Spring 2022

Quilting Topological Phases of Matter with Quantum Thread: A Luttinger Liquid Love Letter

Joseph McCabe Ulysses Sullivan
Yale University Graduate School of Arts and Sciences, jmusullivan@gmail.com

Abstract

Quilting Topological Phases of Matter with Quantum Thread:

a Luttinger Liquid Love Letter

Joseph Sullivan

2022

Kicked off by the discovery of the quantum Hall effect in the early 1980s, the study of topological phases of matter has captured the attention of the condensed matter physics community for over four decades. With topologically ordered phases, symmetry-protected topological phases and, most recently, fracton phases, examples of states of matter beyond the Landau-Ginzburg symmetry breaking paradigm abound. One approach for constructing these novel states of matter is to employ a layered approach; 2-dimensional phases can be built by coupling together 1-dimensional "wires", 3-dimensional phases can be built by coupling together 2-dimensional "layers" and/or 1-dimensional "wires" and so on. Two major advantages of this approach are its analytical tractability and its ability to describe chiral phases.

In this dissertation we will make use of these constructions to study several new and exotic strongly coupled quantum phases of matter. These include necessarily interacting fermionic symmetry-protected topological phases, chiral fracton phases and stable compressible phases which lack any local order parameter.

Quilting Topological Phases of Matter with Quantum Thread:

a Luttinger Liquid Love Letter

A Dissertation

Presented to the Faculty of the Graduate School

Of

Yale University

In Candidacy for the Degree of

Doctor of Philosophy

By

Joseph Sullivan

Dissertation Director: Meng Cheng

May 2022

Acknowledgment

First and foremost, I would like to thank my advisor Meng Cheng. I have learned a tremendous amount from him and he has shown me a great deal of generosity and patience. When struggling with a research question I had the possibly annoying habit on barging into Meng's office at will. I would always preface my question with "If you don't know this off the top of your head don't worry". He would always know it off the top of his head. The combination of clarity of thought, deep knowledge of physics and kindness makes Meng an ideal advisor and I am grateful to have gotten the chance to work with him.

I would also like to acknowledge the members of my committee; Steve Girvin, Leonid Glazman, Xie Chen and particularly Nick Read. I also had the habit of barging into Nick's office and he was always good about steering me in the right direction. The guidance and feedback they provided during the process of putting together this dissertation is greatly appreciated. I am thankful for my collaborators and friends Arpit Dua, Pok Man Tam, Tyler Ellison and especially Tom Iadecola and Dom Williamson.

I was lucky enough to have a few great groups of friends during my time at Yale,

which I will categorize as physics, soccer and other. In the domain of physics I would like to thank James Watson, Oskari Timgren, Emily Kuhn, Emma Castiglia, Connor Hann, Luna Zagorac and Kelly Backes.

On the soccer front, I would like to salute the Yale Men's club soccer team (FCYU). This team and the guys on it ended up being incredibly important part of my time at Yale. I leave the club in a better place than I found it and, due to sheer longevity, as the all time leading goal scorer and assist provider (but not oldest ever member, cf Scott Jensen). I have made countless friends through FCYU but would like to specifically acknowledge Sam Day-Weiss, Scott Jensen, Jack Devlin, Nate Shekita, Rohan Subramanian and Ben Ihenacho.

In the classification of other I want to make a special shout-out to the KBT crew; Jack Treado, Margie Fuchs, Jake Brawer, Sybil Engelby, Chris Harshaw, Sam Bryant, Gwen Gage, Julia Stevenson, Camille Violet, Peter Chen, Jesse Horwitz, Melanie Reschke, Josie Bircher and Henry Balme whose friendships brought levity and welcome distraction during the tumultuous events of the previous few years.

I would like to thank my father, Jim, for instilling in me a sense of curiosity and a fondness for learning, which I have put to good use over the past six years. Finally, I am most grateful for the love and support of three women; my sister Lillie, my mother Nancy and my soon-to-be wife Chloe. Lillie, while I initially wished you had been a boy I could not have asked for a greater sibling and friend. I will never not envy how insightful and charismatic you are. Nancy (Mom), thank you for always being in your children's corner and for showing us firsthand that with competence and determination you will always succeed. Chloe, if I had to come Yale and never

heard the words "topological insulator" or "fracton" it would have been worth it for having met you. Loving and being loved by the person you admire most in the world is an infinitely greater reward than any Ph.D.

Contents

List of Figures

Chapter 1

Introduction

1.1 Topological phases of matter: a brief overview

The early 1980s marked the beginning of a new epoch for condensed matter physics. In the previous era the classification scheme which organized all of the known states of matter relied on the transformation properties of local order parameters under the symmetries of the system. Liquid water, which looks homogeneous in all directions can be differentiated from ice, which has a rigid lattice structure, signaling a reduction in the spatial symmetry of the system. Under the Landau-Ginzburg [3, 4] paradigm, local information was sufficient to distinguish distinct phases of matter.

This method of taxonomy was shown to be incomplete with the discovery of the integer and fractional quantum Hall states [1, 5]. The defining feature of these states is the famous quantized Hall resistances shown in Fig. 1.1 . On the boundary of these systems one finds robust chiral edge modes and in the fractional case, the emergent quasiparticles of the system possess fractionalized quantum numbers (eg

electric charge of $e/3$). It was eventually realized, after efforts were made to fit the quantum Hall states into the Landau-Ginzburg paradigm, that the novel physics just described is incompatible with the existence of a local order parameter [6, 7, 8, 9]. In the subsequent decades myriad examples of phases of matter which elude the symmetry breaking paradigm have been found. The rest of this section will be devoted to providing a cursory introduction to the families relevant to this dissertation.

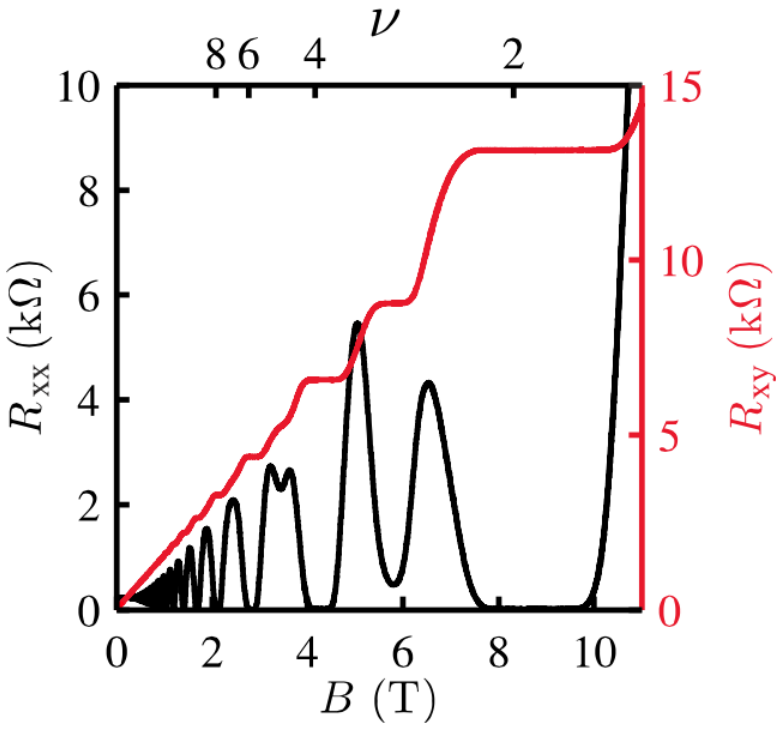

Figure 1.1: The famous plot of quantized hall resistance in the integer quantum hall effect first measured by von Klitzing, Dorda, and Pepper [1]. One can see large regions in which the resistance R is flat as the magnetic field B is increased. Sharp jumps connect these qauntized flat regions, signaling a phase transition.

Topological Order (TO)

In 1990 Wen [9] proposed a description of quantum Hall fluids in terms of *topological order*, the idea being that quantum states may be characterized by their ground

states on different topological manifolds. Heuristically in a gapped system, quantized invariants such as ground state degeneracy (GSD) should be insensitive to local perturbations and provide a natural way to differentiate phases. This idea spurred the search for other gapped states of matter with "topological" features. Soon more examples were recognized in bosonic settings such as quantum spin liquids [10, 11].

Along with a GSD dependent upon the topology of space, a hallmark of TO states are emergent quasiparticles (*anyons*) with fractionalized quantum numbers (charge, spin etc). Another characteristic is a long-range entangled (LRE) ground state wave function. This means that the ground state cannot be converted via a finite-depth local unitary circuit[1] into a product state. LRE can be diagnosed by calculating the entanglement entropy of subsystems [12, 13]. It turns out that these three properties (GSD, fractionalization and LRE) are not independent of one another and are different manifestations of the non-local nature of TO states. In a sense, TO states can be fit into the symmetry breaking paradigm if one allows for the use of non-local order parameters [14, 7, 6].

One potential practical application of TO is to the field of quantum computing. For a given TO state the braiding of anyons is equivalent to acting with a unitary matrix on the degenerate ground state subspace. The idea then is to encode topologically protected qubits in the ground state subspace and use braiding to perform quantum operations. After the theoretical discovery of TOs realizing non-Abelian anyon theories [15] the idea of a topological quantum computer capable of performing the full

[1]Quantum information theory terminology meaning a finite sequence of local unitary transformations. In other words are LRE state cannot be adiabatically evolved into a product state.

set of gates necessary for quantum computation emerged [16]. Tunneling between degenerate ground states necessarily requires a non-local operator in a TO state (see Fig. 1.3 (c)), also making them promising candidates for robust quantum memories[17].

In the infra-red (IR) TO phases are described by quantum field theories which only contain "topological" terms which are independent of the space-time metric. In the case of $\nu = \frac{1}{m}$ Laughlin state for example, the corresponding topological quantum field theory is just level m $U(1)$ Chern-Simons theory [8]. As a rudimentary exercise we will see how exactly this works:

We have at our disposal a compact $U(1)$ gauge field a_μ as well as a background field A_μ, which we can use to probe properties of the system. The idea is to write down an effective action which i) does not depend on any space-time metric ii) couples A_μ to some conserved current J_μ iii) reproduces the interesting phenomenology associated with the Laughlin state [2]. Using natural units ($e = \hbar = 1$) consider the action

$$S_{eff}[a; A] = \int dtdx^2 \ \frac{-m}{4\pi}\epsilon^{\mu\nu\lambda}a_\mu\partial_\nu a_\lambda + \frac{1}{2\pi}A_\mu\epsilon^{\mu\nu\lambda}\partial_\nu a_\lambda \quad . \tag{1.1}$$

Note we have built a conserved current out of the exterior derivative of a_u: $J^\mu = \frac{1}{2\pi}\epsilon^{\mu\nu\lambda}\partial_\nu a_\lambda$. Looking at the $\mu = 0$ term, $\frac{1}{2\pi}A_0\epsilon^{0ij}\partial_i a_j$, we can interpret a 2π gauge flux of a as carrying a unit of electric charge (charged under A). The action in Eq. 1.1 is quadratic in a so we can integrate it out to get a new effective action purely in terms of the background field A :

[2] eg fractional quantized Hall conductance, fractional charge, fractional braiding statistics.

$$S_{eff}[A] = \frac{1}{4\pi m}\int dtdx^2\ \epsilon^{\mu\nu\lambda}A_\mu\partial_\nu A_\lambda \quad . \tag{1.2}$$

From here we can extract the Hall conductivity σ^{xy}

$$\langle J^i\rangle = \frac{\delta S_{eff}[A]}{\delta A_i} = \frac{1}{2\pi m}\epsilon^{i\nu\lambda}\partial_\nu A_\lambda = \frac{1}{2\pi m}E^j \implies \sigma^{xy} = \frac{1}{2\pi m} \quad . \tag{1.3}$$

Comfortingly, the effective theory in Eq. 1.1 successfully reproduces the quantized Hall conductance of the Laughlin state.

The next thing to consider is the symmetry fractionalization associated with the Laughlin state. We should expect to see emergent quasiparticles with $\frac{1}{m}$ the charge of an electron and similarly fractionalized exchange statistics. In order to capture this physics we introduce a current j^μ which couples to the dynamical gauge field a. We need to add

$$\delta S = \int dtdx^2 a_\mu j^\mu \tag{1.4}$$

to Eq. 1.1. To see the effect of this we can turn off the background field: $A = 0$. The equation of motion for a gives

$$\frac{1}{2\pi}\left(\partial_\mu a_\nu - \partial_\nu a_\mu\right) = \frac{1}{m}\epsilon_{\mu\nu\lambda}j^\lambda \implies b = \frac{2\pi}{m}j^0 \tag{1.5}$$

where $b = \epsilon^{0ij}\partial_i a_j$ is the magnetic field for a. Again we have a relationship between fluxes and charges. This is a generic feature of the Chern-Simons theory, the Chern-

Simons term $a \wedge da$ encodes "flux attachment." Getting more specific, suppose a static a quasiparticle of unit charge is placed at the origin. The corresponding current is $j^0 = \delta(x),\ j^{1/2} = 0$ and Eq. 1.5 tells us that $b = \frac{2\pi}{m}\delta(x)$ or that each gauge charge of a also carries gauge $\frac{2\pi}{m}$ flux of a. Furthermore, we have already seen that a gauge flux of a carries electric charge:

$$J^0 = \frac{1}{2\pi} b = \frac{1}{m} j^0 = \frac{1}{m}\delta(x)\ . \tag{1.6}$$

Thus we can conclude that the anyon corresponding to a unit gauge charge of a also carries $\frac{1}{m}$ fractional electric charge.

In order to determine the braiding statistics of the theory let us suppose that our system hosts N anyons with gauge charges q_l and at positions r_l. Consider the following scenarios i) the anyons are static for all time ii) the anyon q_1 moves around a closed loop ∂C bounding a region C over some long time interval T, after which all the anyons remain static for all time. The currents in these scenarios are given by

$$\begin{aligned}
&\text{Scenario i):} \quad j^0(r) = \sum_{l=1}^{N} q_l \delta(r - r_l), \quad j^i(r) = 0 \\
&\text{Scenario ii):} \quad j^0(r) = q_1 \delta(r - r_1(t)) + \sum_{l=2}^{N} q_l \delta(r - r_l), \quad j^i(r) = q_1 \dot{r}_1^i(t) \delta(r - r_1(t)) \quad .
\end{aligned} \tag{1.7}$$

Working in the Coulomb gauge ($a_0 = 0, \partial^i a_i = 0$) there is the following relation between the actions of the two scenarios

$$
\begin{aligned}
S_{ii)}[a] - S_{i)}[a] = \Delta S[a] &= \int d^2r dt\ a_i(r,t)\ \underbrace{j^i(r,t)}_{\text{current of ii)}} \\
&= q_1 \int dt\ \dot{r}_1^i(t) a_i(r_1(t)) \\
&= q_1 \oint_{\partial C} d\vec{n} \cdot \vec{a} = q_1 \int_C dA\ \epsilon^{ij} \partial_i a_j \\
&= q_1 \times (\text{total flux contained in } C)
\end{aligned}
\tag{1.8}
$$

As we have already seen in Eq. 1.5, an anyon of gauge charge q carries gauge flux $\frac{2\pi q}{m}$. Eq. 1.8 tells us then that moving an anyon of charge q_1 around a region C which contains another anyon of charge q_2 results in an additional phase factor of $e^{\frac{2\pi q_1 q_2}{m}}$ in the partition function. Therefore we get the quantized $\frac{2\pi}{m}$ fractional braiding statistics we expected.

The Chern-Simons theory in Eq. 1.1 was very effective at capturing the essential features of the Laughlin state. By adding more gauge fields into the mix we can study more sophisticated quantum Hall systems. For example,

$$
\begin{aligned}
S_{eff}[a_{(1)}, a_{(2)}; A] = \int dt dx^2\ \frac{1}{2\pi} A_\mu \epsilon^{\mu\nu\lambda} \partial_\nu a_{(1),\lambda} + \frac{-m_1}{4\pi} \epsilon^{\mu\nu\lambda} a_{(1),\mu} \partial_\nu a_{(1),\lambda} \\
+ \frac{1}{2\pi} \epsilon^{\mu\nu\lambda} a_{(1),\mu} \partial_\nu a_{(2),\lambda} + \frac{-m_2}{4\pi} \epsilon^{\mu\nu\lambda} a_{(2),\mu} \partial_\nu a_{(2),\lambda}
\end{aligned}
\tag{1.9}
$$

corresponds to a quantum Hall state with rational filling $\nu = \frac{1}{m_1 - \frac{1}{m_2}}$. Using this approach we can build up the hierarchy states [18, 19, 20]. More generally if we have n dynamical gauge fields $\{a_{(q)}\}_{q=1}^n$ we can work with

$$S_{eff}[a_{(q)}; A] = \int dtdx^2 \ \frac{K^{ij}}{4\pi}\epsilon^{\mu\nu\lambda}a_{(i),\mu}\partial_\nu a_{(j),\lambda} + \frac{t^j}{2\pi}A_\mu\epsilon^{\mu\nu\lambda}\partial_\nu a_{(j),\lambda} \tag{1.10}$$

where K is an integer symmetric matrix and t is an integer vector. To describe a gapped phase of matter, such as the quantum Hall states or some other topologically ordered state, K must be non-degenerate. In this case we can get a great deal of information from K and t. For example, the hall conductivity is $\sigma^{xy} = \frac{1}{2\pi}\left(K^{-1}\right)^{ij} t_i t_j$, the electric charge of the quasiparticle coupled to gauge field $a_{(i)}$ is given by $\left(K^{-1}\right)^{ij} t_j$ and the statistical phase from braiding anyon i around anyon j is given by $2\pi\left(K^{-1}\right)^{ij}$. K even gives the topological ground state degeneracy; on a manifold with genus g we have GSD $= |\det K|^g$.

The construction we have just seen is quite powerful. It turns out that any Abelian TO in 2d can be described in this way [21, 22]. In Chapter 5 we will explore some novel 3d phases by associating each gauge field $a_{(q)}$ with a spatial layer and consider the implications of degenerate $K-$matrices in this context.

Symmetry-protected topological phases (SPT)

Entanglement provides a powerful diagnostic for distinguishing phases of matter. As we have just discussed, TO states are LRE, meaning they cannot be evolved into a product state using a finite-depth local unitary circuit. This definition naturally motivates another. We say a state is short-range entangled (SRE) if it **can** be evolved into a product state using a finite-depth local unitary circuit. The family of states

classified by the symmetry breaking paradigm of Landau and Ginzburg are SRE, for example. It is natural to ask whether this is the full story; are all states of matter either classified by TO or according to the symmetry breaking of a local order parameter? A number of historical examples in bosonic [23] and fermionic [24, 25, 26] settings hint at this not being the full story.

To illustrate this, consider the open chain of spin $\frac{1}{2}$ particles shown in Fig. 1.2. The chain, which has $2N$ sites, is partitioned into sub-lattices A and B, each of size N. We will work with the Hamiltonian

$$H = -J_1 \sum_i \left(\vec{S}_i^A + \vec{S}_i^B\right)^2 - J_2 \sum_i \left(\vec{S}_{i+1}^A + \vec{S}_i^B\right)^2 , \quad J_1, J_2 > 0. \tag{1.11}$$

Note that this Hamiltonian has $SO(3)$ rotation symmetry as well as time reversal symmetry. The J_1 term is designed to project the A and B spins in each unit cell i into the triplet state: $\left\{ \left|\uparrow_i^A \uparrow_i^B\right\rangle , \ \frac{1}{\sqrt{2}} \left(\left|\uparrow_i^A \downarrow_i^B\right\rangle + \left|\downarrow_i^A \uparrow_i^B\right\rangle\right) , \ \left|\downarrow_i^A \downarrow_i^B\right\rangle \right\}$. The J_2 term does the same thing but to the A and B spins in neighboring unit cells. In Fig. 1.2 we have shown the gapped ground state of the Hamiltonian in two different regimes. In the case $\frac{J_1}{J_2} \gg 1$ the spins in a given unit cell will form a singlet state and the unique ground state will proportional to $\prod_{i=1}^{L} \left(\left|\uparrow_i^A \downarrow_i^B\right\rangle - \left|\downarrow_i^A \uparrow_i^B\right\rangle\right)$. The other regime, $\frac{J_1}{J_2} \ll 1$, is more interesting. In this situation the B spin from site i and the A spin in site $i+1$ are forced into the singlet state, leaving the leftmost A and rightmost B spins unconstrained. The result is a fourfold degenerate ground state $\left|\sigma_1^A\right\rangle \left(\prod_{i=1}^{L-1} \left(\left|\uparrow_{i+1}^A \downarrow_i^B\right\rangle - \left|\downarrow_{i+1}^A \uparrow_i^B\right\rangle\right)\right) \left|\sigma_L^B\right\rangle$, where σ_1^A and σ_L^B can independently

be either spin up or down.

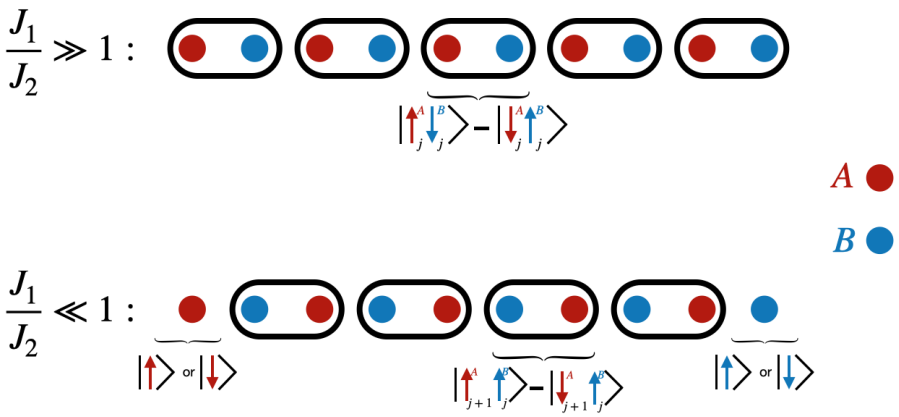

Figure 1.2: Here we depict the ground states of the Hamiltonian in Eq. 1.11 in two separate regimes. Top: when J_1 dominates the spins A and B in the same unit cell form a singlet state. The result is a unique gapped ground state. Bottom: when J_2 dominates the spins A and B from neighboring unit cells form a singlet state, leaving behind a dangling qubit on each end of the chain. In this case the GSD is equal to four. Note that the edge states transform protectively under the symmetries of the Hamiltonian.

The bulk order of these [3] two SRE states is exactly the same yet one has a GSD of four resulting from robust edge modes while the other has a unique ground state. When trying to differentiate these states knowledge of the bulk is insufficient. For the state with dangling edge modes we can lift the degeneracy by adding some local Pauli operator (turning on a magnetic field) but by doing so we are breaking the rotational and time-reversal symmetries. Observe though that if we stack two of these systems on top of one another we can symmetrically pair up the dangling edge modes on the end points of the two chains into the singlet state and end up back in the less interesting phase with a unique ground state. With symmetry imposed as a constraint we can think of these states as being classified by the group $\mathbb{Z}_2$, where the

[3] What we capturing here is the physics of the AKLT chain. Technically to obtain the same state studied in [23] we also need to project the A and B spins in each unit cell into the triplet state. Our interest here is the novel boundary physics (and also brevity) so we have not taken this extra step.

group multiplication corresponds to stacking the chains.

Belaboring the point a bit, it is clear that symmetry considerations are key when coming up with notions of a "phase" capable of differentiating the two qualitatively distinct SRE states above. This motivates the following definition: given the ground state of a local Hamiltonian with symmetry group G, we say the state is a symmetry-protected topological (SPT) phase if i.) it is distinct from and cannot be converted into a trivial product state using a G-symmetric finite-depth local unitary circuit and ii.) it does not possess any TO [4]. Because of the correspondence between ground states and Hamiltonians we may also think of defining SPTs in terms of interpolations between Hamiltonians; given two $G-$symmetric Hamiltonians H_A and H_B we say H_A and H_B describe distinct SPT phases if we cannot find a symmetric path through parameter space which interpolates from $H_A \to H_B$ without closing the spectral gap. As we have already, the seen caveat that the interpolation be symmetry preserving is key to the definition of SPT phases. Symmetry violating interpolations between SRE states A and B which preserve the gap are is generically possible, so it is the symmetry constraint which refines the otherwise trivial classification.

Unsurprisingly, the boundary between distinct SPT states hosts novel physics. More specifically, a nontrivial SPT in n-dimensions will host a n-1 dimensional edge theory which is not realizable in a true n-1 dimensional setting. The protecting symmetries act anomalously on these boundary theories preventing the existence of a symmetric and non-degenerate ground state. Generically then, at the boundary

[4]So the lack of convertibility into a trivial product state in condition i) is not due to some underlying topological order.

of an SPT state one finds gaplessness or in the gapped case, spontaneous symmetry breaking or topological order (when the bulk dimension is 3d or higher). These anomalous edge states characterize the SPT.

A large body of work exists on both fermionic and bosonic SPTs. The first systematic understanding to be established in this area was for non-interacting fermionic SPTs [27, 28]. Group cohomolgy theory provides a complete classification of bosonics SPTs in one and two dimensions [29, 30, 31]. [5]. Applying this to 1d is equivalent to classifying the projective representations of the protecting symmetry group G. The group $SO(3)$, for instance, has two inequivalent classes of projective representations[6] agreeing with the $\mathbb{Z}_2$ classification we found in our above example. This makes quite a lot of sense; the inequivalent classes of $SO(3)$ projective representations correspond to half-integer spin (eg the edge spin $\frac{1}{2}$ particles in the bottom configuration in Fig 1.2) and integer spins (eg the edge spin 0 particles in the top configuration in Fig 1.2). Similar progress has been made in classifying general fermionic SPTs using generalizations of the group-cohomology constructions [32, 33, 34], and classifications based on TQFTs [35, 36, 37, 38]. In Chapter 2 we will discuss an example of an intrinsically interacting fermionic SPT state which cannot actually exist without interactions.

Fracton Topological Order

In the last decade examples of 3d LRE states which do not fit within the framework of TQFT have emerged. So called fracton topological orders (FTO) possess emergent

[5] See Appendices D and J of [30] for an introduction to this subject.
[6] $\mathcal{H}^2[SO(3), U(1)] = \mathbb{Z}_2$

quasiparticles which are mobility restricted in certain (sometimes all) directions. Like TO phases, fracton phases can possess emergent quasiparticles with fractionalized quantum numbers. However, in the fracton case the ground state degeneracy is no longer a topological invariant but instead scales sub-extensively with system size. Where TO phases only care about the topology of space, fracton phases know about the geometry [7]. The history of fracton phases dates back to 2005 in work by Chamon [39] on quantum glassiness. Later Haah discovered the now famous Haah's Code [40], a commuting projector model with completely immobile elementary excitations. Broad interest in the nascent field of fracton physics was sparked by the work of Vijay, Haah and Fu [41, 42] in which they showed that the examples found by Haah and Chamon were part of a much larger family of fracton phases.

The related properties of restricted quasiparticle mobility and subsystem scaling GSD have attracted interest from branches of physics other than condensed matter. These attributes would suggest fracton models make ideal candidates for topological quantum memories [8] and this area of research has garnered attention in the quantum information community[43, 44, 45]. On the less applied side, certain fracton models [40] do not seem to fit within the paradigm of quantum field theory and the renormalization group which have been organizing principles underlying physics for over half a century. This challenge to theoretical physics orthodoxy has been picked up by members of the high energy theory community. Those fracton models which do have tractable IR descriptions give rise to unusual quantum field theories [46, 47, 48, 49, 50, 51, 52].

[7] For example on a 3-torus of size $L \times L \times L$ the GSD of the toric code is 8 while for the X-Cube model GSD= 2^{6L-3}.

[8] The search for a robust quantum memory was the initial motivation for Haah's work.

One common setting for realizing fracton physics is commuting projector models with qudit or majorana degrees of freedom. Another natural place to find mobility restricted phenomenology is higher rank gauge theories [48]. This is somewhat unsurprising because the mobility constraints on the quasiparticles in fracton phases can be understood as stemming from high moment conservation laws (eg dipole moment conservation). In this dissertation we will give several examples of fracton phases built from networks of Luttinger liquids.

Gapless weak symmetry breaking phases

Typically when one speaks about topological phases of matter one is referring to gapped systems. The idea being that a gapped system is far from a critical phase and in this region of phase space quantized properties such as the number of chiral edge states are robust. Certainly, gapless systems can have "topological features." A canonical example is the 2d superfluid which, while symmetry breaking, has gapped vortex excitations whose discrete charge is related to the winding of the phase around closed curves in the fluid. Other examples are the compressible phases [9] which arise in quantum Hall systems [53, 54, 55]. Topology also shows up in 3d gapless systems such as Weyl semi-metals which feature protected surface states [56]. Recently examples of intrinsically gapless SPT phases have been found [57].

In this work we will present several examples of compressible phases of matter which exhibit "weak symmetry breaking." In these phases the global $U(1)$ charge symmetry is spontaneously broken, giving rise to a Goldstone mode, but the corresponding

[9] So very gapless.

order parameter is non-local (eg a string or planar operator) placing them outside of Landau-Ginzburg framework. In addition to the gapless sector these phases often exhibit a topologically ordered sector with deconfined fractonic excitations. We will explore an example of this in depth in Chapter 5.

1.2 Goals and themes of this work

A great deal of progress has been made the study of topological phases (and condensed matter theory in general) by coupling together 0-dimensional building blocks (spins/bosons, fermions) into a reasonable physical model. The low energy physics of these systems can be extracted by coarse-graining the microscopic description, resulting in a quantum field theory. While this approach is good and proper, if one is interested in discrete quantitative (eg topological) or even qualitative emergent properties of the system, using the full microscopic Hamiltonian can be overkill. A useful tactic is to "pre-coarse-grain" part of the system and use 1d or 2d quantum field theories as the building blocks for novel quantum phases of matter.

Coupled wire constructions, in which arrays of quantum wires are coupled together, have been employed to study the full gauntlet of condensed matter systems [58, 59, 60, 61, 62, 63, 64, 65, 66, 67, 68, 69]. Beginning with the work of Kane, Mukhopadhyay, and Lubensky [60] and Kane and Teo [61] on constructions of fractional quantum Hall states, the technique has proved remarkably effective at describing both Abelian and non-Abelian [68, 66] topological phases of matter. The main appeal of the method is its analytical tractability. Strong interactions can be encoded and then handled

using bosonization techniques [70, 71]. More specifically, the interactions correspond to sine-Gordon terms in the Hamiltonian.

Following the example at the end of Sec. 1.1 we will sketch the construction of the Laughlin state using this technique, first presented in [60]. The idea is to begin with a decoupled array of wires, where each wire hosts a chiral (ϕ_L) and anti-chiral (ϕ_R) free boson (see Fig. 1.3 (a)). The degrees of freedom have commutation relations $[\phi_{\eta'}^{(j')}(x'), \partial_x \phi_\eta^{(j)}(x)] = i\pi \,\mathrm{sgn}(\eta)\delta_{\eta\eta'}\delta_{jj'}\delta(x'-x)$ where j labels the wire location, $\eta = L, R$ and $\mathrm{sgn}(\eta = L/R) = +/-$. The Hamiltonian describing the dynamics on each wire j is given by

$$H = \frac{v}{2\pi}\int dx \left(\partial_x \phi_L^{(j)}\right)^2 + \left(\partial_x \phi_R^{(j)}\right)^2 \quad . \tag{1.12}$$

So far our system is just a stack of decoupled Luttinger liquids. The local operators $\psi_{L/R} = e^{i\phi_{L/R}}$ create charged chiral excitations. For concreteness suppose m is odd. Then we can define the bosonic field

$$2\Theta_{j+1/2} = \left(\frac{m+1}{2}\phi_L^{(j)} + \frac{1-m}{2}\phi_R^{(j)} - \frac{1-m}{2}\phi_L^{(j+1)} - \frac{m+1}{2}\phi_R^{(j+1)}\right)$$

and consider the following tunneling term

$$\left(\psi_{L,j}^\dagger \psi_{R,j}\right)^{\frac{m-1}{2}} \left(\psi_{L,j+1}^\dagger \psi_{R,j+1}\right)^{\frac{m-1}{2}} \psi_{L,j}^\dagger \psi_{R,j+1} = \exp\left[i2\Theta_{j+1/2}\right] \quad . \tag{1.13}$$

This describes a process [10] in which $\frac{m-1}{2}$ left moving quasiparticles and right

[10] Technically the chiral quasiparticle created by ψ_η is a fermion so $\psi^n = 0$. What we are really

moving quasiholes are created on wires j and $j+1$ and then a right mover on wire j is converted into a left mover on wire $j+1$. What we do now is condense this process by adding the following interaction term to the Hamiltonian

$$H_{int} = -g \sum_{j=1}^{N} \int dx \cos(2\Theta_{j+1/2}) \ . \tag{1.14}$$

At this point the wires are no longer decoupled. Observe, that all the sine-Gordon terms in Eq. 1.14 commute with one-another and so in the limit $g \gg 1$ [11] the ground state manifold consists of the configurations with $\langle 2\Theta_{j+1/2} \rangle \in 2\pi\mathbb{Z}$. Density fluctuations of the original chiral bosons ϕ_η are gapped out in this regime. The elementary excitations correspond to tunneling events, or solitons, which interpolate between allowed configurations in the ground state manifold: $\Theta_{j+1/2} \to \Theta_{j+1/2} + n\pi$.

The fundamental quasiparticle, a 2π soliton, is shown in Fig. 1.3 (b). It can be moved around using the following operators

$$T_y(j) = e^{i(\phi_{L,j} - \phi_{R,j})} \ \text{ and } \ T_x(x_1, x_2) = e^{\frac{i}{2m}\int_{x_1}^{x_2} \partial_x \left(\frac{m+1}{2}\phi_L^{(j)} + \frac{1-m}{2}\phi_R^{(j)} + \frac{1-m}{2}\phi_L^{(j+1)} + \frac{m+1}{2}\phi_R^{(j+1)} \right)} \tag{1.15}$$

where $T_y(j)$ hops a 2π kink between across wire j and $T_x(x_1, x_2)$ moves a 2π kink from $x_1 \to x_2$ along the wire. We can also interpret these operators as creating particle-hole pairs at their endpoints. Measuring the charge the density at the end point of the T_x operator tells us that these quasiparticles carry charge $\frac{1}{m}$. We can

doing here is point splitting $\psi_\eta^n(x) \equiv \prod_{q=0}^{n-1} \psi_\eta(x + qa) \sim \prod_{q=0}^{n-1} \partial_x^q \psi_\eta(x)$. In the interest of brevity we have ignored subtleties like these.

[11] We can always obtain this by adjusting the kinetic terms in the theory to make $\cos 2\Theta$ relevant. We can also just consider the situation where g has an already large bare value.

compute the braiding statistics of between the elementary quasiparticles (see Fig. 1.3 (c)). This process produces a phase of $e^{\frac{2\pi i}{m}}$. The elementary quasiparticles of this model have charge $\frac{1}{m}$ and mutual braiding statistic $2\pi/m$ signaling we are in the same phase as the Laughlin state. Note that any local operator $e^{2i\Theta'}$ not equivalent to some linear combination $\sum_j n_j 2\Theta_{j+1/2}$ of the interaction terms creates a gapped excitation. The upshot of this is that the model is stable; in order to destabilize it we need to introduce a competing sine-Gordon term $\cos 2\Theta'$ but as we have just seen, such a term will be irrelevant. By the same token the expectation of any local operator $\langle e^{2i\Theta'}\rangle = 0$ ruling out the possibility of symmetry breaking.

On the other hand, it is possible to find a non-local order parameter. For concreteness lets place our system on a torus built from N wires and consider the process of moving an anyon across a full cycle perpendicular to the wire direction. The operator accomplishes this is $\prod_{j=1}^{N} e^{i(\phi_{L,j}-\phi_{R,j})}$. Observe though that $\sum_j(\phi_{L,j}-\phi_{R,j}) = \frac{1}{m}\sum_j 2\Theta_{j+1/2}$. Recalling that in the ground state $\langle\Theta_{j+1/2}\rangle \in \pi\mathbb{Z}$ we see that $\langle\prod_{j=1}^{N} e^{i(\phi_{L,j}-\phi_{R,j})}\rangle = e^{2\pi i/m}$. The expectation value of this non-local operator tells us which of the m degenerate ground states we are in. Furthermore, we can use the operator T_x in Eq. 1.15 to transport an anyon around the cycle along the wire direction. By considering the commutation relations of T_x and T_y we see that this process toggles between the ground states of the Laughlin state.

As the example just discussed shows, this construction can realize rather rich physics in a class of models that are relatively simple to analyze. The condition that the sine-Gordon terms mutually commute, sometimes referred to as the Haldane null vector criterion [72], makes the coupled wire construction reminiscent of commuting

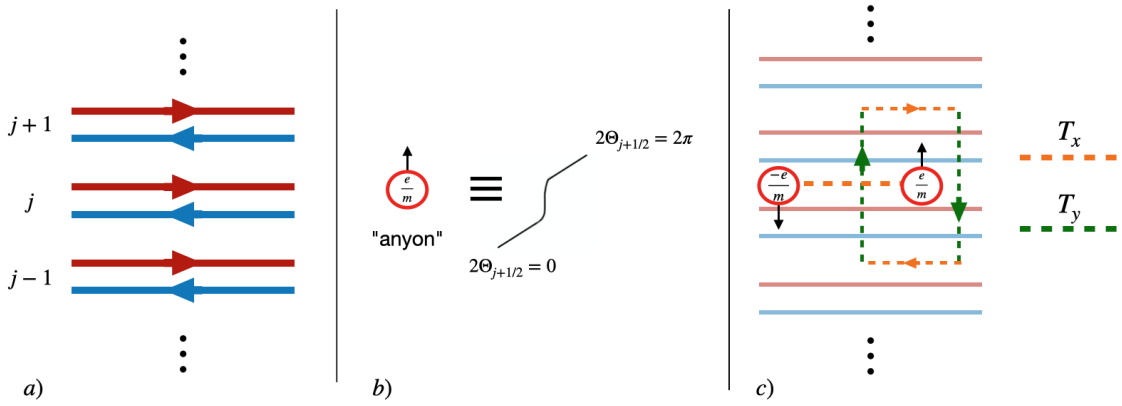

Figure 1.3: a) Here we see the set up for the wire construction. The red/blue wires host $\phi_{L/R}$. b) The anyons of the theory correspond to 2π kinks in the condensed field $2\Theta_{j+1/2}$. Note that the anyon can be thought of as living in the space in between the wires. c) One anyon is moved around another using the sequence of $T_x T_y T_x^{-1} T_y^{-1}$. The failure of the left T_y to commute with the T_x operator connecting the quasiparticle-quasihole pair gives rise to a braiding phase of $\frac{2\pi}{m}$.

projector models with the added capability of being able to describe chiral phases. Further, the similarity to commuting projector models means that the bulk-boundary correspondence is very explicit. The relatively simple task of analyzing coupled wire models makes them an excellent platform for "designing" exotic quantum matter [73]. If lattice degrees of freedom are the "quantum Legos" of condensed matter physics, the Luttinger liquid can be viewed as the "quantum thread" with which one can quilt together novel topological phases.

Moving up one dimension, Coupled layer constructions, where stacks of 2d layers are coupled together, are similarly useful [74, 75, 76, 50]. For one thing, stacking layers (or wires) is a natural way of constructing higher dimensional SPTs. The idea, depicted in Fig 1.4, is to start with a non-anomalous pair of 2d layers (1d wires) featuring the anomalous edge theory S and the inverse theory $\bar{S}$ [12]. By coupling theory

[12]Note that the wire (Fig. 1.3) and dot (Fig. 1.2) examples we have seen also fit into this framework. In the wire case S is a chiral boson theory and in the dot case S is some theory of a

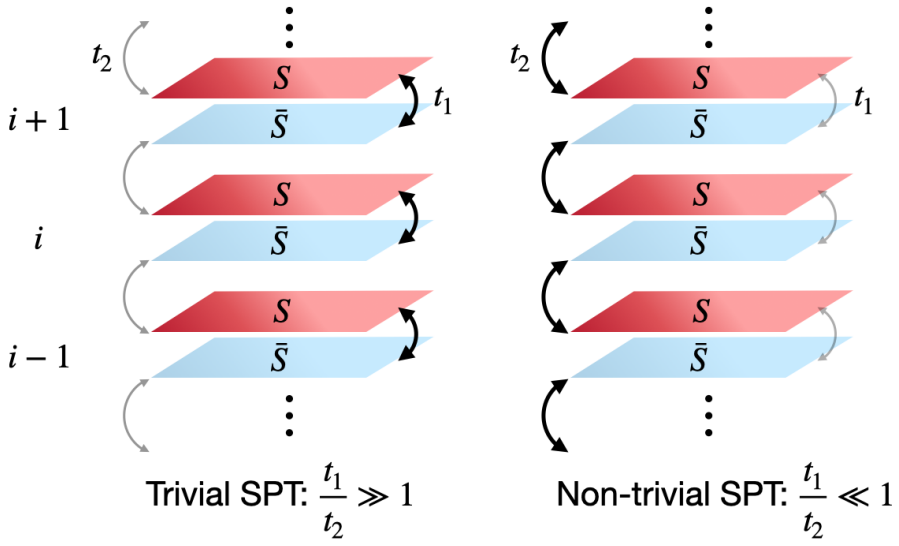

Figure 1.4: Cartoon of the layer construction of a 3+1d SPT phase. A layer, indexed by i, is made up of a pair of $G-$symmetric theories S (top, red) and $\bar{S}$ (bottom, blue). The phase is trivial when the inter-label coupling dominates the intra-layer coupling and non-trivial when this inequality is reversed. In the non-trivial case, when the system has a boundary, there is are anomalous S and $\bar{S}$ boundary theories on the top and bottom surfaces respectively.

S in layer i to layer (wire) $\bar{S}$ in layer (wire) $i+1$ one can drive a phase transition to the 3D (2D) SPT characterized by the anomalous edge theory S. These constructions are also implicit in topological defect networks which provide a framework for a partial classification of fracton phases [77].

In summary the advantage of this coupled wire/layer approach is that by starting with more sophisticated building blocks the study of novel phases of matter is somewhat streamlined. The goal of this dissertation is leverage these strengths to study new strongly coupled quantum phases of matter which have been missed because of their lack of amenability to more standard techniques.

single qubit.

1.3 Outline

The chapters of this dissertation correspond to the following publications [78, 79, 80, 81]. In addition to a general Appendix A at the end of the manuscript, each chapter will contain its own appendix containing further supplementary details. There is some redundancy built into the introductory parts of the chapters, particularly between Chapters 3 and 4. This is done in an effort to make each chapter self contained.

In Chapter 2 we will discuss fermionic SPT phases. We will give a broad review of SPT physics supplementing the discussion in 1.1 before narrowing our focus to an interetsing class of fermionic SPT. Specifically, we investigate an intrinsically interacting 2D fermionic SPT protected by a $\mathbb{Z}_4 \times \mathbb{Z}_2^T$ symmetry. Such phases carry the label "intrinsically interacting" because they cannot be realized in systems of free fermions. We model the edge Hilbert space by replacing the internal $\mathbb{Z}_4$ symmetry with a spatial translation symmetry, and design an exactly solvable Hamiltonian for the edge model. Then we show that at low-energy the edge can be described by a two-component Luttinger liquid, with nontrivial symmetry transformations that can only be realized in strongly interacting systems. We further demonstrate the symmetry-protected gaplessness under various perturbations, and the bulk-edge correspondence in the theory.

Chapter 3 presents a general construction for fracton topological orders (1.1) using the coupled wire method. We find that both gapped and gapless phases with fractonic excitations can emerge from the models. In the gapless case the weak symmetry breaking mechanism discussed in 1.1 is a generic feature. In the gapped case, we

argue that fractonic excitations are mobile along the wire direction, but their mobility in the transverse plane is generally reduced. We show that the excitations in general have infinite-order fusion structure, distinct from previously known gapped fracton models. Like the two-dimensional coupled-wire constructions, many models exhibit gapless (or even chiral) surface states, which can be described by infinite-component Luttinger liquids. Unusually though, the universality class of the surface theory strongly depends on the surface orientation, thus revealing a different type of bulk-boundary correspondence unique to fracton phases.

Chapter 4 lays out an in-depth study of a specific fracton coupled wire model, which we dub the "fractonal quantum Hall state." A complementary coupled layer construction is also discussed. The model combines the known construction of $\nu = 1/m$ Laughlin fractional quantum Hall states with a planar p-string condensation mechanism [76]. The bulk of the model supports gapped immobile fracton excitations that generate a hierarchy of mobile composite excitations. Open boundaries of the model are chiral and gapless, and can be used to demonstrate a fractional quantized Hall conductance where fracton composites act as charge carriers in the bulk. The planar p-string mechanism used to construct and analyze the model generalizes to a wide class of models including those based on layers supporting non-Abelian topological order. We describe this generalization and additionally provide concrete lattice-model realizations of the mechanism.

In Chapter 5 we introduce a new type of 3D compressible quantum phase, in which the $U(1)$ charge conservation symmetry is weakly broken by a rigid string-like order parameter, and no local order parameter exists. We show that this gapless

phase is completely stable and described at low energy by an infinite-component Chern-Simons-Maxwell theory. We determine the emergent symmetry group, which contains $U(1)$ 0-form planar symmetries and an unusual subgroup of the dual U(1) 1-form symmetry supported on cylindrical surfaces. Through the associated 't Hooft anomaly, we examine how the filling condition is fulfilled in the low-energy theory. We also demonstrate that the phase exhibits a kind of fractonic topological order, signified by extensively many different types of topologically nontrivial quasiparticles formed out of vortices of the weak superfluid. A microscopic model realizing the weak superfluid phase is constructed using an array of strongly coupled Luttinger liquid wires, and the connection to the field theory is established through boson-vortex duality.

In the Appendix A we provide background on some useful 1d fermion-boson dualities, namely the Jordan-Wigner transformation and Abelian bosonization.

Chapter 2

Edge theories of intrinsically interacting fermionic SPTs

2.1 Introduction

As discussed in Chapter 1.1 symmetry-protected topological (SPT) phases [30, 82, 83] are characterized by their protected boundary states. The protecting symmetries act anomalously on the boundary states, in such a way that a symmetric and non-degenerate ground state is prohibited. As a result, a boundary without symmetry breaking must be gapless, or gapped with intrinsic topological order when the boundary is two-dimensional or higher [84]. Many examples of SPT phases have been discovered in fermionic systems, in particular in electronic band insulators and BCS superconductors [27, 85, 86, 87]. Due to the non-interacting nature of these states, their boundary physics is well understood and can be described in terms of Dirac or Majorana fermions when the interactions on the boundary are sufficiently weak. Dirac-like surface states have been

observed in 3D time-reversal-invariant topological insulators [86, 87], as well as their generalizations with crystalline symmetries. Strong interactions can drive the gapless surface to symmetry-enriched[1] topologically ordered phases [84, 88, 89, 90, 91, 92].

Beyond free fermions, recently there has been significant theoretical progress in classifying SPT phases in interacting fermionic systems [32, 93, 94, 95, 33, 96], following previous classifications of bosonic SPT phases using group cohomology [30]. A number of different approaches have been put forward, such as fermionic generalizations of the group-cohomology constructions [32, 33, 34], and classifications based on topological quantum field theories [35, 36, 37, 38]. These results have pointed to an interesting possibility, namely interacting Fermionic Symmery-Protected Topological (FSPT) phases, which can only exist with strong interactions. One mechanism for such phases is when fermions first form bosonic molecules/spins under strong interactions, and then these bosons form a SPT state. As an example, imagine in 2D fermions first form charge-$2e$ bosons, and then these bosons are put into a so-called bosonic integer quantum Hall state [97], which has an electric Hall conductance quantized to $\frac{8e^2}{h}$, but a vanishing thermall Hall conductance, violating the Wiedemann-Franz law [62]. Thus this phase can only be found in the presence of strong interactions. However, more interestingly there exist *intrinsically* fermionic phases which can not be realized by weakly interacting systems and have no bosonic counterpart. Examples of such intrinsically FSPT phases have been discovered in one, two and three dimensions [93, 98, 95]. In one dimension, an intrinsically interacting FSPT phase exists when the symmetry group is $\mathbb{Z}_4^f \times \mathbb{Z}_4$ [93, 98], where the edge modes transform as a projective

[1] Topologically ordered states which also feature symmetry protection.

representation of the symmetry group. Here $\mathbb{Z}_4^f$ refers to the conservation of fermion number mod 4. In two dimensions, the simplest symmetry group that allows an interacting FSPT phase is $\mathbb{Z}_2^f \times \mathbb{Z}_4 \times \mathbb{Z}_2^\mathsf{T}$. Here $\mathbb{Z}_2^\mathsf{T}$ denotes the time-reversal symmetry that squares to the identity, i.e. fermions are Kramers singlets. Similar states protected by crystalline symmetries have been found [99, 100].

Given that these new phases require strong interactions to exist, their boundary states cannot be simply free Dirac/Majorana fermions. While exactly-solvable bulk Hamiltonians can in principle be constructed [32, 98], it is very desirable to have a physical understanding of the interacting edge states. Generally, nontrivial dynamics on the edge leads to either gapped phases with broken symmetry, or a symmetric gapless phase. In this chapter will address this question for the 2D $\mathbb{Z}_2^f \times \mathbb{Z}_4 \times \mathbb{Z}_2^\mathsf{T}$ FSPT phase just mentioned. The strategy will be to study a closely related 2D crystalline FSPT phase, where the $\mathbb{Z}_4$ symmetry is replaced by a $\mathbb{Z}$ translation symmetry. The corresponding crystalline SPT phase has a simple bulk wavefunction, and the edge modes can be cleanly separated from the bulk as a stand-alone 1D chain of spinless fermions, which do not allow any quadratic couplings respecting the symmetries. We design an analytically solvable model for the boundary chain, and derive a two-component Luttinger liquid theory that captures the low-energy physics, based on which we propose a very similar theory where the spatial translation $\mathbb{Z}$ is replaced by an internal $\mathbb{Z}_4$ symmetry. We then demonstrate that the theory exhibits the correct quantum anomaly.

2.2 Intrinsically interacting FSPT phases in 2D

We review the physics of intrinsically interacting FSPT phases in 2D, through a decorated domain wall picture [101], and closely related ones with crystalline symmetries. Another construction of FSPT phases using group super-cohomology theory will be briefly summarized in Appendix 2.7.1. We will focus on $G = \mathbb{Z}_4 \times \mathbb{Z}_2^{\mathsf{T}}$. Notice that fermions transform as Kramers singlet, e.g. spinless fermions, unlike the spin-1/2 electrons which are Kramers doublets.

We first briefly recall the non-interacting classification with such a symmetry group [102]. Since there is no charge conservation, in general the BdG Hamiltonian can be compactly written as $H = \Psi^\dagger h \Psi$, where the Nambu spinor Ψ is schematically defined as $\Psi = (c, c^\dagger)$ suppressing all the indices (site, spin, etc.). In the presence of a unitary symmetry, e.g. $\mathbb{Z}_4$ in this case, the first-quantized Hamiltonian h can be block diagonalized, with blocks labeled by $\mathbb{Z}_4$ eigenvalues. Now within each block the only symmetry is the $\mathbb{Z}_2^{\mathsf{T}}$. Because the fermions are Kramers singlets, the classification for each block is given by the BDI class in the ten-fold way, which is completely trivial in 2D. We conclude that the overall classification is trivial as well. Therefore strong interactions are necessary to form any nontrivial FSPT phases with this symmetry.

2.2.1 Decorated domain wall construction

The ground state wavefunction of many SPT phases can be understood through a decorated domain wall construction. One first imagines that a discrete symmetry H is broken spontaneously. We take this discrete symmetry to be a normal subgroup

of the protecting symmetry of the SPT phase. Once the symmetry is broken, there can be domain walls between different symmetry-breaking patterns, e.g. different expectation values of an order parameter. Mathematically, each domain wall is uniquely labeled by a group element $\mathbf{h} \in H$. This process can be reversed: starting from the broken symmetry state, the symmetry can be restored by proliferating domain walls. In other words, the wavefunction of a symmetric state can be viewed as the quantum superposition of all possible domain wall configurations.

Now imagine that the domain walls are "decorated" by 1D SPT states protected by the remaining symmetry G/H. The decoration is in fact the manifestation of the SPT order in the symmetry-breaking phase, and can be understood more intuitively in the presence of a physical edge: while domain walls are closed in the bulk, they can end on the edge, which also terminate the associated 1D SPT states on the domain walls. Thus topologically protected zero-energy modes must appear at a domain wall on the edge. A SPT wavefunction is then obtained by proliferating domain walls decorated by 1D SPT states. Importantly, a consistent symmetric wavefunction requires that the decorated 1D SPT states obey the same group multiplication law as the domain walls. Namely, two domain walls labeled by group elements $\mathbf{h}_1$ and $\mathbf{h}_2$ can fuse into a domain wall labeled by $\mathbf{h_1 h_2}$. The same relation must be satisfied by the associated 1D SPT states.

To illustrate, let us consider the example of class DIII topological superconductor (TSC) in 2D. As a simple model for DIII TSC, consider spin-1/2 electrons with $p_x + ip_y / p_x - ip_y$ pairing for spin up/down fermions. Time-reversal symmetry acts on fermion annihilation operators as $\psi_\alpha \to \sum_\beta (i\sigma^y)_{\alpha\beta}\psi_\beta$, where $\alpha, \beta = \uparrow, \downarrow$ are the spin

z component. Edge states of this TSC are described by helical Majorana fermions, where left- and right-moving modes carry opposite spins. They can be gapped out by turning on a time-reversal breaking mass term. Thus a time-reversal domain wall on the edge corresponds to a mass that changes sign. It is well-known that a Majorana zero-energy bound state is found at the mass domain wall. In the bulk, a domain wall then carries a Majorana chain which gives rise to the Majorana zero mode when it is cut open by the physical edge [2]. Hence the DIII TSC can be thought of as proliferating domain walls decorated by Majorana chains. Such a picture was realized recently in a commuting-projector model for the class DIII TSC [103].

For $G = \mathbb{Z}_4 \times \mathbb{Z}_2^{\mathsf{T}}$ in 2D, we may write the wavefunction as a superposition of $\mathbb{Z}_4$ domain walls, and decorate them with 1D SPT states protected by the remaining $\mathbb{Z}_2^{\mathsf{T}}$ symmetry. Denote the generator of the $\mathbb{Z}_4$ group by $\mathbf{g}$. The classification of 1D FSPT phases with $\mathbb{Z}_2^{\mathsf{T}}$ symmetry is well-understood: non-interacting fermions with this symmetry fall into the class BDI in the periodic table, with a $\mathbb{Z}$ classification [85, 27]. The integer invariant ν counts the number of protected Majorana zero modes on one edge. When interactions are taken into account, the classification collapses to $\mathbb{Z}_8$ [104, 105], i.e. a state with $\nu = 8$, although topologically nontrivial for free fermions, can be trivialized by strong interactions.

Now we consider decorating the fundamental $\mathbb{Z}_4$ domain walls labeled by $\mathbf{g}$ by the $\nu = 2$ 1D FSPT states. Correspondingly, the $\mathbf{g}^2$ domain walls are decorated by the $\nu = 4$ 1D FSPT state, etc. Finally, the $\mathbf{g}^4 = 1$ domain walls are decorated by

[2] At the domain wall, the time-reversal symmetry is broken so the remaining symmetry is just the fermion parity conservation $\mathbb{Z}_2^f$ and the corresponding symmetry class for free fermions is class D.

$\nu = 8$ states which become trivial in the presence of strong interactions, as required by the consistency of the construction. This is also why such a decorated domain wall construction necessarily requires strong interactions to exist.

From the construction, it follows that a defining feature of the edge states in this FSPT phase is that when the $\mathbb{Z}_4$ symmetry is broken, a $\mathbb{Z}_4$ domain wall carries a pair of Majorana zero modes protected by the time-reversal symmetry.

While in principle one can study edge states using the exactly-solvable lattice model, in practice such models are complicated to work with (see for example [32] and [98]). In this work we adopt a different approach, ultilizing the connection between SPT phases with internal symmetry and those with crystalline symmetry with the same group structure.

2.2.2 Correspondence with crystalline SPT phases

The one-to-one correspondence between SPT phases with internal and crystalline symmetries was observed in many examples, and recently formalized in [106]. We provide a heuristic explanation for why this is true, and refer the interested reader to [106] for a more systematic approach.

Suppose that the low-energy physics of a system of interest can be described by a continuum field theory. It is very common that the continuum field theory enjoys a larger symmetry than the microscopic Hamiltonian, for example discrete lattice translations enhanced to continuous ones. A discrete lattice translation operation is implemented on the fields by the corresponding (actually continuous) one, possibly

combined with an internal transformation. However, since the continuous translation itself is a symmetry, the purely internal part of the transformation must be a symmetry of the field theory as well. In other words, one can extract the "internal" action of the lattice translation by simply dropping the coordinate shift. Thus a crystalline symmetry becomes effectively an internal one within the field-theoretical description. We thus expect that the classification of SPT phases with a crystalline symmetry group is the same as those with an internal symmetry as long as the group structures are identical [3].

While the equivalence works at the level of topological classifications, technically it is often the case that crystalline SPT phases are easier to understand thanks to the "block state" construction [107, 108, 109, 110]. For example, consider 2D SPT phases protected by $\mathbb{Z} \times G$ where $\mathbb{Z}$ is lattice translation along the y direction and G is an on-site symmetry group. Besides those SPT phases protected by G alone, the rest can all be constructed by stacking 1D states protected by G, i.e. there is a 1D SPT state 'per unit length' along y.

This argument applies to boundary theories as well. An edge along the same direction preserves the translation (as well as all the internal symmetries). In this construction, the edge is nothing but a chain of end states of the 1D SPT phase which builds up the bulk, and each site transforms projectively under the internal symmetry (i.e. $\mathbb{Z}_2^f \times \mathbb{Z}_2^{\mathsf{T}}$). We will study an exactly solvable lattice model of this edge, and in particular a critical point described by a (1+1)d Luttinger liquid,

[3] For point-group operations on fermions, additional subtleties occur relating to how the symmetry group is extended by the fermion parity symmetry [99], but this subtlety is not relevant for the kind of symmetry we are interested in.

which is invariant under continuous translations. One can then derive the symmetry transformations on the low-energy degrees of freedom and extract the "on-site" part of the transformations. We will show that if the 1D building block of the bulk state is chosen to be the $\nu = 2$ 1D FSPT phase, the resulting edge field theory has all the features expected for the edge of an intrinsically interacting FSPT phase with $\mathbb{Z}_4 \times \mathbb{Z}_2^{\mathsf{T}}$, and the lattice translation is identified with the $\mathbb{Z}_4$ (namely, the "internal" part of the lattice translation has order 4).

Similar methods have been applied to study both bulk and boundary physics of interacting SPT phases in 3D [99, 111, 112].

2.3 The Microscopic Model

We consider a 2D weak topological superconductor, where the bulk is an array of 1D wires in the BDI class. Looking at the edge, we have a 1D chain of Majorana modes:

$$\gamma_i^\dagger = \gamma_i,\ \eta_i^\dagger = \eta_i,\ \gamma_i^2 = \eta_i^2 = 1, i = 1, 2, \ldots, 2N. \tag{2.1}$$

which satisfy the following algebra:

$$\{\gamma_i, \gamma_j\} = \{\eta_i, \eta_j\} = 2\delta_{ij}, \{\gamma_i, \eta_j\} = 0\ \forall\ i, j. \tag{2.2}$$

The time-reversal (TR) symmetry T_r acts as

$$T_r : \begin{pmatrix} \gamma \\ \eta \\ i \end{pmatrix} \longrightarrow \begin{pmatrix} \gamma \\ \eta \\ -i \end{pmatrix} \tag{2.3}$$

We can then pairwise combine the γ_i and η_i into a complex fermion

$$\psi_j = \frac{\gamma_j + i\eta_j}{2}, \tag{2.4}$$

with canonical commutation relation $\{\psi_i, \psi_j^\dagger\} = \delta_{ij}, \{\psi_i, \psi_j\} = 0$. TR symmetry then becomes an anti-unitary particle-hole transformation:

$$T_r : \psi_j \to \psi_j^\dagger. \tag{2.5}$$

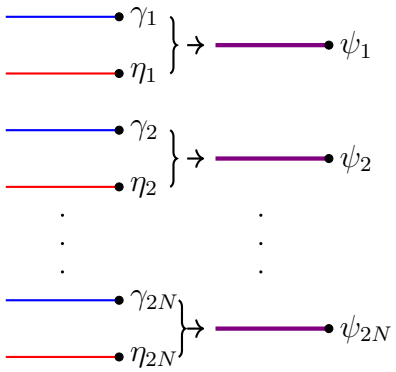

Figure 2.1: Combining $4N$ Majorana edge modes, pairwise, to form $2N$ physical fermions.

It is straightforward to check that any Hamiltonian quadratic in $\psi_i, \psi_j^\dagger$ is not allowed as it breaks TR symmetry. This also follows from the $\mathbb{Z}$ classification of non-interacting Hamiltonians in BDI class in 1D. Any Hamiltonian we write down then

must be interacting. With interactions, it is known that the classification is reduced to $\mathbb{Z}_8$, i.e. eight Majorana zero modes can be gapped out by quartic interactions without spontaneously breaking the TR-symmetry. For the BDI chain, this gapping mechanism must break translation symmetry as one has to group four sites together. In other words, if one is to find a gapped phase without breaking the TR symmetry, the unit cell must be enlarged at least four times.

To explore the possible phases that can occur on edge, we consider the following TR-invariant Hamiltonian for the boundary chain:

$$H = -\sum_i \left(t\psi_{i+1}^\dagger \psi_{i-1} + \Delta\psi_{i+1}\psi_{i-1} + \text{h.c.}\right)\left(2\psi_i^\dagger\psi_i - 1\right). \tag{2.6}$$

For simplicity we assume both t and Δ are real in the following. The model possesses translation symmetry; on our physical fermions translation in the transverse direction acts as $T_t : \psi_i \to \psi_{i+1}$. We will consider closing the chain into a ring with periodic boundary conditions (PBC) (i.e. $\psi_{2N+1} = \psi_1$).

This model is exactly solvable. Employing a Jordan-Wigner (JW) transformation twice we can effectively split the chain in two (even sites and odd sites). One can then think of the model as two copies of a p-wave superconductor, with the caveat that the JW transformation maps a physical fermion to a non-local object in the "free" fermions.

2.3.1 Jordan-Wigner transformation

Recall the JW mapping:

$$\psi_i = \left(\prod_{j=1}^{i-1} \tau_j^z \right) \tau_i^- . \tag{2.7}$$

Here $\tau^{x,y,z}$ are Pauli matrices. There is some subtlety involving the the BC conditions of the chains which we will address in a separate section. As an example of the fermion-spin mapping, away from the boundary site one finds

$$\psi_{i+1}^\dagger \psi_{i-1} (2\psi_i^\dagger \psi_i - 1) = \tau_{i+1}^+ \tau_{i-1}^- . \tag{2.8}$$

Note that we only have next to nearest neighbor interactions. This will be the case for all the other terms in the Hamiltonian as well. Carrying out the JW mapping on the other terms one arrives at

$$H = -\sum_i \left(t\tau_{i+1}^+ \tau_{i-1}^- + \Delta \tau_{i+1}^- \tau_{i-1}^- + \text{h.c.} \right). \tag{2.9}$$

With only next-nearest-neighbor couplings, the Hamiltonian decomposes into two decoupled ones on even and odd sites, respectively. We can further JW transform the two sets (even site and odd site) of spin degrees of freedom resulting in two species of JW fermions. Given the partitioning of the sites into even and odd it makes sense to make this explicit in our notation. Let

$$\tilde{f}_j = \psi_{2j-1}, \quad f_j = \psi_{2j}. \tag{2.10}$$

We will refer to ψ_i (as well as $f_j, \tilde{f}_j$) as physical fermions since they are local operators in the original theory. We will similarly define

$$\sigma_j = \tau_{2j}, \tilde{\sigma}_j = \tau_{2j-1}. \tag{2.11}$$

For later reference, we give the explicit expressions of the JW fermions c in terms of the physical fermions f:

$$c_n = \prod_{j=1}^{n} (-1)^{\tilde{f}_j^\dagger \tilde{f}_j} f_n, \quad \tilde{c}_n = \prod_{j=1}^{n-1} (-1)^{f_j^\dagger f_j} \tilde{f}_n \tag{2.12}$$

Note that on a given chain our JW fermions do have fermionic statistics but JW fermions from different chains actually commute: $[c_m, \tilde{c}_n] = 0 = [c_m, \tilde{c}_n^\dagger]$.

The Hamiltonian becomes

$$H = \sum_j \big(- t c_{j+1}^\dagger c_j + \Delta c_{j+1} c_j + \text{h.c.} \big) + (c \to \tilde{c}) \tag{2.13}$$

2.3.2 Boundary conditions

Define the parity operator

$$P = \prod_{i=1}^{2N} \tau_i^z = \prod_{j}^{N} (1 - 2\tilde{f}_j^\dagger \tilde{f}_j)(1 - 2 f_j^\dagger f_j). \tag{2.14}$$

We can similarly define the parity of the even and odd site chains

$$P_1 = \prod_{j=1}^{N}(1 - 2\tilde{f}_j^\dagger \tilde{f}_j),\ P_2 = \prod_{j=1}^{N}(1 - 2f_j^\dagger f_j) \tag{2.15}$$

Note P, P_1 and P_2 all commute with H. Let μ_f and μ_b denote the boundary conditions on the physical fermions and the JW spin degrees of freedom, respectively. Recall that we are assuming a PBC in the fermionic variables so $\mu_f = 1$. Consider one of the boundary terms of our original H:

$$\begin{aligned}
\tilde{f}_{N+1}^\dagger \tilde{f}_N = \mu_f \tilde{f}_1^\dagger \tilde{f}_N &= \mu_f \tau_1^+ \prod_{i=1}^{2N-2} \tau_i^z \tau_{2N-1}^- \\
&= \tau_{2N+1}^+ P \prod_{i=1}^{2N-2} \tau_i^z \tau_{2N-1}^- \\
&= -\mu_b P \tau_1^+ \prod_{i=1}^{2N-2} \tau_i^z \tau_{2N-1}^-
\end{aligned} \tag{2.16}$$

Therefore we have

$$\mu_f = -\mu_b P. \tag{2.17}$$

When we split the spin chain in two(even sites and odd sites), the resultant chains clearly inherit the same BC, that is $\mu_{b_1} = \mu_b = \mu_{b_2}$, where μ_{b_i} is the BC of the spin degrees of freedom on chain i.

Denote the BCs for the JW operators $\tilde{c}$ and c by μ_{f_1} and μ_{f_2}. Then a similar argument shows

$$\mu_{f_i} = -P_i \mu_{b_i} = -P_i \mu_b = P_i P \mu_f \tag{2.18}$$

so $\mu_{f_1} = P_2 \mu_f$ and $\mu_{f_2} = P_1 \mu_f$. We have imposed a PBC on the physical fermions f

$(\mu_f = 1)$ thus;

$$\mu_{f_1} = P_2 \text{ and } \mu_{f_2} = P_1 \ . \tag{2.19}$$

Note we can divide up our Hilbert space into four parity sectors $(P_1, P_2) = (\pm 1. \pm 1)$ or $(\pm 1, \mp 1)$.

2.4 Phase Diagram: Ising analysis

Since the model is supposed to describe an anomalous edge, the ground state can not be non-degenerate. Due to the one-dimensional nature it is either gapless, or gapped with spontaneous breaking of the symmetries. In this section we analyze the gapped phases of the model Eq. 2.6. After the JW transformation, the Hamiltonian decomposes into two Majorana chains, which are gapped as long as both t and Δ are nonzero. We thus expect that the symmetries must be spontaneously broken. To work out the symmetry breaking properties and gain some intuition about the edge theory, we come back to the spin representation and consider the Ising point: $|t| = |\Delta|$. The behavior at the Ising point should apply to other values of Δ with the same sign since the gap remains open.

Our spin Hamiltonian is

$$H = -\sum_i \left[(\Delta + t)\tau^x_{i-1}\tau^x_{i+1} + (t - \Delta)\tau^y_{i-1}\tau^y_{i+1}\right]. \tag{2.20}$$

We know from the properties of the JW transform on a closed chain that $\mu_b = -P$, this will emerge as the natural choice from the energetics of the ground state as well.

Symmetry transformations of the spin variables can be easily derived:

$$\begin{aligned} T_r &: \tau_i^{\pm} \to (-1)^{i-1}\tau_i^{\mp}, \quad \tau_i^z \to -\tau_i^z, \\ T_t &: \tau_i \to \tau_{i+1}. \end{aligned} \tag{2.21}$$

To diagnose the symmetry breaking, we will work with the order parameter $\tilde{f}_i^\dagger f_i = \tilde{\sigma}_i^+ \tilde{\sigma}_i^z \sigma_i^-$. For a given t we may consider the two Ising points: $\Delta = t$, which corresponds to $H = -2t\sum_i(\sigma_i^x\sigma_{i+1}^x + \tilde{\sigma}_i^x\tilde{\sigma}_{i+1}^x)$, and $\Delta = -t$ which corresponds to $H = -2t\sum_i(\sigma_i^y\sigma_{i+1}^y + \tilde{\sigma}_i^y\tilde{\sigma}_{i+1}^y)$. With regards to the order parameter, we are really working with its projection onto the ground state:

$$\tilde{f}_i^\dagger f_i = \tilde{\sigma}_i^+ \tilde{\sigma}_i^z \sigma_i^- \cong \begin{cases} \tilde{\sigma}_i^x\sigma_i^x, & \Delta = t \\ \\ \tilde{\sigma}_i^y\sigma_i^y, & \Delta = -t \end{cases}. \tag{2.22}$$

where we take $\cong$ to mean equal at the level of projecting onto the ground state space. Consider the transformation properties of the order parameter (and its ground state projection) under T_t and T_r:

$$T_t : \tilde{f}_i^\dagger f_i \to f_i^\dagger \tilde{f}_{i+1} \cong \begin{cases} \sigma_i^x\tilde{\sigma}_{i+1}^x, & \Delta = t \\ \\ \sigma_i^y\tilde{\sigma}_{i+1}^y, & \Delta = -t \end{cases} \tag{2.23}$$

and

$$T_r : \tilde{f}_i^\dagger f_i \to -f_i^\dagger \tilde{f}_i \cong \begin{cases} -\tilde{\sigma}_i^x\sigma_i^x, & \Delta = t \\ \\ -\tilde{\sigma}_i^y\sigma_i^y, & \Delta = -t \end{cases}. \tag{2.24}$$

Below we work out the symmetry breaking properties for the $\Delta = t$ case. From this analysis, it is clear that the symmetry breaking properties of the $\Delta = -t$ case are the same. Flipping the sign of Δ simply rotates between σ^x and σ^y in the Hamiltonian and in the projection of the order parameter on the ground state space. The upshot of this is that that the symmetry breaking of the ground state only depends on the sign of t.

On general grounds, we expect that T_r will always be broken, as an Ising-like Hamiltonian can at most induce translation symmetry breaking with a doubled unit cell. Whether T_t is broken depends on the sign of the coupling t, i.e. ferromagnetic or anti-ferromagnetic. Below we determine the ground state(s) for the different cases of sign of t and even/oddness of N.

2.4.1 N even

Let $t = \Delta$. One can then basically read off the ground states. In each case the spin chains will have PBC; $\mu_B = 1$ means $P = -1$.

$t < 0$

$t < 0$ means we are in a staggered anti-ferromagnetic phase; site i will anti-align with site $i + 2$. Thus we expect that the translation symmetry is broken spontaneously.

Our ground state space will be constructed from the states

$$\{|\uparrow\uparrow\downarrow\downarrow \ldots \downarrow\downarrow\rangle, |\uparrow\downarrow\downarrow\uparrow \ldots \downarrow\uparrow\rangle, |\downarrow\uparrow\uparrow\downarrow \ldots \uparrow\downarrow\rangle, |\downarrow\downarrow\uparrow\uparrow \ldots \uparrow\uparrow\rangle\}. \tag{2.25}$$

Here $|\uparrow\rangle/|\downarrow\rangle$ is the eigenstate of τ^x with eigenvalue $+/-$. The BC-parity relationship can be used to quickly read off the ground state. Note that $P = \prod_i \sigma_i^z$ which, in the x-basis just flips the spin at every site. Since parity is a good quantum number, we have a $d = 2$ ground state space: with basis

$$\begin{aligned} |+\rangle &= |\uparrow\uparrow\downarrow\downarrow \ldots\rangle - |\downarrow\downarrow\uparrow\uparrow \ldots\rangle \\ |-\rangle &= |\uparrow\downarrow\downarrow\uparrow \ldots\rangle - |\downarrow\uparrow\uparrow\downarrow \ldots\rangle \end{aligned} \tag{2.26}$$

with parity eigenvalue -1. Now lets compute expectation values of our order parameter. In the ground states, we find

$$\langle \pm| \tilde{\sigma}_i^x \sigma_i^x |\pm\rangle = \pm 1 = -\langle \pm| \sigma_i^x \tilde{\sigma}_{i+1}^x |\pm\rangle \tag{2.27}$$

Since $\tilde{\sigma}_i^x \sigma_i^x$ is odd under T_r, the TR symmetry is spontaneously broken. From Eq. (2.27) it is also clear that T_t is broken. Therefore, both T_t and T_r are broken, while their product, $T_t T_r$, is preserved.

$t > 0$

Here we are in a staggered ferromagnetic phase. A basis for our ground state, which must have $P = -1$, is

$$\begin{aligned} |+\rangle &= |\uparrow\uparrow\uparrow\uparrow \ldots.\rangle - |\downarrow\downarrow\downarrow\downarrow \ldots..\rangle \\ |-\rangle &= |\uparrow\downarrow\uparrow\downarrow \ldots.\rangle - |\downarrow\uparrow\downarrow\uparrow \ldots..\rangle \end{aligned} \tag{2.28}$$

and we see

$$\langle \pm | \, \tilde{\sigma}_i^x \sigma_i^x \, | \pm \rangle = \pm 1 = \langle \pm | \, \sigma_i^x \tilde{\sigma}_{i+1}^x \, | \pm \rangle \,, \tag{2.29}$$

suggesting T_t is not broken, as one expects.

2.4.2 N odd

$t < 0$

Again we are in a staggered anti-ferromagnetic phase but the oddness of the split chains requires an APBC: Our ground state space will be constructed from the states

$$\{ |\uparrow\uparrow\downarrow\downarrow \, ... \, \uparrow\uparrow\rangle \,, |\uparrow\downarrow\downarrow\uparrow \, ... \, \uparrow\downarrow\rangle \,, |\downarrow\uparrow\uparrow\downarrow \, ... \, \downarrow\uparrow\rangle \,, |\downarrow\downarrow\uparrow\uparrow \, ... \, \downarrow\downarrow\rangle \} \tag{2.30}$$

but now $P = 1$. The $P = 1$ ground state basis is

$$\begin{aligned} |+\rangle &= |\uparrow\uparrow\downarrow\downarrow \, ...\rangle + |\downarrow\downarrow\uparrow\uparrow \, ...\rangle \,, \\ |-\rangle &= |\uparrow\downarrow\downarrow\uparrow \, ...\rangle + |\downarrow\uparrow\uparrow\downarrow \, ...\rangle \,. \end{aligned} \tag{2.31}$$

Checking the order parameter expectation values we see:

$$\begin{aligned} \langle \pm | \, \tilde{\sigma}_i^x \sigma_i^x \, | \pm \rangle &= \pm 1 = - \langle \pm | \, \sigma_i^x \tilde{\sigma}_{i+1}^x \, | \pm \rangle \,, \\ \langle \pm | \, T_r \tilde{\sigma}_i^x \sigma_i^x T_r^{-1} \, | \pm \rangle &= - \langle \pm | \, \tilde{\sigma}_i^x \sigma_i^x \, | \pm \rangle \,. \end{aligned} \tag{2.32}$$

As in the N even case both T_t and T_r are broken, while their product $T_t T_r$ is not.

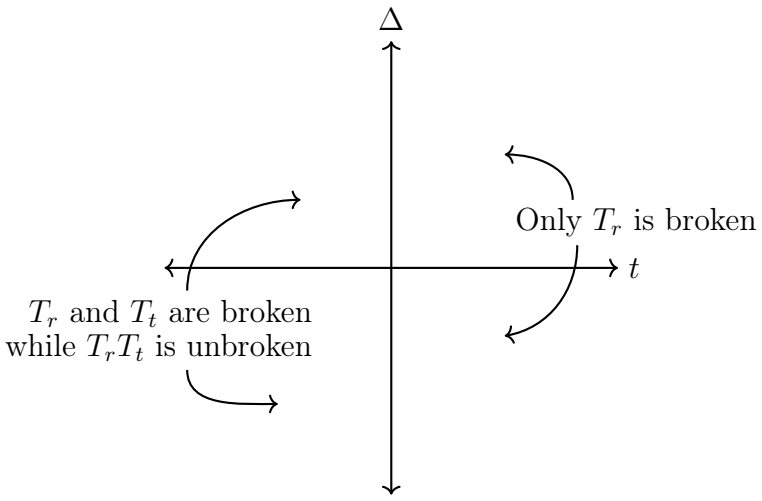

Figure 2.2: Phase diagram of the model Hamiltonian Eq. 2.6. The symmetry breaking pattern only depends on the sign of t..

$t > 0$

This case turns out to be the same as the N even one: only T_r is broken, because of the ferromagnetic coupling.

2.5 Low-energy Field Theory

The model becomes gapless at $\Delta = 0$:

$$H_0 = -t \sum_j (c^\dagger_{j+1} c_j + \text{h.c.}) + (c \to \tilde{c}). \tag{2.33}$$

We will assume $t > 0$. At this point, the Hamiltonian is simply free JW-fermions hopping on the chains and no symmetries are broken. The TR symmetry fixes the chemical potential at 0, i.e. half-filling; so $k_F = \frac{\pi}{2}$. Further interactions can be incorporated by bosonization. However, one must keep in mind that c and $\tilde{c}$ are highly non-local in terms of physical fermions. In the following we will work out the

bosonized theory for this gapless point. Of particular importance is how the low-energy fields transform under the global symmetries, and how physical fermions are represented in the low-energy theory.

2.5.1 Bosonization

Following the standard bosonization prescription, we linearize the spectrum around the two Fermi points $\pm\frac{\pi}{2}$, and define chiral fields:

$$c_{k_F+k} = c_{R,k}, c_{-k_F+k} = c_{L,k} \tag{2.34}$$

where R/L stand for right/left moving. Introduce a continuum field $\psi(x) \sim c_x$, we can write

$$\psi(x) = e^{i\frac{\pi}{2}x}\psi_R(x) + e^{-i\frac{\pi}{2}x}\psi_L(x) \tag{2.35}$$

where the chiral fields are defined as

$$\psi_{R/L}(x) \sim \frac{1}{\sqrt{N}}\sum_k e^{ikx}c_{R/L,k}, \tag{2.36}$$

There is a similar field $\tilde{\psi}$ on the other chain. In the large size limit we see $\{\psi(x), \psi^\dagger(y)\} = 2\pi\delta(x-y) = \{\tilde{\psi}(x), \tilde{\psi}^\dagger(y)\}$ while fields from different chains commute i.e $[\psi(x), \tilde{\psi}(y)] = [\psi(x), \tilde{\psi}^\dagger(y)] = 0$.

Now we can bosonize the fields [71]:

$$\psi_{L/R}(x) \sim e^{i[\theta(x)\pm\phi(x)]} \tag{2.37}$$

where the bosonic fields satisfy the canonical commutation relation $[\phi(x), \partial_y\theta(y)] = i\pi\delta(x-y)$. $\tilde{\theta}, \tilde{\phi}$ are similarly defined. Note that in our definition ϕ, θ and $\tilde{\phi}, \tilde{\theta}$ commute, reflecting the fact that our JW fermions from different chains commute. Anti-commutation between ψ and $\tilde{\psi}$ can be re-enforced by introducing Klein factors, but they are not necessary for our purpose. The non-interacting Hamiltonian can be expressed in terms of the bosonic fields $\Phi = (\phi, \theta, \tilde{\phi}, \tilde{\theta})^T$:

$$H = \frac{v}{2\pi}\int dx\,[(\partial_x\phi)^2 + (\partial_x\theta)^2] + \frac{v}{2\pi}\int dx\,[(\partial_x\tilde{\phi})^2 + (\partial_x\tilde{\theta})^2] \tag{2.38}$$

where $v = ta_0$. The theory is a $c = 2$ Luttinger liquid. The Luttinger parameter is 1 in the free theory, and can be tuned to other values when density-density interactions are included.

While the bosonization is fairly straightforward, an important ingredient of the low-energy theory is how physical electrons are represented, which determine the allowed operator content. In terms of the bosonic fields, physical fermions are given by attaching the JW string to $\psi(x)$ and $\tilde{\psi}(x)$:

$$e^{\pm i\tilde{\phi}\pm\phi\pm\theta}, e^{\pm i\phi\pm\tilde{\phi}\pm\tilde{\theta}}. \tag{2.39}$$

Their combinations give all physical operators. This is a nontrivial requirement, forbiding operators like $\psi^\dagger\tilde{\psi}$. One may understand the constraints as a gauge symmetry, which has important consequences for boundary conditions. One can show that a general vertex operator $e^{i\mathbf{l}^T\Phi}$ is physical if and only if both $l_1+l_2+l_4$ and $l_3+l_2+l_4$ are even integers. Furthermore, if $e^{i\mathbf{l}^T\Phi}$ is a bosonic operator, then $l_1+l_2+l_3+l_4$ must be even, so l_1, l_3 and l_2+l_4 are all even.

2.5.2 Symmetry transformations of Φ

What distinguishes the field theory from an ordinary 1D quantum wire is their anomalous transformation properties under the symmetries. The lattice model has translation whose generator we denote by t, and time-reversal symmetry generated by r. Notice that $r^2 = \mathbb{1}$ and $rt = tr$. In addition, the model also has U(1) charge conservation, but it is not relevant.

From the lattice model (See Appendix 2.7.3 for derivation)

$$T_r : \begin{pmatrix} c_{k,L/R} \\ \tilde{c}_{k,L/R} \end{pmatrix} \to \begin{pmatrix} c^\dagger_{k,R/L} \\ -\tilde{c}^\dagger_{k,R/L} \end{pmatrix}, \tag{2.40}$$

so our fields transform as

$$T_r \begin{pmatrix} \psi_{L/R} \\ \tilde{\psi}_{L/R} \end{pmatrix} \to \begin{pmatrix} \psi^\dagger_{R/L} \\ -\tilde{\psi}^\dagger_{R/L} \end{pmatrix} \Rightarrow T_r : \begin{pmatrix} \phi \\ \theta \\ \tilde{\phi} \\ \tilde{\theta} \end{pmatrix} \to \begin{pmatrix} -\phi \\ \theta \\ -\tilde{\phi} \\ \tilde{\theta}+\pi \end{pmatrix}. \tag{2.41}$$

Our bosonization procedure (definitions of L/R moving fields etc) has assumed $t > 0$ but one can study the $t < 0$ using the same conventions as Sec. 2.5.1 by mapping $t \to -t$ via the unitary transformation $\left(c_i, \tilde{c}_i\right) \to \left((-1)^i c_i, (-1)^i \tilde{c}_i\right)$. Note that boundary terms transform like $c_N^\dagger c_1 \to (-1)^{N-1} c_N^\dagger c_1$. For N odd, we see that the boundary condition is flipped in addition to the sign of t.

With this in mind we can work out the translation transformation properties of Φ given $T_t : \tilde{f}_i \to f_i$ etc. Recall that

$$\begin{aligned} c_i &\sim e^{-i\frac{\pi}{2}x} e^{i(\theta+\phi)} + e^{i\frac{\pi}{2}x} e^{i(\theta-\phi)}, \\ \tilde{c}_i &\sim e^{-i\frac{\pi}{2}x} e^{i(\tilde{\theta}+\tilde{\phi})} + e^{i\frac{\pi}{2}x} e^{i(\tilde{\theta}-\tilde{\phi})}. \end{aligned} \tag{2.42}$$

For $t > 0$, $c_i \to \tilde{c}_{i+1}$ and $\tilde{c}_i \to c_i$ under T_t gives

$$T_t : \begin{pmatrix} \phi \\ \theta \\ \tilde{\phi} \\ \tilde{\theta} \end{pmatrix} \to \begin{pmatrix} \tilde{\phi} - \frac{\pi}{2} \\ \tilde{\theta} \\ \phi \\ \theta \end{pmatrix}. \tag{2.43}$$

For $t < 0$, $c_i \to -\tilde{c}_{i+1}$ and $\tilde{c}_i \to c_i$ giving

$$T_t : \begin{pmatrix} \phi \\ \theta \\ \tilde{\phi} \\ \tilde{\theta} \end{pmatrix} \to \begin{pmatrix} \tilde{\phi} - \frac{\pi}{2} \\ \tilde{\theta} + \pi \\ \phi \\ \theta \end{pmatrix}. \tag{2.44}$$

We have suppressed the coordinate change associated with the translation.

Notice that in all cases we have T_r^2 and T_t^4 acting as the identity on bosonic fields. However, T_r and T_t do not commute when acting on Φ, which seems to contradict the fact that the symmetry group is $\mathbb{Z}_2^{\mathsf{T}} \times \mathbb{Z}_4$. The reason for the inconsistency is because $\phi, \theta, \tilde{\phi}$ and $\tilde{\theta}$ are not local fields. As we will see below, when acting on local degrees of freedom T_t and T_r do represent the group faithfully.

2.5.3 K matrix formulation

We have derived a low-energy theory from the lattice model. Here we discuss an alternative formulation using a K matrix description [113, 114, 115, 116, 117], which has the advantage that only physical degrees of freedom (allowing chiral ones) appear. First we give a brief overview of K matrix theory. A general (chiral or non-chiral) Luttinger liquid is described by the following Lagrangian:

$$\mathcal{L} = \frac{1}{4\pi} \sum_{IJ} K_{IJ} \partial_t \phi_I \partial_x \phi_J - \frac{1}{4\pi} \sum_{IJ} V_{IJ} \partial_x \phi_I \partial_x \phi_J - \cdots \tag{2.45}$$

Here K is a symmetric integer matrix, which determines the commutation relations between fields: $[\phi_I(y), \partial_x \phi_J(x)] = 2\pi i (K^{-1})_{IJ} \delta(y - x)$. Since we are considering an edge of a short-range entangled bulk without fractionalized excitations, we require $\det K = \pm 1$. For such unimodular K matrices, all excitations $e^{i\phi_i}$ are physical. The non-universal V matrix determines velocities of bosonic modes as well as scaling dimensions of operators.

A general symmetry transformation T_g takes the following form

$$T_g^{-1}\phi_I T_g = \sum_j (W_g)_{IJ}\phi_J + (\delta\phi_g)_I. \tag{2.46}$$

To preserve the commutation relations the integer matrix W_g must satisfy

$$W_g K^{-1} W_g^T = \pm K^{-1}, \tag{2.47}$$

$+/-$ for unitary/anti-unitary transformations. In addition, they must obey group multiplication laws: $W_g W_h = W_{gh}$,

The K matrix for a Luttinger liquid is generally not uniquely defined because one can make a change of variable: $\phi_I = \sum_J W_{IJ}\phi'_J$, where W is an invertible integer matrix (i.e. $|\det W| = 1$). For the new fields, the K matrix becomes $\tilde{K}' = W^T K W$, and

$$W'_g = W^{-1} W_g W, \delta\phi'_g = W^{-1}\delta\phi_g. \tag{2.48}$$

To obtain such a description, we first find a basis for local operators in the theory. They can be chosen as $\phi_I = \mathbf{l}_I^T \Phi$ with

$$\begin{aligned} \mathbf{l}_1 &= (1,1,1,0), \\ \mathbf{l}_2 &= (1,0,1,1), \\ \mathbf{l}_3 &= (-1,1,1,0), \\ \mathbf{l}_4 &= (1,0,-1,1). \end{aligned} \tag{2.49}$$

Their commutation relations are given by the following K matrix:

$$K = \begin{pmatrix} 1 & -1 & 0 & 1 \\ -1 & 1 & 1 & 0 \\ 0 & 1 & -1 & -1 \\ 1 & 0 & -1 & -1 \end{pmatrix}. \tag{2.50}$$

Symmetry properties can be readily obtained from Eq. (2.41) and (2.43). We find that under TR symmetry

$$W_r = \begin{pmatrix} 0 & -1 & 1 & 1 \\ -1 & 0 & 1 & 1 \\ 1 & -1 & 0 & 1 \\ -1 & 1 & 1 & 0 \end{pmatrix}, \delta\phi_r = \begin{pmatrix} 0 \\ \pi \\ 0 \\ \pi \end{pmatrix}, \tag{2.51}$$

and under lattice translation:

$$W_t = \begin{pmatrix} 0 & 1 & 0 & 0 \\ 1 & 0 & 0 & 0 \\ 0 & 0 & 0 & 1 \\ 0 & 0 & 1 & 0 \end{pmatrix}, \delta\phi_t = -\frac{\pi}{2} \begin{pmatrix} 1 \\ 1 \\ -1 \\ 1 \end{pmatrix}. \tag{2.52}$$

We can further simplify the K matrix. A change of variables $\phi = W\phi'$ with

$$W = \begin{pmatrix} 1 & 0 & 0 & 0 \\ 1 & 0 & 1 & -1 \\ 0 & 0 & 0 & 1 \\ 1 & 1 & 0 & -1 \end{pmatrix}, \tag{2.53}$$

brings K into the standard diagonal form:

$$W^T K W = \begin{pmatrix} \sigma_z & 0 \\ 0 & \sigma_z \end{pmatrix}. \tag{2.54}$$

This is expected from the general classification of non-chiral, unimodular K matrices.

Using Eq. (2.48) we obtain

$$W'_r = \begin{pmatrix} 0 & 1 & -1 & 1 \\ 1 & 0 & 1 & -1 \\ 1 & 1 & 0 & -1 \\ 1 & 1 & -1 & 0 \end{pmatrix}, \delta\phi'_r = \begin{pmatrix} 0 \\ \pi \\ \pi \\ 0 \end{pmatrix}, \tag{2.55}$$

and

$$W'_t = \begin{pmatrix} 1 & 0 & 1 & -1 \\ 0 & 1 & -1 & 1 \\ 1 & 1 & -1 & 0 \\ 1 & 1 & 0 & -1 \end{pmatrix}, \delta\phi'_t = \frac{\pi}{2} \begin{pmatrix} -1 \\ 1 \\ 1 \\ 1 \end{pmatrix}. \tag{2.56}$$

Using the matrix representations, one can check that $T_r^2 = T_t^4 = \mathbb{1}, T_r T_t = T_t T_r$ and $T_t^2 \neq \mathbb{1}, P$ where P is the global fermion parity, which shows that the symmetry group is indeed $\mathbb{Z}_2^{\mathsf{T}} \times \mathbb{Z}_4$.

While the K matrix now is the same as the one for free fermions, we emphasize that it does not mean the theory is free after the basis transformation, because the symmetry transformations become complicated. For a free theory, we expect that a n-body operator remains n-body under symmetry transformations, which is not the case for W_r' and W_t': for example, they map a 1-body operator to a 3-body one. One can further check that no other basis transformations can bring W_t and W_r into a form expected for a free theory, while keeping K the same.

It is crucial that the K matrix is 4×4, which allows non-trivial transformations such as W_r' and W_t'. We show in the appendix that 2×2 K matrix can not describe such an edge. In fact, we prove that within the K matrix framework, there are no nontrivial fermionic SPT phases with 2×2 K matrix. Therefore the theory found here is in some sense "minimal."

Although we have provided a completely local description of the effective theory, in the following we will still work with the formulation given in Sec. 2.5.2, as it is easier to relate to the lattice model.

2.5.4 Gapped phases in the bosonic field theory

With a complete low-energy gapless theory, we can explore effects of more complicated interactions to understand its stability. Here we first consider the stability with

respect to gapping perturbations of null-vector type [114]. For U(1) bosons, generic local interactions are given by vertex operators of the form $e^{i\mathbf{l}^T\Phi}$, where $\mathbf{l}$ is an integer vector. Given that we are working with non-local variables, additional constraints must be placed on $\mathbf{l}$ to ensure locality, as discussed in Sec. 2.5.1.

In an effort to gap out the theory we can consider adding Higgs terms of the form [114, 115, 62, 97, 116] $\sum_a U_a \cos(\mathbf{l}_a^T\Phi - \alpha_a)$ with $\mathbf{l}_a \in \mathbb{Z}^4$. Restricting our attention to the gapping terms which respect time reversal and translation symmetry provides a verification of the robustness of the gapless edge and the nontrivial symmetry-protected topological order of the bulk. To gap out the edge modes, it is sufficient to choose $\{\mathbf{l}_a\}$ as a set of linearly independent null vectors, namely they satisfy

$$[\mathbf{l}_a^T\Phi, \mathbf{l}_b^T\Phi] = 0 \tag{2.57}$$

for all a, b. Then in the limit of large U_a, all $\mathbf{l}_a^T\Phi$ simultaneously acquire finite expectation values to minimize the cosine potentials. Since there are two conjugate pairs of bosonic fields, two null vectors are needed to freeze all degrees of freedom.

Our basic tactic is the following: consider a set of symmetry-preserving, independent gapping terms $\{\cos(\mathbf{l}_a^T\Phi - \alpha_a)\}$ for a set of null vectors $\mathbf{l}_a$. We then check whether there exists any local, elementary field $\mathbf{v}^T\Phi$ that acquires a finite expectation value in the ground state (meaning that a certain linear combination of $\mathbf{l}_a$'s is a multiple of $\mathbf{v}$). If these fields transform non-trivially under the symmetry transformations, then the ground state spontaneously breaks the symmetry. A more systematic treatment can be found in [14].

Continuum limit of the solvable model

Before considering general gapping terms, let us analyze the continuum limit of the pairing term in the lattice model [118]:

$$\begin{aligned}\sum_j \Delta c_{j+1} c_j + \text{h.c.} &\sim \Delta \int_0^L dx \, [\psi(x+a)\psi(x) + \text{h.c}] \\ &= \Delta \int_0^L dx \, [e^{-i\frac{\pi}{2}} e^{i2\theta(x)} + \text{h.c.}]\end{aligned} \tag{2.58}$$

Here a is the short-distance cutoff.

So the superconducting term $-\Delta(c_{j+1}c_j + \tilde{c}_{j+1}\tilde{c}_j) + \text{h.c.}$ becomes $\Delta(\sin 2\theta + \sin 2\tilde{\theta})$. Without loss of generality, assume $\Delta > 0$. In the large L limit, θ is pinned at the minima of $\Delta \sin 2\theta$, namely $\theta = -\frac{\pi}{4}$ or $\frac{3\pi}{4}$. Recall though that the physical ground states should have definite total fermion parity. One can check that $P_1 = e^{i\int_0^L \partial_x \tilde{\phi}}$ and $P_2 = e^{i\int_0^L \partial_x \phi}$, thus:

$$P = \exp\left(i \int_0^L \partial_x \tilde{\phi} + \partial_x \phi\right) \tag{2.59}$$

From the bosonic commutation relations we see

$$P\theta P^{-1} = \theta + \pi, P\tilde{\theta}P^{-1} = \tilde{\theta} + \pi. \tag{2.60}$$

The Hamiltonian conserves both P_1 and P_2.

We know the parity of our ground state from the lattice model but it is useful to derive it from the field theory. The physical fermion $e^{i(\tilde{\phi}+\phi+\theta)}$ satisfies PBC, which

means

$$\begin{aligned} e^{i[\tilde{\phi}(L)+\phi(L)+\theta(L)]} &= e^{i[\int_0^L \partial_x(\tilde{\phi}+\phi+\theta)+(\tilde{\phi}(0)+\phi(0)+\theta(0))]} \\ &= -e^{i\int_0^L \partial_x(\tilde{\phi}+\phi+\theta)} e^{i[\tilde{\phi}(0)+\phi(0)+\theta(0)]} \end{aligned} \tag{2.61}$$

Because in the ground state manifold θ is pinned, we see that the BC is $-P_1P_2$. Thus we find $P = P_1P_2 = -1$. (For $t > 0$ and odd N, it is the opposite). Similarly we find

$$\begin{aligned} \psi_{L/R}(L) &= -e^{i(\int_0^L dx\partial_x\theta \pm \int_0^L dx\partial_x\phi)}\psi_{L/R}(0) \\ &= -P_2\psi_{L/R}(0), \end{aligned} \tag{2.62}$$

in accordance with the lattice result $c_{N+1} = P_1c_1$.

Now we work out the ground states for the field theory and check the symmetry breaking pattern. For the sake of explicitness consider chain 2. We can form the parity (i.e. P_2) eigenstates $|\pm\rangle_2 = \left|\frac{-\pi}{4}\right\rangle_2 \pm \left|\frac{3\pi}{4}\right\rangle_2$, where $P_2 |\pm\rangle_2 = \pm |\pm\rangle_2$. The analysis of chain 1 is identical. The ground state space of the full chain is spanned by $|\pm\rangle_1 |\pm\rangle_2$, subject to the constraint of a fixed total fermion parity. For $t > 0$, we have shown that $P = -1$, so the two states are $|+\rangle_1 |-\rangle_2$ and $|-\rangle_1 |+\rangle_2$. It is convenient to form the following superpositions:

$$|\pm\rangle = |+\rangle_1 |-\rangle_2 \pm |-\rangle_1 |+\rangle_2 . \tag{2.63}$$

In terms of $\theta, \tilde{\theta}$ eigenstates:

$$\begin{aligned} |+\rangle &= \left|\frac{-\pi}{4}\right\rangle_1 \left|\frac{-\pi}{4}\right\rangle_2 - \left|\frac{3\pi}{4}\right\rangle_1 \left|\frac{3\pi}{4}\right\rangle_2 \\ |-\rangle &= \left|\frac{3\pi}{4}\right\rangle_1 \left|\frac{-\pi}{4}\right\rangle_2 - \left|\frac{-\pi}{4}\right\rangle_1 \left|\frac{3\pi}{4}\right\rangle_2 . \end{aligned} \tag{2.64}$$

Now

$$T_r : (\theta, \tilde{\theta}) \to (\theta, \tilde{\theta} + \pi)$$

meaning $T_r : |\pm\rangle \to -|\mp\rangle$ suggesting T_r is broken.

The symmetry breaking can also be detected by an order parameter. In this case, the order parameter is just $\cos(\theta - \tilde{\theta})$, which is odd under T_r but invariant under T_t. Its expectation value on $|\pm\rangle$ is ± 1. On the other hand, $\sin(\theta - \tilde{\theta})$ is also odd under translation but its expectation value vanishes.

In the lattice theory T_t breaking depended on the sign of t so we should expect the same behavior in the field theory. Recall

$$T_t : (\theta, \tilde{\theta}) \to \begin{cases} (\tilde{\theta}, \theta) & t > 0 \\ \\ (\tilde{\theta} + \pi, \theta) & t < 0 \end{cases} . \tag{2.65}$$

We can see that the field theory reproduces the symmetry breaking properties of the lattice. The same result is seen in the odd case with the small adjustment that in the $t > 0$ case our $P = 1$ ground states are given by $|\pm\rangle = |+\rangle_1 |+\rangle_2 \pm |-\rangle_1 |-\rangle_2$.

General gapping terms

With the above special case worked out we can now consider general gapping terms. We will focus on the $t > 0$ phase and results for the $t < 0$ phase are very similar. Recall how Φ transforms under T_r and T_t:

$$T_t : \begin{pmatrix} \phi \\ \theta \\ \tilde{\phi} \\ \tilde{\theta} \end{pmatrix} \to \begin{pmatrix} \tilde{\phi} + \frac{\pi}{2} \\ \tilde{\theta} \\ \phi \\ \theta \end{pmatrix} \quad \text{and} \quad T_r : \begin{pmatrix} \phi \\ \theta \\ \tilde{\phi} \\ \tilde{\theta} \end{pmatrix} \to \begin{pmatrix} -\phi \\ \theta \\ -\tilde{\phi} \\ \tilde{\theta} + \pi \end{pmatrix}. \tag{2.66}$$

As discussed already, if our goal is to investigate the gapability of the model we need to consider something like $\delta\mathcal{L} = U_1 \cos(\mathbf{l}_1^T\Phi - \alpha_1) + U_2 \cos(\mathbf{l}_2^T\Phi - \alpha_2)$. Verifying that any symmetry-allowed gapping term introduces spontaneous breaking or gapless modes amounts to working through all the allowed cases. We give a proof of the all the cases in Appendix 2.7.4. Here we will show a few examples to demonstrate the approach.

Let us first consider the case in which each gapping term transforms trivially under both of the symmetries:

$$T_g^{-1} \cos(\mathbf{l}^T\Phi - \alpha) T_g = \cos(\mathbf{l}^T\Phi - \alpha), g = t/r. \tag{2.67}$$

let $\mathbf{l}^T = (a, b, c, d)$, then acting with symmetry operators on $\cos(a\phi + b\theta + c\tilde{\phi} + d\tilde{\theta} - \alpha)$ one can derive constraints on the vector $\mathbf{l}$. It follows, via T_t symmetry, that $a = \pm c$ for example. We summarize these constraints in the following table:

Symmetry	Vector constraint	Phase constraint
T_t	$a = \pm c$ and $b = \pm d$	$a \in 4\mathbb{Z}$
T_r	$a, c = 0$ or $b, d = 0$	$d \in 2\mathbb{Z}$

From the table one has gapping terms of the form $\cos\left(4n(\phi \pm \tilde{\phi})\right)$ or $\cos\left(2m(\theta \pm \tilde{\theta})\right)$ which condense. Some fraction of these correspond to physical operators which break T_t and T_r respectively. For example; for $\cos 4n(\phi \pm \tilde{\phi})$, the order parameter $\cos 2(\phi \pm \tilde{\phi})$ has a finite expectation value and breaks translation symmetry.

Now consider the situation in which T_t exchanges the gapping terms and T_r does not. We have an interaction of the form

$$U_1[\cos\left(a\phi + b\theta + c\tilde{\phi} + d\tilde{\theta} - \alpha\right) + \cos\left(c\phi + d\theta + a\tilde{\phi} + b\tilde{\theta} + \frac{a\pi}{2} - \alpha\right)]. \tag{2.68}$$

There are only two Higgs terms so acting with T_t twice must generate a phase of $2n\pi$.

Symmetry	Vector constraint	Phase constraint
T_t		$a + c \in 4\mathbb{Z}$
T_r	$a, c = 0$ or $b, d = 0$	$b, d \in 2\mathbb{Z}$

If $a, c = 0$, because both b and d are even we write $b = 2m, d = 2n$. Then $\delta L \sim \cos\left(2(m\theta + n\tilde{\theta}) - \alpha\right) + \cos\left(2(n\theta + m\tilde{\theta}) - \alpha\right)$. For $m = \pm n$ these two terms collapse into a single one, meaning the edge has a gapless mode. Otherwise, we can combine the two arguments to get $2(m + n)(\theta + \tilde{\theta})$. So there is a symmetry-breaking order parameter $(\theta + \tilde{\theta})$.

If $b, d = 0$ we have a similar scenario: $a + c \in 4\mathbb{Z}$ plus the locality constraint means both a and c are even. If $a = \pm c$ then there is just a single term $\cos[a(\phi \pm \tilde{\phi})]$, and

we require $a \in 4\mathbb{Z}$. As we will show below, translation symmetry is broken by the order parameter $2(\phi + \tilde{\phi})$. For $a \neq \pm c$, we can combine the two arguments to form $(a + c)(\phi + \tilde{\phi})$, which again gives the order parameter $2(\phi + \tilde{\phi})$.

Details of the remaining cases are given in Appendix 2.7.4. It follows that general symmetry allowed gapping terms always lead to spontaneous symmetry breaking. Thus the edge theory describes a non-trivial SPT phase.

2.5.5 The bulk-edge correspondence

Our low-energy edge theory is derived from a microscopic construction of the weak topological superconductor. The connection with the $\mathbb{Z}_4 \times \mathbb{Z}_2^{\mathsf{T}}$ FSPT phase has been somewhat implicit, only established through the general correspondence between topological phases with crsytalline and internal symmetries discussed in Sec. 2.2.2. In this section we directly show that the edge theory captures correctly the anomaly expected for boundary states of the $\mathbb{Z}_4 \times \mathbb{Z}_2^{\mathsf{T}}$ FSPT phase. We provide two arguments for the bulk-edge correspondence. The arguments also provide evidence for stability of the gapless edge against the most general types of perturbations beyond those of null-vector type, since it is known that gapping terms which do not obey null-vector conditions can still open a gap [119, 120].

Domain wall structure

As reviewed in Sec 2.2, the ground state wavefunction of a $\mathbb{Z}_4 \times \mathbb{Z}_2^{\mathsf{T}}$ fermionic SPT phase can be understood using a decorated domain wall picture. While in the bulk domain walls are closed, they can terminate on the edge and a fermionic zero mode

appears at the end point due to the decoration. This can be taken as a defining feature of the edge states: a $\mathbb{Z}_4$ domain wall binds a fermionic zero mode protected by the $\mathbb{Z}_2^{\mathsf{T}}$ symmetry.

We will now show that the edge theory does have the right domain wall structure. We first construct a gapping term which leads to spontaneous breaking of T_t while preserving T_r. Consider a gapping term $U(\cos 4\phi + \cos 4\tilde{\phi})$, with $U < 0$, which condenses ϕ and $\tilde{\phi}$ at minima of the cosine potential $\frac{\pi m}{2}$ with $m \in \mathbb{Z}$. From the derived conditions on physical operators one can see that 2ϕ and $2\tilde{\phi}$ are physical but ϕ and $\tilde{\phi}$ are not. The T_t symmetry cycles through the ground state space

$$\begin{pmatrix} 2\phi \\ 2\tilde{\phi} \end{pmatrix} : \quad \begin{pmatrix} 0 \\ 0 \end{pmatrix} \xrightarrow{T_t} \begin{pmatrix} \pi \\ 0 \end{pmatrix} \xrightarrow{T_t} \begin{pmatrix} \pi \\ \pi \end{pmatrix} \xrightarrow{T_t} \begin{pmatrix} 2\pi \\ \pi \end{pmatrix} \xrightarrow{T_t} \begin{pmatrix} 0 \\ 0 \end{pmatrix} \tag{2.69}$$

while T_r is unbroken.

Suppose we are in the state (denoted by $|0 \to \pi\rangle$) with a domain wall at x separating the $\begin{pmatrix} 0 \\ 0 \end{pmatrix}$ state (denoted by $|0 \to 0\rangle$) and the $\begin{pmatrix} \pi \\ 0 \end{pmatrix}$ state. Note the following specific bosonic commutation relation

$$e^{\pm i\frac{\theta(y)}{2}} 2\phi(x) e^{\mp i\frac{\theta(y)}{2}} = 2\phi(x) + \begin{cases} \pm\pi & 0 < x < y \\ 0 & x > y \end{cases}. \tag{2.70}$$

We can create the domain wall configuration from a uniform ground state in two

ways: two states

$$|0 \to \pi\rangle_{\pm} = e^{\pm i \frac{\theta(x)}{2}} |0 \to 0\rangle \tag{2.71}$$

are degenerate since they are related by the TR transformation. They have the same domain wall at x, separating the $\begin{pmatrix} 0 \\ \\ 0 \end{pmatrix}$ and $\begin{pmatrix} \pi \\ \\ 0 \end{pmatrix}$ states, but differ in local properties. Notice that while $e^{i\theta(x)/2}$ is non-local, in a closed system one always creates domain walls in pairs by applying $\exp\left[\frac{i}{2}\int_{x_0}^{x_1} \partial_x \theta dx\right]$, which is a physical string-like operator. If we look at the charge densities, $\rho_{\pm}(y) = \frac{1}{\pi} \langle 0 \to \pi | \, \partial_y \phi(y) \, |0 \to \pi\rangle_{\pm}$, of the two states we see that

$$\rho_+(y) - \rho_-(y) = \delta(y - x). \tag{2.72}$$

.

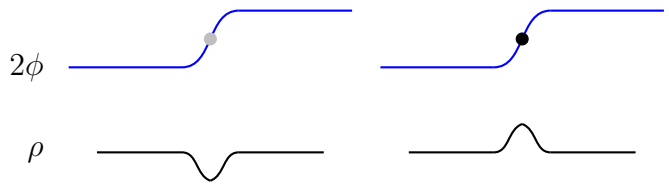

Figure 2.3: Degenerate domain wall states differ in their charge densities..

The degenerate kinked states differ in local charge $\Delta Q = 1$, suggesting the presence of a fermionic zero mode, as the only charge-1 local excitations in our system are physical fermions. In fact, an operator toggling between the two states is $e^{i(\phi+\tilde{\phi}+\theta)}$ (note that ϕ and $\tilde{\phi}$ condense). These two states are related by the TR transformation, protecting the degeneracy.

Gauging fermion parity

An alternative way to characterize the bulk SPT phase is through the symmetry properties of a fermion parity flux. In a nontrivial fermionic SPT phase, a fermion parity flux transforms projectively under the global symmetry group. In [121], a classification of 2D fermionic SPT phases was derived using these ideas. Mathematically, projective representation carried by a fermion parity flux is characterized by a 2-cocycle in $\mathcal{H}^2[G, \mathbb{Z}_2]$, which agrees with the group super-cohomology classification. We briefly summarize these facts about general classification of 2D FSPT phases in Appendix 2.7.1.

We will directly couple the SPT phase to a $\mathbb{Z}_2$ gauge field, sourced by fermions. We will first carry out the gauging construction for the bulk theory. To this end, let us write down a topological field theory for the bulk:

$$\mathcal{L} = \sum_{IJ} \frac{K_{IJ}}{4\pi} a_I \wedge da_J + \cdots \tag{2.73}$$

Here a_I are compact U(1) gauge fields, and the K matrix is given in Eq. (2.54). The same K matrix appears in the bulk Chern-Simons theory and the edge chiral boson theory following from the general bulk-boundary correspondence. da is the fermion current in the bulk. Under symmetries, the gauge field transforms as:

$$T_g : a_I \to \sum_{IJ} (W_g)_{IJ} a_J, \tag{2.74}$$

where W_g is given in Eqs. (2.55) and (2.56).

Now we couple the bulk to a $\mathbb{Z}_2$ gauge field A:

$$\frac{1}{2\pi}(a_1 + a_2 - a_3 - a_4)dA + \frac{1}{\pi}BdA. \tag{2.75}$$

The $\mathbb{Z}_2$ gauge theory is described by the mutual Chern-Simons term $\frac{1}{\pi}BdA$ (corresponding to a K matrix $\begin{pmatrix} 0 & 2 \\ 2 & 0 \end{pmatrix}$. B can be thought of as a Higgs field that Higgs the U(1) gauge structure of A down to $\mathbb{Z}_2$, and it couples to vortex current.

Here we choose $a_1+a_2-a_3-a_4$ because this combination preserves T_t, and under T_r it becomes minus itself. Therefore We let $T_t^{-1}AT_t = A, T_r^{-1}AT_r = A$, and $T_r^{-1}BT_r = -B$. We then integrate out A, which leads to a constraint $a_1 + a_2 - a_3 - a_4 + 2B = 0$. It can be resolved by writing

$$\begin{pmatrix} a_1 \\ a_2 \\ a_3 \\ a_4 \\ B \end{pmatrix} = \begin{pmatrix} 1 & 0 & 0 & 0 \\ -1 & 1 & 0 & 0 \\ 0 & 1 & 1 & 1 \\ 0 & 0 & -1 & 1 \\ 0 & 0 & 0 & -1 \end{pmatrix} \begin{pmatrix} \tilde{a}_1 \\ \tilde{a}_2 \\ \tilde{a}_3 \\ \tilde{a}_4 \end{pmatrix}. \tag{2.76}$$

In fact, one can view the upper 4×4 block as the (non-invertible) similarity transformation between a and $\tilde{a}$. We will denote it by U, with $\det U = 2$. In terms of the new variables

$(\tilde{a}_1, \tilde{a}_2, \tilde{a}_3, \tilde{a}_4)$, the K matrix reads

$$\begin{pmatrix} 0 & 1 & 0 & 0 \\ 1 & 0 & 1 & 1 \\ 0 & 1 & 0 & 2 \\ 0 & 1 & 2 & 0 \end{pmatrix}. \tag{2.77}$$

This K matrix describes a $\mathbb{Z}_2$ topological order, as expected. Symmetry transformations are given by $\tilde{W}_g = U^{-1} W_g U, \delta\tilde{\phi}_g = U^{-1}\delta\phi_g$. The commutator between T_t and T_r acts on the corresponding edge fields as

$$\tilde{\Phi} \to \tilde{\Phi} + \begin{pmatrix} 0 \\ 0 \\ \pi \\ \pi \end{pmatrix}. \tag{2.78}$$

Notice that $e^{i\tilde{\phi}_3}$ are $e^{i\tilde{\phi}_4}$ are the two fermion parity fluxes, so they do transform projectively under T_t and T_r, corresponding to the nontrivial cohomology class in $\mathcal{H}^2[\mathbb{Z}_4 \times \mathbb{Z}_2^{\mathsf{T}}, \mathbb{Z}_2]$. Physically, a fermion parity flux has a two-fold degeneracy protected by the symmetry.

2.6 Summary

In this chapter we find that edge modes of an intrinsically interacting FSPT phase can be described by a Luttinger liquid theory. It is possible that the same is true for

all 2D FSPT phases in the group super-cohomology construction. We have proved that within K matrix theory, 4×4 is the minimal dimension required for the $\mathbb{Z}_4 \times \mathbb{Z}_2^{\mathsf{T}}$ FSPT phase. An interesting question to ask is whether this $c = 2$ edge theory is the "minimal" (as measured by central charge) among all conformal field theories with the quantum anomaly. Another example of interacting 2D FSPT phase was found in Ref. [93], with symmetry group $\mathbb{Z}_4^f \times \mathbb{Z}_4 \times \mathbb{Z}_4$. Here the physics is somewhat different from the example discussed in this work: in the decorated domain wall construction, the state can be obtained by decorating $\mathbb{Z}_4$ domain walls with 1D $\mathbb{Z}_4^f \times \mathbb{Z}_4$ FSPT states. As mentioned in the introduction, the 1D FSPT phase itself can only exist in the presence of strong interactions, so is the 2D phase. It will be very interesting to construct a gapless edge theory for this interacting FSPT phase.

An important open problem is to understand the edge physics of intrinsically interacting FSPT phases beyond group super-cohomology [121, 33, 96]. An example of such phases in 2D arises with $\mathbb{Z}_8 \times \mathbb{Z}_2^{\mathsf{T}}$ symmetry. If the $\mathbb{Z}_8$ symmetry is replaced by translation, the bulk is a stack of Majorana chains, and the edge is a 1D chain with one Majorana per unit cell. The simplest Hamiltonian must involve four-site interactions. An example is the following Hamiltonian studied in [122]:

$$H = g \sum_i \gamma_i \gamma_{i+1} \gamma_{i+3} \gamma_{i+4}. \tag{2.79}$$

Remarkably, such a Hamiltonian is actually integrable [122], and realizes a gapless phase with a dynamical exponent $z = 3/2$. The nature of this phase is not fully understood. An interesting future direction is to construct other gapless theories, in

particular conformal field theories, and develop field-theoretical descriptions.

Intrinsically interacting fermionic SPT phases also exist in three spatial dimensions [95, 33, 96]. Recent works have found general conditions on gapped surface topological order in the group super-cohomology cases [111, 123]. It will be interesting to explore gapless surface theories in these systems.

2.7 Appendix

2.7.1 Group super-cohomology classification

Suppose the symmetry group is $G = \mathbb{Z}_2^f \times G_b$, where G_b denotes the "bosonic" part of the symmetry group. In the group super-cohomology classification, 2D FSPT phases are labeled by a pair (ν, ω) where $[\nu] \in \mathcal{H}^2[G_b, \mathbb{Z}_2]$ and $\omega \in C^3[G_b, \mathrm{U}(1)]$. Here $[\cdot]$ denotes cohomology class. The $\mathbb{Z}_2$-valued 2-cocycle ν's are responsible for all the "intrinsically" FSPT phases. Note that ν needs to satisfy an obstruction-free condition, see Ref. [33] for a recent summary.

There are two ways to understand the physical meaning of ν. First, in a decorated domain wall construction, domain walls are labeled by $\mathbf{g} \in G_b$. At a junction of three domain walls $\mathbf{g}, \mathbf{h}$ and $\mathbf{gh}$, one has a fermion mode whose occupation is determined by ν. Denote $\mathbb{Z}_2$ additively as $\{0, 1\}$, then the occupation number is just $\nu(\mathbf{g}, \mathbf{h})$. Therefore ν determines the complex fermion decoration on domain wall junctions.

Alternatively, let us consider inserting a superconducting vortex into the FSPT phase. More precisely, such a vortex is a π flux for fermions, i.e. a fermion picks up -1

phase factor when moving around the π flux. Since the π flux is not a local object, the symmetry group can be represented projectively on the flux. The projective representation, or more precisely the factor set, is given by $(-1)^{\nu}$.

Let us work this out for $G_b = \mathbb{Z}_4 \times \mathbb{Z}_2^{\mathsf{T}}$. The second cohomology group $\mathcal{H}^2[G_b, \mathbb{Z}_2] = \mathbb{Z}_2$. The nontrivial element of the $\mathbb{Z}_2$ corresponds to a two-dimensional projective representation, on which the generators of $\mathbb{Z}_4$ and $\mathbb{Z}_2^{\mathsf{T}}$ anticommute. In other words, the π flux in the FSPT phase carries this projective representation.

2.7.2 2×2 K matrix

We show that a 2×2 K matrix can not describe the edge. For a non-chiral fermionic system, the K matrix can be fixed to be $K = \sigma^z$. Then it is straightforward to show that the only invertible similarity transformations that leave σ^z invariant are $\mathbb{1}$ and σ^z. Similarly, the only ones that take σ^z to $-\sigma^z$ are σ^x and σ^y.

The time-reversal symmetry squaring to the identity is then implemented by σ^x. Because the $\mathbb{Z}_4$ generator W_t has to commute with both K and the time-reversal transformation, only $W_t = \mathbb{1}$ is allowed. At this point, notice that within 2×2 K matrix, the theory can be realized by free fermions.

We have found that the two symmetry transformations are given by

$$T_r : W_r = \sigma^x, \delta\phi_r = \begin{pmatrix} \alpha \\ \\ -\alpha \end{pmatrix}, \tag{2.80}$$

and

$$T_t : W_t = \mathbb{1}, \delta\phi_t = \frac{\pi}{2} \begin{pmatrix} n_1 \\ \\ n_2 \end{pmatrix}, n_{1,2} \in \{0, 1, 2, 3\}. \tag{2.81}$$

Further requiring $\mathbb{Z}_4$ commuting with T fixes $n_1 = n_2$.

With these transformations, the following perturbation is allowed $\cos(\phi_L - \phi_R - \alpha)$, which fully gaps out the edge without breaking symmetries.

2.7.3 Symmetry actions on various operators

Let us work out how T_r and T_t act on the fermionic operators. From Eq. (2.12) we see

$$\begin{aligned} T_r : c_i &\longrightarrow (-1)^i \prod_{j=1}^{i} (1 - 2\tilde{f}_j^\dagger \tilde{f}_j) f_i^\dagger = (-1)^i c_i^\dagger, \\ T_r : \tilde{c}_i &\longrightarrow (-1)^{i-1} \prod_{j=1}^{i} (1 - 2 f_j^\dagger f_j) \tilde{f}_i^\dagger = (-1)^{i-1} \tilde{c}_i^\dagger. \end{aligned} \tag{2.82}$$

It should be noted also that $T_r : P_i \longrightarrow (-1)^N P_i$. Under translation our physical fermions transform trivially as $f_i \to f_{i+1}$, adapting this to our partitioning of the even and odd sites gives $f_i \to \tilde{f}_{i+1}$ and $\tilde{f}_i \to f_i$ leading to

$$\begin{aligned} T_t : c_i &\to \prod_{j=1}^{i} (1 - 2 f_j^\dagger f_j) \tilde{f}_{j+1} = \tilde{c}_{i+1} \\ T_t : \tilde{c}_i &\to \prod_{j=1}^{i-1} (1 - 2\tilde{f}_{j+1}^\dagger \tilde{f}_{j+1}) f_i = c_i \end{aligned} \tag{2.83}$$

Recalling $c_k = \frac{1}{\sqrt{M}} \sum_{j=1}^{M} e^{-ikj} c_j$ we can use the transformation properties derived

above to see what happens in the momentum basis.

$$T_r : c_k \longrightarrow \frac{1}{\sqrt{N}} \sum_{j=1}^{N} e^{ikj} (-1)^j c_j^\dagger = \frac{1}{\sqrt{N}} \sum_{j=1}^{N} e^{i(k+\pi)j} c_j^\dagger$$
$$= c_{k+\pi}^\dagger$$

Similarly, $T_r : \tilde{c}_k \longrightarrow -\tilde{c}_{k+\pi}^\dagger$. For translation, using 2.83 we see

$$\begin{aligned} T_t : c_k &\longrightarrow \frac{1}{\sqrt{N}} \sum_{j=1}^{N} e^{ikj} \tilde{c}_{j+1} = e^{-ik} \tilde{c}_k \\ T_t : \tilde{c}_k &\longrightarrow \frac{1}{\sqrt{N}} \sum_{j=1}^{N} e^{ikj} c_j = c_k \end{aligned} \tag{2.84}$$

2.7.4 Perturbative stability of the edge theory

Here we give a proof via exhaustion that symmetry allowed Higgs terms push the edge theory away from a trivial phase. If we wish to gap out the system we must have exactly two linearly independent Higgs terms: $\delta\mathcal{L} = U_1 \cos(\mathbf{l}_1^T \Phi - \alpha_1) + U_2 \cos(\mathbf{l}_2^T \Phi - \alpha_2)$. We will focus on the $t > 0$ phase, the proof for the $t < 0$ phase follows in the same way. Recall how Φ transforms under T_r and T_t:

$$T_t : \begin{pmatrix} \phi \\ \theta \\ \tilde{\phi} \\ \tilde{\theta} \end{pmatrix} \to \begin{pmatrix} \tilde{\phi} + \frac{\pi}{2} \\ \tilde{\theta} \\ \phi \\ \theta \end{pmatrix} \quad \text{and} \quad T_r : \begin{pmatrix} \phi \\ \theta \\ \tilde{\phi} \\ \tilde{\theta} \end{pmatrix} \to \begin{pmatrix} -\phi \\ \theta \\ -\tilde{\phi} \\ \tilde{\theta} + \pi \end{pmatrix} \tag{2.85}$$

a particular symmetry may act internally on each Higgs terms or it may exchange them. We will consider all the cases and show in each instance gapless modes or SSB

are present.

No exchange

Consider the case in which each gapping term transforms trivially under both of the symmetries:

$$T_g^{-1} \cos\left(\mathbf{l}^T \Phi - \alpha\right) T_g = \cos\left(\mathbf{l}^T \Phi - \alpha\right), g = t/r. \tag{2.86}$$

let $\mathbf{l}^T = (a, b, c, d)$, then acting with symmetry operators on $\cos\left(a\phi + b\theta + c\tilde{\phi} + d\tilde{\theta} - \alpha\right)$ we arrive at the following constraints:

Symmetry	Vector constraint	Phase constraint
T_t	$a = \pm c$ and $b = \pm d$	$a \in 4\mathbb{Z}$
T_r	$a, c = 0$ or $b, d = 0$	$d \in 2\mathbb{Z}$

If we explicitly consider some specific allowed term we can derive constraints on α (e.g something like $\cos\left(2n(\theta + \tilde{\theta}) - \alpha\right)$ is symmetry allowed for any α but T_t constrains α in a term like $\cos\left(2n(\theta - \tilde{\theta}) - \alpha\right)$ to be $0, \pi$.) but this will not influence the presence of symmetry breaking behavior so we will ignore working these constraints out in general. From the table one has gapping terms of the form $\cos\left(4n(\phi \pm \tilde{\phi})\right)$ or $\cos\left(2m(\theta \pm \tilde{\theta})\right)$ which condense. Some fraction of these correspond to physical operators which break T_t and T_r respectively.

T_r **exchange**

Now consider the case in which time reversal exchanges the two Higgs terms: explicitly this has the form

$$\begin{aligned}\delta L = U_1[&\cos(a\phi + b\theta + c\tilde{\phi} + d\tilde{\theta} - \alpha) \\ &+ (-1)^{d\pi}\cos(-a\phi + b\theta - c\tilde{\phi} + d\tilde{\theta} - \alpha)]\end{aligned} \tag{2.87}$$

Recall that if we are to condense the gapping terms the operators $\mathbf{l}_1^T\Phi, \mathbf{l}_2^T\Phi$ must commute with themselves and with each other. Suppose T_t does not exchange the terms. One can check that the requirement that $\mathbf{l}_i K^{-1}\mathbf{l}_j = 0$ for $i, j = 1, 2$ is met only iff $a = 0$ or $b = 0$. We summarize the constraints in the following table

Symmetry	Vector constraint	Phase constraint
T_t	$a = \pm c$ and $b = \pm d$	$a \in 4\mathbb{Z}$
$\mathbf{l}_i^T K^{-1}\mathbf{l}_j = 0$	$a = 0$ or $b = 0$	

Note now that $T_r^{-1}(\phi \pm \tilde{\phi})T_r \sim a(\phi \pm \tilde{\phi})$ and $T_r^{-1}(\theta \pm \tilde{\theta})T_r \sim b(\theta \pm \tilde{\theta})$. We are back to the previous case.

In the case where T_t exchanges the Higgs terms we get:

Symmetry	Vector constraint	Phase constraint
T_t	$a = \pm c$ and $b = \mp d$	$a \in 4\mathbb{Z}$
$\mathbf{l}_i^T K^{-1}\mathbf{l}_j = 0$	$a = 0$ or $b = 0$	

Again, the two gapping terms turn out to be proportional, and there is a symmetry breaking.

T_t exchanges

Finally, consider the last case in which T_t exchanges the Higgs terms and T_r does not. We have an interaction of the form

$$U_1[\cos(a\phi + b\theta + c\tilde{\phi} + d\tilde{\theta} - \alpha) + \cos(c\phi + d\theta + a\tilde{\phi} + b\tilde{\theta} + \frac{a\pi}{2} - \alpha)] \quad .$$

There are only two Higgs terms so acting with T_t twice must generate a phase of $2n\pi$.

Symmetry	Vector constraint	Phase constraint
T_t		$a + c \in 4\mathbb{Z}$
T_r	$a, c = 0$ or $b, d = 0$	$b, d \in 2\mathbb{Z}$

If $a, c = 0$ then $\delta L \sim \cos(2(n\theta + m\tilde{\theta}) - \alpha) + \cos(2(m\theta + n\tilde{\theta}) - \alpha)$ and there is either a gapless mode (if $n = \pm m$) or a physical fraction of $n\theta + m\tilde{\theta}, m\theta + n\tilde{\theta}$ and/or $(n + m)\theta + (m + n)\tilde{\theta}$ breaks symmetry.

If $b, d = 0$ we have a similar scenario: $a + c \in 4\mathbb{Z}$, together with the locality constraint we find that a, c are both even, and we have the same situation as the $a, c = 0$ case treated just above.

Chapter 3

Fractonic phases in coupled wire models

3.1 Introduction

It is a common belief that gapped phases of quantum many-body systems can be described by topological quantum field theories (TQFT). There is strong evidence to support TQFT-based classifications in one and two spatial dimensions, but in three dimensions, a large family of gapped topological states have been constructed [39, 124, 125, 126, 41, 42], whose properties do not easily fit within the TQFT framework. They all feature quasiparticle excitations with reduced mobility, and sometimes even completely immobile ones. When put on a three torus, these fracton orders exhibit a topological ground state degeneracy (GSD) which, asymptotically, grows exponentially with linear system size.

In searching for the unified structure underlying fracton order, it was realized that

certain (type-I) fracton models can be built from coupling stacks of 2D topological phases [76, 127]. In fact, a simple stack of layers of 2D gapped states already exhibits some of the characteristics of fracton topological order, e.g. size-dependent GSD, quasiparticles with reduced mobility (i.e. they can only move in planes). This observation has inspired more general constructions of fracton topological order [128, 129, 130, 131, 132, 133], as well as shedding light on the precise meaning of fracton phases [134, 135, 136]. More recently, systematic constructions of fracton models from networks of 2D TQFTs (possibly embedded in a 3D TQFT) have been proposed [77, 137, 138], encompassing many existing models including type-II examples. Ref. [77] further conjectured that all 3D gapped phases can be obtained this way.

In this chapter, we explore a different avenue to construct 3D fracton topological phases. The starting point of our construction is an array of 1D quantum wires, each described at low energy by a Luttinger liquid. Couplings between wires are then turned on to lift the extensive degeneracy. This approach is known as a coupled wire construction [60, 61] and has been widely applied to construct explicit models for 2D topological phases (for a recent survey of these applications see Ref. [139]). The advantage of the coupled wire construction is that the correspondence between the bulk topological order and the edge theory can be made very explicit and chiral topological phases arise naturally. While being more general than other exactly solvable models (i.e. string-net models), the construction still remains analytically tractable. The method has previously been applied to 3D systems, however the examples have fallen under TQFT-type topological orders [68, 75].

Here we will systematically study 3D coupled wire constructions. We will find

that the construction can easily give rise to both gapped and gapless phases. In both cases, there can exist gapped fractonic excitations. Notably, these excitations generally have fusion structures distinct from all previously known gapped fracton models: they are labeled by an integer-valued (internal) topological charge, much like electric charges in a gapless U(1) gauge theory, even though the system can be fully gapped. When it is gapped, we will see that the excitations are mobile along the wires (but require a quasi-local string operator), but generally have reduced mobility in the transverse directions. We will demonstrate in a class of examples that all excitations are immobile in the transverse directions, thus exhibiting a new type of lineon topological order.

Similar to the 2D case, the coupled wire construction allows direct access to surface states, at least when the surface is parallel to the wires. The surface states can be described by an infinite-component Luttinger liquid, defined by an infinite K matrix, which would ordinarily correspond to an (infinite-component) Abelian Chern-Simons theory in the bulk. However, the bulk-boundary relation is highly unusual in the gapped lineon phases: in most cases the surface K matrix strongly depends on the orientation of the surface, so in a sense different surfaces can host qualitatively different gapless states.

This chapter is organized as follows: In Sec. 3.2 we provide a systematic overview of the coupled wire construction. We classify excitations in a general coupled wire model, emphasizing the important role of Gaussian fluctuations overlooked in previous studies. A polynomial formalism is introduced for these models which allows for the use of powerful algebraic methods. In Sec. 3.3 we consider a class of models built

from wires hosting of a single Luttinger liquid, which we term the chiral plaquette models. There prove to be both gapped and gapless models within this class. Specific examples of each case are analyzed. In Sec. 3.4 an example with each wire hosting a two-component Luttinger liquid is considered. These "CSS" models are shown to be gapped, with all quasiparticles being lineon. In Appendix 3.6.1 we give a general treatment of 2D coupled wire construction. Appendix 3.6.2 discusses the spectrum of Gaussian fluctuations for 3D coupled wire models. This analysis shows that models which naively appear gapped can actually posses gapless fluctuations. Appendix 3.6.3 gives an algorithm for computing the GSD of these models. In Appendix 3.6.4 we give an algorithm for finding the charge basis of the models. Finally, in Appendix 3.6.5 we prove that all of the excitations of the CSS models of Sec. 3.4 are lineons.

3.2 Coupled wire construction

In this section we lay out the general theory of coupled wire construction. While our focus is on the 3D case, the formalism applies to 2D without much modification and in fact is more tractable there. We provide a detailed account of the general theory in 2D in Appendix 3.6.1.

Consider quantum wires arranged in a square lattice, as illustrated in Fig. 3.1(a). Each wire is described by an M component Luttinger liquid, with a K matrix K_{w}. If the wire is bosonic (fermionic), we take $K_{\mathrm{w}} = \sigma^x \otimes \mathbb{1}_{M\times M}$ ($K_{\mathrm{w}} = \sigma^z \otimes \mathbb{1}_{M\times M}$). The

Lagrangian for one wire is

$$\mathcal{L} = \frac{1}{4\pi}\partial_t \Phi^{\mathsf{T}} K_{\mathrm{w}} \partial_x \Phi - \frac{1}{4\pi}\partial_x \Phi^{\mathsf{T}} V \partial_x \Phi. \tag{3.1}$$

Throughout this paper we choose the wires to extend along the x direction. V is the velocity matrix, which we take to be $V = v\mathbb{1}$ for simplicity. Here Φ denotes the bosonic fields collectively

$$\Phi = (\phi_1, \phi_2, \ldots, \phi_{2M})^{\mathsf{T}}. \tag{3.2}$$

They satisfy canonical commutation relations

$$[\Phi_a(x_1), \partial_{x_2}\Phi_b(x_2)] = 2\pi i (K_{\mathrm{w}}^{-1})_{ab}\delta(x_1 - x_2). \tag{3.3}$$

Since $K_{\mathrm{w}}^{-1} = K_{\mathrm{w}}$, we do not distinguish the two throughout the paper. Denote the bosonic field of the wire at site $\mathbf{r} = (j, k)$ by $\Phi_{\mathbf{r}}(x)$. Bosonic fields on different wires commute. Importantly, all these fields are 2π periodic, which means that local operators in the theory are built out of derivatives of ϕ's, together with vertex operators of the form $e^{i\mathbf{l}^{\mathsf{T}}\Phi_{\mathbf{r}}(x)}$ with $\mathbf{l}$ being an arbitrary integer vector.

We add the following type of interactions to gap out the wires:

$$-U\sum_{\mathbf{r}}\int \mathrm{d}x \sum_{\alpha=1}^{q} \cos\Theta_{\mathbf{r}}^{\alpha}(x),\ U > 0. \tag{3.4}$$

Each of the $\Theta_{\mathbf{r}}^{\alpha}(x)$ is a linear combination of fields at nearby sites, with integer coefficients. We demand that the system is translation-invariant, including the continuous

translation along x and the discrete translations along y and z. We write $\Theta^{\alpha}_{\mathbf{r}}(x) = \sum_{\mathbf{r}'}(\Lambda^{\alpha}_{\mathbf{r}-\mathbf{r}'})^{\mathsf{T}}\Phi_{\mathbf{r}'}(x)$. The gapping terms should satisfy the null conditions [114, 140, 115, 116]:

$$[\Theta^{\alpha}_{\mathbf{r}}(x), \Theta^{\beta}_{\mathbf{r}'}(x')] = 0. \tag{3.5}$$

This guarantees that the each $\Theta^{\alpha}_{\mathbf{r}}$ can be simultaneously frozen out in the large U limit.

Additionally, we demand that $\Theta^{\alpha}_{\mathbf{r}}$ are asymptotically linearly-independent, so there are sufficiently many of them to pin all bosonic fields. More precisely, consider the array of wires with periodic boundary conditions, the total number of independent Θ's should be $MN_w - c$ where N_w is the number of wires, and c is bounded (c may vary with system size). This means that there should be no local linear relations for Θ's, so all possible linear relations involve infinitely many fields in the thermodynamic limit.

We further assume that the gapping terms are "locally primitive," which roughly says there is no local order parameter. More generally, we impose the condition that there exist no nontrivial local fields that commute with all Θ's, except the Θ's themselves and their linear combinations with integer coefficients. This is analogous to the topological order condition for stabilizer codes in qubit systems. Therefore, when U is sufficiently large, the gapping terms freeze all bosonic fields, at least at the classical level.

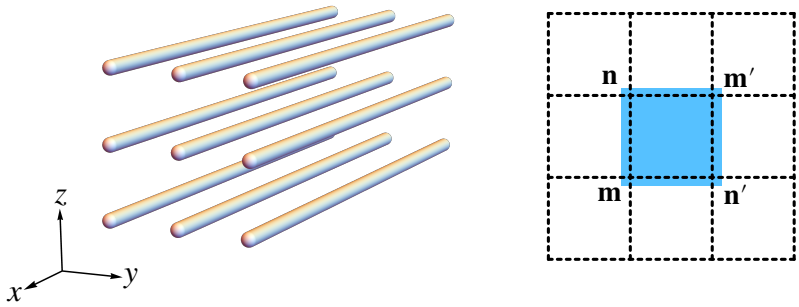

(a) (b)

Figure 3.1: (a) Illustration of the 3D coupled wires construction an (b) the gapping interaction in the chiral plaquette model..

3.2.1 Energy spectrum and excitations

We now give a semi-classical description of the low-energy excitations. In the limit of large U, the cosine potentials pin all $\Theta_{\mathbf{r}}$ at the minima and so the ground state manifold corresponds to the configurations with $\Theta_{\mathbf{r}} \in 2\pi\mathbb{Z}$. Excitations can be classified into the following two types.

The first type of excitations correspond to small oscillations of the fields $\Theta_{\mathbf{r}}$ around the minima. The spectrum of such oscillations can be found by a Gaussian approximation, i.e. $\cos\Theta_{\mathbf{r}} \approx 1 - \frac{1}{2}\Theta_{\mathbf{r}}^2$ at $\Theta_{\mathbf{r}} = 0$ and diagonalizing the resulting quadratic Hamiltonian (more details can be found in Appendix 3.6.2). Physically, these excitations can be interpreted as density waves. We note that the spectrum of such oscillations may be gapless or gapped depending on the form of the gapping interactions. One may wonder whether the conditions on gapping terms listed in the previous section imply that the Gaussian fluctuations are gapped (which might be implicitly assumed in most coupled wire constructions in the literature, where such Gaussian fluctuations were not considered), but this is far from obvious and most likely incorrect.

The other type of excitations are known as "kinks" or "solitons," where some of the fields $\Theta_{\mathbf{r}}$ tunnel from one minima to another. More concretely, for the gapping term $\cos\Theta^l_{\mathbf{r}}(x)$, a n-kink where $n \in \mathbb{Z}$ is a configuration where $\Theta^\alpha_{\mathbf{r}}$ varies by $2\pi n$ over a short distance ξ. Such kink excitations are localized, and may be topologically nontrivial (i.e. cannot be created locally). They represent gapped quasiparticle excitations, which are of most interest to us in this work.

To characterize the quasiparticle excitations, in particular their superselection sectors as well as the mobility, it is important to understand the structure of local excitations, i.e. how local operators act on the ground state.

As mentioned in the previous section, local operators come in two types: spatial derivatives of Φ and vertex operators. First, a local vertex operator $e^{i\mathbf{l}^\mathsf{T}\Phi_{\mathbf{r}}(x_0)}$ acting on the ground state generally creates multiple kinks in the yz plane located at $x = x_0$. From the commutation algebra, one can easily find that a $(\mathbf{l}^\mathsf{T}K_w\Lambda_{\mathbf{r}-\mathbf{r}'})$-kink is created for the $\Theta_{\mathbf{r}'}$ gapping term. It should be clear that such patterns of local creations of kinks determine the mobility of quasiparticles in the yz plane, i.e. the plane perpendicular to the wire direction.

The other type of local operators, namely derivatives of Φ, can be used to transport excitations along the wire direction. In particular, one can construct string operators of the general form

$$\exp\left(i\sum_{\mathbf{r}}\mathbf{w}^\mathsf{T}_{\mathbf{r}}\int_{x_1}^{x_2}\partial_x\Phi_{\mathbf{r}}\right). \tag{3.6}$$

Here $\mathbf{w}_{\mathbf{r}}$ can be real numbers. Without loss of generality, they can be restricted to $[0, 1)$ as the integral part corresponds to a local vertex operator. For Eq. 3.6 to be a

legitimate string operator, it should create allowed kink excitations (of strength $2\pi\mathbb{Z}$) at x_1 and x_2. We further demand that $\mathbf{w_r}$ should be "quasi-localized" in the yz plane, either strictly short-range, or exponentially localized.

For a coupled wire model in two dimensions, under quite general conditions we are able to completely classify superselection sectors (i.e. anyon types) of excitations and show that they are generally given by the determinant group of an integer K matrix determined from the gapping terms. We further show that lattice translations across wires can permute anyon types. Unfortunately for 3D models, we do not have results of similar generality and will have to work case-by-case.

3.2.2 Ground state degeneracy

In the limit of large U, the ground state of the coupled wire model on a torus is obtained by minimizing the gapping potentials $\cos\Theta^\alpha_{\mathbf{r}} = 0$, in other words $\Theta^\alpha_{\mathbf{r}} = 2\pi n^\alpha_{\mathbf{r}}$ where $n^\alpha_{\mathbf{r}} \in \mathbb{Z}$. The 2π-periodicity of the underlying bosonic fields ϕ's induces equivalence relations between different configurations of $\Theta^\alpha_{\mathbf{r}}$. For example, shifting ϕ_i at site $\mathbf{r}$ by 2π leads to the following shifts of n's:

$$n^\alpha_{\mathbf{r}'} \to n^\alpha_{\mathbf{r}} + [K_w \Lambda^\alpha_{\mathbf{r}-\mathbf{r}'}]_i. \tag{3.7}$$

Thus these two configurations are actually equivalent. Physically distinct ground states then correspond to equivalence classes of the integer configurations $\{n^\alpha_{\mathbf{r}}\}$.

A more systematic algorithm to compute the ground state degeneracy is presented in Appendix 3.6.3. The degenerate space is spanned by non-local string operators

running along x and surface operators in the yz plane, referred to as logical operators, and therefore topologically protected as least when the system is fully gapped.

3.2.3 Surface states

With open boundary conditions, generally there exist boundary local fields unconstrained by the bulk gapping terms, which may form gapless surface states. This is most easily seen when the surface is parallel to the wire direction. For such a surface, "free" surface fields can be obtained as "incomplete" gapping terms, which by construction commute with the bulk ones. These incomplete gapping terms however do not commute with each other in general. Denote the corresponding fields on the boundary by $\tilde{\Theta}_n(x)$, where $n \in \mathbb{Z}$ indexes the transverse direction on the surface. Their commutation relation generally should take the form

$$[\tilde{\Theta}_m(x_1), \partial_{x_2}\tilde{\Theta}_n(x_2)] = 2\pi i (K_{\text{surf}})_{mn}\delta(x_1 - x_2). \tag{3.8}$$

Here K_{surf} is an integer symmetric matrix. The algebra is formally equivalent to that of local bosonic fields in a multi-component Luttinger liquid with K_{surf} as the K matrix. As a result, the surface degrees of freedom can be viewed as a 2D extension of a Luttinger liquid. Interestingly, in general K_{surf} depends on the surface orientation, which is a very unusual form of bulk-boundary correspondence.

3.2.4 Polynomial representation

Here we introduce a polynomial representation for the coupled wire construction, inspired by Haah's polynomial formalism for Pauli stabilizer codes [40, 141]. It gives a compact form of the gapping terms and allows applications of powerful algebraic methods.

We denote using y and z, the unit translations along the two directions perpendicular to wires, and by $\bar{y} = y^{-1}, \bar{z} = z^{-1}$, the inverse translations along the same directions respectively. The Hamiltonian can be represented as a $2M \times M$ matrix, where each column represents one Θ^α. Rows of a given column give the Laurent polynomial for the corresponding bosonic field that shows up in Θ^α. More explicitly, suppose $\Lambda^\alpha_{\mathbf{r}\mathbf{r}'} \equiv \Lambda^\alpha_{\mathbf{r}'-\mathbf{r}}$ as required by translation invariance, the p-th row of the column is

$$\sigma_{p\alpha} = \sum_{jk} \Lambda^\alpha_{jk,p} y^j z^k, \tag{3.9}$$

where $1 \leq p \leq 2M, 1 \leq \alpha \leq M$. Following Ref. [40], σ is called a stabilizer map (and each gapping term is a stabilizer).

The null condition can then be summarized as

$$\sigma^\dagger K_{\mathrm{w}} \sigma = 0, \tag{3.10}$$

where $\sigma^\dagger \equiv \bar{\sigma}^{\mathsf{T}}$. This is again reminiscent of Haah's formalism for stabilizer codes, except that now the polynomials have $\mathbb{Z}$ coefficients, instead of $\mathbb{Z}_2$. The other important difference is that K is symmetric, not symplectic.

We also define $\epsilon = \sigma^\dagger K_\mathrm{w}$ as the excitation map. The rows in the excitation map correspond to the different gapping terms. Acting the excitation map on local operators tells the excited gapping terms i.e. the kink excitations. In other words, it is a map between local operators and the kink excitations created by the action of those local operators, hence the name. The null condition in Eq. (3.10) implies $\mathrm{Im}\,\sigma \subset \ker \epsilon$. We further require that $\mathrm{Im}\,\sigma = \ker \epsilon$ on an infinite system, which means that there are no gapless degrees of freedom left, which is the primitive condition discussed previously.

We study two families of stabilizer maps. For the first family, we consider $M = 1$ and $K_\mathrm{w} = \sigma^z$. The stabilizer map is given by:

$$\sigma = \begin{pmatrix} m_1 + n_2 y + n_1 z + m_2 yz \\ \\ m_2 + n_1 y + n_2 z + m_1 yz \end{pmatrix}. \tag{3.11}$$

We refer to these stabilizer maps as chiral plaquette models.

The second general family of models is defined for even M and bosonic wires. We use $M = 2$ as example with $K_\mathrm{w} = \sigma^x$, and denote the two bosonic fields on each wire as ϕ and θ. The stabilizer map is given by

$$\sigma = \begin{pmatrix} f & 0 \\ \\ g & 0 \\ \\ 0 & \bar{g} \\ \\ 0 & -\bar{f} \end{pmatrix}, \tag{3.12}$$

where f and g are finite-degree polynomials of y and z. The Hamiltonian is similar to the "CSS" codes for Pauli stabilizer models, in the sense that one term only involves ϕ and the other only involves θ.

The polynomial formalism, besides providing an economic representation of the Hamiltonian, allows for the use of powerful mathematical tools from the theory of polynomial rings. We use the representation to compute the basis of nontrivial superselection sectors or the "charge basis" of a given model. In other words, the charge basis is defined as the set of quotient equivalence classes of charges modulo trivial charge configuration. A charge configuration is trivial if and only if it can be created out of the ground state (e.g. two charges created by applying a string operator) using a local operator. For conventional topological phases, the charge basis is a finite set. In contrast, a fracton phase necessarily has an infinitely large charge basis. An efficient algorithm to compute the charge basis is described in Appendix 3.6.4 along with the calculation for some models.

3.3 Chiral plaquette models

The chiral plaquette model is illustrated in Fig. 3.1(b). Specifically, the gapping term is given by

$$\Theta_{\mathbf{r}} = \mathbf{m}^{\mathsf{T}}\Phi_{\mathbf{r}} + \mathbf{n}^{\mathsf{T}}\Phi_{\mathbf{r}+\hat{\mathbf{z}}} + [\mathbf{n}']^{\mathsf{T}}\Phi_{\mathbf{r}+\hat{\mathbf{y}}} + [\mathbf{m}']^{\mathsf{T}}\Phi_{\mathbf{r}+\hat{\mathbf{y}}+\hat{\mathbf{z}}}. \tag{3.13}$$

Here we define $\mathbf{m} = (m_1, m_2), \mathbf{n} = (n_1, n_2)$ and $\mathbf{m}' = (m_2, m_1)$, similarly for $\mathbf{n}'$. The components $m_{1,2}, n_{1,2}$ are integers. Using the single wire K matrix $K_{\mathrm{w}} = \sigma^z$, we define a dot product between vectors as $\mathbf{x} \cdot \mathbf{y} = \mathbf{x}^{\mathsf{T}} K_{\mathrm{w}} \mathbf{y}$, for example $\mathbf{m} \cdot \mathbf{m}' = 0$. We also

write $\mathbf{x}^2 = \mathbf{x} \cdot \mathbf{x}$.

In the following we assume $\gcd(m_1, m_2) = \gcd(n_1, n_2) = 1$. We further assume that $\mathbf{m}$ and $\mathbf{n}$ are linearly independent, the same with $\mathbf{m}$ and $\mathbf{n}'$. Equivalently, both $\mathbf{m} \cdot \mathbf{n}'$ and $\mathbf{m} \cdot \mathbf{n}$ must be non-zero.

In Appendix 3.6.2 we find the density wave spectrum

$$E_{\mathbf{k}} = \sqrt{v^2 k_x^2 + vU|f_{\mathbf{k}}|^2}, \tag{3.14}$$

where

$$f_{\mathbf{k}} = m_1 + n_2 e^{ik_y} + n_1 e^{ik_z} + m_2 e^{i(k_y + k_z)}. \tag{3.15}$$

The spectrum is fully gapped if and only if

$$[(m_1 + m_2)^2 - (n_1 + n_2)^2][(m_1 - m_2)^2 - (n_1 - n_2)^2] > 0. \tag{3.16}$$

Otherwise there are gapless points, near which the dispersion is linear.

3.3.1 Surface theory

First we study the surface states. Consider the $(0, 1, 0)$ surface, parallel to the xz plane. The bulk occupies the $y > 0$ region. We follow the general procedure outlined in Sec. 3.2.3 to find the K matrix. At $y = 0$, consider vertex operators supported on two adjacent wires $e^{i(\mathbf{l}_1^\mathsf{T} \Phi_z + \mathbf{l}_2^\mathsf{T} \Phi_{z+1})}$. If they commute with all bulk terms, $\mathbf{l}_1$ and $\mathbf{l}_2$ should satisfy

$$\mathbf{l}_2 \cdot \mathbf{m} = 0, \mathbf{l}_1 \cdot \mathbf{n} = 0, \mathbf{l} \cdot \mathbf{m} + \mathbf{l}_2 \cdot \mathbf{n} = 0. \tag{3.17}$$

We find that the only nonzero solution is $\mathbf{l}_2 = \mathbf{m}', \mathbf{l}_1 = \mathbf{n}'$. Indeed, these terms can be viewed as "half" of a hypothetical plaquette term on the boundary.

Denote $\tilde{\Theta}_z = \mathbf{n}'^{\mathsf{T}}\Phi_{0,z} + \mathbf{m}'^{\mathsf{T}}\Phi_{0,z+1}$. It is not difficult to show that any local vertex operators can be expressed as linear superposition of Φ_z. Therefore they form a basis for local vertex operators. Their commutation relations define the K matrix on the surface, according to Eq. (3.8). The nonzero entries of the K matrix are

$$K_{zz} = \mathbf{m}^2 + \mathbf{n}^2, K_{z,z+1} = \mathbf{m} \cdot \mathbf{n} \tag{3.18}$$

One can similarly find the K matrix on the xy surface. It is easy to see that all one needs to do is to replace $\mathbf{n}$ and $\mathbf{n}'$.

Next we turn to the $(0, 1, 1)$ surface, illustrated in Fig. 3.2(b). Due to the zigzag shape, there are two kinds of vertex operators surviving at low energy, which can again be viewed as "incomplete" plaquette terms, as illustrated in Fig. 3.2(b). The surface K matrix reads:

$$-\begin{pmatrix} \mathbf{m}\cdot\mathbf{n} & \mathbf{m}^2 & \mathbf{m}\cdot\mathbf{n}' & & & \\ & \mathbf{m}\cdot\mathbf{n}' & \mathbf{m}^2 & \mathbf{m}\cdot\mathbf{n} & & \\ & & \mathbf{m}\cdot\mathbf{n} & \mathbf{m}^2 & \mathbf{m}\cdot\mathbf{n}' & \\ & & & \ddots & \ddots & \ddots \end{pmatrix}, \tag{3.19}$$

which is generally distinct from the K matrices on the other surfaces. This example illustrates that in general surfaces of different orientations have very different K matrices.

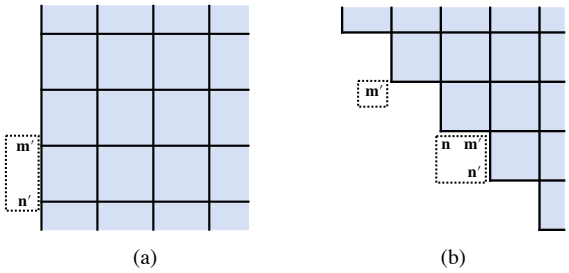

Figure 3.2: Illustrations of surface states, for two different orientations: (a) $(0, 1, 0)$ surface and (b) $(0, 1, 1)$ surface. Representative local vertex operators are shown in dashed boxes..

Since the surfaces are gapless, one may wonder whether they have any instabilities. The stability can be analyzed à la Haldane [114] by attempting to find a complete set of null vectors to gap out the edge, for example. We just point out that in some of our examples, the $(0, 1, 0)$ and $(0, 0, 1)$ surfaces are stable with respect to any local perturbations, and in fact fully chiral (i.e. all modes are moving in the same direction).

3.3.2 Mobility of fundamental kinks

Below we consider the mobility of the most fundamental excitation, a kink on a single plaquette. Following the discussions in Sec. 3.2.1, we first consider mobility in the yz plane, and then mobility along x, the wire direction.

Mobility in the yz plane.

Determining if a quasiparticle is mobile is equivalent to finding a string operator for the excitation. We now show that it is sufficient to consider string operators of a minimal width, i.e. one site. To see this, we consider a string operator of width 2 creating a single plaquette excitation at one end, illustrated by the following figure:

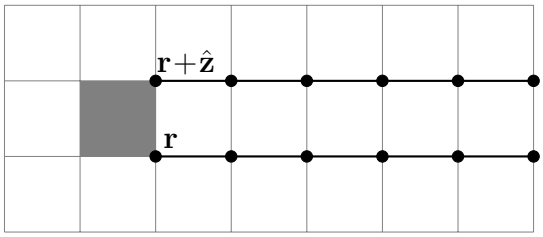

Suppose the operator at the corner site $\mathbf{r}+\hat{\mathbf{z}}$ is $e^{i\mathbf{l}\cdot\Phi_{\mathbf{r}+\hat{\mathbf{z}}}}$. Because it should only excite the plaquette on the bottom left, but not on the top left, we must have $\mathbf{l}\cdot\mathbf{n}'=0$, which means $\mathbf{l}=a\mathbf{n}$ for some $a\in\mathbb{Z}$. We thus multiply the string operator by a stabilizer $e^{-ia\Theta_{\mathbf{r}}}$ to clean the operator at site $\mathbf{r}+\hat{\mathbf{z}}$. This "cleaning" can be repeatedly applied to the other sites on the same line, so now the width is reduced to just 1. It should be clear that a similar argument works when the width is greater than 2.

First we study a string operator directed along z direction, which can be written as

$$\prod_z e^{i\mathbf{l}_z^{\mathrm{T}}\Phi_{yz}} \tag{3.20}$$

where $\mathbf{l}_z$ are integer vectors. If the string commutes with the Hamiltonian, the following conditions must be satisfied:

$$\mathbf{l}_k\cdot\mathbf{m}+\mathbf{l}_{k+1}\cdot\mathbf{n}=0,\mathbf{l}_k\cdot\mathbf{n}'+\mathbf{l}_{k+1}\cdot\mathbf{m}'=0. \tag{3.21}$$

We write $\mathbf{l}_k=a_k\mathbf{m}+b_k\mathbf{n}$, which is always possible when $\mathbf{m}\cdot\mathbf{n}'\neq 0$. The second equation gives $b_{k+1}=a_k$. The first equation gives the following recursion relation

$$a_k(\mathbf{m}^2+\mathbf{n}^2)+(a_{k+1}+b_k)\mathbf{m}\cdot\mathbf{n}=0, \tag{3.22}$$

which can be written as (when $\mathbf{m} \cdot \mathbf{n} \neq 0$)

$$a_{k+1} + \lambda_z a_k + a_{k-1} = 0, \lambda_z = \frac{\mathbf{m}^2 + \mathbf{n}^2}{\mathbf{m} \cdot \mathbf{n}}. \tag{3.23}$$

A general solution can be expressed as powers of the roots of the characteristic polynomial:

$$a_k = A \left(\frac{-\lambda_z + \sqrt{\lambda_z^2 - 4}}{2} \right)^k + B \left(\frac{-\lambda_z - \sqrt{\lambda_z^2 - 4}}{2} \right)^k. \tag{3.24}$$

Here A and B can be fixed by initial conditions of the sequence $\{a_k\}$. Notice that when $|\lambda_z| > 2$, one of the two roots has absolute value greater than 1 and the other smaller than 1, so $|a_k|$ generally grows exponentially with k.

For concreteness, suppose that at the bottom of the string one finds a single kink excitation. This corresponds to the initial condition $\mathbf{l}_1 = \mathbf{m}$, which excites a $(\mathbf{m} \cdot \mathbf{n})$-kink. Thus the whole string is fixed by $a_1 = 1, b_1 = 0$. We can easily find $A = -B = \frac{1}{\sqrt{\lambda_z^2 - 4}}$. The coefficients a_k should all be integers. This is possible only when λ_z is an integer:

1. $|\lambda_z| = 0$: the string repeats with period-4 $\mathbf{m}, \mathbf{n}, -\mathbf{m}, -\mathbf{n}$.

2. $|\lambda_z| = 1$: $\{a_k\}_{k=1}^{\infty}$ is $\{1, -1, 0, 1, -1, 0, 1, \dots\}$ for $\lambda_z = 1$, and $\{1, 1, 0, -1, -1, 0, 1, \dots\}$ for $\lambda_z = -1$.

3. $|\lambda_z| = 2$: then $a_k = (-\operatorname{sgn} \lambda)^{k+1} k$.

4. $|\lambda_z| > 2$: $|a_k|$ grows exponentially.

Only for $\lambda_z = 0, \pm 1$, can the string operator actually move the excitation, at least for appropriate lengths. When $|\lambda_z| \geq 2$, the excitation created at the end of the string operator has a strength growing with the length of the string, thus costing more and more energy as the distance increases. Therefore we conclude that a $(\mathbf{m} \cdot \mathbf{n})$-kink can move along z only when $\lambda_z = 0, \pm 1$.

For the mobility along y, a similar calculation can be done and the ratio $\lambda_y = \frac{-\mathbf{m}^2+\mathbf{n}^2}{\mathbf{m}'\cdot\mathbf{n}}$ determines the mobility (basically $\mathbf{m} \to \mathbf{m}'$).

For certain choices of $\mathbf{m}$ and $\mathbf{n}$, e.g. when $\mathbf{n} = \mathbf{n}'$, it is necessary to consider string operators along the $z = \pm y$ diagonal directions. We study an example of this type below in Sec. 3.3.3.

Mobility along x

We now consider the mobility along the wire direction. As discussed in Sec. 3.2.1, in general kinks can be moved along x with the following string operator:

$$\exp\left(i \sum_{\mathbf{r}} \mathbf{w}_{\mathbf{r}}^{\mathsf{T}} \int_{x_1}^{x_2} \mathrm{d}x \, \partial_x \Phi_{\mathbf{r}}\right), \tag{3.25}$$

where $\mathbf{w}_{\mathbf{r}}$ are real numbers. Locality requires that these $\mathbf{w}_{\mathbf{r}}$ must have a (quasi-)localized profile, i.e. either completely short-range, or decaying exponentially away from the location of the excitation. Below we present a method to construct such a quasi-local string operator, whose profile in the yz plane is strictly short-range in one direction, but only quasi-localized in the other direction. In fact, using a cleaning argument similar to the one in Sec. 3.3.2, one can prove that no string operator of

strictly *finite* support in the yz plane can move a single plaquette excitation in the wire direction, so a string operator, if it exists, must be quasi-localized.

The construction is most easily explained when the system is compactified to a quasi-2D one. Such a process has been used in Ref. [142] to understand properties of fracton models. Without loss of generality, we choose the compactification direction to be z, i.e. a periodic boundary condition is imposed along z. Denote the length of the z direction by L_z. Basically, a whole column of wires at a given y is viewed a "super"-wire, with L_z bosonic degrees of freedom. Denote these fields on one "super"-wire collectively by Φ_y, and we write the gapping Hamiltonian in the following way:

$$-U\sum_{z}\cos(P_z^{\mathsf{T}}\Phi_y + Q_z^{\mathsf{T}}\Phi_{y+1}). \tag{3.26}$$

It is straightforward to read off P_z's from Eq. 3.13. In particular, the K matrix K^{xz} can be expressed as $[K^{xz}]_{zz'} = P_z \cdot P_{z'}$. We consider the following form of string operator:

$$\exp\left(i\sum_{z} u_z \int_{x_1}^{x_2} \mathrm{d}x\, P_z^{\mathsf{T}}\partial_x\Phi_y\right). \tag{3.27}$$

One can prove that it only creates excitations at the y-th "super"-wire. It is shown in Appendix 3.6.1 that to move an elementary excitation located at the $(0, z_0)$ plaquette, we can set

$$u_z = (K^{xz})^{-1}_{zz_0}. \tag{3.28}$$

In order to have a quasi-localized string, u_z must be sufficiently localized. For $|\lambda_z| > 2$,

u_z decays exponentially

$$|(K^{xz})^{-1}_{zz_0}| \sim e^{-|z-z_0|/\xi}, \tag{3.29}$$

where $\xi \sim \cosh^{-1} \frac{|\lambda_z|}{2}$. Because of the exponential decay, the choice of of boundary condition is inessential.

If $|\lambda_z| < 2$, the string operator is at best algebraically localized, and for certain system size the K matrix K^{xz} can become degenerate. Therefore the construction does not yield a quasi-localized string operator for a fundamental, single-plaquette excitation (it is possible that for composite excitations a localized string operator still exists).

In principle, the construction can be applied to compactification along any direction, and a quasi-localized string operator can be defined as long as the corresponding K matrix is "gapped." Here, a gapped K matrix means that the eigenvalues of K are separated from 0 by a finite spectral gap in the infinite size limit. Otherwise the K matrix is said to be gapless. If for any compactification direction the K matrix is gapless, we believe that the bulk must be gapless (i.e. the condition Eq. 3.16 must be violated).

3.3.3 Example of gapped phases

We now consider two examples of the chiral plaquette model with fully gapped bulk. Both examples are not covered by the general discussions in the previous section due to the special choices of $\mathbf{m}$ and $\mathbf{n}$, and in fact turn out to be planon models.

Planon phase I

Consider $\mathbf{m} = (p+1, p), \mathbf{n} = (1, 1)$. One can easily check that the bulk is fully gapped. The K matrix reads

$$[K^{xz}]_{kk'} = (2p+1)\delta_{kk'} + \delta_{k,k'+1} + \delta_{k,k'-1}, \tag{3.30}$$

which is also gapped since $\lambda_z = 2p+1 > 2$. In this model, the 1-kink can move along $y = z$ lines. The string operator is given by

$$\prod_j e^{i(1,1)^{\mathsf{T}}\Phi_{j,j}} \tag{3.31}$$

From the analysis in Sec. 3.3.2, they can also move along the wires, but not along y or z directions. Therefore all excitations are at least planons. We conjecture that there are no fully mobile excitations in this model.

Consistent with the planar structure, since $\mathbf{n}^2 = \mathbf{n}'^2 = 0$, the K matrices on all surfaces different from $(0, 1, -1)$ are actually the same (up to an overall sign). On the other hand, the surface $(0, 1, -1)$ can be made completely gapped: the K matrix becomes

$$[K^{(0,1,-1)}]_{ij} = (p+1)(\delta_{i,j+1} + \delta_{i,j-1}). \tag{3.32}$$

Therefore, boundary fields $\tilde{\Theta}_{2j}, j \in \mathbb{Z}$ mutually commute and form a complete set of

null vectors. The surface can be gapped by the following interactions:

$$-U' \sum_j \int \mathrm{d}x \, \cos \tilde{\Theta}_{2j}(x). \tag{3.33}$$

From these results, it is plausible to conjecture that the model realizes a pure planon phases in the $(0, -1, 1)$ planes. Such a phase can be described by an infinite Chern-Simons theory [50] with a K matrix given in Eq. 3.30. To further check this conjecture, we compute the ground state degeneracy for a $L_y \times L_z$ grid of wires, with periodic boundary condition imposed. We find that

$$\mathrm{GSD}(L_y, L_z) = \begin{cases} 2p+3 & l = 1 \\ \det K^{xz}(l) & l > 1 \end{cases}. \tag{3.34}$$

Here $l = \gcd(L_y, L_z)$ is the number of (effective) 2D planes with this boundary condition, which naturally explains the degeneracy except the special $\gcd(L_y, L_z) = 1$ case.

Planon phase II

Consider $\mathbf{m} = (p, 0), \mathbf{n} = (0, 1)$, with $p > 1$. The bulk is fully gapped according to Eq. 3.16. The surface K matrices can be easily found:

$$[K^{xz}]_{kk'} = (p^2 - 1)\delta_{kk'}, \tag{3.35}$$

and

$$[K^{xy}]_{jj'} = (p^2+1)\delta_{jj'} + (p+1)(\delta_{j,j'+1} + \delta_{j,j'-1}). \tag{3.36}$$

The K matrix on $(0,1,1)$ surface is block diagonalized. Each block is the following 2×2 matrix:

$$\begin{pmatrix} p^2-1 & p-1 \\ p-1 & p^2-1 \end{pmatrix}. \tag{3.37}$$

It is not difficult to see that the kink charge on each plaquette is defined mod p^2-1, namely charge (p^2-1) can be created locally. An elementary 1-kink can move along y, with a period-2 string operator, and the mobility along x is also clear from K^{xz}. We have computed the charge basis in Appendix 3.6.4, and the result, $\{a + bz^{\mu_z} | a, b \in \mathbb{Z}_{p^2-1}\}$, is indeed consistent with our observations here.

The GSD is found to be

$$\begin{cases} (p^2-1)^{L_z} & L_y \text{ is even} \\ (p+1)^{L_z} & L_y \text{ is odd} \end{cases}. \tag{3.38}$$

Note that $(p^2-1)^{L_z} = \det K^{xz}(L_z)$. The reduction for odd L_y can be understood as follows: under T_x, n-kink becomes $-pn$, mod p^2-1. T_x-invariant kinks must satisfy $n \equiv -pn \mod p^2-1$, or n is a multiple of $p-1$, which form a $\mathbb{Z}_{p+1}$ subgroup.

While the degeneracy and the mobility of bulk excitations seem to be compactible with the model describing decoupled xy planes, this picture is inconsistent with the fully chiral surface theory given by Eq. 3.36 in the xy plane (it would be gappable if the decoupled layer picture was correct).

3.3.4 Examples of gapless phases

In this section we study two examples of chiral plaquette model, whose Gaussian fluctuations are gapless. We will analyze the properties of the gapped sectors, and leave the effect of gapless modes for future work.

Gapless fracton phase

Consider $\mathbf{m} = (p, q), \mathbf{n} = (-p, q)$. We assume p and q are coprime, $|p| \neq |q|$ and both nonzero. The Gaussian spectrum is found to be gapless.

It is useful to first give the surface K matrices. For the xz surface, the nonzero elements are

$$[K^{xz}]_{kk} = 2(p^2 - q^2), [K^{xz}]_{k,k+1} = -(p^2 + q^2). \tag{3.39}$$

For the xy surface:

$$[K^{xy}]_{kk} = \mathbf{m}^2 - \mathbf{n}^2 = 0, [K^{xy}]_{k,k+1} = \mathbf{m} \cdot \mathbf{n}' = 2pq. \tag{3.40}$$

Similar to the K matrix in Eq. 3.32, the xy surface can be fully gapped.

One can easily see, from previous discussions that a 1-kink is immobile in the yz plane (a $2pq$-kink can move along y). Since both surface K matrices have $|\lambda| < 2$, the construction in Sec. 3.3.2 fails to produce a quasi-localized string operator (only an algebraically-localizedd one). As mentioned in Sec. 3.3.2, since $(p, q) = 1$ no string operator of bounded support in the yz plane can move this excitation. With this body of evidence we conjecture that the 1-kinks are fractons. As we show below, they

can be created at corners of a rectangular sheet operator in the yz plane.

The GSD has interesting dependence on L_y and L_z. We will specfically consider the case when $p+q$ is odd an L_z is even, to illustrate the physics. From numerical computations we find the GSD is given by the following formula:

$$\text{GSD} = \begin{cases} 2 \cdot (2pq)^{L_y} & L_y \text{ is odd} \\ (2pq)^{L_y - 1} |\det \tilde{K}^{xz}| & L_y \equiv 0 \,(\text{mod } 4) \cdot \\ 4 \cdot (2pq)^{L_y} & L_y \equiv 2 \,(\text{mod } 4) \end{cases} \tag{3.41}$$

An interesting feature of the GSD is that when L_y is a multiple of 4, the additional factor $|\det \tilde{K}^{xz}|$ appears in the GSD. Here $\tilde{K}^{xz}$ will be defined below, but it is related to K^{xz} by an order one factor, and grows exponentially with L_z. We will now explain the exponential factor $(2pq)^{L_y}$ as well as the dependence on $L_y \bmod 4$. We note that the odd L_z case has a similar L_y dependence.

xz planons. The exponential dependence on L_y can be understood in terms of planons in the xz plane. These excitations take the form of two 1-kinks $\mathbf{1}_{y,z}\mathbf{1}_{y+2,z}$. Here we label plaquettes by the coordinate of the down-left corner.

First we show that $\mathbf{1}_{y,z}\mathbf{1}_{y+2,z}$ can move along z. We explicitly construct the string operator. Place the two kinks at $(0,0)$ and $(2,0)$, and the string is supported on $y=1$ and $y=2$:

$$\prod_{k \geq 1} e^{i(\mathbf{x}_k^\intercal \Phi_{1,k} + \mathbf{y}_k^\intercal \Phi_{2,k})}, \tag{3.42}$$

where

$$\mathbf{y}_k = i\sigma^y \mathbf{x}_k, \mathbf{x}_{k+1} = -\sigma^z \mathbf{x}_k, \mathbf{y}_{k+1} = \sigma^z \mathbf{y}_k. \tag{3.43}$$

It is straightforward to check that the string operator commtes with the gapping terms. The initial condition $\mathbf{x}_1 = (a, b)$ should satisfy $qa - pb = 1$, which is always solvable over $\mathbb{Z}$ if $(p, q) = 1$. We notice that the string operator has period-2 along z.

Furthermore one can show that $(2pq)_{y,z}(2pq)_{y+2,z}$ is a local excitation. This should be evident from the following figure:

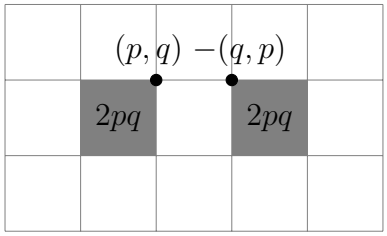

Here (a, b) denotes a vertex operator $e^{i(a\phi_1 + b\phi_2)}$. Thus these planons satisfy $\mathbb{Z}_{2pq}$ fusion rules. This construction also immediately shows that $\mathbf{1}_{y,z}\mathbf{1}_{y+2,z}$ can move along the x direction.

From now on we refer to $\mathbf{1}_{y-1,z}\mathbf{1}_{y+1,z}$ as the y-th planon. From the string operators one can easily determine the braiding statistics of these planons. We find that they are all bosons, and there is a $e^{\frac{i\pi}{pq}}$ mutual braiding phase between neighboring planons.

We note that with the planon string operators can be easily extended to a rectangular sheet operator that creates four 1-kinks on the corners, similar to what happens in the X-cube model.

Compactification. To understand the L_y dependence of the GSD, it is useful to consider compactification along z. Closed string operators wrapping around the z cycle for the xz planons become local order parameters, which must be fixed under

compactification. We give their explicit expressions:

$$W_{1y} = \frac{1}{2q}\sum_z \Theta_{y,z}, W_{2y} = \frac{1}{2p}\sum_z (-1)^z \Theta_{y,z}. \tag{3.44}$$

We may view W_1 as moving the planon q, q around the z cycle, and W_2 as moving the $-p, -p$ planon. Notice that these two string operators are not totally independent, due to the relation $qW_{1y}+pW_{2y} \equiv 0$ (mod local stabilizers). Diagonalizing these order parameters, the theory is partitioned into different sectors labeled by eigenvalues of W_{1y} and W_{2y}. They naturally form a $\mathbb{Z}_{2q} \times \mathbb{Z}_{2p}$ group. We now prove that with the additional condition it is in fact $\mathbb{Z}_{2pq}$. In fact, consider the element $(1, 1)$, whose order is obviously $2pq$. Now for a general element (a, b) in $\mathbb{Z}_{2q} \times \mathbb{Z}_{2p}$, we look for an integer n such that $n \equiv a \mod 2q, n \equiv b \mod 2p$. In other words, there must exist $x_1, x_2 \in \mathbb{Z}$ such that $n = a + 2qx_1 = b + 2px_2$, or $a - b = 2(px_2 - qx_1)$. Since $a + b$ is even and $(p, q) = 1$, one can always find x_1 and x_2 to satisfy this equation.

In this compactified system, we have to fix the local "order parameters," which are generated by W_{1y} and W_{2y} when summing over all z. In analyzing the quasi-2D system, it is convenient to just add another term $-\cos W_{1y}$ or $-\cos W_{2y}$. For simplicity, consider $p = 1$, then we just need to add $-\cos W_1$. A linearly independent set of gapping terms are $W_{1y}, \Theta_{y,z}, z = 1, 2, \cdots, L_z - 1$. With this choice of gapping vectors, the local degeneracy is completely removed. We denote the new K matrix computed from this set of gapping vectors as $\tilde{K}^{xz}$.

The GSD of the compactified system reads:

$$\begin{cases} 2 & L_y \text{ is odd} \\ |\det \tilde{K}^{xz}| & L_y \equiv 0 \,(\text{mod } 4) \\ 4 & L_y \equiv 2 \,(\text{mod } 4) \end{cases}, \tag{3.45}$$

which almost replicates the L_y dependence of the GSD in Eq. 3.41, up to a factor of $2pq$ when L_y is a multiple of 4 due to an additional relation among the compactified planon string operators.

The L_y dependence here can be traced to the y-translation symmetry action on anyons in the compactified system. It turns out that $|\det \tilde{K}^{xz}|$ is always a perfect square, so denote $M = \sqrt{|\det \tilde{K}^{xz}|}$. The fusion group of Abelian anyons turns out to be $\mathbb{Z}_M^2$. Denote the unit translation action on anyons by T_y. We show quite generally that $T_y^2 = -\mathbb{1}$ (i.e. the charge conjugation).

If we choose the basis to be $(1, 0, \ldots, 0)$ and $(0, 0, \ldots, 1)$, we have numerically found that the translation action along y is given by the following $\mathrm{SL}(2, \mathbb{Z})$ matrix:

$$T_y = \begin{pmatrix} 2 & -5 \\ 1 & -2 \end{pmatrix}, \tag{3.46}$$

which satisfies $T_y^2 = -\mathbb{1}$, so T_y is order-4. The only order-4 element for $\mathrm{SL}(2, \mathbb{Z})$ is in fact the S matrix, so T_y is in the same conjugacy class. We assume that a basis transformation has been done to make $T_y = \begin{pmatrix} 0 & -1 \\ 1 & 0 \end{pmatrix}$. For odd L_y, the only anyon

invariant under $T_y^{L_y}$ is $(\frac{M}{2}, \frac{M}{2})$. For $L_y \equiv 2 \,(\mathrm{mod}\, 4)$, the $\mathbb{Z}_2^2$ group generated by $(\frac{M}{2}, 0)$ and $(0, \frac{M}{2})$ is invariant under $T_y^{L_y}$. When L_y is a multiple of 4, all anyons are invariant. The number of $T_y^{L_y}$-invariant anyons gives the GSD of the compactified system [121].

Gapless planon phase

Consider the following gapless model inspired by the construction in Ref. [61]. Let $\mathbf{m} = (\frac{1-q}{2}, \frac{1+q}{2})$ and $\mathbf{n} = (q, -q)$ where q is odd. We choose a slightly different stabilizer map which corresponds to flipping the sign of the top-right and bottom-right corner terms in the plaquette of the chiral plaquette model:

$$\sigma = \begin{pmatrix} m_1 - n_2 y + n_1 z - m_2 yz \\ \\ m_2 - n_1 y + n_2 z - m_1 yz \end{pmatrix}. \tag{3.47}$$

Using the the results of Appendix 3.6.2 one can confirm that the Gaussian fluctuations above the ground state manifold are gapless for this model. The gapless points occur at momenta $(0, \pm\frac{2\pi}{3}, \mp\frac{2\pi}{3})$.

Denote $l = \gcd(L_y, L_z)$. The GSD is given by

$$\mathrm{GSD} = \begin{cases} q^{l-1} \cdot 3q & \text{if } l = 6k+3 \\ \\ q^{l-2} 2q \cdot 2q & \text{if } l = 6k \pm 2 \\ \\ q^{l-2} & \text{if } l = 6k \\ \\ q^l & \text{otherwise} \end{cases}. \tag{3.48}$$

To understand the size-dependence of the GSD, we need to know the mobility of

certain elementary excitations. First of all, a 1-kink $\mathbf{1}_{yz}$ is a lineon with mobility along the diagonal line $z = y + \alpha$ with $\alpha \in \mathbb{Z}$. The string operator $\prod_j e^{\frac{i}{q}\mathbf{n}\cdot\Phi_{y+j,z+j}}$ translates the 1-kink along this path. However, a q-kink can move along both y and z directions (in steps of 6). The composite, $\mathbf{1}_{y-1,z}(-\mathbf{1})_{yz}\mathbf{1}_{y,z-1}$ is a planon with mobility in the planar surface with normal vector $(0, 1, -1)$. The planon is moved in the discrete direction by combinations of the lineon string operator and is moved along the wire by the string operator $e^{\frac{i}{q}\int_0^L \mathbf{m}\cdot\partial_x\Phi}$.

For those familar, we can interpret that the plaquette term in the formalism of Ref. [61]: $\Theta_{y,z} = \tilde{\phi}^L_{y,z} - \tilde{\phi}^R_{y+1,z+1} + q\theta_{y,z+1} + q\theta_{y+1,z}$ where $\phi^{L/R}_{\mathbf{r}} = \phi_{\mathbf{r}} \pm q\theta_{\mathbf{r}}$. This observation along with the mobility of the excitations gives the heuristic picture of a stack of $\nu = \frac{1}{q}$ Laughlin states lying in the planes defined by normal vector $(0, 1, -1)$ which are then coupled by the $q\theta_{y,z+1} + q\theta_{y+1,z}$ terms.

If PBC are imposed in the discrete directions, which have length L_y and L_z, one can see there are $\gcd(L_y, L_z)$ distinct paths of slope $z = y$. This is shown in Fig 3.3. Since each plane hosts Laughlin-like planons, naively this suggests $q^{\gcd(L_y,L_z)}$ superselection sectors of planons living on the 2D surfaces partitioning the three torus, therefore explaining the q^l factor in GSD. Let $\alpha = 1, 2, \ldots, \gcd(L_y, L_z)$ label these distinct diagonal planes.

With the picture of layers of Laughlin states in mind, we write down a naive basis

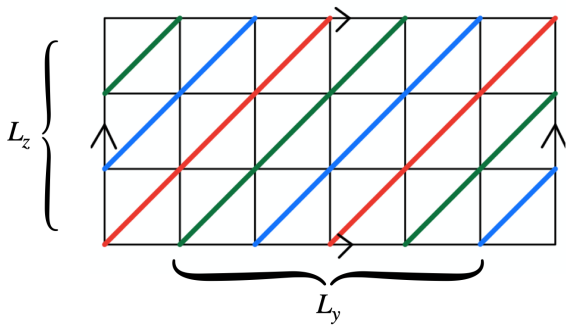

Figure 3.3: An example of the partitioning of lattice with PBC into $\gcd(L_y, L_z)$ cycles along the direction $z = y$. Here $L_y = 6$ and $L_z = 3$ results in 3 distinct closed paths: $\alpha = 1, 2, 3$ correspond to the blue, green and red paths respectively..

of logical operators for the system. Fixing a diagonal plane labeled by α, we define

$$\begin{aligned} X_\alpha &= \frac{1}{q}\mathbf{m} \cdot \int_0^L \mathrm{d}x\, \partial_x \Phi_{yz} \\ Z_\alpha &= \frac{1}{q} \sum_{yz \,\in\, \alpha} \Theta_{yz}(x) \end{aligned} \tag{3.49}$$

where $yz \in \alpha$ for X_α. The operator X_α cycles the planon $\mathbf{1}_{y-1,z}(-\mathbf{1})_{yz}\mathbf{1}_{y,z-1}$ around the wire direction while Z_α moves the planon around a cycle in the discrete direction. However one can check this pairing does not produce a diagonal commuation matrix. Following the procedure in Appendix 3.6.3 one may consider the commutation matrix of

$$[X_\alpha, Z_\beta] = \frac{2\pi i}{q}\left(\delta_{\alpha\beta} - \delta_{\alpha,\beta\pm1}\right). \tag{3.50}$$

Computing the Smith normal form of this matrix allows one to construct a set of canonical logical operators $\tilde{X}_\alpha, \tilde{Z}_a$ with $[\tilde{X}_a, \tilde{Z}_b] = \frac{2\pi i \delta_{ab}}{d_a}$ such that $\prod_a d_a = |\mathrm{GSD}|$, where GSD is given in Eq. (3.48). This procedure is necessary because while the model may superficially resemble stacks of Laughlin states, the inter-planar couplings can induce relations amongst logical operators. As an example, consider the case

when $\gcd(L_y, L_z) = 6k$. One may verify, using Eq. (3.49) the following relations between the operators Z_α:

$$\begin{aligned} &\sum_{i=0}^{k-1} (Z_{6i+1} + Z_{6i+2} - Z_{6i+4} - Z_{6i+5}) = 0, \\ &\sum_{i=0}^{k-1} \left(Z_{6i+1} - Z_{6i+3} - Z_{6i+4} + Z_{6(i+1)}\right) = 0. \end{aligned} \tag{3.51}$$

This lack of linear independence only holds at system size $\gcd(L_y, L_z) = 6k$ and is reflected in the value of the GSD which is q^{6k-2}.

3.4 CSS models

We study an example of the CSS model, given by the following polynomials:

$$\begin{aligned} f(y, z) &= y + z + yz, \\ g(y, z) &= n + y + z. \end{aligned} \tag{3.52}$$

For general CSS models, the Gaussian spectrum is found to be

$$E_{\mathbf{k}} = \sqrt{\frac{v^2 k_x^2}{\pi^2} + \frac{2Uv}{\pi}(|f_{\mathbf{k}}|^2 + |g_{\mathbf{k}}|^2)}. \tag{3.53}$$

In this case, we find that the spectrum is fully gapped for any value of n.

If $n > 4$, it is further shown in Appendix 3.6.5 that *all* excitations are lineons moving along the x direction (i.e. the direction of the wires). In other words, since the excitations can move only along x, it is a "type-II" model in the yz plane. This

is somewhat similar to Yoshida's Sierpinski spin liquid [126], which is a $\mathbb{Z}_2$ stabilizer model with only lineons. To prove this result we generalize the cleaning argument for Pauli stabilizer models [125, 143] to the present case. The details of the proof can be found in Appendix 3.6.5. Notice that unlike the proof in Ref. [125] showing that there are no string operators at all in Haah's cubic code, here the model actually has "string operators" in the yz plane. This string operator, if cut into a segment, however, does not create a charge and its inverse. In fact, if one fixes the charge at one end of the string operator, the magnitude of the charge on the other end grows exponentially with the separation between them, costing an exponentially large energy to create the configuration. Therefore, the charges are still immobile. In Appendix 3.6.4 we compute a charge basis of this model, and the result is given by $a+by$, where $a, b \in \mathbb{Z}$. Physically it means that there are infinitely many types of excitations at the (arbitrarily chosen) origin $(0, 0)$ or $(1, 0)$, labeled by two integers, and any other excitation can be transformed to an excitation at the two sites by applications of local operators.

3.5 Summary

In this work we have uncovered new classes of 3D fracton models through coupled wire constructions. When gapped, they are found to be lineon models, exhibiting integral fusion structures and some with highly unusual bulk-surface correspondence. All these features distinguish them from previously studied fracton phases, which either arise in stabilizer models, or are constructed from condensation transitions in coupled

2D topologically ordered states. A related class of planon phases was recently studied in Ref. [iCS], whose surface states are similar to the models in this work, but with clearer layered structures. These models demonstrate the existence of fully gapped fracton phases with infinite, integral fusion groups, typically associated with gapless fractonic U(1) gauge theories [144, 145, 146, 147], and it is an important question for future works to characterize such fracton orders. For example, it is known that in certain fracton models lineons can have nontrivial braiding statistics [148, 147]. Are there similar statistical phases for lineons in our models?

Many of our models have gapless modes, and currently we do not have a clear physical understanding of the nature of these gapless excitations. One possibility is that they can be interpreted as photons of certain U(1) gauge fields. It will be of great interest to identify an effective field theory for these phases, perhaps along the lines of Ref. [67]. It is also important to understand the interactions between the gapped quasiparticles and the gapless modes, e.g. whether the gapless modes mediate long-range interactions between gapped excitations. A related question is the stability of the gapless phase against perturbations.

Another possible direction for generalization is to consider more complicated, interacting conformal field theories, such as Wess-Zumino-Witten theories with higher levels, replacing the Luttinger liquid (essentially free bosons) in each wire [61]. This may lead to interesting non-Abelian lineon phases.

3.6 Appendix

3.6.1 Coupled wire construction in 2D

Here we consider the coupled wire construction in 2D and show that under fairly general assumptions the model is an Abelian topological phase. While this result is certainly expected and a well-known folklore, it has not been explicitly shown in literature.

The wires are labeled by a single index j. Each wire is a Luttinger liquid described by a K matrix K_w. We define $\mathbf{l}_1 \cdot \mathbf{l}_2 = \mathbf{l}_1^\mathsf{T} K_\mathrm{w} \mathbf{l}_2$. For the gapping term, without loss of generality we only include interactions between nearest-neighboring wires:

$$H_\mathrm{int} = -U \sum_j \sum_{\alpha=1}^{N} \int \mathrm{d}x \, \cos \Theta^\alpha_{j,j+1}. \tag{3.54}$$

Here $\Theta^\alpha_{j,j+1} = P_\alpha^\mathsf{T} \Phi_j + Q_\alpha^\mathsf{T} \Phi_{j+1}$ where P_α, Q_α are integer vectors.

We make the following assumptions about P, Q's:

1. They should satisfy the null conditions

$$P_\alpha \cdot P_\beta + Q_\alpha \cdot Q_\beta = 0, P_\alpha \cdot Q_\beta = 0. \tag{3.55}$$

   So that the gapping terms commute with each other.

2. All bosonic fields are gapped out when the system is closed. Since the number of gapping terms is the same as the fields, as long as the gapping terms are linearly independent the condition is satisfied.

3. Topological order condition: if a local vertex operator creates no excitations, it must be a linear superposition of the "stabilizers" (with integer coefficients). For example, on each site, if $\mathbf{l} \in \mathbb{Z}^{2N}$ satisfies $\mathbf{l} \cdot P_\alpha = \mathbf{l} \cdot Q_\alpha = 0$ for all α, then $\mathbf{l} = 0$. Therefore, viewed as vectors over $\mathbb{R}^{2N}$, $\{P_\alpha, Q_\alpha\}$ span a complete basis. Moreover, the subspace spanned by $\{P_\alpha\}$ and that of $\{Q_\alpha\}$ are orthogonal.

   Two useful corollaries follow: 1) $K_{\alpha\beta} = P_\alpha \cdot P_\beta$ is an invertible matrix. 2) if $\mathbf{l} \cdot P_\alpha = 0$ for all α, then $\mathbf{l}$ is a linear superposition of Q_α's (over $\mathbb{Z}$), and vice versa.

   As a special but important case of the topological order condition, there should be no local degeneracy. In other words, there exist no integers m_α such that $\sum_\alpha m_\alpha \Theta^\alpha_{j,j+1}$ is a non-primitive vector. This leads to the following condition: let M denote the following $N \times 4N$ matrix

$$M = \begin{pmatrix} P_1 & Q_1 \\ P_2 & Q_2 \\ \vdots & \vdots \\ P_N & Q_N \end{pmatrix} \tag{3.56}$$

   then the Smith normal form of M must have all non-zero diagonals being ± 1.

   In fact one should allow superposition of $\Theta^\alpha_{j,j+1}$'s from a finite cluster of wires.

Now we classify the superselection sectors of kink excitations, which give anyon types of the topological phase. They are defined as the equivalence classes of localized excitations, up to local ones. In the coupled wire model, first consider kinks of Θ^α at

the $j, j+1$ bond. They can be labeled by a vector $\mathbf{e} = (e_1, e_2, \ldots, e_N) \in \mathbb{Z}^N$ with a e_α-kink in $\Theta^\alpha_{j,j+1}$.

Next we classify which kinks can be locally created. It is not difficult to show from the topological order condition that it is sufficient to consider a two-wire local operator $e^{i(\mathbf{l}_1^\intercal \Phi_j + \mathbf{l}_2^\intercal \Phi_{j+1})}$. In order for the operator to only create excitations on the bond $j, j+1$, one must have

$$\mathbf{l}_1 \cdot Q_\alpha = 0, \mathbf{l}_2 \cdot P_\alpha = 0, \forall \alpha. \tag{3.57}$$

From our non-degeneracy assumption, we see that $\mathbf{l}_1 = \sum_\beta m_{1\beta} P_\beta, \mathbf{l}_2 = \sum_\beta m_{2\beta} Q_\beta$. Thus the excitation vector is $e^{\text{loc}}_\alpha = \sum_\beta (m_{1\beta} P_\alpha \cdot P_\beta + m_{2\gamma} Q_\alpha \cdot Q_\gamma) = \sum_\beta (m_{1\beta} - m_{2\beta}) K_{\alpha\beta}$.

Therefore, the equivalence class is given by $\mathbb{Z}^N$ mod out vectors generated by row (or column) vectors of K. Formally this agrees with the superselection sectors of an Abelian Chern-Simons theory with the K matrix K.

We also need to understand how kinks on different bonds are related. Suppose there is a kink $\mathbf{e}^{(j-1)}$ on $j-1, j$ bond. To locally transform it into a kink on $j, j+1$ bond, apply a vertex operator $e^{i\mathbf{l}^\intercal \Phi_j}$ at site j, where $\mathbf{l}$ must satisfy.

$$Q_\alpha \cdot \mathbf{l} = -e^{(j-1)}_\alpha. \tag{3.58}$$

Let Q denote the $N \times 2N$ matrix formed by Q_α's. Eq. 3.58 is solvable for any $\mathbf{e}$ if and only if the Smith normal form of Q has only ± 1 entries. It is not clear whether

this follows from the conditions imposed on P and Q, but we do not know of any counterexamples. Assuming this is the case, then $e^{i\mathbf{l}^{\mathsf{T}}\Phi}$ annihilates the kinks on $j-1, j$ bond and create new kinks on $j, j+1$ bond, given by $\mathbf{e}' = P \cdot \mathbf{l}$. The superselection sector $[\mathbf{e}']$ may be different from $[\mathbf{e}]$, but since there are only a finite number of them, after sufficiently many steps the kinks can be transported without changing its charge type.

Now we consider moving excitations along the wire direction. Consider an excitation $\mathbf{e}$ on bond $j, j+1$, and an operator $W_j(x) = e^{i\sum_\alpha w_\alpha P_\alpha^{\mathsf{T}} \Phi_j(x)}$, where w_α are rational numbers. W_j commutes with the gapping terms at the $j-1, j$ bond and creates excitations at the $j, j+1$ bond, in particular $w_\alpha P_\alpha \cdot P_\beta$ for $\Theta^\beta_{j,j+1}$. Then if we choose $\mathbf{w} = K^{-1}\mathbf{e}$, W_j defines a string operator to move $\mathbf{e}$ along the wire:

$$W^\dagger(x_2)W(x_1) \sim e^{i\sum_\alpha w_\alpha P_\alpha^{\mathsf{T}} \int_{x_1}^{x_2} \partial_x \Phi_j}. \tag{3.59}$$

We have essentially described the anyon string operators, and can compute their braiding statistics. However, the string operator that moves an anyon across wires does not have explicit form, so we do not have general expressions for the braiding statistics.

We also need to consider the spectrum of Gaussian fluctuations. While we do not have closed-form expressions for the general case, we expect that the Gaussian spectrum should be gapped when all the conditions on P and Q are satisfied and the K matrix is invertible.

Example with $N = 1$

We consider fermionic systems with $N = 1$. We take $P = (p_1, p_2)$ and $Q = (p_2, p_1)$, where $\gcd(p_1, p_2) = 1$. It is easy to check that all our conditions are satisfied. Local excitations are of the form $\pm(p_1^2 - p_2^2)$, so the group is just $\mathbb{Z}_{|p_1^2 - p_2^2|}$.

A period-1 string is given by $\mathbf{l} = (1, 1)^\mathsf{T}$, which generates an excitation $p_1 - p_2$. If $p_1 - p_2 \neq \pm 1$, to get a "unit" excitation one needs to consider $\mathbf{l}_1 = (x, y)^\mathsf{T}, \mathbf{l}_2 = (y, x)^\mathsf{T}$, where $xp_1 - yp_2 = 1$ (always solvable as $\gcd(p_1, p_2) = 1$). It implies that translation along y can act nontrivially on anyons: under translation T_y, a kink of strength $p_1 x - p_2 y$ becomes $p_1 y - p_2 x$. Notice that $T_y^2 = 1$. As an example, if $p_1 = 5, p_2 = 2$, the anyons form a $\mathbb{Z}_8$ group and T_y takes $a \in \mathbb{Z}_8$ to a^5. Ref. [60] considered $p_1 = \frac{m+1}{2}, p_2 = \frac{m-1}{2}$ to obtain $K = (m)$. In this case, T_y does not act. This kind of Laughlin states enriched nontrivially by lattice translation was also studied in Ref. [149].

Now consider the system has an edge at $j = 0$. It is easy to check that the only local vertex operator is $e^{iQ^\mathsf{T}\Phi_0}$. The edge theory is thus a chiral Luttinger liquid, with 1×1 K matrix: $K = (p_2^2 - p_1^2)$.

3.6.2 Gaussian spectrum

In the $U \to \infty$ limit of coupled wire models, the gapping terms pin the fields $\Theta = 0$. Here we study small oscillations of Θ around the minima by expanding $\cos\Theta \sim -1 + \frac{\Theta^2}{2}$ and solve the resulting quadratic theory. Below we introduce a mode expansion for the various bosonic fields involved and review how one finds single-particle spectrum

of a quadratic Hamiltonian of bosonic creation and annihilation operators. We work out the spectrum of the chiral plaquette model as an example.

Mode expansion of bosonic fields

Mean field theory gives the following translationally invariant effective Hamiltonian

$$H_{\text{eff}} = \int_0^L \mathrm{d}x \sum_{\mathbf{r},q} \left\{ \frac{v}{2\pi} \left[\left(\partial_x \phi_{\mathbf{r}}^{(q)}\right)^2 + \left(\partial_x \theta_{\mathbf{r}}^{(q)}\right)^2 \right] + \frac{U}{2} \Theta_{\mathbf{r}}^2 \right\}. \tag{3.60}$$

where the index q allows for more than one Luttinger liquid per wire. We use the following mode expansion

$$\begin{aligned} \theta_{\mathbf{r}}^{(q)}(x) &= i\sqrt{\frac{\pi}{LN_{\text{w}}}} \sum_{k_x \neq 0} \sum_{\mathbf{k}} \frac{1}{\sqrt{|k_x|}} \left(a_{k,q}^\dagger - a_{-k,q} \right) e^{-i(k_x x + \mathbf{k}\cdot\mathbf{r})} \\ \phi_{\mathbf{r}}^{(q)}(x) &= -i\sqrt{\frac{\pi}{LN_{\text{w}}}} \sum_{k_x \neq 0} \sum_{\mathbf{k}} \frac{\operatorname{sgn} k_x}{\sqrt{|k_x|}} \left(a_{k,q}^\dagger + a_{-k,q} \right) e^{-i(k_x x + \mathbf{k}\cdot\mathbf{r})}, \end{aligned} \tag{3.61}$$

where the index $k = (k_x, \mathbf{k})$ and N_w is the number of wires. Canonical commutation relations are imposed on a and $a^\dagger$'s: $[a_{k,q}, a_{l,q'}^\dagger] = \delta_{kl}\delta_{qq'}, [a_{k,q}, a_{l,q'}] = [a_{k,q}^\dagger, a_{l,q'}^\dagger] = 0$.

Consider the Fourier representation of the kinetic part of H_{eff}:

$$\begin{aligned} \int \mathrm{d}x \sum_{\mathbf{r}} \left(\partial_x \theta_{\mathbf{r}}^{(q)}\right)^2 &= \sum_k |k_x| \left(a_{k,q}^\dagger a_{k,q} + a_{-k,q}^\dagger a_{-k,q} - a_{-k,q}^\dagger a_{k,q}^\dagger - a_{k,q} a_{-k,q} \right) \\ \int \mathrm{d}x \sum_{\mathbf{r}} \left(\partial_x \phi_{\mathbf{r}}^{(q)}\right)^2 &= \sum_k |k_x| \left(a_{k,q}^\dagger a_{k,q} + a_{-k,q}^\dagger a_{-k,q} + a_{-k,q}^\dagger a_{k,q}^\dagger + a_{k,q} a_{-k,q} \right). \end{aligned} \tag{3.62}$$

The term Θ^2 will involve terms of the form $\phi_{\mathbf{r}}^{(q)} \phi_{\mathbf{r}+\boldsymbol{\Delta}}^{(q')}$, $\theta_{\mathbf{r}}^{(q)} \theta_{\mathbf{r}+\boldsymbol{\Delta}}^{(q')}$ and $\phi_{\mathbf{r}}^{(q)} \theta_{\mathbf{r}+\boldsymbol{\Delta}}^{(q')}$ where

Δ is some vector in the yz plane. The mode expansion for these terms is as follows

$$\begin{aligned}
\int dx \sum_{\mathbf{r}} \phi^{(q)}_{\mathbf{r}} \phi^{(q')}_{\mathbf{r}+\mathbf{\Delta}} &\sim \sum_{k_x \neq 0, \mathbf{k}} \frac{e^{i\mathbf{k}\cdot\mathbf{\Delta}}}{|k_x|} \left(a^\dagger_{k,q} a_{k,q'} + a^\dagger_{k,q} a^\dagger_{-k,q'} + a_{-k,q} a^\dagger_{-k,q'} + a_{-k,q} a_{k,q'} \right) \\
\int dx \sum_{\mathbf{r}} \theta^{(q)}_{\mathbf{r}} \theta^{(q')}_{\mathbf{r}+\mathbf{\Delta}} &\sim - \sum_{k_x \neq 0, \mathbf{k}} \frac{e^{i\mathbf{k}\cdot\mathbf{\Delta}}}{|k_x|} \left(-a^\dagger_{k,q} a_{k,q'} + a^\dagger_{k,q} a^\dagger_{-k,q'} - a_{-k,q} a^\dagger_{-k,q'} + a_{-k,q} a_{k,q'} \right) \\
\int dx \sum_{\mathbf{r}} \phi^{q}_{\mathbf{r}} \theta^{q'}_{\mathbf{r}+\mathbf{\Delta}} &\sim \sum_{k_x \neq 0, \mathbf{k}} \frac{\mathrm{sgn}(k_x)}{|k_x|} e^{i\mathbf{k}\cdot\mathbf{\Delta}} \left(-a^\dagger_{k,q} a_{k,q'} + a^\dagger_{k,q} a^\dagger_{-k,q'} + a_{-k,q} a^\dagger_{-k,q'} - a_{-k,q} a_{k,q'} \right)
\end{aligned} \tag{3.63}$$

Using these expressions above one can construct a BdG type Hamiltonian for the corresponding quadratic bosonic theory.

Bogoluibov transformation for bosons

We will be studying theories which are quadratic in bosonic creation/annihilation operators. Here we describe how to find the spectrum for a general quadratic Hamiltonian of bosons:

$$\begin{aligned}
H &= \sum_{ij} \left(T_{ij} a^\dagger_i a_j + U_{ij} a^\dagger_i a^\dagger_j + U^*_{ij} a_j a_i \right) \\
&= (a^\dagger \; a) h \begin{pmatrix} a \\ a^\dagger \end{pmatrix}
\end{aligned} \tag{3.64}$$

where the "first-quantized" Hamiltonian h is defined as:

$$h = \begin{pmatrix} T & U \\ U^* & T^* \end{pmatrix}. \tag{3.65}$$

Here T is Hermitian and U is symmetric. a_i's satisfy the canonical commutation relations $[a_i, a_j^\dagger] = \delta_{ij}$. We perform a canonical transformation to a new set of annihilation operators b in which the Hamiltonian is diagonalized:

$$H = (b^\dagger \; b) \begin{pmatrix} \Lambda & 0 \\ 0 & \Lambda \end{pmatrix} \begin{pmatrix} b \\ b^\dagger \end{pmatrix} \quad \text{where} \quad \begin{pmatrix} a \\ a^\dagger \end{pmatrix} = W^\dagger \begin{pmatrix} b \\ b^\dagger \end{pmatrix} \tag{3.66}$$

Here Λ is the diagonal matrix of single-particle energy eigenvalues. Note the requirement that b_i satisfy the canonical commutation relations for bosons means that the Bogoluibov transformation W is symplectic:

$$WJW^\dagger = J, J = \begin{pmatrix} \mathbf{1} & 0 \\ 0 & -\mathbf{1} \end{pmatrix}. \tag{3.67}$$

So Λ does not simply correspond to the eigenvalues of the "first-quantized" Hamiltonian matrix h. However, using the fact that $JW^\dagger J = W^{-1}$, we can rewrite the diagonalization equation

$$\begin{pmatrix} T & U \\ U^* & T^* \end{pmatrix} = W \begin{pmatrix} \Lambda & 0 \\ 0 & \Lambda \end{pmatrix} W^\dagger \tag{3.68}$$

as a more standard eigenvalue problem:

$$\begin{pmatrix} T & -U \\ U^* & -T^* \end{pmatrix} = W \begin{pmatrix} \Lambda & 0 \\ 0 & -\Lambda \end{pmatrix} W^{-1}. \tag{3.69}$$

So we can solve for the spectrum by diagonalizing the matrix

$$\begin{pmatrix} T & -U \\ U^* & -T^* \end{pmatrix}.$$

Spectrum of the chiral plaquette models

Here, as an example, we calculate the spectrum of the chiral plaquette models. These models were written in the chiral basis, where $\mathbf{m}\cdot\Phi = m_1\phi_L + m_2\phi_R$. We work, because of the simplicity of the mode expansion, in the (ϕ, θ) basis with $\mathbf{m}\cdot\Phi = a\phi + b\theta$, where $a = m_1 + m_2$ and $b = m_1 - m_2$ is clear. Similarly $c = n_1 + n_2, d = n_1 - n_2$.

Define the following functions of $\mathbf{k}$

$$f_\phi = a^2 + c^2 + a^2\cos(k_y + k_z) + c^2\cos(k_y - k_z) + 2ac(\cos k_z + \cos k_y),$$

$$f_\theta = b^2 + d^2 - b^2\cos(k_z + k_y) - d^2\cos(k_y - k_z) + 2bd(\cos k_z - \cos k_y),$$

$$f_{\phi\theta} = 2i\,\mathrm{sgn}(k_x)\left[(ad - bc)\sin k_z - (ad + cb)\sin k_y - ab\sin(k_y + k_z) - cd\sin(k_y - k_z)\right]. \tag{3.70}$$

Schematically, Θ^2 term involves terms of the form $\phi\phi$, $\theta\theta$ and $\phi\theta + \theta\phi$. Using the

results of Appendix 3.6.2 one can check that

$$\begin{aligned}(\phi\phi)_k &\sim \frac{f_\phi(k)}{|k_x|}\left(a_k^\dagger a_k + a_k^\dagger a_{-k}^\dagger + a_{-k}a_{-k}^\dagger + a_{-k}a_k\right),\\ (\theta\theta)_k &\sim \frac{f_\theta(k)}{|k_x|}\left(a_k^\dagger a_k + a_k^\dagger a_{-k}^\dagger - a_{-k}a_{-k}^\dagger - a_{-k}a_k\right),\\ (\phi\theta+\theta\phi)_k &\sim \frac{f_{\phi\theta}(k)}{|k_x|}\left(a_k^\dagger a_{-k}^\dagger - a_{-k}a_k\right).\end{aligned} \tag{3.71}$$

The single particle hamiltonian h_k then has the following form

$$h_k = \begin{pmatrix} a_k^\dagger & a_{-k}\end{pmatrix}\begin{pmatrix} T_k & U_k \\ U_k^* & T_k\end{pmatrix}\begin{pmatrix} a_k \\ a_{-k}^\dagger\end{pmatrix} \tag{3.72}$$

where

$$\begin{aligned}T_k &= \frac{v}{\pi}|k_x| + \frac{U}{|k_x|}\left(f_\phi + f_\theta\right)\\ U_k &= \frac{U}{|k_x|}\left(f_\phi - f_\theta + f_{\phi\theta}\right).\end{aligned} \tag{3.73}$$

Diagonalizing the matrix

$$\begin{pmatrix} T_k & -U_k \\ U_k^* & -T_k\end{pmatrix}$$

gives the spectrum

$$E_k = \sqrt{v^2|k_x|^2 + vU\left(f_\phi + f_\theta\right)}. \tag{3.74}$$

So to determine if the fluctuations are gapped one needs to check that $\min(f_\phi + f_\theta) > 0$.

We define $\alpha = \frac{k_y+k_z}{2},\ \beta = \frac{k_y-k_z}{2}$. One can show that $f_\phi(\mathbf{k}) + f_\theta(\mathbf{k}) = |f_\mathbf{k}|^2 \geq 0$ where

$$|f_\mathbf{k}| = |m_1 e^{i\alpha} + m_2 e^{-i\alpha} + n_2 e^{i\beta} + n_1 e^{-i\beta}|. \tag{3.75}$$

Thus one just needs to find the zero locus of $|f_\mathbf{k}|$, given by the following equations:

$$\begin{aligned} (m_1 + m_2)\cos\alpha + (n_1 + n_2)\cos\beta = 0, \\ (m_1 - m_2)\sin\alpha + (n_2 - n_1)\sin\beta = 0. \end{aligned} \tag{3.76}$$

Let us define

$$\begin{aligned} s &= (m_1 + m_2)^2(n_1 - n_2)^2, \\ t &= (m_1 - m_2)^2(n_1 + n_2)^2, \\ u &= (n_1^2 - n_2^2)^2. \end{aligned} \tag{3.77}$$

Assume for now $u \neq 0$. We can easily find

$$\cos^2\alpha = \frac{t-u}{t-s}, \sin^2\alpha = \frac{s-u}{s-t}. \tag{3.78}$$

So for both expressions to be positive-definite, we must have

$$(t-s)(t-u) \geq 0, (s-t)(s-u) \geq 0, \tag{3.79}$$

which implies that either $t \leq u \leq s$ or $s \leq u \leq t$. It is easy to see that the $s = t$ case is included.

Therefore, if $(t-u)(s-u) > 0$, there are no zeros for $|f_{\mathbf{k}}|^2$, which implies that it must have a positive minimum. One can further check that this condition also covers the $u = 0$ case.

3.6.3 Ground state degeneracy on torus

When the model is fully gapped, an interesting quantity to consider is the ground state degeneracy (GSD) with periodic boundary conditions imposed. The GSD can be computed using a method introduced by Ganeshan and Levin [150]. In their approach, all fields are treated as real-valued, with the Hamiltonian still given by Eq. 3.4. Compactness is then imposed dynamically by adding

$$-V\sum_{\mathbf{r}}\cos 2\pi Q^a_{\mathbf{r}},\ Q^a_{\mathbf{r}} = \frac{1}{2\pi}\int \mathrm{d}x\,\partial_x\Phi^a_{\mathbf{r}}(x). \tag{3.80}$$

Collecting all the pinned fields $C = \{\Theta^\alpha_{\mathbf{r}}(x), Q^a_{\mathbf{r}}\}$, we compute their commutation matrix $\mathcal{Z}$. Notice that $\Theta^\alpha_{\mathbf{r}}$ commute with each other, so do the $Q^a_{\mathbf{r}}$'s, thus the nonzero commutators only occur between Θ and Q, and the commutation matrix takes an off-diagonal form:

$$\mathcal{Z} = \begin{pmatrix} 0 & \mathcal{Z}_1 \\ -\mathcal{Z}_1^{\mathsf{T}} & 0 \end{pmatrix}. \tag{3.81}$$

We then find the Smith normal form of $\mathcal{Z}_1$:

$$A\mathcal{Z}_1 B = \mathcal{D}, \tag{3.82}$$

where A and B are unimodular integer matrices. Then define

$$\mathcal{V} = \begin{pmatrix} 0 & A \\ B^{\mathsf{T}} & 0 \end{pmatrix}, \tag{3.83}$$

and one obtains

$$\mathcal{V}\mathcal{Z}\mathcal{V}^{\mathsf{T}} = \begin{pmatrix} 0 & -\mathcal{D} \\ \mathcal{D} & 0 \end{pmatrix}. \tag{3.84}$$

We assume that diagonal elements of $\mathcal{D}$ are ordered such that the first I of them, $d_1, d_2, \cdots, d_I$ are non-zero. Then the GSD is given by $|d_1 d_2 \cdots d_I|$. The matrix $\mathcal{V}$ in fact gives the logical operators that span the ground state space [150]. More precisely, the commutation matrix is "diagonalized" in the new basis

$$C' = \mathcal{V}C = \begin{pmatrix} AQ \\ B^{\mathsf{T}}\Theta \end{pmatrix}. \tag{3.85}$$

This form of C' suggests that the logical operators come in two conjugate groups, one being AQ (with additional $1/d_i$ factors that we haven't included yet), physically string operators along x, the other being $B^{\mathsf{T}}\Theta$, which can be generally interpreted as surface operators in the transverse directions.

3.6.4 Algorithm to find a charge basis

We first define the charge basis in terms of the excitation map discussed in the main text.

Definition 3.6.1. Charge basis

Any local operator is said to create a trivial charge configuration. In other words, any charge cluster that belongs to Imϵ where ϵ is the excitation map, is trivial. We now denote the set of all excitations by E, also referred to as the excitation module. We use Theorem 1 of Ref. [141] which states that the equivalence class of excitations modulo trivial ones is a torsion element of the cokernel of the excitation map. In other words, any topologically nontrivial local charge is an element of $T\,\mathrm{coker}\,\epsilon = T(E/\mathrm{Im}\epsilon)$. Torsion submodule $T(M)$ of a module M is defined as $T(M) = \{m \in M | \exists r \in R\backslash\{0\}$ such that $rm = 0\}$.

In order to calculate the charge basis given by $T\,\mathrm{coker}\,\epsilon = T(E/\mathrm{Im}\epsilon)$, we first note that we consider the excitation map represented by a matrix with matrix elements belonging to a polynomial ring $R[x, y, z]$ over the ring of integers $\mathbb{Z}$ i.e. each element is polynomials in variables y and z with coefficients of monomials in $\mathbb{Z}$. We can always bring the excitation map to this form i.e. with non-negative exponents of translation variables since we can choose any translate of the stabilizer generators as our generating set to write down a polynomial representation of the excitation map. The same holds for the charge basis. Even though an arbitrary charge configuration is expressed as a Laurent polynomial, if it is finite, we can change our choice of origin to write it as a polynomial with non-negative exponents of translation variables i.e. over a polynomial ring. We will use this idea to compute the charge basis using the trivial charge polynomials expressed in the non-negative cone i.e. with non-negative exponents of translation variables. Any non-trivial charge configuration can

be expressed using the elements of this charge basis up to a translation.

We now introduce some definitions and concepts needed in the calculation of the charge basis. These definitions are taken from Ref. [151].

Definition 3.6.2. Groebner basis of an ideal

Groebner basis of an ideal I is defined as a basis in which the leading term of every element divides the leading term of any polynomial in the ideal I.

Consider the Groebner basis $G = \{g_1, g_2, ..., g_t\}$ for the ideal I. With respect to the set $\{\text{lt}(g_1), ...\text{lt}(g_t)\}$ of leading terms of G, consider the saturated subsets $J \subset \{1, ..., t\}$.

Definition 3.6.3. Saturated subset

For any subset $J \subseteq \{1, ..., s\}$, set monomials $X_J = \text{LCM}(X_j | j \in J)$ where X_j are monomials. We say that J is saturated with respect to $X_1, ..., X_s$ provided that for all $j \in \{1, ..., s\}$, if X_j divides X_J, then $j \in J$. In other words, it is saturated if all the monomial from X_1 to X_s divide the LCM of the smaller subset defined by J. For example, consider the set $(X_1 = xy, X_2 = x^2, X_3 = y, X_4 = x^4)$ and choose the subset $(X_1 = xy, X_2 = x^2)$. The LCM of elements in the subset is x^2y which is divisible by X_3 but $X_3 \notin J$ and hence the subset (X_1, X_2) is not saturated.

For each saturated subset $J \subseteq \{1, \ldots, t\}$, we let I_J denote the ideal of R generated by $\{\text{lc}(g_i) | i \in J\}$ where lc denotes the leading coefficient. C_J be the complete set of coset representatives for R/I_J. Assume that $O \in C_J$ and also for each power product X, let $J_X = \{\text{lm}(g_i) | \text{lm}(g_i) \text{ divides } X\}$ where $\text{lm}(g_i)$ denotes the leading monomial of g_i.

Definition 3.6.4. Totally reduced polynomial

A polynomial $r \in A$ is totally reduced provided that for every power product X, if cX is the corresponding term of r, then $c \in C_{J_X}$. For a given polynomial $r \in A$, a normal form for f provided that $f \equiv r \,(\mathrm{mod} I)$ and r is totally reduced.

Now we state the main theorem (Theorem 4.3.3. of Ref. [151] that describes the result for the coset representatives of the quotient R/I_J

Theorem 3.6.5. *Let G be a Groebner basis for the non-zero ideal I of A. Assume that for each saturated subset $J \subseteq \{1, ..., t\}$, a complete set of coset representatives C_J for the ideal I_J is chosen. Then, every $f \in A$ has a unique normal form. The normal form can be computed effectively provided linear equations are solvable in R and R has effective coset representatives.*

The actual calculation is best understood through examples. We now show an example from different classes of models mentioned in the main text.

Charge basis for different models

- We first consider the CSS model.

$$\epsilon = \begin{pmatrix} 0 & 0 & yz + y + z & n + y + z \\ n + \overline{y} + \overline{z} & -(\overline{yz} + \overline{y} + \overline{z}) & 0 & 0 \end{pmatrix}. \tag{3.86}$$

  where n is an integer. Since there is a duality between the ϕ and θ sectors, we can consider only one sector, let's say ϕ and calculate the charge basis in the ϕ sector. The excitation map (3.86) implies that any excitation pattern that belongs to

the im ϵ is a linear combination of the two polynomials as shown in the map i.e. it belongs to the ideal $\langle yz + y + z, n + y + z\rangle$. The Groebner basis of the ideal with lexicographic ordering is given by $\{g_1 = y + z + n, g_2 = z^2 + nz + n\}$. The leading terms are then given by y and z^2 i.e. leading monomials y and z^2 with coefficients 1 and 1. Now we use the definition that for each power product X, $J_X = \{m_i|\ \mathrm{lm}(g_i) \text{ divides } X\}$ where lm denotes the leading monomial. Then we get the saturated subsets $J_1 = \varnothing$, $J_{y^{\mu_y}} = \{m_1\}$, $J_z = \varnothing$, $J_{z^{\mu_z>1}} = \{m_2\}$, $J_y = \{m_1\}$ and $J_{y^{\mu_y} z^{\mu_z>1}} = \{m_1, m_2\}$ where μ_y and μ_z are non-zero integer exponents of y and z. Thus, the corresponding ideals I_J are $I_{J_1} = I_{J_z} = 0$, $I_{J_{y^{\mu_y}}} = \langle 1\rangle$, $I_{J_{z^{\mu_z\geq 2}}} = \langle 1\rangle$ and $I_{J_{y^{\mu_y} z^{\mu_z}}} = \langle 1\rangle$. We get $C_{J_1} = C_{J_z} = \mathbb{Z}$ while all other coset representatives are 0. Thus, a complete set of coset representatives for $\mathbb{Z}[y, z]/I$ is the set $\{a + bz|a, b \in \mathbb{Z}\}$.

We can also simply arrive at this result by writing down relations $y = -n - z$ and $yz = n$ from the relations $y+z+n = 0$ and $y+z+yz = 0$ in the ideal. Using these two relations, we get $z^2 + nz + n = 0$. Hence, an arbitrary polynomial in y and z can be expressed only in terms of monomials 1 and z since y and z^2 can be reduced to polynomials in 1 and z. The choice of basis monomials is not unique. Notice that because our original ideal is symmetric in y and z, we can also use the relation $y^2 + ny + n = 0$ and express an arbitrary polynomial in terms of basis monomials 1 and y i.e. as $\{a + by|a, b \in \mathbb{Z}\}$.

- We now consider a family of models described by

$$\epsilon = \begin{pmatrix} m_1 + n_2 y + n_1 z + m_2 yz & m_2 + n_1 y + n_2 z + m_1 yz \end{pmatrix}. \tag{3.87}$$

1. $\mathbf{m} = (p, q)$ and $\mathbf{n} = (-p, q)$
2. $\mathbf{m} = (p + 1, p)$ and $\mathbf{n} = (1, 1)$
3. $\mathbf{m} = (p, 0)$ and $\mathbf{n} = (0, 1)$

1. We consider the first example in this family for particular values of p and q as $p = 3, q = 2$ such that

$$\epsilon = \begin{pmatrix} 3 + 2y - 3z + 2yz & 2 - 3y + 2z + 3yz \end{pmatrix}. \tag{3.88}$$

The excitation map (3.88) implies that the trivial charge configuration ideal is given by

$$\langle 3 + 2y - 3z + 2yz, 2 - 3y + 2z + 3yz \rangle \ .$$

The Groebner basis of the ideal with lexicographic ordering is given by $\{g_1 = yz - 5y + 5z - 1, g_2 = 12y - 13z + 5, g_3 = 13z^2 - 10z + 13\}$. The leading terms are then given by yz, $12y$ and $13z^2$ i.e. leading monomials $m_1 = yz$, $m_2 = y$ and $m_3 = z^2$ with coefficients 1, 12 and 13. Then, we write the saturated subsets, $J_1 = \varnothing$, $J_y = \{m_2\}$, $J_z = \varnothing$, $J_{z^{\mu_z > 1}} = \{m_3\}$, $J_{y^{\mu_y} z} = \{m_1, m_2\}$ and $J_{y^{\mu_y} z^{\mu_z > 1}} = \{m_1, m_2, m_3\}$ where μ_y and μ_z are non-

zero integer exponents of y and z. Thus, the corresponding ideals I_J are $I_{J_1} = I_{J_z} = 0$, $I_{J_{y^{\mu_y}}} = \langle 12 \rangle$, $I_{J_{z^{\mu_z \geq 2}}} = \langle 13 \rangle$ and $I_{J_{y^{\mu_y} z^{\mu_z}}} = \langle 1 \rangle$. We get $C_{J_1} = C_{J_z} = \mathbb{Z}$, $C_{J_{y^{\mu_y}}} = \mathbb{Z}_{12}$, $C_{J_{z^{\mu_z \geq 2}}} = \mathbb{Z}_{13}$ while all other coset representatives are 0. Thus, a complete set of coset representatives for $\mathbb{Z}[y,z]/I$ is the set $\{a + by^{\mu_y} + cz + dz^{\mu_z > 1} | a, c \in \mathbb{Z}, b \in \mathbb{Z}_{12}, d \in \mathbb{Z}_{13}\}$.

2.

$$\epsilon = \begin{pmatrix} (p+1) + y + z + pyz & p + y + z + (p+1)yz \end{pmatrix}. \tag{3.89}$$

The excitation map (3.89) implies that the trivial charge configuration ideal is given by

$$\langle (p+1) + yz + pyz, p + y + z + (p+1)yz \rangle \ .$$

The Groebner basis of the ideal with lexicographic ordering is given by $\{g_1 = y+z+2p+1, g_2 = z^2+(2p+1)z+1\}$. The leading terms are then given by y and z^2 i.e. leading monomials $m_1 = y$ and $m_2 = z^2$ with coefficients 1 and 1. Then, we get the saturated subsets $J_1 = \varnothing$, $J_{y^{\mu_y}} = \{m_1\}$, $J_z = \varnothing$, $J_{z^{\mu_z > 1}} = \{m_2\}$, $J_{y^{\mu_y} z} = \{m_1\}$ and $J_{y^{\mu_y} z^{\mu_z > 1}} = \{m_1, m_2\}$ where μ_y and μ_z are non-zero integer exponents of y and z. Thus, the corresponding ideals I_J are $I_{J_1} = 0$, $I_{J_z} = 0$, $I_{J_{y^{\mu_y}}} = \langle 1 \rangle$, $I_{J_{z^{\mu_z \geq 2}}} = \langle 1 \rangle$ and $I_{J_{y^{\mu_y} z^{\mu_z}}} = \langle 1 \rangle$. We get $C_{J_1} = C_{J_z} = \mathbb{Z}$ while all other coset representatives are 0. Thus, a complete set of coset representatives for $\mathbb{Z}[y,z]/I$ is the set $\{a+bz | a, b \in \mathbb{Z}\}$.

3.

$$\epsilon = \begin{pmatrix} p+y & z+pyz \end{pmatrix}. \tag{3.90}$$

where p is an integer. The excitation map (3.90) implies that the trivial charge configuration ideal is given by $\langle p+y, 1+py\rangle$. The Groebner basis of the ideal with lexicographic ordering is given by $\{g_1 = y+p, g_2 = p^2-1\}$. The leading terms are then given by y and p^2-1 i.e. the leading monomials $m_1 = y$ and $m_2 = 1$ with coefficients 1 and p^2-1. Then we get the saturated subsets $J_1 = \{m_2\}$, $J_{y^{\mu_y}} = \{m_1, m_2\}$, $J_{z^{\mu_z}} = \{m_2\}$ and $J_{y^{\mu_y} z^{\mu_z}} = \{m_1, m_2\}$ where μ_y and μ_z are positive integer exponents of y and z. Thus, the corresponding ideals I_J are $I_{J_1} = \langle p^2-1\rangle$, $I_{J_{y^{\mu_y}}} = \langle 1\rangle$, $I_{J_{z^{\mu_z}}} = \langle p^2-1\rangle$ and $I_{J_{y^{\mu_y} z^{\mu_z}}} = \langle 1\rangle$. We get $C_{J_1} = \mathbb{Z}_{p^2-1}$ and $C_{J_{z^{\mu_z}}} = \mathbb{Z}_{p^2-1}$ while the other coset representatives are 0. Thus, a complete set of coset representatives for $\mathbb{Z}[y,z]/I$ is the set $\{a + bz^{\mu_z} | a, b \in \mathbb{Z}_{p^2-1}\}$.

- We now consider another family of models given by

$$\epsilon = \begin{pmatrix} m_1 - n_2 y + n_1 z - m_2 yz & m_2 - n_1 y + n_2 z - m_1 yz \end{pmatrix}. \tag{3.91}$$

where $\mathbf{m} = \left(\frac{1-q}{2}, \frac{1+q}{2}\right)$ and $\mathbf{n} = (q, -q)$. where q is odd. For $q = 3$, we get

$$\epsilon = \begin{pmatrix} -1 + 3y + 3z - 2yz & 2 - 3y - 3z + yz \end{pmatrix}. \tag{3.92}$$

The excitation map (3.92) implies that the trivial charge configuration ideal is given by

$$\langle -1 + 3y + 3z - 2yz, 2 - 3y - 3z + yz \rangle \ .$$

The Groebner basis of the ideal with lexicographic ordering is given by $\{g_1 = yz - 1, g_2 = 3y + 3z - 3, g_3 = 3z^2 - 3z + 3\}$. The leading terms are then given by yz, $3y$ and $3z^2$ i.e. leading monomials $m_1 = yz$, $m_2 = y$ and $m_3 = z^2$ with coefficients 1, 3 and 3. Then, we get the saturated subsets $J_1 = \varnothing$, $J_{y^{\mu_y}} = \{m_2\}$, $J_z = \varnothing$, $J_{z^{\mu_z > 1}} = \{m_3\}$, $J_{y^{\mu_y} z} = \{m_1, m_2\}$ and $J_{y^{\mu_y} z^{\mu_z > 1}} = \{m_1, m_2, m_3\}$ where μ_y and μ_z are non-zero positive integer exponents of y and z. Thus, the corresponding ideals I_J are $I_{J_1} = I_{J_z} = 0$, $I_{J_{y^{\mu_y}}} = \langle 3 \rangle$, $I_{J_{z^{\mu_z \geq 2}}} = \langle 3 \rangle$ and $I_{J_{y^{\mu_y} z^{\mu_z}}} = \langle 1 \rangle$. We get $C_{J_1} = C_{J_z} = \mathbb{Z}$, $C_{J_{y^{\mu_y}}} = \mathbb{Z}_3$ and $C_{J_{z^{\mu_z}}} = \mathbb{Z}_3$ while all other coset representatives are 0. Thus, a complete set of coset representatives for $\mathbb{Z}[y, z]/I$ is the set $\{a + by^{\mu_y} + cz + dz^{\mu_z > 1} | a, c \in \mathbb{Z}, b, d \in \mathbb{Z}_3\}$.

3.6.5 Proof that the model Eq. 3.52 has only lineons

Recall that the stabilizer map is given by

$$\sigma = \begin{pmatrix} x + y + xy & & \\ n + x + y & & \\ & n + \overline{x} + \overline{y} & \\ & -(\overline{x} + \overline{y} + \overline{xy}) & \end{pmatrix} . \tag{3.93}$$

Formally the stabilizers can be written as

$$\begin{array}{ccc} XX & \text{———} & XI \\ \Big| & & \Big| \\ IX^n & \text{———} & XX \end{array} \qquad \begin{array}{ccc} ZZ^{-1} & \text{———} & Z^nI \\ \Big| & & \Big| \\ IZ^{-1} & \text{———} & ZZ^{-1} \end{array} \tag{3.94}$$

Here for brevity and in analogy with stabilizer codes we denote $XI \equiv e^{i\phi_1}, IX \equiv e^{i\phi_2}, ZI \equiv e^{i\theta_1}, IZ \equiv e^{i\theta_2}$, suppressing the x coordinate dependence. We consider cleaning of arbitrary pair creation operators to show that there is nontrivial logical string operator. Since the code is "CSS," cleaning the pair creation operators of one type would be enough. Thus, we consider Z pair creation operators.

Cleaning to a minimal box containing the excitation patches

We can clean an arbitrary pair creation operator that creates a pair of excitation patches to a minimal box that contains the two patches. This can be done by using the commutation constraints due to the corners shared with X stabilizers, i.e. where the independent vertices XI and XX of the X stabilizer operator hits the pair creation operator enclosing the excitation patches. There are two orthogonal edges with these type of independent vertices, XX and XI, in the X stabilizer. Such edges are called good edges for cleaning [125] and having two of them here implies that one can clean the Z pair creation operator down to a minimal box containing the excitation patches as shown in Figs. 3.4, 3.5 and 3.6 using commutation constraints with the corners of the kind XX and XI of the X stabilizer.

Diagonal pair creation operators

The figures 3.4(a) and 3.5(a) can be cleaned to flat-rod configurations by just stepwise cleaning of corners. For example, in Fig. 3.4a, use $[O, XX] = 0$ which gives $O = ZZ^{-1}$ and thus it can be cleaned by multiplying the Z-stabilizer. The process can be repeated for O_1 and O_2 and so on to yield Fig. 3.4(c). The same process can be carried out for configuration in fig. 3.5(a) to yield Fig 3.5c using the constraint $[O, XI] = 0$ which yields $O = IZ, II$.

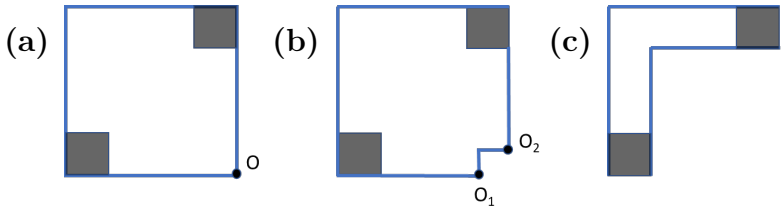

Figure 3.4: Cleaning of pair creation operators.

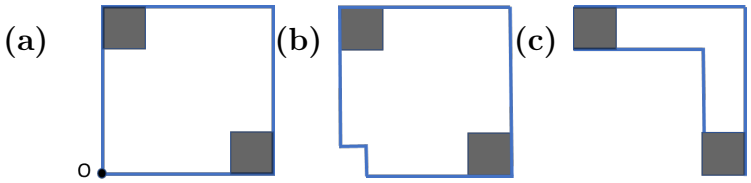

Figure 3.5: Cleaning of pair creation operators.

Horizontal and vertical strips

The horizontal and vertical strips can be reduced again to the lines. For the horizontal line, we can show the deformation result for recursion as follows. Suppose the operator

on site i is (a_i, b_i). Then they must satisfy

$$a_i + b_i + a_{i+1} = 0, nb_i + a_{i+1} + b_{i+1} = 0. \tag{3.95}$$

It follows that $a_{i+2} = nb_i$, and

$$n(a_i + a_{i+1}) + a_{i+2} = 0. \tag{3.96}$$

The characteristic polynomial is $x^2 + nx + n = 0$, with roots $\omega_{1,2} = \frac{-n \pm \sqrt{n(n-4)}}{2}$. So we can generally write

$$a_i = u_1\omega_1^i + u_2\omega_2^i. \tag{3.97}$$

Then

$$b_i = -a_i - a_{i+1} = -u_1(1+\omega_1)\omega_1^i - u_2(1+\omega_2)\omega_2^i. \tag{3.98}$$

It is easy to see that if $n > 4$, both $\omega_{1,2}$ are real and $|\omega_{1,2}| > 1$, so a_i or b_i grows exponentially large with i.

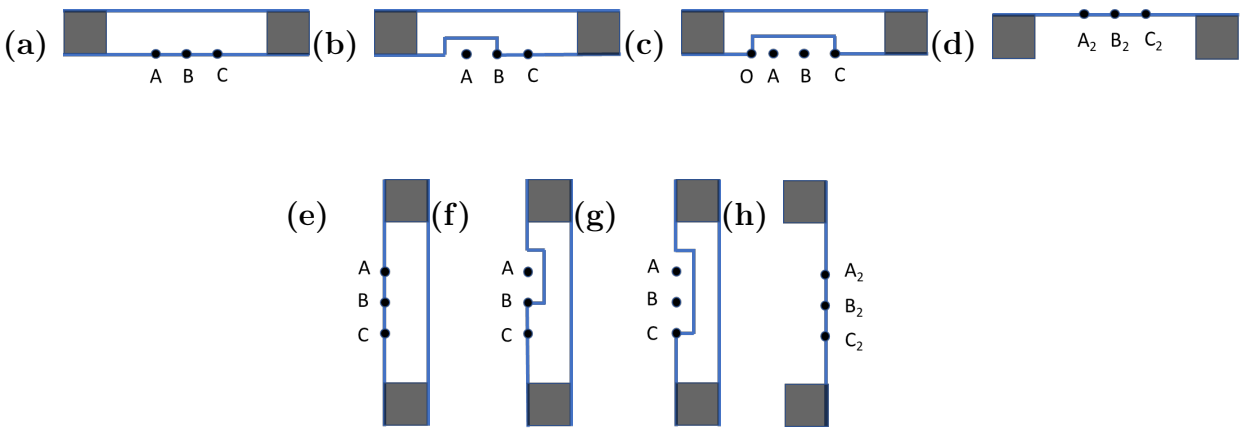

Figure 3.6: Cleaning of pair creation operators.

Similarly, for the vertical line, we have the recursion relations

$$a_i + a_{i+1} + b_{i+1} = 0, a_i + b_i + nb_{i+1} = 0. \tag{3.99}$$

It follows that $a_i = nb_{i+2}$, and

$$nb_{i+2} + nb_{i+3} + b_{i+1} = 0. \tag{3.100}$$

The characteristic polynomial is $nx^2 + nx + 1 = 0$, with roots $\lambda_{1,2} = -\frac{1}{2} \pm \sqrt{\frac{1}{4} - \frac{1}{n}}$. So we can generally write

$$b_i = u_1\lambda_1^i + u_2\lambda_2^i. \tag{3.101}$$

Then

$$a_i = -b_i - nb_{i+1} = -u_1(1 + n\lambda_1)\lambda_1^i - u_2(1 + n\lambda_2)\lambda_2^i. \tag{3.102}$$

When $n \geq 4$, both roots $|\lambda_{1,2}| < 1$. As a result, a_i and b_i decays exponentially and the string can not extend to arbitrarily long length.

We have shown that both horizontal and vertical string operators must create charges exponentially large in the length of the string at least on one end. Now we further prove explicitly that no string operators can create charges of opposite values, meaning $nb_i = -a_0 - b_0$ and $a_i + b_i = -a_0$. Consider the horizontal line. This implies

$$n[u_1(1 + \omega_1)\omega_1^i + u_2(1 + \omega_2)\omega_2^i] = u_1(2 + \omega_1) + u_2(2 + \omega_2), \tag{3.103}$$

and

$$u_1\omega_1^{i+1} + u_2\omega_2^{i+1} = u_1 + u_2. \tag{3.104}$$

They have no non-zero solution for any i. Similar holds for the vertical relations.

L shaped operators

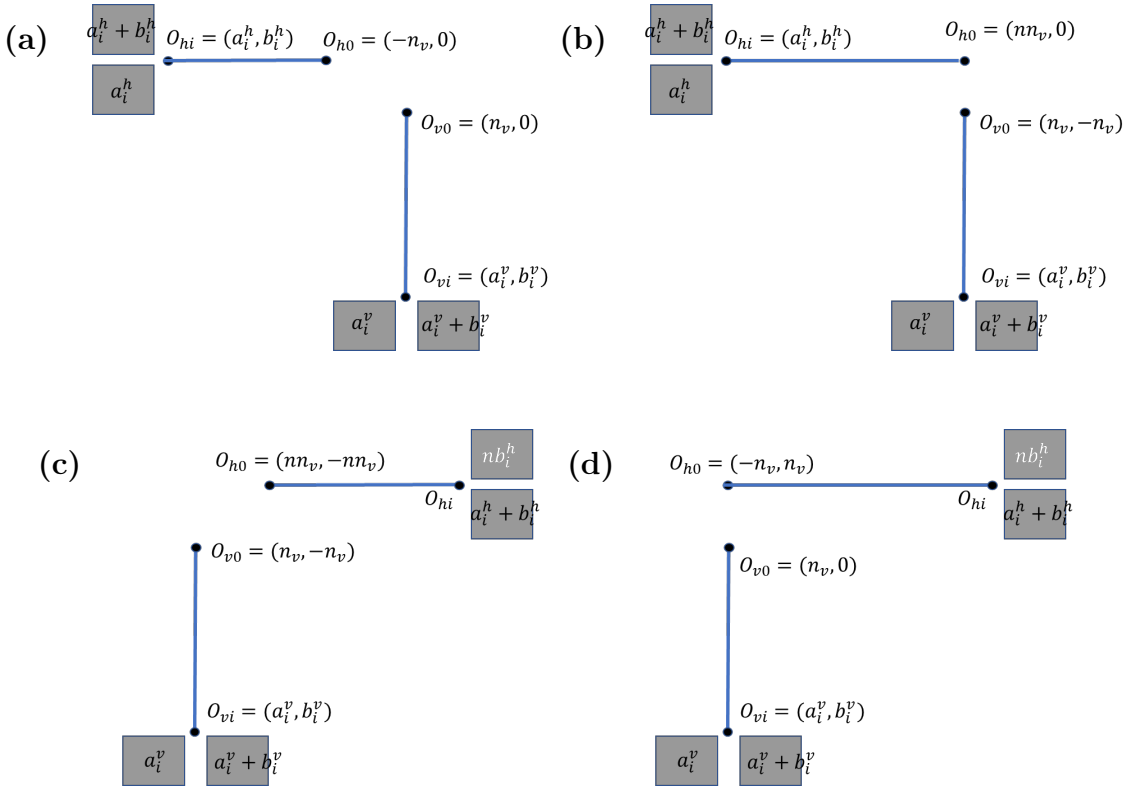

Figure 3.7: L shaped operators.

We now consider string operators that could be formed from L shaped operators in Fig. 3.4(c) and Fig. 3.5(c). Using the cleaning done for the horizontal and vertical strips, we can reduce these operators to width 1 operators shown in Fig. 3.7. The lines do not join exactly at the corner in order to cancel out the excitations around it. The patches shown at the ends show the excitation strengths at those ends. We now

show string operator formed from such joining L shaped width 1 operators cannot form a nontrivial logical operator.

L shaped operators in Fig. 3.7(a) and (b)

In Fig.3.7a, due to the commutation with stabilizer generators, the vertices O_{h0} and O_{v0} have constraints $[O_{h0}, IX^n] = [O_{v0}, IX^n] = 0$ which imply $O_{h0} = (ZI)^{n_h} \equiv (n_h, 0)$ and $O_{v0} = (ZI)^{n_v} \equiv (n_v, 0)$. In order to cancel the excitation shared by the two lines of the L shape as shown, we get $n_h + n_v = 0$. Along the horizontal line, we have the recursion constraints due to the commutation as follows

$$a^h_{i+1} + b^h_{i+1} + a^h_i = 0 \tag{3.105}$$

$$nb^h_{i+1} + a^h_i + b^h_i = 0 \tag{3.106}$$

which give the recursive equation

$$nb^h_{i+2} + nb^h_{i+1} + b^h_i = 0. \tag{3.107}$$

This can be solved using the quadratic $ny^2 + ny + 1 = 0$ which has two roots λ_1, λ_2. Thus, we get for the other corner (a^h_i, b^h_i),

$$b^h_i = u^h_1 \lambda^i_1 + u^h_2 \lambda^i_2 \tag{3.108}$$

$$a^h_i = -u^h_1(1 + n\lambda_1)\lambda^i_1 - u^h_2(1 + n\lambda_2)\lambda^i_2. \tag{3.109}$$

Using the constraint $O_{h0} \equiv (a^h_0, b^h_0) = (-n_v, 0)$, we get $u^h_1 = -u^h_2 = \frac{-n_v}{n(\lambda_2 - \lambda_1)}$.

Similarly, for the vertical line, we have

$$a_i^v + a_{i+1}^v + b_{i+1}^v = 0 \tag{3.110}$$

$$a_i^v + b_i^v + n b_{i+1}^v = 0 \tag{3.111}$$

which gives the recursive equation

$$n b_{i+2}^v + n b_{i+1}^v + b_i^v = 0 \tag{3.112}$$

with roots $\lambda_{1,2}$ of the same characteristic equation as before i.e. $ny^2 + ny + 1 = 0$. Hence, we again get

$$b_i^v = u_1^v \lambda_1^i + u_2^v \lambda_2^i \tag{3.113}$$

$$a_i^v = -u_1^v (1 + n\lambda_1)\lambda_1^i - u_2^v (1 + n\lambda_2)\lambda_2^i. \tag{3.114}$$

Using $O_{v0} \equiv (a_0^v, b_0^v) = (n_v, 0)$, we get $u_1^v = -u_2^v = \frac{n_v}{n(\lambda_2 - \lambda_1)}$. Now, in order for the L shape to form a string operator, we need to cancel out the excitation created at the two ends. Hence, we require $a_i^v = 0$, $a_i^h = 0$ and $b_i^v + b_i^h = 0$. But

$$a_i^v = \frac{n_1}{\lambda_2 - \lambda_1}(\lambda_1^{i+2} - \lambda_2^{i+2}). \tag{3.115}$$

We notice that both λ_1 and λ_2 are negative with $|\lambda_2| > |\lambda_1|$ and thus $a_i^v = 0$ is not possible for $n > 4$.

We can have the same L shape with different boundary operators at the corner for

the horizontal and vertical segments, as shown in Fig.3.7b. In this case, in order to cancel the excitations in the plaquettes, we get $O_{h0} = (nn_v, 0)$ and $O_{v0} = (n_v, -n_v)$. The recursion relations are the same as the L shape in Fig.3.7a because of the same commutation constraints along the edge. Thus, the solutions are of the form (3.113) and (3.114) for the horizontal segment and of the form (3.113) and (3.114) for the vertical segment. Only the boundary conditions are different i.e. $O_{h0} = (a_0^h, b_0^h) = (n_v, 0)$ and $O_{v0} = (a_0^v, b_0^v) = (n_v, -n_v)$. Hence the solutions for u_i^v are modified to be $u_1^v = \frac{n_v\lambda_2}{\lambda_2-\lambda_1}$ and $u_2^v = \frac{-n_v\lambda_1}{\lambda_2-\lambda_1}$. To form a string operator, we require as in Fig. 3.7a, $a_i^v = 0$, $a_i^h = 0$ and $b_i^v + b_i^h = 0$. We have

$$a_i^v = \frac{n_v\lambda_1\lambda_2}{\lambda_1 - \lambda_2}\left[(1+n\lambda_2)\lambda_2^{i-1} - (1+n\lambda_1)\lambda_1^{i-1}\right]. \tag{3.116}$$

We again notice that both λ_1 and λ_2 are negative with $|\lambda_2| > |\lambda_1|$, and so it is impossible to have $a_i^v = 0$.

L shaped operators in Fig. 3.7(c) and (d)

In Fig. 3.7c, we have $[O_{h0}, XX] = [O_{v0}, XX] = 0$ such that $O_{h0} = (ZZ^{-1})^{n_h}$ and $O_{v0} = (ZZ^{-1})^{n_v}$. In order to cancel the common excitation, we require $n_h = nn_v$. Thus, $O_h = (ZZ^{-1})_h^n \equiv (nn_v, -nn_v)$ and $O_v = (ZZ^{-1})_v^n \equiv (n_v, -n_v)$. For the vertical line, we have the same constraints as (3.110) and (3.111), thus we get

$$b_i^v = u_1^v\lambda_1^i + u_2^v\lambda_2^i \tag{3.117}$$

$$a_i^v = -u_1^v(1+n\lambda_1)\lambda_1^i - u_2^v(1+n\lambda_2)\lambda_2^i. \tag{3.118}$$

with roots $\lambda_{1,2}$ of the same characteristic equation as before i.e. $nx^2 + nx + 1 = 0$. Using $O_2 \equiv (a_0^v, b_0^v) = (n_2, -n_2)$, we get $u_1^v = \frac{n_2\lambda_2}{\lambda_1 - \lambda_2}$ and $u_2^v = \frac{-n_2\lambda_1}{\lambda_1 - \lambda_2}$. For the horizontal line, we get

$$nb_i^h + a_{i+1}^h + b_{i+1}^h = 0 \tag{3.119}$$

$$a_i^h + b_i^h + a_{i+1}^h = 0 \tag{3.120}$$

which leads to $n(a_i^h + a_{i+1}^h) + a_{i+2}^h = 0$. This leads to

$$a_i^h = u_1^h \omega_1^i + u_2^h \omega_2^i \tag{3.121}$$

$$b_i^h = n^{-1}(u_1^h \omega_1^{i+2} + u_2^h \omega_2^{i+2}), \tag{3.122}$$

where ω_1, ω_2 are roots of the characteristic equation $x^2 + nx + n = 0$. Using $a_0^h = u_1^h + u_2^h = nn_v$ and $b_0^h = -nn_v$, we get $u_1^h = \frac{-nn_v(n+\omega_2^2)}{\omega_1^2 - \omega_2^2}$ and $u_2^h = \frac{-nn_v(n+\omega_2^2)}{\omega_1^2 - \omega_2^2}$. We get

$$a_i^h + b_i^h = \frac{n^2 n_v}{\omega_2^2 - \omega_1^2}(1 + n^{-1}\omega_1^2)(1 + n^{-1}\omega_2^2)(\omega_1^i - \omega_2^i). \tag{3.123}$$

The cancellation of excitations requires $a_i^v + b_i^v = 0$, $a_i^v + nb_i^h = 0$ and $a_i^h + b_i^h = 0$. From (3.123), we see $a_i^h + b_i^h = 0$ is not possible for $n > 4$.

We can have the same L shape with different boundary operators at the corner for the horizontal and vertical segments, as shown in Fig.3.7d. In this case, in order to cancel the excitations in the plaquettes, we get the boundary conditions $O_{h0} = (a_0^h, b_0^h) = (-n_v, n_v)$ and $O_{v0} = (a_0^v, b_0^v) = (n_v, 0)$. Hence the solutions for $u_i^{h/v}$ are

modified as follows

$$u_1^h = \frac{nn_v + n_v\omega_2^2}{\omega_1^2 - \omega_2^2} \tag{3.124}$$

$$u_2^h = \frac{-n_v\omega_1^2 - nn_v}{\omega_1^2 - \omega_2^2} \tag{3.125}$$

which gives

$$a_i^h + b_i^h = u_1^h(1 + n^{-1}\omega_1^2)\omega_1^i + u_2^h(1 + n^{-1}\omega_2^2)\omega_2^i \tag{3.126}$$

$$= \frac{n_v}{\omega_1^2 - \omega_2^2}\left\{[(n + \omega_1^2) + (1 + n^{-1}w_1^2)\omega_2^2]\omega_1^i - [(n + \omega_2^2) + (1 + n^{-1}\omega_2^2)\omega_1^2]\omega_2^i\right\} \tag{3.127}$$

$$= \frac{n_v n^2}{\omega_1^2 - \omega_2^2}\left(\omega_1^i - \omega_2^i\right). \tag{3.128}$$

The condition $a_i^h + b_i^h$ to cancel the excitation at the ends to form a string operator cannot be satisfied for $n > 4$.

Chapter 4

The "fractonal" quantum Hall effect: Fracton phases from chiral layers

4.1 Introduction

As discussed in Chapter 3 fracton phases are a new class of topological states of matter characterized by "subdimensional" quasiparticles with emergent mobility restrictions (see Refs. [152, 153] for a recent review). Initially of interest for their glassy features [39, 154] and utility as topological quantum memories [125, 155, 156, 43, 124, 157, 158] due to constrained quasiparticle dynamics [159, 160], the subject has grown to challenge the classification of topological phases of matter via topological quantum field theory [134, 161, 137, 77, 162] and demonstrated the possibility of heretofore unforeseen field theories [144, 145, 163, 52, 164, 146, 165, 166, 167, 131, 48, 168, 169, 170, 171, 172, 173, 49].

While many constructions of fracton phases have been proposed, a systematic

understanding of all possible phases is yet to be rigorously established. Most works so far have relied on constructing exactly solvable "commuting-projector" models whose Hamiltonians are sums of commuting terms [39, 154, 125, 155, 126, 174, 41, 42, 76, 127, 129, 175, 176, 128, 130, 177, 178, 179, 143, 180, 133]. However, many topological phases, including *chiral* phases with broken time-reversal symmetry, cannot be realized by such models [181]. Such phases include many of the most famous (2+1)-dimensional topological orders, including fractional quantum Hall (FQH) phases [182]. Different tools are thus required to build, study, and classify models of chiral fracton phases, the prospect of which has only recently been raised [183, 75].

Chiral topological phases nevertheless admit analytically tractable microscopic models in the form of coupled-wire constructions. These constructions, which were also discussed in Chapter 3, model topological phases as arrays of (1+1)-dimensional quantum wires with suitably chosen many-body interactions. Coupled-wire constructions allow for the use of powerful techniques from (1+1)-dimensional systems, including bosonization and conformal field theory (CFT), to describe strongly interacting phases of matter in higher dimensions. They have been used to build and analyze numerous models of topological phases in (2+1) [58, 59, 60, 61, 62, 63, 64, 65, 66, 67], (3+1) [68, 69], and higher dimensions [68], including both Abelian and non-Abelian examples.

Expanding upon the results of Chapter 3, we show that the coupled-wire formalism can be applied to realize new chiral fracton phases in (3+1) dimensions. We focus primarily on a model inspired by the wire construction of the $\nu = 1/m$ Laughlin FQH states [60, 61] that realizes subdimensional excitations with anyonic statistics inherited from those of Laughlin quasiparticles. The models we consider have a useful

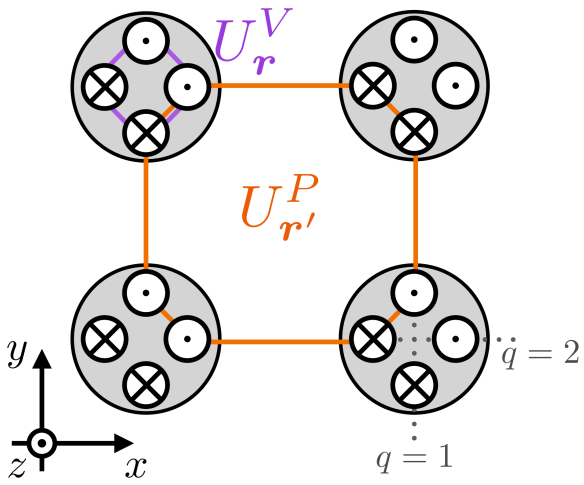

Figure 4.1: Schematic depiction of the coupled-wire array with vertex and plaquette terms $U^V_{\boldsymbol{r}}$ (purple) and $U^P_{\boldsymbol{r}}$ (orange). Gray circles represent the wires, and crossed and dotted circles represent right and left movers, respectively. The labels $q = 1, 2$ arise from viewing each wire as the intersection of a vertical and horizontal plane, respectively. .

interpretation in terms of anyon condensation, wherein stacks of $\nu = 1/m$ Laughlin phases on x-z and y-z planes are coupled by condensing "p-strings" composed of Laughlin quasiparticles at the lines of intersection of each pair of planes. This planar p-string condensation mechanism allows for the rapid determination of broad classes of new fracton phases, including examples based on non-Abelian topological orders.

The chapter is laid out as follows. In Section 4.2 we introduce our coupled-wire model and study the topological properties of its bulk and boundary. In Section 4.3 we provide a high level description of planar p-string condensation. In Appendix 4.5.1 we provide detailed calculations on the coupled-wire model that complement the discussion in the main text. In Appendix 4.5.7 we generalize our coupled-wire construction to a non-Abelian model. In Appendix 4.5.8 we present further details about planar p-string condensation, including examples and relations to existing mechanisms to generate fracton topological order.

4.2 Chiral Fracton Phase in a Laughlin Coupled-Wire Model

In this section we introduce and analyze a coupled wire model that realizes a chiral fracton phase. In Sec. 4.2.1 we define the model; starting from a decoupled array of two-component Luttinger liquids and then introducing two types of sine-Gordon terms to produce a strongly coupled phase. In Sec. 4.2.2 we explore an interpretation of the model through the lens of the planar p-string condensation mechanism. The bulk excitations are discussed in the Sec. 4.2.3. In Sec. 4.2.4 we discuss the surface theory of the model. Finally, the topological degeneracy is addressed in Sec. 4.2.5.

4.2.1 Model Definition

We consider a set of (1+1)-dimensional quantum wires oriented along the z-axis and placed on the vertices $\boldsymbol{r} = (x, y)$ of an $L_x \times L_y$ square lattice Λ in the x-y plane (see Fig. 4.1). Each vertex contains two quantum wires labeled by $q = 1, 2$, and each wire contains two chiral channels labeled by $\eta = L, R$. The wires consist of free fermions, which we write in bosonized form as $\Psi^q_{\eta,\boldsymbol{r}} \sim e^{i\phi^q_{\eta,\boldsymbol{r}}}$, where the chiral bosonic fields $\phi^q_{\eta,\boldsymbol{r}}(z)$ obey the equal-time canonical commutation relations

$$[\phi^q_{L/R,\boldsymbol{r}}(z), \phi^{q'}_{L/R,\boldsymbol{r}'}(z')] = \pm\delta_{q,q'}\delta_{\boldsymbol{r},\boldsymbol{r}'}\, i\pi\ \mathrm{sgn}(z-z'), \tag{4.1}$$

where we associate the signs + and − with $\eta = L$ and R, respectively. To specify the couplings between wires, we define new fields and commutation relations

$$\tilde{\phi}^q_{L/R,\boldsymbol{r}} = [(\phi^q_{L,\boldsymbol{r}} + \phi^q_{R,\boldsymbol{r}}) \pm m(\phi^q_{L,\boldsymbol{r}} - \phi^q_{R,\boldsymbol{r}})]/2 \tag{4.2}$$

$$[\tilde{\phi}^q_{L/R,\boldsymbol{r}}(z), \tilde{\phi}^{q'}_{L/R,\boldsymbol{r}'}(z')] = \pm\, \delta_{q,q'}\delta_{\boldsymbol{r},\boldsymbol{r}'}\, i\pi m\ \mathrm{sgn}(z-z'),$$

with m an odd integer, which are appropriate for describing Laughlin quasiparticles at filling $\nu = 1/m$. In these new variables, the local vertex operator $e^{i\tilde{\phi}^q_{\eta,\boldsymbol{r}}}$ defines a chiral quasiparticle with fermionic statistics, while the nonlocal vertex operator $e^{i\tilde{\phi}^q_{\eta,\boldsymbol{r}}/m}$ defines a chiral Laughlin quasiparticle with anyonic statistical angle $2\pi/m$.

We now couple the wires with interactions $H_{\mathrm{int}} = -\sum_{\boldsymbol{r}} \int_0^{L_z} \mathrm{d}z\ \left(\lambda_V\, U^V_{\boldsymbol{r}} + \lambda_P\, U^P_{\boldsymbol{r}}\right)$, where

$$U^V_{\boldsymbol{r}} = \cos\left[\frac{1}{m}\left(\tilde{\phi}^1_{L,\boldsymbol{r}} - \tilde{\phi}^1_{R,\boldsymbol{r}} + \tilde{\phi}^2_{L,\boldsymbol{r}} - \tilde{\phi}^2_{R,\boldsymbol{r}}\right)\right] \equiv \cos(\theta^V_{\boldsymbol{r}}) \tag{4.3}$$

$$U^P_{\boldsymbol{r}} = \cos\left[2\left(\tilde{\theta}^1_{\boldsymbol{r},\hat{\boldsymbol{y}}} + \tilde{\theta}^2_{\boldsymbol{r}+\hat{\boldsymbol{y}},\hat{\boldsymbol{x}}} - \tilde{\theta}^1_{\boldsymbol{r}+\hat{\boldsymbol{x}},\hat{\boldsymbol{y}}} - \tilde{\theta}^2_{\boldsymbol{r},\hat{\boldsymbol{x}}}\right)\right] \equiv \cos(\theta^P_{\boldsymbol{r}}),$$

and $2\tilde{\theta}^q_{\boldsymbol{r},\hat{\boldsymbol{a}}} = \tilde{\phi}^q_{L,\boldsymbol{r}} - \tilde{\phi}^q_{R,\boldsymbol{r}+\hat{\boldsymbol{a}}}$, with $\hat{\boldsymbol{a}} = \hat{\boldsymbol{x}}, \hat{\boldsymbol{y}}$ the unit vectors in the x and y directions. Importantly, these interactions are local when written in terms of the "fundamental" fermions $\Psi^q_{\eta,\boldsymbol{r}}$; this can be checked explicitly using Eq. (4.2) (see also Ref. [61]). Furthermore, it is straightforward to check using Eq. (4.2) that the interaction terms $U^V_{\boldsymbol{r}}$ and $U^P_{\boldsymbol{r}}$ commute among themselves and can therefore be simultaneously diagonalized. In the strong-coupling limit $\lambda_P, \lambda_V \to \infty$, the ground state manifold is obtained by pinning the arguments of $U^V_{\boldsymbol{r}}$ and $U^P_{\boldsymbol{r}}$ to integer multiples of 2π.

We remark that, strictly speaking, the vertex terms $U_{\boldsymbol{r}}^V$ appearing in Eq. (4.3) are not translation invariant in the z-direction when written in terms of the original fermions due to the presence of oscillatory factors $\sim e^{i\,4k_F\,z}$, where k_F is the Fermi wavenumber. These factors can be removed by making a global change of variables $\tilde{\phi}^2_{\eta,\boldsymbol{r}} \to -\tilde{\phi}^2_{\eta,\boldsymbol{r}}$, which amounts to choosing different bosonization conventions depending on the index $q = 1, 2$. This effectively redefines $k_F \to -k_F$ for the $q = 2$ layers, leading to the pairwise cancellation of the $2k_F$ factors giving rise to the oscillations, while maintaining commutativity of the vertex and plaquette terms and preserving the canonical commutation relations. This transformation does not affect any of the properties of the model considered here, so we continue to use the original convention of Eq. (4.3).

4.2.2 Planar p-String Condensation Interpretation

The interactions (4.3) have an appealing interpretation in terms of coupled layers. Consider a system of initially decoupled $\nu = 1/m$ Laughlin FQH systems stacked along y-z and x-z planes of the cubic lattice. We assign the labels $q = 1, 2$ to y-z and x-z planes, respectively. Now define a square lattice in the x-y plane whose vertices $\boldsymbol{r}$ are the locations of the lines of intersection of pairs of x-z and y-z planes. We can now couple pairs of Laughlin planes where they intersect by condensing a bosonic bound state of local excitations. The simplest nontrivial object we can condense is a bound state of two quasiparticle-quasihole pairs, one pair for each $q = 1, 2$. A microscopic model for this setup is obtained by representing each Laughlin plane

using a coupled-wire construction. Within this construction, the local operator that creates a Laughlin quasiparticle-quasihole pair within a layer is given by [61]

$$Q^q_{\boldsymbol{r}} = e^{i\frac{1}{m}(\tilde{\phi}^q_{L,\boldsymbol{r}} - \tilde{\phi}^q_{R,\boldsymbol{r}})}. \tag{4.4}$$

Adding $-\lambda_V \sum_{\boldsymbol{r}} \int_0^{L_z} \mathrm{d}z\, U^V_{\boldsymbol{r}}$ to the Hamiltonian and taking $\lambda_V \to \infty$ thus condenses the bound state of two such quasiparticle-quasihole pairs for all z along the intersection line $\boldsymbol{r}$. This four-body composite can be viewed as a small loop composed of Laughlin quasiparticles (i.e. a p-string, see below), which fluctuates in the presence of condensation terms $U^V_{\boldsymbol{r}'}$ located at lattice sites $\boldsymbol{r}' \neq \boldsymbol{r}$. The plaquette terms $U^P_{\boldsymbol{r}}$ emerge by performing degenerate perturbation theory in the coupling g that couples the wires within a given x-z or y-z plane to form the Laughlin FQH layer building blocks [see Appendix 4.5.2].

The coupled-wire model with interactions (4.3) is thus one simple instance of a large class of models obtained by coupling two interpenetrating stacks of (2+1)-dimensional topological phases. The condensation process implemented by the vertex terms $U^V_{\boldsymbol{r}}$ is an example of *p-string* condensation [76, 127, 128], because it proliferates closed loops composed of Laughlin quasiparticles. This distinguishes p-string condensation from standard anyon condensation [184], which proliferates pointlike anyon composites. Anyon condensation has also been used to build 3D topological orders from 2D building blocks [185, 69, 75], but such constructions do not yield totally immobile fracton excitations. In contrast, p-string constructions generically lead to fractons (for a summary, see Sec. 4.3).

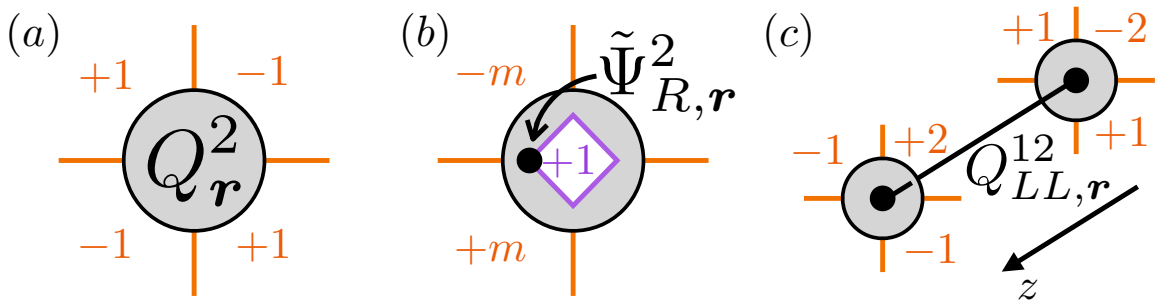

Figure 4.2: Action of (a) the Laughlin quasiparticle operator 4.4, (b) the chiral electron operator 4.6, and (c) the composite chiral quasiparticle operator $Q^{12}_{LL,\boldsymbol{r}}$ 4.7. Integer charges of the vertex and plaquette solitons are indicated in purple and orange, respectively. .

The present class of models is distinguished from other p-string condensation constructions [76, 127, 128, 183] by the fact that p-strings are only allowed to fluctuate within x-y planes. This new restriction enables the condensation of p-strings composed of anyons with nontrivial mutual statistics—the Laughlin p-strings defined above being a simple example. In prior p-string constructions, such condensates could not be consistently defined due to the nontrivial braiding of p-strings from intersecting planes. The construction introduced here thus enables a host of new fracton phases not obtainable by other means that are explored further in Sec. 4.3 and Appendix 4.5.8.

4.2.3 Bulk Excitations of the Coupled-Wire Model

The coupled-wire array supports two kinds of excitations: charged solitons, i.e. abrupt jumps of the pinned fields $\theta^V_{\boldsymbol{r}}, \theta^P_{\boldsymbol{r}}$ between integer multiples of 2π, and neutral Gaussian fluctuations of these fields around their minima. The solitons constitute gapped topological excitations of the theory. The Gaussian fluctuations become gapless in the thermodynamic limit $L_x, L_y \to \infty$ [80] [see Appendix 4.5.3]. However, they are topologically trivial and do not contribute to the charge response at the level

of Eq. (4.3). Furthermore, numerical results indicate a scaling limit $L_x = L_y \to \infty$, $U \gtrsim L_x^{2.8}$ in which they are gapped [see Appendix 4.5.3]. We defer further analysis of the Gaussian fluctuations and their stability to future work.

Pointlike charged excitations of the coupled-wire array are identified with solitons:

$$\partial_z \theta_{\boldsymbol{r}}^{V,P} \to \partial_z \theta_{\boldsymbol{r}}^{V,P} + 2\pi n\, \delta(z - z_0), \tag{4.5}$$

for $n \in \mathbb{Z}$ and some $0 \leq z_0 < L_z$. A basis for these excitations is obtained by considering the action of all local vertex operators in a given wire. The vertex operators at our disposal are the Laughlin quasiparticle-quasihole pair operator $Q_{\boldsymbol{r}}^q(z)$ [Eq. (4.4)], the chiral "electron" operator

$$\tilde{\Psi}_{\eta,\boldsymbol{r}}^q = e^{i\tilde{\phi}_{\eta,\boldsymbol{r}}^q}, \tag{4.6}$$

and the chiral operator

$$Q_{\eta,\boldsymbol{r}}^q(z_1, z_2) = \exp\left(\frac{i}{m}\int_{z_1}^{z_2} \mathrm{d}z\; \partial_z \tilde{\phi}_{\eta,\boldsymbol{r}}^q\right), \tag{4.7}$$

which moves a Laughlin quasiparticle from $z = z_1$ to z_2. (Note that $Q_{\boldsymbol{r}}^2 = e^{i\theta_{\boldsymbol{r}}^V} Q_{\boldsymbol{r}}^{1\dagger}$, so that $Q_{\boldsymbol{r}}^{1\dagger} \simeq Q_{\boldsymbol{r}}^2$ when acting on the ground state, where $\theta_{\boldsymbol{r}}^V$ is pinned.) Of these three operator types, the first two create genuine integer solitons in $U_{\boldsymbol{r}}^{V,P}$, see Fig. 4.2(a) and (b). $Q_{\eta,\boldsymbol{r}}^q(z_1, z_2)$ creates pairs of integer solitons in $U_{\boldsymbol{r}}^P$, but a pair of *fractional solitons* in $U_{\boldsymbol{r}}^V$. This constitutes a *linelike* excitation, because it shifts $U_{\boldsymbol{r}}^V$ by a noninteger

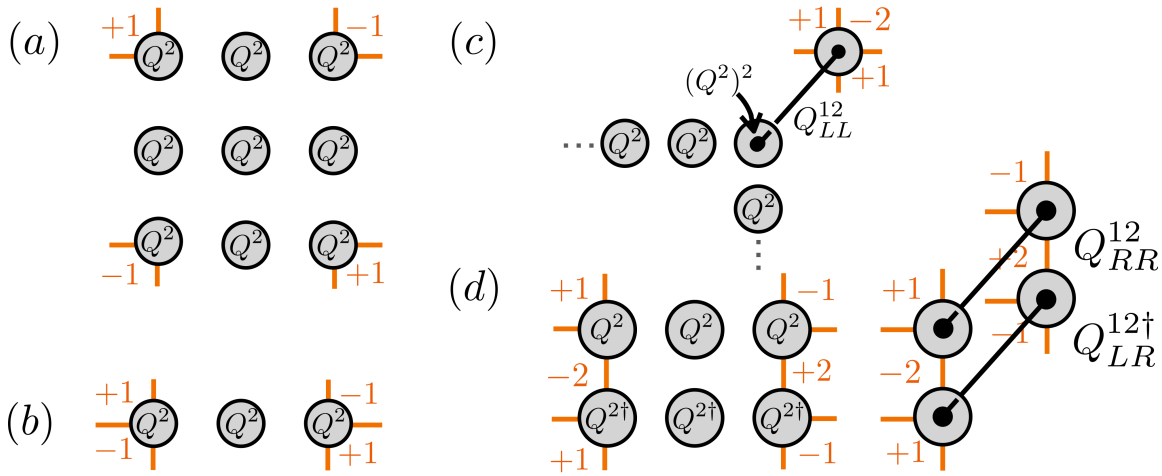

Figure 4.3: Subdimensional excitations of the coupled-wire array include (a) immobile fractons, (b) lineons mobile only along fixed lattice directions, and (d) planons mobile only within 2D planes. Panel (c) depicts the fusion of x and y lineons into a z lineon, while (d) depicts a pair of operators that can be multiplied to allow a planon to "turn a corner" between the x- and z-directions. .

multiple of 2π in the region between $z_{1,2}$. However, one can build composite operators

$$Q^{qq'}_{\eta\eta',\boldsymbol{r}}(z_1,z_2) = Q^{q}_{\eta,\boldsymbol{r}}(z_1,z_2)[Q^{q'}_{\eta',\boldsymbol{r}}(z_1,z_2)]^\dagger \tag{4.8}$$

for which such linelike excitations cancel; for example, $Q^{12}_{LL,\boldsymbol{r}}(z_1,z_2)$ creates a pair of three integer plaquette solitons separated by $z_2 - z_1$ along a wire [see Fig. 4.2(c)].

A hierarchy of quasiparticle mobility restrictions follows from the observation that a single plaquette excitation cannot be moved by a local operator. This mobility restriction in the x-y plane is visible in Fig. 4.2, which demonstrates that plaquette solitons of strength ± 1 are created in groups of at least four. Immobility of the plaquette solitons in the z-direction can be deduced from a "Gauss's-law" constraint;

for any compact region M in the x-y plane, we have

$$\sum_{\boldsymbol{r}\in M} \theta^P_{\boldsymbol{r}}(z) = \sum_{(\boldsymbol{r},\hat{\boldsymbol{a}})\in\partial M} 2\,\tilde{\theta}^q_{\boldsymbol{r},\hat{\boldsymbol{a}}}(z), \tag{4.9}$$

where the sum on the right-hand side runs over bonds contained in the boundary ∂M of M. [Note that q and $\hat{\boldsymbol{a}}$ are correlated in this sum: $\hat{\boldsymbol{a}} = \hat{\boldsymbol{x}}$ ($\hat{\boldsymbol{y}}$) implies $q = 2$ (1).] Suppose there exists a local operator $\mathcal{O}$ that moves a single ± 1 plaquette soliton from z_1 to z_2. Such an operator shifts the left-hand side of Eq. (4.9) by $\pm 2\pi$. However, because $\mathcal{O}$ is local, we can always choose M larger than $\mathcal{O}$'s support; hence, $\mathcal{O}$ commutes with the right-hand side of (4.9), a contradiction. Thus all local operators must create plaquette solitons in pairs of charge ± 1 at fixed z, establishing charge-neutrality as a necessary (but not sufficient) condition for mobility in z.

The immobility of a single plaquette soliton implies that these excitations are fractons. Since they are created by the same operators $Q^q_{\boldsymbol{r}}$ that create Laughlin quasiparticle-quasihole pairs in the $\nu = 1/m$ FQH state, we conclude that the condensation transition described in the coupled-layer picture transmutes quasiparticles with planar mobility into immobile subdimensional excitations. A group of four fractons created by applying, e.g., $Q^2_{\boldsymbol{r}}$ to the ground state can be separated from one another by sequential application of Q^2 operators on contiguous vertices, creating a rectangular membrane operator with fractons at its corners [see Fig. 4.3(a)]. Alternatively, $Q^2_{\boldsymbol{r}}$ can be used to propagate *pairs* of fractons in the x- or y-direction, indicating that such pairs become "lineons," i.e. quasiparticles mobile only along one-dimensional submanifolds of the wire array [see Fig. 4.3(b)]. As shown in Fig. 4.3(c), lineons

mobile in the x- and y-directions can "fuse" to become a lineon mobile in the z-direction. Fig. 4.3(d) shows how pairs of lineons can be combined to form "planons" with mobility in, e.g., x-z planes. This hierarchy of quasiparticle mobility is a familiar feature of many fracton models and also follows directly from the planar p-string condensation interpretation of the coupled-wire model [see Section 4.3].

Finally, we note that the braiding statistics of these subdimensional quasiparticles reveals their fractionalized nature. The notion of mutual and self-statistics of fractons, lineons, and planons has been defined [186, 147] and follows from the phase acquired upon exchanging the membrane and string operators used to propagate the corresponding excitations. In the present case, this exchange phase follows from the commutation relations (4.2) and reflects the relationship between fractons and Laughlin quasiparticles. For example, the statistical angle obtained from braiding two lineons [e.g., those depicted in Figs. 4.2(c) and 4.3(b)], or two planons in vertically offset x-z planes [Fig. 4.3(d)], is $\pm 2\pi/m$.

4.2.4 Surface Theory

We now show that the coupled-wire model with interactions (4.3) possesses chiral surface states that are gapless at any system size, evoking a (3+1)-dimensional generalization of FQH physics. To see this, we consider a square lattice with $L_x L_y$ vertices, each containing four chiral modes, and place periodic boundary conditions (PBC) in the z-direction and open boundary conditions (OBC) in the x- and y-directions. This leaves a 2D boundary with the topology of a 2-torus. Next, we apply

a counting argument due to Haldane [114] to determine how many of the $4L_xL_y$ chiral modes are gapped by the interactions (4.3). Recalling that a single cosine term gaps out two modes with opposite chirality in the strong-coupling limit, and noting that there are L_xL_y vertex terms $U^V_{\boldsymbol{r}}$ and $(L_x-1)(L_y-1)$ plaquette terms $U^P_{\boldsymbol{r}}$, we conclude that the interactions (4.3) are sufficient to gap out all but $N = 2(L_x + L_y - 1)$ modes in the array. For the remainder of this paper we assume a fixed finite L_x, L_y.

In Appendix 4.5.1, we show that these N gapless modes are strictly localized on the 2D surface of the array by explicitly identifying a set of surface modes that commute with the bulk couplings. Here, we summarize several notable features of these modes. First, they are chiral, with modes localized on opposite faces of the wire array having opposite chirality. Second, they are spatially overlapping and have nontrivial commutation relations that follow directly from Eq. (4.2) and can be encoded in an $N \times N$ integer matrix K. Third, the K-matrix for modes living on the same face of the array closely resembles that of a stack of fractional quantum Hall states coupled by long-range Coulomb interactions [187, 188, 189, 190].

The spatially overlapping and noncommuting chiral gapless surface modes discussed above can be disentangled by coupling additional boundary wires into the array as shown in Fig. 4.4. We add $2(L_x + L_y)$ wires, each carrying one right- and one left-mover governed by the commutation relation (4.2). The number of gapless modes in the array then increases to $N + 4(L_x + L_y) = 3N + 4$. We now add additional strong commuting interaction terms to the Hamiltonian until $N + 2$ gapless chiral modes remain. First we introduce $2(L_x - 1) + 2(L_y - 1)$ truncated plaquette terms along the left, right, top, and bottom $(\mathrm{L}, \mathrm{R}, \mathrm{T}, \mathrm{B})$ faces of the array. For example, on the T

face we add the couplings [compare to Eq. (4.3)]

$$U^{\mathrm{T}}_{(x,L_y)} = \cos\Big[2\Big(\tilde{\theta}^1_{(x,L_y),\hat{\boldsymbol{y}}} - \tilde{\theta}^1_{(x+1,L_y),\hat{\boldsymbol{y}}} - \tilde{\theta}^2_{(x,L_y),\hat{\boldsymbol{x}}}\Big)\Big] \tag{4.10}$$

for $x = 1, \ldots, L_x - 1$, and likewise for the remaining three faces. Here, $2\tilde{\theta}^1_{(x,L_y),\hat{\boldsymbol{y}}} = \tilde{\phi}^1_{L,(x,L_y)} - \tilde{\phi}^1_{R,(x,L_y+1)}$, where $\tilde{\phi}^1_{R,(x,L_y+1)}$ is one of the additional boundary fields. This removes $2N - 4$ gapless modes, leaving 6 outstanding gapless modes. To dispose of these modes, it suffices to add truncated plaquette terms to three "corners" of the array; for example, on the top-left (TL) corner we add the coupling [compare to Eq. (4.3)]

$$U^{\mathrm{TL}}_{(1,L_y)} = \cos\Big[2\Big(\tilde{\theta}^1_{(1,L_y),\hat{\boldsymbol{y}}} + \tilde{\theta}^2_{(0,L_y),\hat{\boldsymbol{x}}}\Big)\Big], \tag{4.11}$$

and likewise for the TR and BR corners. Here $\tilde{\theta}^2_{(0,L_y),\hat{\boldsymbol{x}}} = \tilde{\phi}^2_{L,(0,L_y)} - \tilde{\phi}^2_{R,(1,L_y+1)}$, where $\tilde{\phi}^2_{L,(0,L_y)}$ is one of the additional boundary fields. Note that we could also add a truncated plaquette term to the BL corner, but the argument of this plaquette term is linearly dependent with the other plaquette terms in the array and hence is not necessary for the construction.

The modified surface theory constructed above is that of $N + 2 = 2(L_x + L_y)$ *commuting* chiral gapless modes—precisely what one would obtain for a stack of $L_x + L_y$ decoupled $\nu = 1/m$ Laughlin states. In fact, the surface theory defined above arises perturbatively within the coupled-layer interpretation of the model when the underlying Laughlin layers are arranged such that their chiral edges do not undergo

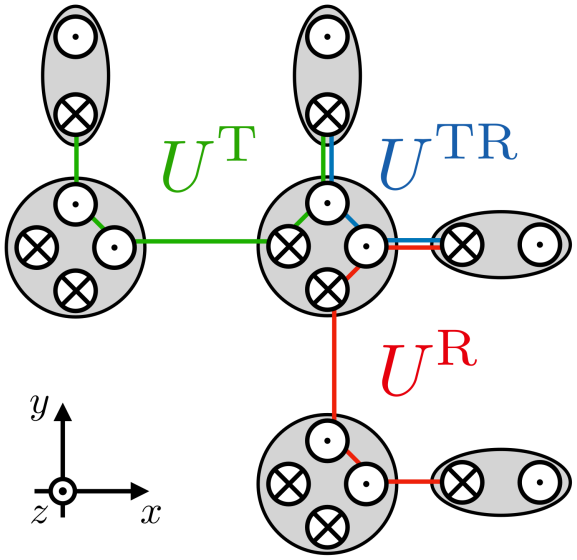

Figure 4.4: Schematic of the surface termination obtained by adding auxiliary boundary wires (gray ovals) and new boundary couplings (green, blue, and red). Dangling chiral gapless modes on the top and right surfaces are clearly visible. .

p-string condensation [see Appendix 4.5.2].

One advantage of this alternative surface termination is that it makes the system's nontrivial Hall response transparent. Since the low-energy theory consists of $N+2$ decoupled chiral gapless modes that are identical to $\nu = 1/m$ Laughlin edge states, inserting a vector potential in the z-direction corresponding to one flux quantum pumps a fractional charge eL_x/m (eL_y/m) between the T/B (L/R) faces of the array [191], corresponding to quantized fractional Hall conductivity σ_{yz} (σ_{xz}) [192, 193]. This response is ultimately mediated by the bulk fractons, which descend from Laughlin quasiparticles and whose bound states are the only charged bulk excitations.

4.2.5 Topological Degeneracy

In order to calculate the topological degeneracy of the ground-state manifold, we add additional couplings to remove the remaining chiral gapless surface modes. Starting from the surface termination shown in Fig. 4.4, we add $N/2+1 = L_x + L_y$ strong interaction terms of the form $\cos(2\tilde{\theta}^q_{\boldsymbol{r},\hat{\boldsymbol{a}}})$ that couple gapless chiral modes on opposing faces of the array. The resulting model can be viewed as a three-torus containing two intersecting surface defects, each with the topology of a two-torus, on which the final interaction terms reside. This unusual boundary condition simplifies the analysis relative to the case of standard PBCs without auxiliary boundary wires [see Appendix 4.5.6].

We calculate (in Appendix 4.5.5) the topological degeneracy using the method of Ref. [67], starting from the set of strong-coupling ground states labeled by the values of the pinned bulk fields $\theta^{V,P}_{\boldsymbol{r}} \in 2\pi\mathbb{Z}$ and their boundary counterparts. Naively, this implies an infinite-dimensional ground state manifold; however, many of these ground states are equivalent since the bosonic fields $\phi^q_{\eta,\boldsymbol{r}}$ are only defined modulo 2π. Accounting for this redundancy, we find that the ground-state manifold has dimension $m^{L_x+L_y}$. This subextensive ground-state degeneracy is a hallmark of "type-I" fracton phases. We remark that the model also exhibits a subextensive number of superselection sectors with standard PBC, as shown in Appendix 4.5.6. In Appendix 4.5.10 we define an exactly solvable lattice model containing a chiral sector whose bulk topological excitations and ground-state degeneracy exactly match those of the coupled-wire model.

4.3 Planar p-String Condensation Mechanism

In this Section we expound upon the planar p-string condensation mechanism for constructing fracton phases of matter. This was introduced in the context of the coupled-wire model in the previous section, but here we study the mechanism more abstractly from the point of view of coupled layers of topological orders that support nontrivial anyonic excitations. In Sec. 4.3.1, we discuss how to perform the planar p-string condensation procedure at the level of the anyon theory of the underlying 2D layers. In Sec. 4.3.2, we apply this condensation procedure to the example of chiral $\mathbb{Z}_N$ anyon layers, providing a high-level description of the topological fracton sectors in the coupled-wire model from the previous section. A lattice model that is foliated equivalent [134] to this chiral fracton theory is described in Appendix 4.5.8 alongside further examples, as well as the connection between planar p-string condensation, gauging planar subsystem symmetries [183] and topological defect networks [77].

To date, several constructions of fracton models from coupled layers have appeared in the literature. They can all be understood as some form of p-string condensation on a stack of 2D layers with topological order. First we review Refs. [76, 127, 128], where the authors consider stacking topological layers along xy, yz, and xz planes of the cubic lattice. These layers must support a group (under fusion) of Abelian bosons $\mathcal{A}$. The authors consider abstract $\mathcal{A}$-net configurations, which correspond to general stringlike objects that satisfy $\mathcal{A}$ fusion rules (for $\mathbb{Z}_2$ these are simply loops). Composite p-string excitations, with fusion rules given by $\mathcal{A}$, are formed along these $\mathcal{A}$-nets in three dimensional space by pinning the appropriate Abelian g boson in a

topological layer to its intersection point with a string segment labelled by g in the $\mathcal{A}$-net. These p-string excitations are then condensed to form a cage-net fracton phase. This is achieved by adding local perturbations to the edges where layers intersect that fluctuate small loops of the p-string excitations, by creating particle-antiparticle pairs of g bosons in both intersecting layers. The effect of the condensation is to confine any particles that braid nontrivially with the p-strings, and to promote the defect appearing at the open end of a p-string into a deconfined fracton excitation. Particles that braid trivially with the p-strings remain deconfined planons, and the $\mathcal{A}$ bosons in particular become equivalent to a pair of fractons (they can be viewed as a small segment of p-string). Particles that braid nontrivially with the p-string can be paired up across different layers to form deconfined lineons (for perpendicular layers) or planons (for parallel layers).

More recently, in Ref. [183], a construction was presented for a single stack of topological layers along the xy planes of a cubic lattice, also supporting a group $\mathcal{A}$ of Abelian bosons or fermions. Once again p-string excitations with fusion rules given by $\mathcal{A}$ can be constructed. However, in this construction, the p-strings are only condensed within yz and xz planes of the cubic lattice (this can be done simultaneously as the p-strings braid trivially). This renders particles that braid nontrivially with the p-strings immobile fractons, as their movement in the $\hat{x}$ and $\hat{y}$ directions becomes confined. Pairs of such fractons, separated along $\hat{x}$ or $\hat{y}$, are equivalent to charges under the condensing p-strings, and have planon mobility. The defects that appear at the ends of p-strings become lineons. Again particles that braid trivially with the p-strings remain deconfined planons. The $\mathcal{A}$ particles in particular are equivalent to

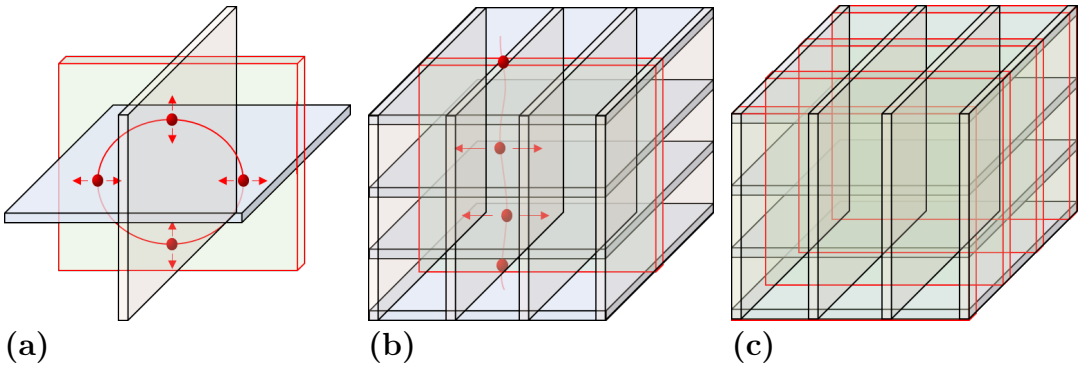

Figure 4.5: (a) A loop of p-string excitation, confined to the xy plane (green), at the junction of two topological layers. Anyons (red) are pinned to the p-string where it pierces through a topological layer. The p-string, and attached anyons, fluctuates over the xy plane (shown by red arrows).
(b) A system of topological layers in xz and yz planes with an extended p-string excitation fluctuating over an xy plane (green), as indicated by red arrows.
(c) A fracton model obtained from topological layers in xz and yz planes via p-string condensation within xy layers (green). .

a pair of lineons, as they can be viewed as small segments of p-string.

Here, we describe yet another p-string construction. We consider topological layers stacked along the xz and yz planes of the cubic lattice that support a group $\mathcal{A}$ of Abelian anyons that do not need to be bosons or fermions (to construct a consistent lattice model they must have on-site string operators, which excludes semions in particular). We then consider condensing p-strings, made up of $\mathcal{A}$ excitations, within xy planes of the cubic lattice only. This promotes particles in the layers that braid nontrivially with the Abelian $\mathcal{A}$ anyons into lineons. The defect at the open end of a p-string is promoted to a fracton. Particles in the layers that braid trivially with the $\mathcal{A}$ anyons remain planons. In particular, an $\mathcal{A}$ anyon in an xz or yz plane is equivalent to a pair of fractons, as it can be viewed as a small segment of p-string.

4.3.1 Anyon theory description

We consider layers described by an emergent anyon theory (modular tensor category) $\mathcal{M}$ [194, 11] that contains a group $\mathcal{A}$ of Abelian anyons. The anyon theory can be broken up into a direct sum according to the braiding phases of the anyons with the Abelian particles in $\mathcal{A}$, which form characters χ of the group $\mathcal{A}$,

$$\mathcal{M} = \bigoplus_{\chi \in \widehat{\mathcal{A}}} \mathcal{C}_\chi \,. \tag{4.12}$$

Specifically, an anyon $a_\chi \in \mathcal{C}_\chi$ and an Abelian anyon $g \in \mathcal{A}$ have S-matrix element $S_{a_\chi,g}|S_{a_\chi,g}|^{-1} = \chi(g)$.

We start from a system of decoupled topological layers, stacked along the xz and yz planes of a cubic lattice, that support anyon theories denoted by $\mathcal{M}_{xz}$ and $\mathcal{M}_{yz}$ respectively (The anyon theories need not be the same in every layer, so long as each supports a subgroup of Abelian anyons isomorphic to $\mathcal{A}$). We utilize the cubic lattice to label anyons by their position, where $a_{x\tilde{y}z}$ denotes an anyon in the yz layer at coordinate x, located between xz layers at y and $y+1$, and contained within the xy plane at coordinate z. Since the $a_{x\tilde{y}z}$ anyon is free to move throughout the yz layer with coordinate x (before the layers are coupled) we also utilize the notation a_x to indicate the anyon is located somewhere in that layer. Similarly, we use the notation $a_{x\tilde{z}}$ to denote that the anyon is located in a strip of the yz layer with coordinate x, between the xy planes at z and $z+1$. We employ similar notation throughout this section and Appendix 4.5.8.

Next, we add coupling terms to the decoupled-layer Hamiltonians, at every triple

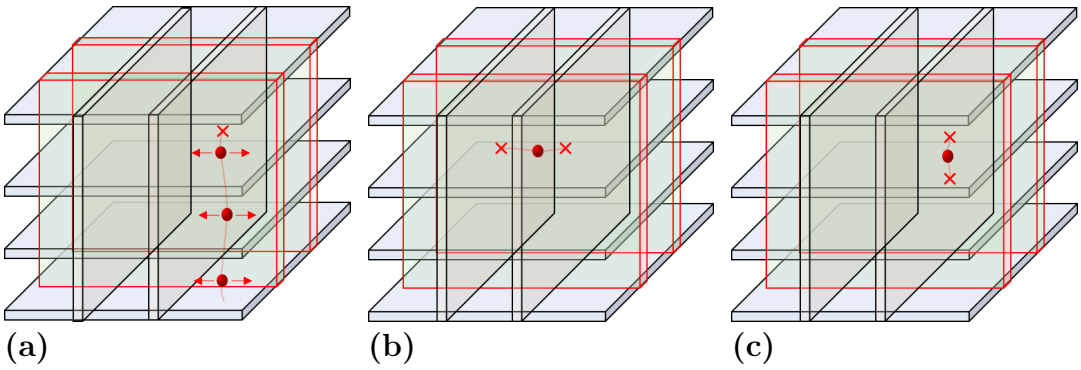

Figure 4.6: (a) The red $\times$ depicts a fracton excitation in the planar p-string condensed layer model. It appears at the end of a p-string that has been condensed in an xy-plane (indicated by red arrows) and so does not incur an energy penalty except at the open endpoint. Hence the excitation is pointlike.
(b) A fracton dipole oriented along $\hat{x}$. This is equivalent to an open p-string piercing a single yz layer, which pins a single Abelian anyon (red sphere). For bosonic (fermionic) p-strings this composite excitation is a yz planon. For p-strings consisting of Abelian anyons with a modular braiding this excitation is a $\hat{y}$ lineon as it cannot pass through the p-string condensates on the xy planes without incurring an energy penalty.
(c) A fracton dipole oriented along $\hat{y}$. Similar to (b) for bosonic (fermionic) p-string condensation this is an xz planon. For modular Abelian anyon p-strings this is an $\hat{x}$ lineon.
.

intersection point of an xz and yz layer with an xy plane, that simultaneously create g-$\overline{g}$ pairs, for $g \in \mathcal{A}$, in both $\mathcal{M}_{xz}$ and $\mathcal{M}_{yz}$, see Fig. 4.5a. In the limit of infinitely strong coupling this induces p-string excitations, formed by composites of $\mathcal{A}$ anyons, to fluctuate and condense in the xy planes, see Fig. 4.5b. For the planar p-string condensate to lead to a consistent gapped phase the F-symbols restricted to $\mathcal{A}$ must be trivial. The limit of the inter-plane spacing along $\hat{z}$ going to zero is particularly relevant for the coupled-wire construction from the main text.

In the p-string condensed phase, the topological excitations are generated by fusion products of:

- Fractons $f^g_{\tilde{x}\tilde{y}z} \sim \prod_{a<\tilde{x}} g_{a\tilde{y}z}$, with $\mathcal{A}$ fusion rules, that appear on xy plaquettes of the cubic lattice. Where $\tilde{x}$ denotes the point between layers x and $x+1$, and

similarly for $\tilde{y}$. These fractons appear at the open endpoints of p-strings that consist of a line of g anyons, such as the fusion product of all $g_{a\tilde{y}z}$ with $a < \tilde{x}$, see Fig. 4.6a.

- Lineons along $\hat{x}$ given by $(a_\chi)_{x\tilde{z}}$ and similarly along $\hat{y}$ given by $(b_\chi)_{y\tilde{z}}$, for anyons $a_\chi, b_\chi \in \mathcal{C}_\chi$, see Figs. 4.7a, 4.7b. There are also composite lineons along $\hat{z}$, given by $\ell^{ab}_{xy} \sim (a_\chi)_{x\tilde{z}}(b_{\overline{\chi}})_{y\tilde{z}}$, see Fig. 4.7c.

- Planons $(a_1)_{x/y}$. For bosonic or fermionic p-string excitations this includes any nontrivial $(g_1)_x = f^g_{\tilde{x}\tilde{y}z} f^{\overline{g}}_{(\tilde{x}-1)\tilde{y}z}$, see Fig. 4.6b, and similarly for y, see Fig. 4.6c. For p-strings formed by more general Abelian anyons with a modular braiding the fracton composites $(g_\chi)_{x\tilde{z}} = f^g_{\tilde{x}\tilde{y}z} f^{\overline{g}}_{(\tilde{x}-1)\tilde{y}z}$ are in fact $\hat{y}$ lineons, and similarly $(g_\chi)_{y\tilde{z}}$ are $\hat{x}$ lineons. (Since modular subtheories of an anyon model factor out [195], this case corresponds to the chiral $\mathbb{Z}_N$ fracton model described below stacked with some other layers.) There are also composite planons $(a_\chi)_x(b_{\overline{\chi}})_{(x-1)}$, see Fig. 4.7f, and similarly for y and z, see Figs. 4.7e, 4.7d.

In this class of models the fractons are Abelian, while the lineons may be non-Abelian. The braidings of the quasiparticles are inherited from the $\mathcal{M}$ layers. In particular, the fracton-composite planons may have nontrivial mutual braidings. Similarly the lineon-composite planons may have nontrivial mutual braidings. Single lineons and planons may also have nontrivial topological spin [147].

In the limit that the inter-plane spacing goes to zero there is no space for excitations supported between layers. However, all the topological excitations can be pushed onto p-string layers and these representatives survive the limit. This is required to match

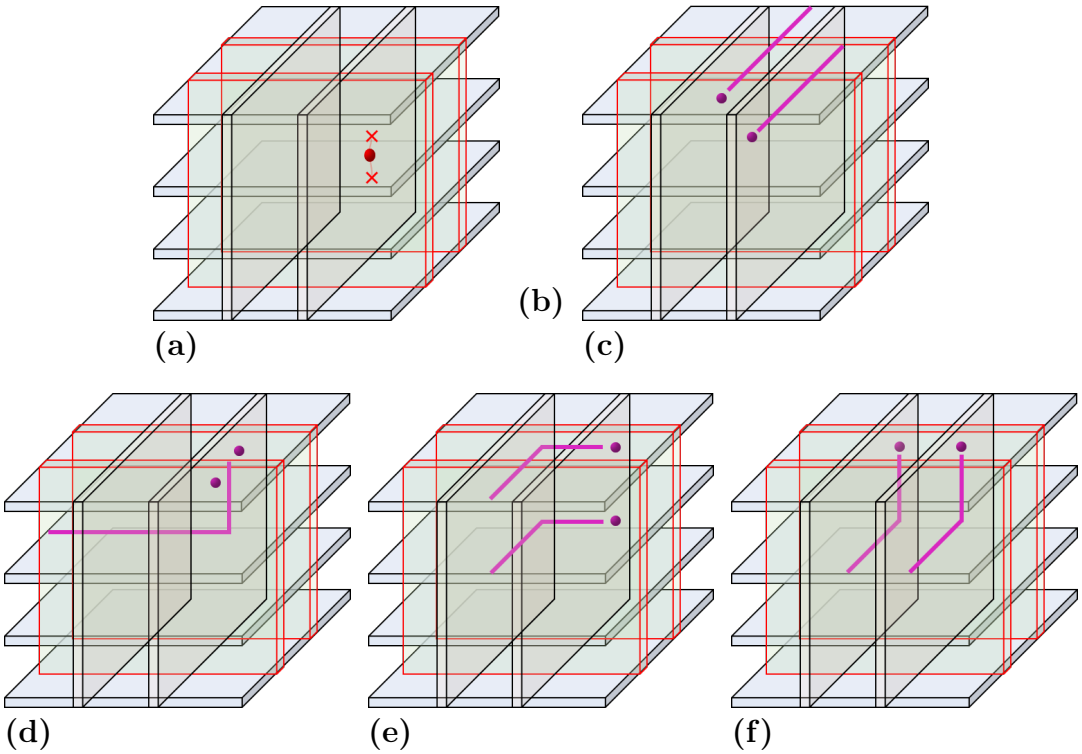

Figure 4.7: (a) An anyon in an xz layer that braids nontrivially with the p-strings becomes an $\hat{x}$ lineon after condensation.
(b) Similarly an anyon in a yz layer that braids nontrivially with the p-strings becomes a $\hat{y}$ lineon.
(c) A composite of $\hat{x}$ and $\hat{y}$ lineons that, together, braid trivially with the p-strings is a $\hat{z}$ lineon.
(d) A dipole of $\hat{x}$ (or $\hat{y}$) lineons that can be created by a local string operator oriented along $\hat{z}$, is an xy planeon.
(e) A dipole of $\hat{x}$ lineons separated along $\hat{y}$ that, together, braid trivially with the p-strings is an xz planeon.
(f) Similarly a dipole of $\hat{y}$ lineons separated along $\hat{x}$ that, together, braid trivially with the p-strings is a yz planeon. .

the excitations with those arising in the coupled-wire model from the previous section.

4.3.2 Example: $\mathbb{Z}_N$ anyon layers

We now present an example of the construction outlined above that reproduces the topological fracton sectors found in the Abelian coupled-wire construction from Section 4.2.3. We consider Abelian chiral topological layers with $\mathbb{Z}_N^{(n)}$ anyons, in the

notation of Ref. [196], for N an odd integer and n coprime to N. For $n = 2, N = m$, this describes the anyon theory of a Laughlin FQH state at filling fraction $\nu = \frac{1}{m}$, modulo the physical fermion. The topological charges, and their fusion, are described by the cyclic group $\mathbb{Z}_N$ under addition. The S-matrix and topological spins of the anyons are

$$S_{a,b} = \frac{1}{\sqrt{N}} e^{i\frac{4\pi n}{N}ab}, \qquad \theta_a = e^{i\frac{2\pi n}{N}a^2}, \tag{4.13}$$

while the quantum dimensions and F symbols are trivial. The obvious $\mathbb{Z}_N$ grading on the anyons is induced by braiding with the 1 anyon that generates the $\mathbb{Z}_N$ under fusion with itself (using additive notation for the composition rule i.e. 0 denotes the vacuum). The 1 anyon is not a boson or fermion as it has topological spin $e^{i\frac{2\pi n}{N}}$.

A fracton model is constructed by driving a $\mathbb{Z}_N$ p-string condensation transition within the xy planes of a stack of $\mathbb{Z}_N$ anyon theories along the xz and yz planes of a cubic lattice. This case is slightly degenerate and unusual in an interesting way, since there are no nontrivial particles in the trivial sector (i.e. the sector containing the particles that braid trivially with 1), as n is coprime to N. Even the generating particle 1 braids nontrivially with itself. The resulting model contains topological charges with a hierarchy of subdimensional topological excitations generated by:

- $\mathbb{Z}_N$ fractons that appear on the open ends of condensed p-strings. These fractons are more exotic than the usual fractons appearing in p-string condensation, as the p-strings are formed by anyons and impart a vestige of the anyonic statistics onto the fractons.

- $\hat{x}$ lineons from nontrivial anyons in an xz layer, trapped between p-string planes. Similarly there are $\hat{y}$ lineons from the yz layers. There are also $\hat{z}$ lineons from composites of an $\hat{x}$ and $\hat{y}$ lineon trapped between the same p-string planes. A pair of fractons adjacent on either side of a p-string plane is equivalent to a single p-string condensed anyon, and hence is also a lineon in this example. These lineons can be obtained by moving an $\hat{x}$ or $\hat{y}$ lineon onto a p-string plane. We remark that this behavior is due to the anyonic nature of the p-strings, and does not occur for bosonic or fermionic p-string condensations.

- Planons that arise from pair composites of lineons, which are themselves composites of fractons, that have opposite braiding phases with the condensed p-strings. In this example a composite formed by only a pair of fractons is not a planon due to the anyonic nature of the p-strings.

In this example we have considered a planar p-string condensation involving anyonic p-strings. Attempting to apply the conventional 3D p-string condensation to these anyonic p-strings would not succeed in producing a gapped phase due to their nontrivial braidings. This is even true for planar p-string condensation with intersecting planes, again due to the nontrivial braidings. However, as we have only considered the anyonic p-string planes to be nonoverlapping, and the F-symbols are trivial, there is no inconsistency in the above construction. This inconsistency can be formulated as the anomaly of a subsystem symmetry in the gauging formulation of planar p-string condensation [183], see Appendix 4.5.8.

A lattice model with fracton topological order that is foliated equivalent to the

example in this section is presented in Appendix 4.5.10 where it is used to calculate the ground space degeneracy of the current example for various boundary conditions.

4.4 Summary

In this chapter we have introduced a coupled-wire construction for a family of chiral fracton phases in (3+1) dimensions with chiral gapless boundary modes. This construction inspired a planar p-string condensation mechanism which we elaborated upon in the main text, as well as Appendix 4.5.8, where it is shown to yield a wide variety of fracton models, including ones based upon non-Abelian layers. In Appendix 4.5.7, we also propose a coupled-wire realization of such non-Abelian models.

The models constructed here motivate further exploration of coupled-wire constructions for fracton phases and new potential paths towards experimental realizations of fracton physics. They also raise the challenge of developing a deeper theoretical understanding of chiral fracton phases.

Finally, this work points towards intriguing field theories obtained by taking the continuum limit in the remaining two directions that were left discrete in the current work. This brings to the forefront challenging technical issues surrounding the continuum limit of a system with an exponentially scaling topological degeneracy.

4.5 Appendix

4.5.1 Details on the coupled-wire model

In this Appendix we provide some of the details for calculations relating to the wire model. First, in Sec 4.5.1 we review the 2D coupled wire construction for the Laughlin state. In Sec 4.5.2 we analyze, via perturbation theory, a model of intersecting Laughlin layers with pairs of Laughlin quasiparticles condensed at vertices and show that the leading order effective Hamiltonian for this model is the one presented in Sec. 4.2. The gap to neutral Gaussian fluctuations is discussed in Sec 4.5.3. We give a thorough discussion of the surface theory in Sec 4.5.4. Lastly, we calculate the ground state degeneracy of the model with the alternative boundary conditions considered in the body of the text (Sec 4.5.5) and with fully periodic boundary conditions (Sec 4.5.6)

Coupled-wire construction of the Laughlin state

Here we review the coupled-wire construction of the $\nu = 1/m$ Laughlin state, first presented in [60, 61]. The building blocks of this construction are a collection of 1D quantum wires of free fermions oriented along the z direction and labelled by a site index j. Upon bosonization; one has $\Psi_{\eta,j}(z) \sim e^{i\phi_{\eta,j}(z)}$ for sites j and chirality $\eta = L, R$. This construction involves only a single species of fermion on each wire so there is no need for the additional superscript q used in the main text. Any local vertex operator must be decomposable into an integer combination of $\phi_{\eta,i}$. The chiral bosons have the familiar commutation relations:

$$[\phi_{L/R,j}(z), \phi_{L/R,i}(z')] = \pm i\pi\delta_{ij}\,\mathrm{sgn}(z - z') \quad \text{and} \quad [\phi_{L,j}(z), \phi_{R,i}(z')] = 0 \tag{4.14}$$

Next, for $m \in 2\mathbb{Z} + 1$, consider the new composite fields

$$\tilde{\phi}_{L/R,j} = \frac{(\phi_{L,j} + \phi_{R,j}) \pm m\,(\phi_{L,j} - \phi_{R,j})}{2} \quad \text{with} \quad [\tilde{\phi}_{L/R,j}(z), \tilde{\phi}_{L/R,i}(z')] = \pm im\pi\delta_{ij}\,\mathrm{sgn}(z - z') \tag{4.15}$$

Note that because m is odd $e^{i\tilde{\phi}_\eta}$ is a local operator and creates a chiral quasiparticle with fermionic statistics. The non-local vertex operator $e^{i\tilde{\phi}_\eta/m}$ creates an anyonic quasiparticle with self-statistics $2\pi/m$. Finally consider the field defined by

$$2\tilde{\theta}_{j,\hat{\boldsymbol{a}}} = \tilde{\phi}_{L,j} - \tilde{\phi}_{R,j+\hat{\boldsymbol{a}}} \tag{4.16}$$

where $\hat{a}$ is a unit vector indexing the lattice site direction. In this situation one can equivalently think of the site $j + \hat{\boldsymbol{a}}$ as $j + 1$. More generally, and in the case of the main text, one may consider unit vectors $\hat{\boldsymbol{a}}$ in more than one direction and so the notation used here is chosen so as to reinforce the notation used in the main text. With all of the relevant fields defined consider a collection of evenly spaced parallel wires with the following Hamiltonian:

$$H = H_0 + H_{\text{int}} = \sum_j \int_0^{L_z} \mathrm{d}z \left[\left(\partial_z \phi_{L,j}\right)^2 + \left(\partial_z \phi_{R,j}\right)^2 \right] - \lambda \sum_j \int_0^{L_z} \mathrm{d}z \cos\left(2\tilde{\theta}_{j,\hat{\boldsymbol{a}}}\right) \quad (4.17)$$

In the $\lambda \to \infty$ limit, the interaction term condenses and $2\tilde{\theta}_{j,\hat{\boldsymbol{a}}} = 0 \ \forall \ i$. In this regime the model is gapped and has an m-fold ground state degeneracy. The gapped excitations correspond to solitons in the condensed fields: $2\tilde{\theta}_{j,\hat{\boldsymbol{a}}}(z) \to 2\tilde{\theta}_{j,\hat{\boldsymbol{a}}}(z) + 2\pi n \Theta(z - z_0)$. The model has anyonic excitations corresponding to minimal strength solitons (kinks of size 2π) which are fully mobile in 2D. The anyons are moved along the wire direction by an operator such as $e^{\frac{i}{m}\int_{z_1}^{z_2} \mathrm{d}z\, \partial_z \tilde{\phi}_{\eta,j}}$ and are moved along the lattice direction by the operator $e^{i(\tilde{\phi}_{L,j} - \tilde{\phi}_{R,j})/m} = e^{i(\phi_{L,j} - \phi_{R,j})}$. Using these quasiparticle translation operators one can compute the anyonic braiding statistics of $2\pi/m$ by considering, e.g., the commutator

$$\left(\prod_j e^{\frac{i}{m}(\tilde{\phi}_{L,j} - \tilde{\phi}_{R,j})} \right) e^{\frac{i}{m}\int_0^L \mathrm{d}z\, \partial_z \tilde{\phi}_{L,i}} = e^{\frac{i}{m}\int_0^L \mathrm{d}z\, \partial_z \tilde{\phi}_{L,i}} \left(\prod_j e^{\frac{i}{m}(\tilde{\phi}_{L,j} - \tilde{\phi}_{R,j})} \right) e^{-2\pi i/m}, \quad (4.18)$$

which follows directly from Eq. (4.15).

4.5.2 Perturbation theory

We claim that the model discussed in the main text emerges as the lowest (fourth) order term in perturbation theory in a model of interpenetrating stacks of $\nu = 1/m$ Laughlin planes coupled by condensing Laughlin quasiparticles using the vertex terms $U^V_{\boldsymbol{r}}$. Heuristically one can see that the plaquette terms are related to products of four

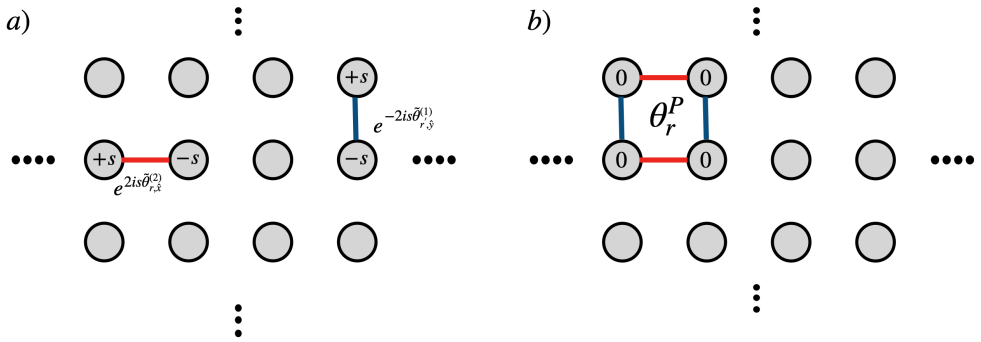

Figure 4.8: (a) Dipole configurations are created in the vertex terms by the Laughlin interaction operators $\exp(2is\tilde{\theta})$. (b) To avoid being projected out of the low-energy subspace, these operators must enter the effective Hamiltonian in the form of a plaquette term. In such configurations, the vertex solitons generated by different Laughlin interaction operators cancel. .

Laughlin interaction terms, $\cos(2\tilde{\theta}^q_{\boldsymbol{r},\hat{\boldsymbol{a}}})$ (see Appendix 4.5.1).

Let's see how this emerges. The Hamiltonian can be decomposed into two parts:

$$H_0 = H_{\text{kin}} - \lambda_V \sum_{\boldsymbol{r}} \int_0^{L_z} \mathrm{d}z \, \cos\left(2\theta^1_{\boldsymbol{r}} + 2\theta^2_{\boldsymbol{r}}\right) \tag{4.19a}$$

$$H_1 = g \sum_{\boldsymbol{r}} \int_0^{L_z} \mathrm{d}z \, \left[\cos\left(2\tilde{\theta}^1_{\boldsymbol{r},\hat{\boldsymbol{y}}}\right) + \cos\left(2\tilde{\theta}^2_{\boldsymbol{r},\hat{\boldsymbol{x}}}\right)\right], \tag{4.19b}$$

where H_{kin} is the kinetic term for the wires in the absence of the couplings λ_V, g.

In the limit $\lambda_V \to \infty$, solitons in the argument of the vertex term in H_0 do not lie in the spectrum of low-energy states. The aim is to find an effective theory which describes the physics in this low-energy subspace. This can be accomplished using Wigner-Brillouin perturbation theory: we introduce the operator P which projects onto the ground-state subspace of H_0 and in particular throws out any states with

solitons in the λ_V terms. Our effective Hamiltonian is then given by $H_0 + H_{\text{eff}}$, where

$$H_{\text{eff}} = PH_1 \sum_{n=0}^{\infty} \left\{ \left[E_0 - (1-P)H_0(1-P) \right]^{-1} H_1 \right\}^n P \tag{4.20}$$

In the limit $\lambda_V \to \infty$, eigenstates of H_0 can be labeled schematically by occupation numbers associated with solitons in each vertex term. Occupied states will be projected out, so we need to determine the lowest-order term in the series which does not excite any vertices. Suppressing the integral over z, we can express H_1 as

$$H_1 = \frac{g}{2} \sum_{\boldsymbol{r}, s=\pm} \left[\exp\left(2is\tilde{\theta}^1_{\boldsymbol{r},\hat{\boldsymbol{y}}} \right) + \exp\left(2is\tilde{\theta}^2_{\boldsymbol{r},\hat{\boldsymbol{x}}} \right) \right].$$

As one can see from Fig. 4.8(a), $\exp(2is\tilde{\theta}^1)$ creates a $\pm s$ dipole of vertex solitons in the y-direction while $\exp(2is\tilde{\theta}^2)$ creates an analogous dipole in the x-direction. The terms in H_{eff} correspond to products of these dipoles. One needs to go to 4^{th} order to create a dipole configuration that leaves behind no vertex solitons and avoids being projected out:

$$\begin{aligned} H^{(4)}_{\text{eff}} = P \sum \frac{g^4}{16\Delta^3_{\text{kink}}} \Bigg[& \exp\left(2is\tilde{\theta}^1_{\boldsymbol{r},\hat{\boldsymbol{y}}} + 2is'\tilde{\theta}^2_{\boldsymbol{r}',\hat{\boldsymbol{x}}} + 2is''\tilde{\theta}^1_{\boldsymbol{r}'',\hat{\boldsymbol{y}}} + 2is'''\tilde{\theta}^2_{\boldsymbol{r}''',\hat{\boldsymbol{x}}} \right) + \text{H.c.} \Bigg] P \\ & + \text{terms w/ unequal numbers of } x\text{- and } y\text{-dipoles that get projected out,} \end{aligned} \tag{4.21}$$

where Δ_{kink} is the energy gap to creating a vertex-soliton dipole. Applying the projection operators one can see that the only terms that survive form a unit square

with $s = -s' = -s'' = s'''$, see Fig. 4.8(b). This yields

$$H_{\text{eff}} \sim \frac{g^4}{\Delta_{\text{kink}}^3} \sum_{\boldsymbol{r}} \cos\left(2\tilde{\theta}^1_{\boldsymbol{r},\hat{\boldsymbol{y}}} - 2\tilde{\theta}^2_{\boldsymbol{r},\hat{\boldsymbol{x}}} - 2\tilde{\theta}^1_{\boldsymbol{r}+\hat{\boldsymbol{x}},\hat{\boldsymbol{y}}} + 2\tilde{\theta}^2_{\boldsymbol{r}+\hat{\boldsymbol{y}},\hat{\boldsymbol{x}}}\right) + \text{higher-order terms}, \tag{4.22}$$

which is, up to subleading corrections, precisely the plaquette term defined in Eq. (4.3) in the main text.

The above analysis can be extended to describe the case where strong vertex terms are only turned on in a bounded subregion, which we take to be an $L_x \times L_y$ rectangle for simplicity, of the full lattice of wires. In the perturbative treatment, strong vertex terms on the boundary of this subregion generate truncated plaquette operators which contain the only edges of a full plaquette that touch one of the strong vertex terms. For example, vertex terms along the top boundary of the subregion generate the interaction $\cos\left[2\left(\tilde{\theta}^1_{(x,L_y),\hat{\boldsymbol{y}}} - \tilde{\theta}^1_{(x+1,L_y),\hat{\boldsymbol{y}}} - \tilde{\theta}^2_{(x,L_y),\hat{\boldsymbol{x}}}\right)\right]$, while the vertex term in the top-right corner of the subregion generates the interaction $\cos\left[2\left(\tilde{\theta}^1_{(L_x,L_y),\hat{\boldsymbol{y}}} - \tilde{\theta}^2_{(L_x,L_y),\hat{\boldsymbol{x}}}\right)\right]$. These are precisely the boundary interactions used in the surface termination discussed in the main text, which can be viewed as a minimal example in which the topmost and bottommost $q = 2$ Laughlin layers and the leftmost and rightmost $q = 1$ Laughlin layers are omitted.

Given this perturbative analysis, we can try to understand the excitations of the model from the perspective of p-string condensation, as discussed in the main text. The term λ_V condenses two pairs of anyons created by $\exp 2i\theta^1_{xy}$ and $\exp 2i\theta^2_{xy}$. This condensate proliferates in the limit $\lambda_V \to \infty$. Low energy excitations must commute

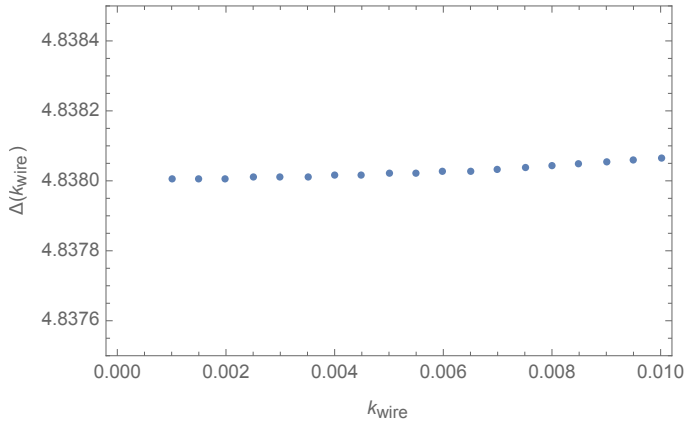

Figure 4.9: A plot of the smallest eigenvalue at a given k_z along the wire direction with $U = 100$ and system size $L = 15$. One can see that the gap $\Delta_{k_z \to 0} \to 4.8380 + \epsilon$ ($\epsilon \ll 1$) reflecting the fact that the model is gapped at finite system size..

with the condensate and so the emergent mobility restrictions can be understood as stemming from this constraint. For more on this perspective, we refer the reader to Appendix 4.5.8.

4.5.3 Scaling of the gap

While gapped to charged topological excitations (solitons), the model studied in the main text possesses gapless neutral excitations in the thermodynamic limit. These neutral excitations, which we refer to as "phonons," correspond to Gaussian density fluctuations and do not participate in the transport of charge.

In this Appendix we present numerical results on the phonon spectrum for PBC in the z-direction and the boundary conditions in the x-y plane used to calculate the topological degeneracy in the main text and in Appendix 4.5.5. For these calculations, we set $L_x = L_y \equiv L$ and consider a vertex coupling $\lambda_V = 100\,U$, with all other couplings including λ_P and the boundary and corner couplings set to U; in turn, we take $U \gg v$, where v is the kinetic energy scale of the decoupled wires. We set

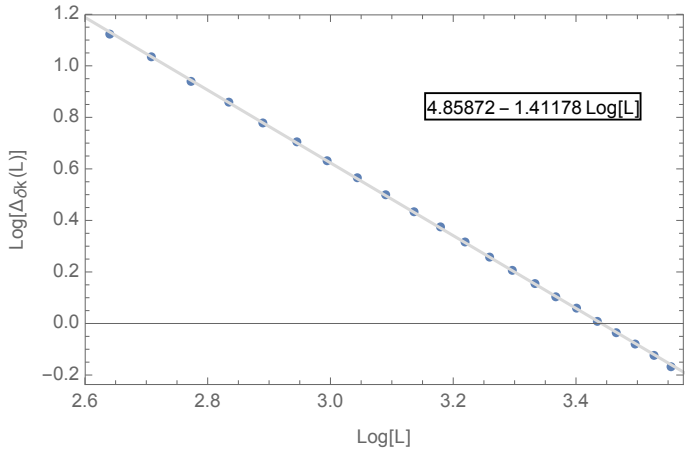

Figure 4.10: Log-Log plot of $\Delta_{\delta k_z}(L)$ vs L at $U = 100$. We see that the scaling relation $\Delta_{\delta k_z}(L) \sim L^{\alpha}$ with $\alpha \approx -1.4118$. .

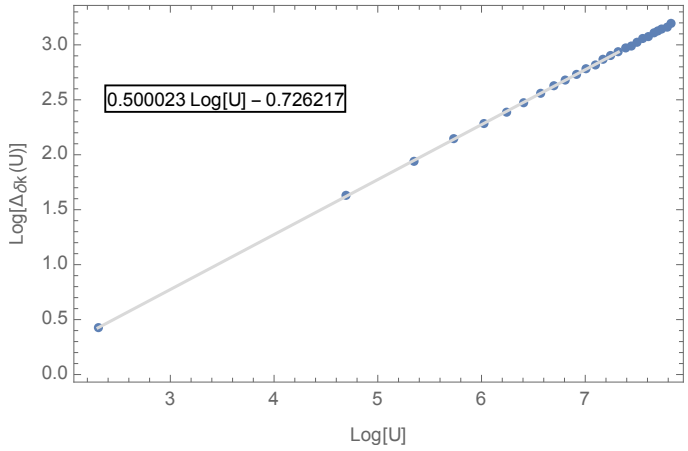

Figure 4.11: Log-Log plot of $\Delta_{\delta k_z}(U)$ vs U at $L = 20$. We see that the scaling relation $\Delta_{\delta k_z}(U) \sim U^{\beta}$ with $\beta \approx .500023$. This points to a scaling $\Delta_{\delta k_z}(U) \sim \sqrt{U}$..

$v = 1$ unless specified otherwise. This hierarchy of energy scales is consistent with the perturbative treatment of Appendix 4.5.2. We analyze the scaling of the phonon gap with the momentum k_z along the wire direction, the system size L, and the strong coupling U. Our results indicate that the phonons are gapped at finite system size, and in a particular scaling limit in which U scales at least as a sufficiently large power of L as $L \to \infty$.

Following [80], for each pinning term we make the replacement $\cos(\Lambda \cdot \Phi) \sim$

$1-\frac{(\Lambda\cdot\Phi)^2}{2}$ and analyze the corresponding Bogoliubov-de-Gennes mean field theory. The alternate boundary conditions break translation symmetry in the discrete directions x, y so the model must be solved using a mixed basis $\{a^\dagger_{\boldsymbol{r}}(k_z), a_{\boldsymbol{r}}(k_z)\}$, which create/destroy bosonic fluctuations of momentum k_z on wire $\boldsymbol{r} = (x, y)$. Since k_z is a well defined quantum number, let us define $\Delta_{k_z}(U, L)$ to be the smallest energy eigenvalue with momentum k_z at system size L and coupling strength U (note that we identify this quantity with the phonon gap since the Hamiltonian is positive semidefinite). We suppress the arguments U and L when convenient.

First let us consider the behavior of Δ_{k_z} as we let $k_z \to 0$. Since the real space calculation is done numerically one cannot actually evaluate the Δ_{k_z} at $k_z = 0$ because the BdG Hamiltonian will involve terms proportional to $\frac{1}{|k_z|}$ coming from factors ϕ^2 and θ^2 (see Ref. [80]). An analytical expression for the eigenenergies is prohibitively complicated but should be a function $f(vk_z, vU)$ in order to the prevent divergence as $k_z \to 0$. Fig. 4.9 shows Δ_{k_z} at system size $L = 15$. Evidently, at this system size $\Delta_{k_z} \to \Delta_0 \in [4.380 - \epsilon, 4.380 + \epsilon]$ with $\epsilon \ll 1$, reflecting the fact that the model is gapped at finite L. In other words, at finite L, $\Delta_{k_z}(L) \to \Delta_0(L) > 0$ as $k_z \to 0$. With this justification, we henceforth approximate Δ_0 by $\Delta_{\delta k_z}$ with a small $\delta k_z = 10^{-5}$.

We now consider the scaling of the gap with L and U. Determining how $\Delta_0(L)$ depends on L enables us to check if the gap persists in the thermodynamic limit. We find that $\Delta_{\delta k_z}(L) \to 0$ as $L \to \infty$. Thus, while gapped at finite L, the phonons become gapless in the limit of infinite system size. In Fig. 4.10 we see a power-law dependence of the form $\Delta_{\delta k_z}(L) \sim L^\alpha$ with $\alpha \sim -1.412$. Lastly, the scaling of $\Delta_{\delta k_z}(U)$ with U is shown in Fig 4.11: $\Delta_{\delta k_z} \sim U^{.500023}$. Since we use a δk of order 10^{-5},

our numerical results are consistent with the dependence $\Delta_{k_z \to 0} \sim \sqrt{U}$, which is also found in Ref. [80]'s analysis of translation-invariant coupled-wire models with gapless fluctuations. Putting these dependences together, we conclude that $\Delta_{k_z \to 0} \sim \sqrt{U} L^{\alpha}$.

One interesting take-away from this analysis is that there exists a scaling limit, in which the strong-coupling limit $U \to \infty$ is taken alongside the thermodynamic limit $L \to \infty$ such that $U \gtrsim L^{-2\alpha}$, in which the fluctuations are gapped. In this limit, one has $\Delta_0 \gtrsim L^{\frac{1}{2}(-2\alpha)} L^{\alpha} \sim O(1)$. At first glance this may seem a somewhat artificial limit to take. Recall though that the $U \to \infty$ limit has been assumed throughout in our discussion of both the charged and neutral sectors of the theory. Thus the scaling limit merely demands that the $U \to \infty$ limit be taken sufficiently "fast" compared to the $L \to \infty$ limit.

4.5.4 Details on surface theory

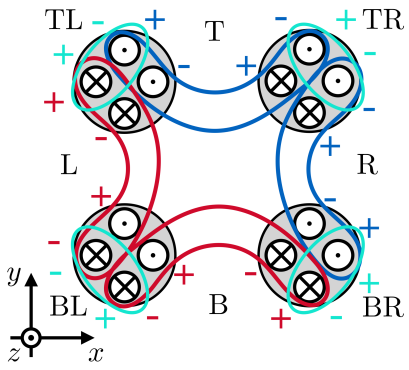

Figure 4.12: Pictorial definition of the gapless surface $(\mathrm{L}, \mathrm{R}, \mathrm{T}, \mathrm{B})$ and corner $(\mathrm{TL}, \mathrm{TR}, \mathrm{BL}, \mathrm{BR})$ modes with open boundary conditions in the x- and y-directions. Chiral modes belonging to the same surface or corner mode are encircled, and $\pm$ indicates the relative sign with which each chiral mode appears [see, e.g., Eq. 4.23]. .

In this Appendix we provide further details on the construction of the surface

theory for the case of open boundary conditions in x and y and periodic boundary conditions in z. In particular, we construct the $2(L_x + L_y)$-dimensional K-matrix of the surface theory, which encodes the commutation relations among the gapless surface modes, and show that it has two zero modes that correspond to bulk degrees of freedom that are gapped in the strong coupling limit. This leaves $N = 2(L_x + L_y - 1)$ gapless modes residing on the surface, as expected from the counting argument presented in the main text.

We identify the chiral gapless boundary modes by finding linear combinations of bosonic fields on the surface that commute with the bulk interaction terms (4.3). The boundary of the coupled-wire array can be divided into left, right, top, and bottom (L, R, T, B) faces. The L and R faces each contain $L_y - 1$ bonds, and the Tand B faces each contain $L_x - 1$ bonds. Each such bond is associated with a chiral mode that commutes with the bulk interactions. For example, on the L surface [$\boldsymbol{r} = (1, y)$, $y = 1, \ldots, L_y - 1$], one finds using Eq. (4.2) that the $L_y - 1$ chiral modes

$$\hat{\phi}^{\mathrm{L}}_{R,\boldsymbol{r}} = \tilde{\phi}^{2}_{R,\boldsymbol{r}} - \tilde{\phi}^{1}_{R,\boldsymbol{r}} + \tilde{\phi}^{1}_{L,\boldsymbol{r}-\hat{\boldsymbol{y}}} - \tilde{\phi}^{2}_{R,\boldsymbol{r}-\hat{\boldsymbol{y}}} \tag{4.23}$$

all commute with the interactions (4.3). Analogous definitions for the R, T, B surfaces can be read off from Fig. 4.12. In addition to the $2(L_x + L_y - 2)$ chiral modes from the L, R, T, B surfaces, there are four gapless modes associated with the TL, TR, BL, BR corners of the array; for example, at the BL corner we have

$$\hat{\phi}^{\mathrm{BL}}_{R} = \tilde{\phi}^{2}_{R,(1,1)} - \tilde{\phi}^{1}_{R,(1,1)}, \tag{4.24}$$

and similar expressions for the other corners can be read off from Fig. 4.12. We thus find a total of $2(L_x + L_y) = N + 2$ boundary modes that commute with the bulk interactions. Of these, all but the modes at the TL and BR corners are chiral, i.e. contain an excess of right- or left-movers.

Each of the surface modes identified above has a nontrivial commutation relation both with itself and with its immediate neighbors; these commutation relations follow directly from Eq. (4.2). We organize these commutation relations into an $(N + 2)$-dimensional square matrix K defined by

$$[\hat{\phi}_\alpha(z), \hat{\phi}_\beta(z')] = i\pi\, K_{\alpha\beta}\ \mathrm{sgn}(z - z'), \tag{4.25}$$

where $\alpha, \beta = 1, \ldots, N + 2$ label the surface modes identified above. We compute K as an 8×8 block matrix whose diagonal blocks describe the $\mathrm{L}, \mathrm{R}, \mathrm{T}, \mathrm{B}$ faces and the $\mathrm{TL}, \mathrm{TR}, \mathrm{BL}, \mathrm{BR}$ corners, and whose off-diagonal blocks encode nontrivial commutation relations among the corners and faces.

We first focus on the block-diagonal part of K. Each of the $\mathrm{L}, \mathrm{R}, \mathrm{T}, \mathrm{B}$ faces has an $(L_a - 1)$-dimensional $(a = x, y)$ K-matrix for the modes identified in Eq. (4.23)

that is proportional to

$$K_a = \begin{pmatrix} -2m & m & 0 & \dots & 0 & 0 \\ m & -2m & m & 0 & \dots & \\ 0 & m & -2m & m & 0 & \dots \\ \vdots & \vdots & \vdots & \vdots & \vdots & \vdots \\ 0 & 0 & \dots & 0 & m & -2m \end{pmatrix}. \tag{4.26}$$

This K matrix is (up to an unimportant sign on the diagonal entries) proportional to that of the so-called "121" phase of a stack of fractional quantum Hall layers identified in Ref. [189]. The K-matrices for the T, B, L, and R surfaces are

$$K_{\mathrm{T}} = -K_x, \qquad K_{\mathrm{B}} = K_x, \qquad K_{\mathrm{L}} = K_y, \qquad K_{\mathrm{R}} = -K_y, \tag{4.27}$$

indicating that opposite surfaces have opposite chiralities, as expected. The remaining diagonal blocks of K describe the self-commutation relations of the TL, TR, BL, BR corner modes identified in Eq. (4.24); they are

$$K_{\mathrm{TL}} = 0, \qquad K_{\mathrm{TR}} = 2m, \qquad K_{\mathrm{BR}} = 0, \qquad K_{\mathrm{BL}} = -2m. \tag{4.28}$$

Note that $K_{\mathrm{TL}} = K_{\mathrm{BL}} = 0$ because these modes are nonchiral.

We now determine the off-diagonal blocks of K. Each of the corner modes has a nontrivial algebra with neighboring modes from the two surfaces it touches. This

algebra is encoded in the $1 \times (L_x - 1)$ K-matrices

$$K_{\mathrm{TLT}} = \begin{pmatrix} -m & 0 & \dots & 0 \end{pmatrix} = -K_{\mathrm{BRB}}, \tag{4.29a}$$

the $(L_x - 1) \times 1$ K-matrices

$$K_{\mathrm{TTR}} = \begin{pmatrix} 0 \\ \vdots \\ 0 \\ -m \end{pmatrix} = -K_{\mathrm{BBL}}, \tag{4.29b}$$

the $1 \times (L_y - 1)$ K-matrices

$$K_{\mathrm{TRR}} = \begin{pmatrix} m & 0 & \dots & 0 \end{pmatrix} = -K_{\mathrm{BLL}}, \tag{4.29c}$$

and the $(L_y - 1) \times 1$ K-matrices

$$K_{\mathrm{RBR}} = \begin{pmatrix} 0 \\ \vdots \\ 0 \\ m \end{pmatrix} = -K_{\mathrm{TLL}}^{\mathsf{T}}. \tag{4.29d}$$

Combining Eqs. (4.26), (4.27), (4.28), and (4.29), we can write the full $2(L_x + L_y)$-

dimensional K-matrix in block form as

$$K = \begin{pmatrix} K_{\mathrm{TL}} & K_{\mathrm{TLT}} & 0 & 0 & 0 & 0 & 0 & K_{\mathrm{TLL}} \\ K_{\mathrm{TLT}}^{\mathsf{T}} & K_{\mathrm{T}} & K_{\mathrm{TTR}} & 0 & 0 & 0 & 0 & 0 \\ 0 & K_{\mathrm{TTR}}^{\mathsf{T}} & K_{\mathrm{TR}} & K_{\mathrm{TRR}} & 0 & 0 & 0 & 0 \\ 0 & 0 & K_{\mathrm{TRR}}^{\mathsf{T}} & K_{\mathrm{R}} & K_{\mathrm{RBR}} & 0 & 0 & 0 \\ 0 & 0 & 0 & K_{\mathrm{RBR}}^{\mathsf{T}} & K_{\mathrm{BR}} & K_{\mathrm{BRB}} & 0 & 0 \\ 0 & 0 & 0 & 0 & K_{\mathrm{BRB}}^{\mathsf{T}} & K_{\mathrm{B}} & K_{\mathrm{BBL}} & 0 \\ 0 & 0 & 0 & 0 & 0 & K_{\mathrm{BBL}}^{\mathsf{T}} & K_{\mathrm{BL}} & K_{\mathrm{BLL}} \\ K_{\mathrm{TLL}}^{\mathsf{T}} & 0 & 0 & 0 & 0 & 0 & K_{\mathrm{BLL}}^{\mathsf{T}} & K_{\mathrm{L}} \end{pmatrix}. \tag{4.30}$$

The existence of the $2(L_x + L_y)$-dimensional K-matrix (4.30) seems to imply the existence of $2(L_x+L_y) = N+2$ gapless modes that commute with the bulk interaction terms, rather than the N modes expected based on counting the bulk interaction terms. However, it is possible that some linear combinations of these surface modes can be rewritten in terms of pinned bulk fields, since these bulk fields also commute with the interaction Hamiltonian. Indeed, we find that the K-matrix (4.30) has two zero modes at any system size, and that these zero modes correspond to linear combinations of pinned bulk fields. The first zero mode can be written compactly in $(N + 2)$-dimensional vector form as

$$\Upsilon_+ = \begin{pmatrix} -1 & -\mathbf{1}_{L_x-1} & -1 & +\mathbf{1}_{L_y-1} & -1 & -\mathbf{1}_{L_x-1} & -1 & +\mathbf{1}_{L_y-1} \end{pmatrix}^{\mathsf{T}}, \tag{4.31}$$

where $\mathbf{1}_d$ is a d-dimensional vector with unit entries. The second is

$$\Upsilon_- = \left(\tfrac{L_x+L_y}{2} \quad C_{+-} \quad \tfrac{L_y-L_x}{2} \quad C_{-+} \quad -\tfrac{L_x+L_y}{2} \quad -C_{+-} \quad \tfrac{L_x-L_y}{2} \quad -C_{-+} \right)^{\mathsf{T}}, \tag{4.32a}$$

where the $(L_x - 1)$-dimensional vector

$$C_{+-} = \left(\tfrac{L_x+L_y}{2} - 1 \quad \tfrac{L_x+L_y}{2} - 2 \quad \dots \quad \tfrac{L_y-L_x}{2} + 1 \right) \tag{4.32b}$$

and the $(L_y - 1)$-dimensional vector

$$C_{-+} = \left(\tfrac{L_x-L_y}{2} + 1 \quad \tfrac{L_x+L_y}{2} + 2 \quad \dots \quad \tfrac{L_x+L_y}{2} - 1 \right). \tag{4.32c}$$

Writing these zero modes as linear combinations of the underlying bosonic surface fields defined by Eqs. (4.23) and (4.24) and their analogs, we find that they can be reexpressed as linear combinations of the pinned bulk vertex and plaquette fields. For example,

$$\Upsilon_+ = \sum_{\boldsymbol{r} \in \Lambda} \theta^P_{\boldsymbol{r}}, \tag{4.33}$$

where the sum runs over all vertices $\boldsymbol{r}$ in the square lattice Λ with OBC and where $\theta^P_{\boldsymbol{r}}$ is the pinned (i.e. gapped) plaquette field. Υ_- can also be expressed as a linear combination of pinned vertex and plaquette fields $\theta^V_{\boldsymbol{r}}$ and $\theta^P_{\boldsymbol{r}}$, respectively, but the expression is more complicated (in particular, it depends on system size) and we omit it here. Pictorial examples of the expressions for $\Upsilon_\pm$ in terms of pinned bulk fields

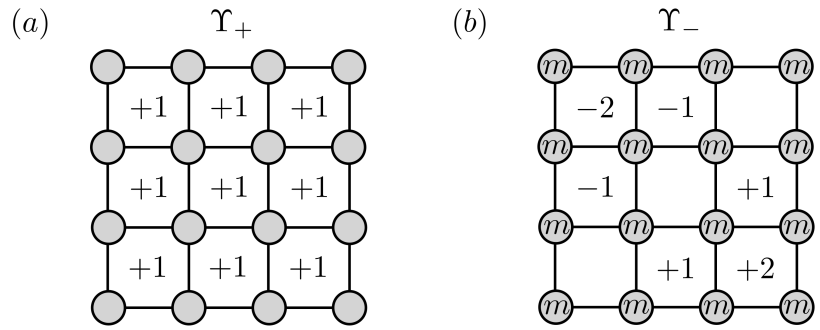

Figure 4.13: Schematic depiction of the expressions for the zero modes Υ_+ (a) and Υ_- (b) in terms of pinned bulk fields $\theta_{\boldsymbol{r}}^{V,P}$ at system size $L_x = L_y = 4$. Integers appearing in a plaquette or vertex of the square lattice signify the coefficient with which the corresponding $\theta_{\boldsymbol{r}}^P$ or $\theta_{\boldsymbol{r}}^V$ field (respectively) enters the expression of $\Upsilon_\pm$ as a linear combination of these fields. .

for $L_x = L_y = 4$ are shown in Fig. 4.13. In summary, while a naive identification of surface modes commuting with the bulk interaction terms finds $N + 2$ such modes, a closer look shows that two of these modes can be reexpressed as linear combinations of pinned bulk fields. We thus find N gapless surface modes, as expected from the counting of bulk interaction terms.

We note in passing that the Lagrangian for the surface theory constructed in this Appendix can be written as

$$L_{\text{bdy}} = \int_0^{L_z} \frac{\mathrm{d}z}{4\pi} \left[(\partial_t \hat{\boldsymbol{\phi}})^{\mathsf{T}} K^+ (\partial_z \hat{\boldsymbol{\phi}}) - (\partial_z \hat{\boldsymbol{\phi}})^{\mathsf{T}} V (\partial_z \hat{\boldsymbol{\phi}}) \right], \tag{4.34}$$

wherein we have collected the boundary modes into an $(N+2)$-component vector $\hat{\boldsymbol{\phi}}$, and where the $(N+2)$-dimensional symmetric rational matrix K^+ is the pseudoinverse of K. The matrix V encodes the kinetic energy of the boundary modes and depends on microscopics. This surface theory is unusual because K^+ is generically not sparse, and deserves further study.

4.5.5 Topological ground-state degeneracy

Here we compute the topological ground-state degeneracy (GSD) for the coupled-wire model with the alternative "unusual" boundary conditions defined in the main text. The method used is presented in Ref. [67]. The closed model is shown in Fig. 4.14 a). Note that in the strong coupling limit any configuration in the ground state manifold is labeled by a set of integers defined by $\theta^{V,P}_{\boldsymbol{r}}, 2\tilde{\theta}^{q}_{i} \in 2\pi\mathbb{Z}$ where $\boldsymbol{r} \in \Lambda$ labels wires in the original 2D array and $i = 1, \ldots, N/2+1$ labels pairs of added boundary wires. Naively then, a general ground state can be labelled by assigning each plaquette, vertex, and oval in 4.14(a) a value in $\mathbb{Z}$. However, because of the compact nature of the degrees of freedom ($\phi^{q}_{\eta,\boldsymbol{r}} \equiv \phi^{q}_{\eta,\boldsymbol{r}} + 2\pi$), many of these ground-state configurations should, in fact, be identified. Starting with an arbitrary configuration, one can "clean" the set of ground-state labels by using local shifts $\phi^{q}_{\eta,\boldsymbol{r}} \to \phi^{q}_{\eta,\boldsymbol{r}} + 2\pi$ to set extraneous labels to zero. The patterns of these local 2π shifts are the same as those produced by the application of vertex operators, some of which are displayed in Figs. 4.2 and 4.3. Patterns of particular use are displayed in Fig. 4.14(b); we refer to the patterns therein by the labels A-E in the cleaning argument below.

First we address the configuration of the vertex terms which are represented in Fig 4.14(a) by the grey circles. We claim that any configuration of vertex terms is trivial and can by cleaned so that $\theta^{V}_{\boldsymbol{r}} = 0$ at each $\boldsymbol{r}$ while the other terms remain unchanged. First note that, by repeated application of D, all vertex terms except one can be set to zero. Suppose the remaining nonzero vertex term is in the top edge and has value $\theta^{V} = q$. Then, by combining B and C, we can set $\theta^{V} = 0$ at the expense

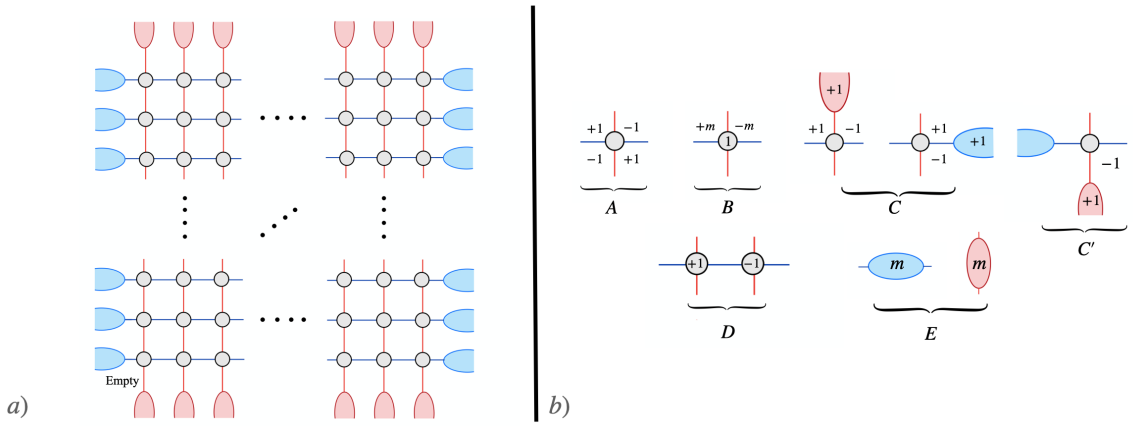

Figure 4.14: (a) A representation of the model with the alternative boundary conditions discussed in the main text. The grey circles correspond to the vertex terms $\theta^V_{\boldsymbol{r}}$ and the squares (both complete and partially complete) correspond to the plaquette terms $\theta^P_{\boldsymbol{r}}$. The blue and red ovals, which are shared between the left/right and top/bottom faces, respectively, correspond to the argument of the Laughlin interaction term, $2\tilde{\theta}^{1,2}$. Note that the bottom-left corner does not have a plaquette term, as discussed in the main text. (b) Here we provide examples of some useful phase shift patterns which are employed to clean a general configuration in the ground state manifold. Note C' in particular, which is a special case of pattern C in the bottom left-corner where the plaquette term is absent. This will be key for cleaning the entire configuration of plaquettes..

of shifting the red oval directly above, corresponding to $\tilde{\theta}^1$, by mq. Finally, using E, this factor of mq can be cleaned.

Next we consider the plaquette terms $\theta^P_{\boldsymbol{r}}$. First we assign some value in $\mathbb{Z}$ to each square in 4.14(a) except for the bottom-left corner, which is assumed to be free of a truncated plaquette term as discussed in the main text. Observe that by using pattern A one can set all plaquettes to 0 except those in an "L"-shaped region on the perimeter. Suppose all nonzero plaquettes are confined to the top and right edge. By applying C from left to right and then top to bottom, the values of the plaquettes can be shifted onto the red or blue ovals. This procedure leaves one remaining nonzero plaquette in the bottom-right corner. For this term, we can apply C to shift its value to the left until it reaches the bottom-left corner, where it can be removed using C'.

At this point all plaquettes and vertices have been set to zero, leaving only the integers corresponding to interaction terms represented by the red and blue ovals in Fig. 4.14. Using E one can now clean the red and blue ovals modulo m. This analysis yields

$$\text{GSD} = m^{L_x+L_y} \tag{4.35}$$

where $L_x \times L_y$ is the size of the square lattice Λ of vertices in the array. Another method for computing topological ground-state degeneracies for coupled-wire models was introduced in [197]. Applying it here produces the same answer.

4.5.6 Periodic boundary conditions

We now briefly comment on the coupled-wire model when the natural periodic boundary conditions (PBC) are imposed in all directions, so that the coupled-wire array has the topology of a three-torus. In this case, the Gauss law defined in Eq. (4.9) in the main text can be applied with $M = \Lambda$, leading to the global constraint

$$\sum_{\boldsymbol{r}\in\Lambda} \theta^P_{\boldsymbol{r}} = 0. \tag{4.36}$$

Now we can apply the Haldane counting argument summarized in the main text. The number of chiral gapless modes in the array is $4L_xL_y$, and with PBC there are L_xL_y vertex terms and L_xL_y plaquette terms. Since each interaction term gaps a pair of chiral modes, the number of interaction terms at first appears sufficient to fully gap all chiral modes. However, the constraint (4.36) reduces by one the number

of linearly independent interaction terms in the Hamiltonian. We thus arrive at the conclusion that the model retains one pair of gapless chiral modes with opposite chirality when PBC are imposed in all directions. We remark that that the model with open boundary conditions (OBC) also has chiral gapless modes, but, as shown in Appendix 4.5.4, these modes are associated entirely with the surface. We expect that local bulk properties of the coupled-wire array—e.g., the energy gap for *local* excitations—cannot depend on boundary conditions. We therefore expect that the remaining chiral gapless modes cannot be excited by any local operator. We attribute these modes to an infinite ground-state degeneracy that occurs when the continuum limit of a closely related fracton lattice model (see Appendix 4.5.8) is taken in the wire direction. This subtlety, which is also present in Ref. [68] but was overlooked there, will be investigated in future work.

Under the plausible assumption of an energy gap to all topological excitations created by local operators, the topological ground-state degeneracy with PBC can be computed using the techniques of Appendix 4.5.5. This calculation finds that the ground-state manifold has dimension

$$\mathrm{GSD} = m^{L_x+L_y-2}\ \gcd(L_x, L_y). \tag{4.37}$$

This differs from Eq. (4.35) by the factor $\gcd(L_x, L_y)/m^2$. The numerator of this factor comes from the fact that the final vertex in the vertex-cleaning procedure described in Appendix 4.5.5 can no longer be eliminated in the case of PBC, and the minimal shift of this remaining vertex is $2\pi\ \gcd(L_x, L_y)$. The denominator of

this factor comes from relations among the plaquette terms that only arise for PBC. One factor of m comes from the fact that cleaning all plaquettes into an "L" shape as in Appendix 4.5.5 yields only $L_x + L_y - 1$ unique plaquette terms for PBC. The remaining factor of m comes from the global constraint (4.36), which reduces by one the number of independent plaquette terms.

4.5.7 Generalization to non-Abelian coupled-wire models

We now propose a direct generalization of the coupled-wire construction depicted in Fig. 4.1 that yields models with non-Abelian excitations. The idea is to promote each Luttinger-liquid wire in Fig. 4.1 to a rational conformal field theory (CFT), and to couple these CFTs in such a way that chiral non-Abelian topological phases (rather than Abelian Laughlin $\nu = 1/m$ phases) reside on x-z and y-z planes of the square lattice. We then couple the planes by adding strong local interactions at the vertices where they intersect; similar to the Laughlin construction, these interactions condense p-strings consisting of fractionalized excitations from different planes. This condensation process generates plaquette terms that give rise to subdimensional non-Abelian excitations. For a high-level analysis of related models, we refer the reader to Appendix 4.5.8.

A relatively simple and very interesting class of examples uses $SU(2)_k$ CFTs as building blocks. These CFTs can be realized using spin chains at criticality or fermionic wires with $2k$ fermion species. They can be coupled using current-current interactions within the x-z and y-z planes of the square lattice to yield chiral $SU(2)_k$

topological phases in each plane. Specifically, we define the $SU(2)_k$ current operators using the decomposition $SU(2)_k = \mathbb{Z}_k \times U(1)_k$ as [66]

$$J^{q,+}_{\eta,\boldsymbol{r}} = \sqrt{k}\, \psi^{q}_{\eta,\boldsymbol{r}}\, e^{+i\tilde{\phi}^{q}_{\eta,\boldsymbol{r}}/k} \tag{4.38}$$

$$J^{q,-}_{\eta,\boldsymbol{r}} = \sqrt{k}\, \psi^{q\,\dagger}_{\eta,\boldsymbol{r}}\, e^{-i\tilde{\phi}^{q}_{\eta,\boldsymbol{r}}/k} \tag{4.39}$$

$$J^{q,z}_{\eta,\boldsymbol{r}} = i\frac{\sqrt{k}}{2}\, \partial_z \phi^{q}_{\eta,\boldsymbol{r}}, \tag{4.40}$$

where $\boldsymbol{r} \equiv (x, y)$, $q = 1, 2$ labels whether the CFT belongs to a vertical or horizontal plane, respectively, and $\eta = L, R$ labels the chirality. Here, $\psi^{q}_{\eta,xy}$ and $\psi^{q\,\dagger}_{\eta,xy}$ are parafermion operators that are the simple currents in the $\mathbb{Z}_k$ CFT, and $\phi^{q}_{\eta,xy}$ are chiral boson operators from the $U(1)_k$ CFT. The parafermion operators in a given wire obey the exchange algebra

$$\psi^{q}_{L/R,\boldsymbol{r}}(z)\psi^{q'}_{L/R,\boldsymbol{r}'}(z') = \psi^{q'}_{L/R,\boldsymbol{r}'}(z')\psi^{q}_{L/R,\boldsymbol{r}}(z)\, e^{\pm i\frac{\pi}{k}\delta_{q,q'}\delta_{\boldsymbol{r},\boldsymbol{r}'}\,\mathrm{sgn}(z-z')} \tag{4.41}$$

$$\psi^{q\,\dagger}_{L/R,\boldsymbol{r}}(z)\psi^{q'\,\dagger}_{L/R,\boldsymbol{r}'}(z') = \psi^{q'\,\dagger}_{L/R,\boldsymbol{r}'}(z')\psi^{q\,\dagger}_{L/R,\boldsymbol{r}}(z)\, e^{\pm i\frac{\pi}{k}\delta_{q,q'}\delta_{\boldsymbol{r},\boldsymbol{r}'}\,\mathrm{sgn}(z-z')} \tag{4.42}$$

$$\psi^{q}_{L/R,\boldsymbol{r}}(z)\psi^{q'\,\dagger}_{L/R,\boldsymbol{r}'}(z') = \psi^{q'\,\dagger}_{L/R,\boldsymbol{r}'}(z')\psi^{q}_{L/R,\boldsymbol{r}}(z)\, e^{\mp i\frac{\pi}{k}\delta_{q,q'}\delta_{\boldsymbol{r},\boldsymbol{r}'}\,\mathrm{sgn}(z-z')}, \tag{4.43}$$

while the chiral bosons obey the algebra

$$[\tilde{\phi}^{q}_{L/R,\boldsymbol{r}}(z), \tilde{\phi}^{q'}_{L/R,\boldsymbol{r}'}(z')] = \pm i\pi\, k\, \delta_{q,q'}\delta_{\boldsymbol{r},\boldsymbol{r}'}\,\mathrm{sgn}(z - z'). \tag{4.44}$$

We can then couple the wires using current-current interactions of the form

$$H = \lambda \sum_{x,y} \sum_{a=1}^{3} \left(U^1_{\boldsymbol{r},\boldsymbol{r}+\hat{\boldsymbol{y}}} + U^2_{\boldsymbol{r},\boldsymbol{r}+\hat{\boldsymbol{x}}} \right), \tag{4.45}$$

where

$$U^q_{\boldsymbol{r},\boldsymbol{r}'} = J^{q,+}_{L,\boldsymbol{r}} J^{q,-}_{R,\boldsymbol{r}'} + J^{q,-}_{L,\boldsymbol{r}} J^{q,+}_{R,\boldsymbol{r}'} \tag{4.46}$$

$$= k \Big[\psi^q_{L,\boldsymbol{r}} \psi^{q\,\dagger}_{R,\boldsymbol{r}'} \, e^{i\left(\tilde{\phi}^q_{L,\boldsymbol{r}} - \tilde{\phi}^q_{R,\boldsymbol{r}'}\right)/k} + \text{H.c.} \Big]. \tag{4.47}$$

The interactions (4.45) are marginally relevant under the renormalization group, so the coupling constant λ flows to infinity when it has the appropriate sign. Each plane then enters a gapped phase with $SU(2)_k$ non-Abelian topological order [65, 66].

Next we seek vertex terms that couple intersecting x-z and y-z planes. The simplest local operators are products of primary operators $\Phi^{q,(\ell)}_{\boldsymbol{r}}$ in each CFT, from which we can construct Hamiltonian terms

$$U^{V,\ell\ell'}_{\boldsymbol{r}} = \Phi^{1,(\ell)}_{\boldsymbol{r}} \Phi^{2,(\ell')}_{\boldsymbol{r}} + \text{H.c.} \tag{4.48}$$

Here, the index $\ell = 0, \ldots, k$ labels the $k+1$ primary fields of the $SU(2)_k$ CFT. These primary operators can be expressed in terms of operators in the $\mathbb{Z}_k$ and $U(1)_k$ CFTs as (suppressing the labels q and $\boldsymbol{r}$ for compactness) [198]

$$\Phi^{(\ell)} = \Phi^{\ell}_L \Phi^{\ell}_R \; e^{i\frac{\ell^2}{4k}\tilde{\phi}_L} \, e^{-i\frac{\ell^2}{4k}\tilde{\phi}_R}, \tag{4.49}$$

where $\Phi_L^\ell \Phi_R^\ell$ is a primary operator in the $\mathbb{Z}_k$ CFT. (Note that $\Phi_L^0 \Phi_R^0 = \Phi_L^k \Phi_R^k = \mathbb{1}$.) The primary operators $\Phi^{(\ell)}$ are in one-to-one correspondence with anyons in the gapped bulk of the coupled-wire array, creating quasiparticle-quasihole pairs consisting of anyons with label ℓ. The vertex terms (4.48) thus create bound states of anyonic excitations in the intersecting layers; adding such a term to the Hamiltonian and manually imposing a large coupling $\lambda_V \gg \lambda$ leads to condensation of p-strings composed of these anyons. The natural anyon to condense in this fashion is the one with label $\ell = k$. This anyon is always Abelian and carries topological spin $e^{i\frac{\pi k}{2}}$—thus, it is a boson when $k = 0 \mod 4$, a fermion when $k = 2 \mod 4$, and a semion or antisemion when $k = 1$ or $3 \mod 4$. To condense p-strings composed of these anyons, we choose $\ell = \ell' = k$ in Eq. (4.48).

Implementing p-string condensation using the vertex terms $U_{\boldsymbol{r}}^{V,kk}$ leads to modified couplings between wires arising from perturbation theory in λ/λ_V. Based on our understanding of the Abelian case, it is clear that the current-current couplings (4.46) generically excite the vertex terms (4.48)—this can be seen, for example, by inspection of the Abelian components of the current operators (4.38) and the primary operators (4.49), whose commutation is governed by Eq. (4.44). Thus, perturbation theory generates products of the current-current interactions (4.46). An example of a term generated at fourth order is

$$U_{\boldsymbol{r}}^P \sim J_{L,\boldsymbol{r}}^{1,+} J_{R,\boldsymbol{r}+\hat{\boldsymbol{y}}}^{1,-} J_{L,\boldsymbol{r}+\hat{\boldsymbol{y}}}^{2,+} J_{R,\boldsymbol{r}+\hat{\boldsymbol{y}}+\hat{\boldsymbol{x}}}^{2,-} J_{R,\boldsymbol{r}+\hat{\boldsymbol{y}}+\hat{\boldsymbol{x}}}^{1,+} J_{L,\boldsymbol{r}+\hat{\boldsymbol{x}}}^{1,-} J_{R,\boldsymbol{r}+\hat{\boldsymbol{x}}}^{2,+} J_{L,\boldsymbol{r}}^{2,-} + \text{H.c.}, \tag{4.50}$$

whose sign structure mimics that of its Abelian counterpart, see Eq. (4.3). To see

that this indeed commutes with $U_{\boldsymbol{r}}^{V,kk}$, we first consider the Abelian sector. The commutator of the Abelian parts of the current operators in Eq. (4.50) with the Abelian part of $U_{\boldsymbol{r}}^{V,kk}$ can be shown to vanish using (4.44). Next, we consider the non-Abelian sector. In order for the non-Abelian parts of Eqs. (4.50) and $U_{\boldsymbol{r}}^{V,kk}$ to commute, we must demand that the combination of $\mathbb{Z}_k$ primary operators entering Eq. (4.48) with $\ell = \ell' = k$ has trivial monodromy with the parafermion operators entering Eq. (4.50). For general ℓ, ℓ', this is achieved when the following two relationships hold:

$$\Delta_{\Phi^\ell} + \Delta_\psi - \Delta_{\Phi^\ell \times \psi} = -(\Delta_{\Phi^{\ell'}} + \Delta_{\psi^\dagger} - \Delta_{\Phi^{\ell'} \times \psi^\dagger}) \bmod 1 \tag{4.51}$$

$$\Delta_{\Phi^\ell} + \Delta_{\psi^\dagger} - \Delta_{\Phi^\ell \times \psi^\dagger} = \Delta_{\Phi^{\ell'}} + \Delta_\psi - \Delta_{\Phi^{\ell'} \times \psi} \bmod 1, \tag{4.52}$$

where $\Delta_{\mathcal{O}}$ is the chiral scaling dimension of the operator $\mathcal{O}$ and $\mathcal{O} \times \mathcal{O}'$ denotes the fusion product of the operators $\mathcal{O}$ and $\mathcal{O}'$. Using the data [198]

$$\Delta_{\Phi^\ell} = \frac{\ell(\ell+2)}{4(k+2)} - \frac{\ell^2}{4k} \tag{4.53}$$

$$\Delta_\psi = -\frac{1}{k} \tag{4.54}$$

$$\Delta_{\psi^\dagger} = -\frac{(k-1)^2}{k} \tag{4.55}$$

$$\Delta_{\Phi^\ell \times \psi} = \frac{\ell(\ell+2)}{4(k+2)} - \frac{(\ell+2)^2}{4k} \tag{4.56}$$

$$\Delta_{\Phi^\ell \times \psi^\dagger} = \frac{\ell(\ell+2)}{4(k+2)} - \frac{(\ell+2k-2)^2}{4k} \tag{4.57}$$

we see that Eq. (4.51) reduces to $\ell = \ell' \bmod k$, while Eq. (4.52) reduces to $\ell =$

$-\ell'$ mod k. The only nontrivial solution satisfying both constraints is $\ell = \ell' = k$.

We thus arrive at the interesting conclusion that condensing p-strings composed of $\ell = k$ $SU(2)_k$ anyons yields a class of models that naturally generalizes the Abelian construction depicted in Fig. 4.1.

Having constructed a nontrivial class of models, we now discuss how to determine the allowed quasiparticles after condensation. Here we can take advantage of the connection between anyon condensation in topological quantum field theories (TQFTs) and chiral algebra extensions in CFTs [184]. Namely, when a primary operator in a CFT is "condensed" (or, algebraically speaking, added to the representation of the vacuum sector) by adding a term of the form (4.48) to the Hamiltonian, the operator content of the CFT reorganizes itself in a manner reminiscent of anyon condensation in TQFT. In particular, the new primary operators in the "extended" CFT are in one-to-one correspondence with deconfined quasiparticles after condensation in the TQFT. Each new primary operator corresponds to a quasiparticle species, as we saw in the Abelian case where each local nonchiral product of vertex operators makes a bound state of fractons. Non-Abelian excitations are created by primary operators in the extended CFT that have a nontrivial fusion algebra, i.e. if their fusion with one or more other primary operators has multiple possible channels.

As an example, consider a wire construction based on $SU(2)_4$ CFTs coupled by current-current interactions (4.46) and vertex terms (4.48) with $\ell = \ell' = 4$. The effect of adding the vertex terms at strong coupling can be understood heuristically by viewing the $p = 1, 2$ copies of $SU(2)_4$ as two separate $SU(2)_4 \times \overline{SU(2)_4}$ topological orders, whose anyons we label by $(\ell, \ell')_p$ with $\ell, \ell' = 0, \ldots, 4$ and $p = 1, 2$. In this

analogy, each anyon with integer topological spin in either of the two copies, including the "diagonal" anyons $(\ell, \ell)_p$, corresponds to a local operator in the associated CFT. These two topological orders are then coupled by condensing the anyon $(4,4)_1(4,4)_2$. One can verify by explicit calculation along the lines of Ref. [184] that the condensed theory hosts a pair of diagonal non-Abelian anyons that can be labeled by $(1,1)_1(0,0)_2$ and $(0,0)_1(1,1)_2$. The corresponding local operators in the CFT thus create non-Abelian quasiparticles.

Although it is interesting that we can generate non-Abelian generalizations of the coupled-wire model studied in the main text, the analysis of this model is cumbersome to carry out at the level of the underlying CFTs. In Appendix 4.5.8, we introduce a general algebraic prescription for carrying out the planar p-string condensation procedure discussed here. Applying this construction to $SU(2)_k$ layers allows for a much more rapid analysis of quasiparticle mobility in the resulting fracton models.

4.5.8 Further aspects of planar p-string condensation

In this Appendix we present further details about examples of and connections between planar p-string condensation and existing mechanisms that generate fracton topological order.

In Sec. 4.5.9, we present further high-level examples of planar p-string condensation, one of which is non-Abelian. In Sec. 4.5.10, we introduce several spin lattice models constructed via planar p-string condensation, including a model that is foliated equivalent [134] to the chiral fracton theory that emerges in the bulk of the coupled-wire model

introduced in the main text. We go on to discuss in Sec. 4.5.11 how this mechanism is related to gauging planar subsystem symmetries [183], and in Sec. 4.5.12 how it fits into the recently developed framework of topological defect networks [77].

4.5.9 Further high-level examples

In this section we present a pair of examples, the first generalizing the $\mathbb{Z}_N$ layer examples to even N, the second realizing non-Abelian fracton sectors that emerge from the coupled-wire construction in Appendix 4.5.7.

Semion layers

There is a closely related family of examples to those presented in Section 4.3 with N even. These correspond to the semion theory (and related theories). Again the topological charges and their fusion is given by $\mathbb{Z}_N$ with N an even integer in this case. The S-matrix and topological spins are

$$S_{a,b} = \frac{1}{\sqrt{N}} e^{i\frac{2\pi}{N}ab}, \qquad \theta_a = e^{i\frac{\pi}{N}a^2}, \tag{4.58}$$

and the quantum dimensions are all 1. However, in this case the F symbols are nontrivial, namely

$$F^{abc}_{[a+b+c]} = e^{i\frac{\pi}{N}a(b+c-[b+c])}, \tag{4.59}$$

where [ ] denotes addition modulo N.

There is an obvious $\mathbb{Z}_N$ grading generated by braiding with the 1 anyon, which is semionic (or a generalization thereof). The planar p-string condensation construction of a fracton model can be formally followed through exactly as above. However, in this case the string operators for the anyonic p-strings being condensed in disjoint layers do in fact have a nontrivial anomaly due to the nontrivial F-symbol. This F-symbol implies that the string operators making up the membrane operator that creates a p-string cannot be realized as on-site operators, and hence cannot be condensed in a consistent way, see Sec. 4.5.11. Another way to say this is that the p-strings cannot be condensed into the vacuum of a gapped phase, as that would allow a vacuum to vacuum process involving the creation and annihilation of p-strings resulting in the vacuum state being equal to minus itself due to the nontrivial F-symbol, which takes values ± 1.

$SU(2)_k$ anyon layers

For an example that is related to the non-Abelian coupled-wire construction proposed in Appendix 4.5.7, we consider chiral topological layers supporting $SU(2)_k$ anyons. The topological charges of the $SU(2)_k$ anyon theory are labelled by half integers $\{0, \frac{1}{2}, \ldots, \frac{k}{2}\}$. Their fusion rules, quantum dimensions, S-matrix and topological spins are

$$j_1 \times j_2 = \sum_{j=|j_1-j_2|}^{\min(j_1+j_2,k-j_1-j_2)} j\,, \qquad d_j = \frac{\sin\frac{(2j+1)\pi}{k+2}}{\sin\frac{\pi}{k+2}}\,,$$
$$S_{j_1,j_2} = \sqrt{\frac{2}{k+2}}\sin\frac{(2j_1+1)(2j_2+1)\pi}{k+2}\,, \qquad \theta_j = e^{2\pi i\frac{j(j+1)}{k+2}}\,, \tag{4.60}$$

respectively. See Ref. [196] for a review of the F and R symbols of the $SU(2)_k$ anyon theory.

The $\frac{k}{2}$ particle is an Abelian $\mathbb{Z}_2$ anyon; it is a boson for $k = 0 \mod 4$, a semion for $k = 1 \mod 4$, a fermion for $k = 2 \mod 4$, and an antisemion for $k = 3 \mod 4$. The braiding phases $S_{j,\frac{k}{2}}|S_{j,\frac{k}{2}}|^{-1} = \pm 1$ with $\frac{k}{2}$ induce a $\mathbb{Z}_2$ grading on the topological charges, organizing them into integers and half-integers $\{0, 1, \dots\}_+ \oplus \{\frac{1}{2}, \frac{3}{2}, \dots\}_-$. The half-integer -1 sector contains a non-Abelian anyon for any $k > 1$.

We construct a fracton model by driving $\mathbb{Z}_2$ p-string condensation of $\frac{k}{2}$ anyons within xy planes of a stack of $SU(2)_k$ anyon layers along the xz and yz planes of the cubic lattice. The resulting fracton model has a hierarchy of subdimensional topologial excitations generated by:

- Abelian $\mathbb{Z}_2$ fractons that appear on the open ends of condensed p-strings.
- Non-Abelian (and Abelian) $\hat{x}$ lineons from the half-integer anyons in an xz layer, trapped between p-string planes. Similarly there are $\hat{y}$ lineons from the yz layers. There are also non-Abelian $\hat{z}$ lineons from composites of an $\hat{x}$ and $\hat{y}$ lineon trapped between the same p-string planes.
- Planons, that may be non-Abelian, coming from the integer anyons in an xz or yz layer or from composites of fractons or lineons that have an overall trivial braiding with the p-strings.

We remark that for odd k there is an anomaly of the string operators preventing the p-strings from condensing to form a consistent condensate, due to the nontrivial F-symbols of the semions or antisemions. For this reason we do not expect that driving

such a p-string condensation in odd-k $SU(2)_k$ planes can lead to a gapped phase. In Sec. 4.5.11, this is expressed as an anomaly of the planar subsystem symmetry that applies semion or antisemion string operators to layers intersected by the plane.

For $k/2$ an odd integer, the p-strings being condensed in layers are made up of emergent fermions. For conventional p-string condensation throughout the whole 3D bulk this would be anomalous, due to the nontrivial topological spin of the emergent fermions. However, as was shown in Ref. [183], a planar subsystem symmetry generated by fermion string operators is not anomalous and can be gauged. This is equivalent to the condensation of p-strings consisting of emergent fermions, see Sec. 4.5.11 for a further discussion.

4.5.10 Lattice models

We now present several lattice-model constructions using the planar p-string condensation mechanism. We highlight in particular that the lattice model discussed in Sec. 4.5.10 is closely related to the coupled-wire model studied in the main text and to the abstract model discussed in Sec. 4.3.2.

X-cube from $\mathbb{Z}_2$ gauge theory layers

As a warm up we consider 2D layers of toric code, i.e. $\mathbb{Z}_2$ lattice gauge theory, stacked along the xz and yz planes of the cubic lattice. We introduce couplings that induce p-loop condensation of m anyons on the xy planes. The resulting planar p-string condensed model is simply the well-known X-cube model [42].

The Hamiltonian governing the edge qubits in each 2D layer is

$$H_{\mathrm{TC}} = -\sum_{v}\prod_{e\ni v} Z_e - \sum_{p}\prod_{e\in p} X_e\,. \tag{4.61}$$

where $e \ni v$ denotes the edges e containing a vertex v and p is used to denote plaquettes. The layers are stacked along the xz and yz planes of the cubic lattice, leading to a single qubit per edge in each xy plane and two qubits per $\hat{z}$ edge e, which we label e_{xz} and e_{yz}. The m anyon p-string creation operators are given by $Z_{e_{xz}}Z_{e_{yz}}$. These couplings are introduced to the decoupled layer Hamiltonian

$$H_\lambda = \sum_{\ell_{xz}} H_{\mathrm{TC}}^{\ell_{xz}} + \sum_{\ell_{yz}} H_{\mathrm{TC}}^{\ell_{yz}} - \lambda \sum_{e\perp\hat{z}} Z_{e_{xz}}Z_{e_{yz}}\,, \tag{4.62}$$

where ℓ_{xz} and ℓ_{yz} denote xz and yz planes, respectively. In the limit of infinitely strong coupling $\lambda \to \infty$ the two qubit Hilbert space on each xy-plane edge is projected onto a single qubit described by the operators $Z_{e_{xz}} \sim Z_{e_{yz}} \mapsto Z_e$ and $X_{e_{xz}}X_{e_{yz}} \mapsto X_e$. The resulting strongly coupled Hamiltonian has cube terms, given by products of four plaquette terms, arising at leading order in degenerate perturbation theory (higher order terms are not independent and hence simply shift the energetics of gapped excitations). This is simply the X-cube model at leading order:

$$H_{\mathrm{condensed}} = -\sum_{v}\prod_{e\ni v, e\perp\hat{x}} Z_e + \prod_{e\ni v, e\perp\hat{y}} Z_e - \sum_{c}\prod_{e\in c} X_e\,. \tag{4.63}$$

The anyons in the toric code layers have $\mathbb{Z}_2\times\mathbb{Z}_2$ fusion generated by the $\mathbb{Z}_2$ electric charge e, which are created by X string operators along edges of the graph,

and magnetic flux m, which are created by Z string operators along dual edges. Since the m particles are planar p-string condensed in this example, the e particles are promoted to lineons, while m becomes a planon composite of a pair of fractons, as described in the general treatment above.

We remark that this example extends directly to planar p-loop condensing $\mathbb{Z}_N$ lattice gauge theory layers to obtain the $\mathbb{Z}_N$ X-cube model. In the next example we introduce an alternate anyonic planar p-loop condensation transition that drives $\mathbb{Z}_N$ lattice gauge theory layers to a twisted $\mathbb{Z}_N$ X-cube model that is foliated equivalent to the chiral fracton model introduced in the main text and discussed in Sec. 4.3.2.

Anomalous string operators in $\mathbb{Z}_N$ gauge theory

For our next example we consider anyonic planar p-string condensation in layers containing $\mathbb{Z}_N$ gauge theory. The resulting fracton model is equivalent to the coupled-wire fracton model introduced in the main text and Sec. 4.3.2, up to stacking with decoupled 2D layers (also known as foliated equivalence).

To describe the model we denote the $\mathbb{Z}_N$ clock and shift matrices by X and Z. They satisfy the relations

$$X^N = Z^N = \mathbb{1}\,, \qquad\qquad XZ = \overline{\omega} ZX\,, \tag{4.64}$$

where ω is a primitive Nth root of unity. The 2D layer Hamiltonians act on edge

qubits of a square lattice via

$$H_{2D} = -\sum_v A_v - \sum_p B_p + \text{H.c.} \tag{4.65}$$

where the vertex and star terms are given by

$A_v =$ 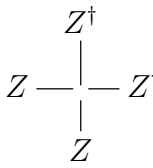 , $B_p =$ 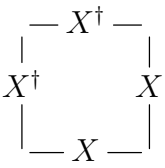 . (4.66)

The above terms generate Z string operators on the dual lattice, and X string operators on the lattice. These string operators create emergent anyons corresponding to gauge flux and charge, which we denote by m and e respectively, that generate $\mathbb{Z}_N \times \mathbb{Z}_N$ fusion rules. The anyon theory describing these particles is formally denoted by the Drinfeld center $\mathcal{Z}(\text{Vec}_{\mathbb{Z}_N})$, which is discussed further in the next section. The braiding S-matrix of this anyon theory is

$$S_{e^i m^j, e^k m^\ell} = \frac{1}{N} \omega^{i\ell + jk} \,. \tag{4.67}$$

For N odd this theory can be decomposed into layers of opposite chirality, $\mathcal{Z}(\text{Vec}_{\mathbb{Z}_N}) \cong \mathbb{Z}_N^{(n)} \boxtimes \mathbb{Z}_N^{(-n)}$, for $n = 1, 2$, or any other integer coprime to N, where we have used the notation of Ref. [196]. The $\boxtimes$ notation we have used refers to the operation of stacking decoupled layers. The generating anyon for the $\mathbb{Z}_N^{(n)}$ chiral layer is given by $e^n m$, while the generator of the antichiral $\mathbb{Z}_N^{(-n)}$ layer is $e^n m^{N-1}$. Denoting anyons in

terms of the chiral-antichiral generators as (i,j) the S-matrix is then written

$$S_{(i,j),(k,\ell)} = \frac{1}{N}\omega^{2n(ik-j\ell)} = S^{(n)}_{i,k} S^{(-n)}_{j,\ell}\,, \tag{4.68}$$

where $S^{(n)}_{i,k}, S^{(-n)}_{j,\ell}$, are the S-matrices of the chiral and antichiral layers respectively.

The anyon theory describing the superselection sectors of the Laughlin state at filling fraction $\nu = \frac{1}{m}$, modulo the physical fermion, is $\mathbb{Z}_N^{(2)}$ for $N = m$, see Ref. [196] for example. Below we utilize the embedding of the $\mathbb{Z}_N^{(2)}$ anyons into the $\mathcal{Z}(\mathrm{Vec}_{\mathbb{Z}_N})$ anyons of the $\mathbb{Z}_N$ lattice gauge theory to construct a lattice model via p-string condensation that is foliated equivalent [134] (i.e. equivalent up to stacking decoupled $\mathbb{Z}_N^{(-2)}$ layers) to the fracton model arising from the coupled-wire construction in the main text when a lattice cutoff is introduced in the wire direction. We explicitly consider $n = 2$, which is relevant to the Laughlin case, but a more general family of models starting from hierarchy FQH states can be obtained using $n \neq 2$.

The string operators for the chiral Abelian anyons in a given 2D layer, as viewed from above, are of the form

$$\cdots \quad \overset{Z}{\big|}\!-\!X^2\!-\!\overset{Z}{\big|}\!-\!X^2\!-\!\overset{Z}{\big|}\!-\!X^2\!-\!\overset{Z}{\big|}\!-\!X^2\!-\!\overset{Z}{\big|}\!-\!X^2 \quad \cdots \tag{4.69}$$

For convenience we conjugate the model by the following local unitary circuit to simplify the horizontal string operators

$$U = \prod_v H_{v+\frac{\hat{x}}{2}} CX^2_{v+\frac{\hat{x}}{2},v+\frac{\hat{y}}{2}} H^\dagger_{v+\frac{\hat{x}}{2}}\,, \tag{4.70}$$

where $\hat{x}$ and $\hat{y}$ denote the axes of the square lattice depicted above. where H_i is a generalized Hadamard matrix, or $\mathbb{Z}_N$ Fourier transform, which satisfies

$$HXH^\dagger = Z^\dagger \,, \qquad\qquad HZH^\dagger = X \,, \tag{4.71}$$

while $CX_{i,j}$ is a generalized controlled-X matrix, which satisfies

$$CX(XI)CX^\dagger = XX \,, \quad CX(IX)CX^\dagger = IX \,, \quad CX(ZI)CX^\dagger = ZI \,, \quad CX(IZ)CX^\dagger = Z^\dagger Z \,, \tag{4.72}$$

where XI, IX denote X_i, X_j, and similarly for Z. The conjugated string operator becomes

$$\cdots \quad \begin{array}{l} Z \\ |\_\_\_ \end{array} \; \begin{array}{l} \quad Z \\ \_\_\_|\_\_\_ \end{array} \; \begin{array}{l} \quad Z \\ \_\_\_|\_\_\_ \end{array} \; \begin{array}{l} \quad Z \\ \_\_\_|\_\_\_ \end{array} \; \begin{array}{l} \quad Z \\ \_\_\_|\_\_\_ \end{array} \quad \cdots . \tag{4.73}$$

The B_p terms in the Hamiltonian are left invariant under conjugation by U, while the A_v terms become

$$UA_vU^\dagger = \begin{array}{ccccc} X^{-2} & & Z^\dagger X^2 & & \\ | & & | & & \\ |\_\_ & Z \,\_\_ & | & - \; Z^\dagger X^2 & \\ & & | & & \\ & & Z & & \\ & & | & & \\ & & |\_ & X^{-2} & \end{array} \quad . \tag{4.74}$$

To facilitate the coupled-layer construction we modify our choice of the Hamiltonian vertex terms by multiplying the above operators with plaquette terms, which preserves

the topological phase, as follows:

$$\widetilde{A}_v = \begin{array}{ccc} & X^2 - & \\ & | & \\ & Z^\dagger & \\ ZX^{-2} - & | & - Z^\dagger X^2 \\ & | & \\ & Z & \\ & | & \\ & - X^{-2} & \end{array} \quad . \tag{4.75}$$

The planar p-string coupled-layer model is obtained by stacking the 2D Hamiltonian along xz and yz planes of the cubic lattice, such that there are two qudits per $\hat{z}$ edge coming from the vertical edges of the intersecting 2D layers, and driving a phase transition with a strong uniform $ZZ^\dagger$ field applied to these edges, i.e.

$$H(\alpha) = \sum_{xz,\, yz \text{ planes}} H_{2D} - \alpha \sum_{e \| \hat{z}} ZZ^\dagger + \text{H.c.} \tag{4.76}$$

In the planar p-string condensed limit, as $\alpha \to \infty$, the low energy subspace has one effective qudit per $\hat{z}$ edge with logical operators $ZI \sim IZ \mapsto Z, XX \mapsto X$ and the leading order Hamiltonian on this Hilbert space is given by

$$H = -\sum_v (\widetilde{A}_v^{xz} + \widetilde{A}_v^{yz}) - \sum_c B_c + \text{H.c.}, \tag{4.77}$$

where $\widetilde{A}_v^{xz}$ and $\widetilde{A}_v^{yz}$ are modified star terms that now act on a common set of qubits on the $\hat{z}$ edges, and

$$B_c = \prod_{e \in c} X_e^{\sigma_e} \tag{4.78}$$

is the cage term of the $\mathbb{Z}_N$ X-cube model, where $\sigma_e = \pm 1$ depending upon the edge. Hence we refer to the Hamiltonian (4.77) as a twisted $\mathbb{Z}_N$ X-cube model, though we remark that the way this model is twisted is distinct from previously considered generalizations of X-cube [76, 128].

We now discuss the ground space degeneracy of the model (4.77) with periodic and open boundary conditions and describe how these results compare with the coupled-wire model discussed in the main text and Appendices 4.5.5 and 4.5.6.

Periodic boundary conditions: On an $L_1 \times L_2 \times L_3$ torus there are an equal number of qubits and local stabilizer generator terms in the Hamiltonian and so we can compute the ground space degeneracy by counting the number of independent relations between the generators, i.e. nontrivial products of generators equal to the identity. The cube terms are identical to those in the X-cube model, where it is known that the product over any dual lattice plane gives rise to a relation. Furthermore, there are two redundancies in these relations as the product over all dual xy planes is identical to the product over all dual yz planes, and similarly for dual xz planes. The vertex terms in Eq. (4.77) are twisted relative to those in the X-cube model, however a similar set of relations still hold: the product of the $\widetilde{A}_v^{xz}$ terms over an xz plane gives a relation, and similarly for the product of the $\widetilde{A}_v^{yz}$ terms over a yz plane. Finally, we can take the product of $\widetilde{A}_v^{xz}(\widetilde{A}_v^{yz})^\dagger$ over an xy plane, leaving a product of Pauli $X^{\pm 2}$ operators over the edges in a pair of xy planes, which can be cancelled out by multiplication with cube terms B_c between the planes, provided L_x, L_y, are multiples of N. There is one redundancy in these relations as the product of the $\widetilde{A}_v^{xz}$ relations over all xz planes, and the $(\widetilde{A}_v^{yz})^\dagger$ relations over all yz planes is identical to

the product of the $\widetilde{A}_v^{xz}(\widetilde{A}_v^{yz})^\dagger$ relations over all xy planes.

The counting of the relations modulo redundancies gives a total ground space degeneracy of $N^{2(L_x+L_y+L_z)-3}$, matching that of the untwisted X-cube model. As explained above, the lattice model in this section is foliated-equivalent to the topological phase of the coupled-wire model, up to stacking with $L_x + L_y$ decoupled $\mathbb{Z}_N^{(-2)}$ layers, which are not affected by the p-string condensation. The degeneracy of the decoupled antichiral layers after planar p-string condensation is $N^{L_x+L_y}$, leaving a degeneracy of $N^{L_x+L_y+2L_z-3}$ associated to the chiral fracton model.

To match with the degeneracy of the wire model we must take the continuum limit in the $\hat{z}$ direction, which sends the number of sites in that direction to infinity, i.e. $L_z \to \infty$. Hence we see from the lattice model that there is necessarily some infinite topological degeneracy due to the continuum limit along $\hat{z}$. This infinite degeneracy is quite subtle, although a similar phenomenon can already be seen to occur for the continuum limit of decoupled topological layers stacked along $\hat{z}$. It is topologically protected in the sense that splitting by local operators is exponentially suppressed as a function of L_x and L_y but it can be lifted by local operators to give a nontrivial dispersion in the $\hat{z}$ direction within the exponentially suppressed window. We leave a more in-depth study of this limit to future work. In the continuum limit along $\hat{z}$, relations that limit to a product over a continuum are lumped into the infinite degeneracy, i.e. we separate out the component of the degeneracy that becomes infinite via $N^{2L_z-2} \to \infty$. This leaves a degeneracy of $N^{L_x+L_y-1}$ which matches that of the coupled-wire model with PBC (see Appendix 4.5.6) for $N = m$ and L_x, L_y such that $\gcd(L_x, L_y) = N$.

Open boundaries: It is simple to modify the above example to match the alternative boundary conditions used to calculate the ground space degeneracy in the main text and in Appendix 4.5.5. To see this, we first note that by picking gapped open boundary conditions at $x = 0, L_x$, for an xz layer, and $y = 0, L_y$, for a yz layer, we can induce the chiral layer to fold over and become the antichiral layer. Equivalently, with electric charge-condensing rough boundaries [199] we have that pairs of chiral and antichiral anyons condense at the boundary. Combining this with periodic boundary conditions in the $\hat{z}$ direction we have a system that can be viewed as decoupled tori on xz and yz planes supporting chiral $\mathbb{Z}_N^{(2)}$ anyons. Inducing p-string condensation on the chiral layers only, as described above, drives the chiral layers to enter the phase of the fracton model described in the main text, but with gapped boundary conditions where the $x = 0$ and $x = L_x$ ($y = 0$ and $y = L_y$) boundaries of the fracton model are connected via a stack of 2D antichiral layers.

To construct the lattice model we again start from decoupled 2D Hamiltonians that we write as

$$H_{2D}^{RBC} = -\sum_v A_v - \sum_p B_p - \sum_{p\in L} B_p^L - \sum_{p\in R} B_p^R + \text{H.c.}, \tag{4.79}$$

where the A_v terms are the same as above, and the B_p terms on plaquettes not touching the left or right open boundaries (as viewed from above) are also the same. The plaquette terms touching the left, or right, boundaries (viewed from above) are

given by

$B_p^L =$ 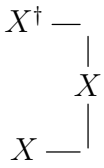 , $B_p^R =$ 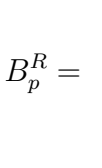 , (4.80)

respectively. At this rough boundary, e anyons condense as single vertex terms A_v can be excited by an open string of X operators ending on the boundary. In terms of the decomposition into chiral and antichiral layers $\mathbb{Z}_N^{(2)} \boxtimes \mathbb{Z}_N^{(-2)}$ generated by e^2m and e^2m^{N-1}, respectively, this gapped boundary corresponds to a simple fold, since $e^2m \times e^2m^{N-1} = e^4$ generates the condensate there.

As above, we apply the local unitary circuit from Eq. (4.70), restricted to the vertices not on the boundaries. All but the leftmost vertex terms take the same form as in Eq. (4.74). After a phase preserving redefinition of the vertex terms they are all brought into the form of Eq. (4.75) (including the leftmost vertex terms, by way of multiplication with the B_p^L terms). The coupled-layer model is found by driving planar p-string condensation on the xy planes of a stack of $\mathbb{Z}_N^{(2)}$ layers in xz and yz planes with rough boundary conditions on the $x = 0, L_x$, and $y = 0, L_y$, planes

$$H(\alpha) = \sum_{xz,\, yz \text{ planes}} H_{2D}^{RBC} - \alpha \sum_{e \| \hat{z}} ZZ^\dagger + \text{H.c.} \tag{4.81}$$

Taking the planar p-string condensed limit, $\alpha \to \infty$, projects each edge into a single qudit subspace spanned by operators $ZI \sim IZ \mapsto Z, XX \mapsto X$. The Hamiltonian on

this Hilbert space is given by

$$H = -\sum_v (\widetilde{A}_v^{xz} + \widetilde{A}_v^{yz}) - \sum_c B_c - \sum_{c\in\partial} B_c^{\partial} + \text{H.c.} \tag{4.82}$$

where $\widetilde{A}_v^{xz}$, $\widetilde{A}_v^{yz}$ and B_c are as above and

$$B_c^{\partial} = \prod_{e\in c} X_e^{\sigma_e}\,, \tag{4.83}$$

is a partial cage term of the X-cube model in the presence of a rough gapped boundary [186], where c contains eight edges for a boundary term and five edges for a corner term, while $\sigma_e = \pm 1$ depending upon the edge. To count the ground space degeneracy in the above stabilizer Hamiltonian we first note that with the gapped open boundary conditions there are $3L_xL_y + L_x + L_y$ edge qubits, $2L_xL_y$ star terms, and $L_xL_y + L_x + L_y + 1$ cube terms (including truncated edge and corner cubes) per xy layer. There are $(L_y + 1) + (L_x + 1) + L_z$ constraints from products of cube terms over dual xz, yz, and xy planes that give identity. However there are two global redundancies between the product of the relations over all dual xz and yz planes, and all xz and xy planes, respectively. Combining the above contributions yields a ground state degeneracy of

$$N^{L_x+L_y} = N^{(3L_xL_y+L_x+L_y)L_z-(3L_xL_y+L_x+L_y+1)L_z+(L_x+1+L_y+1+L_z)-2} \tag{4.84}$$

which for $N = m$ matches the result quoted in the main text and derived in Appendix 4.5.5.

String-net layers

Finally, we consider a class of examples based on inducing planar p-string condensation on decoupled layers supporting models from the general class of 2D string-net Hamiltonians.

Any nonchiral anyon theory that admits a gapped boundary to vacuum (technically Witt trivial [200]) can be realized by a string-net lattice model [201]. The starting point is a theory $\mathcal{C}$ consisting of a finite number of string types $\{s\}$, including the vacuum 1, together with a fusion operation described by coefficients N_{ab}^{c} that is not strictly associative, which is captured by F-symbols. This mathematical object is formalised by a unitary fusion category (UFC) [202].

The string-net Hamiltonian based on $\mathcal{C}$ is defined on a honeycomb lattice (and more generally on any directed trivalent planar graph)

$$H_{\mathrm{SN}} = -\sum_{v} A_v - \sum_{p} B_p \,, \tag{4.85}$$

where the vertex term enforces the fusion rule at every vertex of the lattice

$A_v \Big|$ 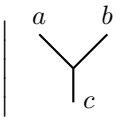 $\Big\rangle = \delta_{ab}^{c} \Big|$ 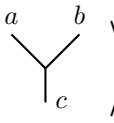 $\Big\rangle \,,$ (4.86)

with

$$\delta_{ab}^{c} = \begin{cases} 0 & N_{ab}^{c} = 0 \,, \\ 1 & N_{ab}^{c} > 0 \,, \end{cases} \tag{4.87}$$

and the plaquette term further decomposes as

$$B_p = \frac{1}{\mathcal{D}^2} \sum_{s \in \mathcal{C}} d_s B_p^s \,, \tag{4.88}$$

where d_s is the quantum dimension of string type s, $\mathcal{D}^2 = \sum_s d_s^2$ is the total quantum dimension of $\mathcal{C}$ and

$B_p^s \Big| \quad \Big\rangle = \Big| \quad s \quad \Big\rangle \,,$ 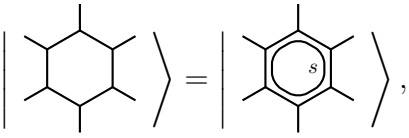 (4.89)

inserts a loop of string type s into the plaquette p, which is then fused into the lattice.

The emergent anyons in the topological phase containing the string-net model based on the UFC $\mathcal{C}$ are described by the Drinfeld center $\mathcal{Z}(\mathcal{C})$. In the special case that $\mathcal{C}$ already describes an algebraic theory of anyons, known as a modular tensor category (MTC), the Drinfeld center is simply given by stacking the anyon theory with its time-reverse, $\mathcal{Z}(\mathcal{C}) \cong \mathcal{C} \boxtimes \overline{\mathcal{C}}$. Another important special case is where the string types are given by elements of a finite group G and the F-symbols are trivial, denoted Vec_G, in which the emergent anyons $\mathcal{Z}(\mathrm{Vec}_G)$ correspond to the charges, fluxes and dyons of G gauge theory.

If the emergent anyon theory $\mathcal{Z}(\mathcal{C})$ contains a group G of Abelian bosons that are closed under fusion, then the above lattice model can be constructed so as to have an on-site 1-form G symmetry [203, 204, 205, 206]. This is achieved by taking an input UFC $\mathcal{C}_G$ that is G-graded, without loss of generality. This simply means that the string types decompose into nonempty g-sectors $\mathcal{C}_g$ containing string types we denote

$\{s_g\}$. The full UFC is recovered by a direct sum over these sectors, i.e.

$$\mathcal{C}_G = \bigoplus_g \mathcal{C}_g \,, \tag{4.90}$$

and the fusion rule respects the grading, i.e.

$$N_{a_g b_h}^{c_k} = \delta_{gh\bar{k}} N_{a_g b_h}^{c_k} \,, \tag{4.91}$$

where $\bar{k} = k^{-1}$. The plaquette terms of the string-net Hamiltonian can then be rearranged to form a projection onto the symmetric sector of a G representation

$$B_p = \frac{1}{|G|} \sum_g B_p^g \,, \tag{4.92}$$

where

$$B_p^g = \frac{1}{\mathcal{D}_0^2} \sum_{s \in \mathcal{C}_g} d_s B_p^s \,, \tag{4.93}$$

and $\mathcal{D}_0^2 = \sum_{s \in \mathcal{C}_0} d_s^2$ is the total quantum dimension of the trivial sector.

To describe the 1-form symmetry we first fix a decomposition of the Abelian group

$$G \cong \mathbb{Z}_{p_1^{n_1}} \times \cdots \times \mathbb{Z}_{p_k^{n_k}} \,, \tag{4.94}$$

for primes p_i, and their powers $n_i \in \mathbb{N}$. Using this decomposition we can express an

arbitrary group element and its inverse as

$$g = (g_1, \ldots, g_k)\,, \qquad\qquad \bar{g} = (-g_1, \ldots, -g_k)\,. \tag{4.95}$$

where $g_i = 0, \ldots, p_i^{n_i} - 1$ and group composition is given by addition in $\mathbb{Z}_{p_i^{n_i}}$. We can now define a generalized clock matrix on the G-graded vector space of string types. Denoting a basis element from sector g as $|a_g\rangle$, the generalized clock matrix acts via

$$\widetilde{Z}^g \, |a_h\rangle = \prod_{i=1}^{k} \omega_i^{g_i h_i} \, |a_h\rangle \ , \tag{4.96}$$

where ω_i is a primitive $p_i^{n_i}$-th root of unity and $g_i h_i$ denotes multiplication in $\mathbb{Z}_{p_i^{n_i}}$. This clock operator has commutation relation

$$\widetilde{Z}_e^g B_p^h = \prod_{i=1}^{k} \omega_i^{\sigma_e^p g_i h_i} B_p^h \widetilde{Z}_e^g \,, \tag{4.97}$$

with the plaquette representation of G, where $e \in \partial p$ and $\sigma_e^p = 1$ if the orientation of e matches p and -1 otherwise.

The 1-form symmetry is then generated by string operators

$$\widetilde{Z}_\gamma^g := \prod_{e \cap \gamma} (\widetilde{Z}_e^g)^{\sigma_e^\gamma} \,, \tag{4.98}$$

where γ denotes a closed curve in the dual lattice, and $\sigma_e^\gamma = 1$ if γ intersects e at a right handed crossing, and -1 otherwise. When applied to an open curve γ, running from plaquette γ_- to γ_+, the string operator $\widetilde{Z}_\gamma^g$ creates a $\bar{g}$ boson at γ_- and a g boson

at γ_+.

We now utilize this 1-form symmetry, and the Abelian bosons created by open string operators, to construct a lattice model by layering graded string-nets along the xz and yz planes of a cubic lattice and inducing p-string condensation of these bosons in xy planes. We consider layers of graded string-net models on the square lattice, where each vertex is resolved into a pair of trivalent vertices, making it equivalent to the honeycomb lattice. The decoupled layer model is then described by the Hamiltonian

$$H_{\text{Decoupled}} = \sum_{\ell_x} H_{SN}^{yz,\ell_x} + \sum_{\ell_y} H_{SN}^{xz,\ell_y} \,, \tag{4.99}$$

where the sums are taken over yz and xz planes of the cubic lattice, respectively. This system has one qudit per $\hat{x}$ and $\hat{y}$ edge, two qudits per $\hat{z}$ edge of the cubic lattice, one coming from each layer intersecting at that edge, and several qudits per vertex, coming from the resolved vertices of the 2D square lattice string-net. A basis for the qudits on each $\hat{z}$ edge of the cubic lattice is given by a pair of string types, one from each intersecting layer, which we take to share a common orientation.

To induce p-string condensation we first note that $\widetilde{Z}^g_{e_{xz}} \widetilde{Z}^{\bar{g}}_{e_{yz}}$ creates two pairs of g bosons adjacent to e that are equivalent to a small loop of the p-string excitation in the xy plane labelled by g. Hence adding these operators to the Hamiltonian and taking the limit of large coupling strength induces condensation of these p-strings

within xy planes. The coupled-layer Hamiltonian is

$$H(\Delta) = H_{\text{Decoupled}} - \Delta \sum_{e \| \hat{z}} \sum_{g \in G} \widetilde{Z}^g_{e_{xz}} \widetilde{Z}^{\bar{g}}_{e_{yz}} \,, \tag{4.100}$$

and in the limit of large Δ it enters the planar p-string condensed phase. For $\Delta \to \infty$ the on-site Hilbert space is projected into the subspace given by $\bigoplus_g \mathcal{C}^{xz}_g \boxtimes \mathcal{C}^{yz}_g$ which is spanned by pairs of strings with matching sector label $\left|s_g, s'_g\right\rangle$. At leading order in perturbation theory the p-string condensed Hamiltonian on this Hilbert space is

$$H_{\text{condensed}} = -\sum_v A^{xz}_v + A^{yz}_v - \sum_c B_c \,, \tag{4.101}$$

where A^{xz}_v includes the vertex terms for the resolved vertex in the xz layers, and similarly for A^{yz}_v. We remark that the A_v terms appear unchanged as they commute with the $\widetilde{Z}^{\bar{g}}_e$ operators. The cube term B_c is given by

$$B_c = \frac{1}{|G|^4} \sum_g B^g_c \,, \tag{4.102}$$

where $B^g_c = B^g_{pxz} B^g_{p'xz} B^g_{qyz} B^g_{q'yz}$ with p, p' the xz plaquettes in ∂c and similarly for q, q' and yz.

The emergent excitations of the model are described by the general theory of excitations that arise by applying planar p-string condensation to the g bosons in layers of $\mathcal{Z}(\mathcal{C})$ anyons, see Sec. 4.3.1.

$SU(2)_k$ string-net layers: When the input UFC is given by the $SU(2)_k$ anyon

theory introduced in Sec. 4.5.9, the string types are $\mathbb{Z}_2$-graded into integer and half-integer sectors with the generalized clock operator given by $\widetilde{Z}\,|j\rangle = (-1)^{2j}\,|j\rangle$, where $j = 0, \frac{1}{2}, \ldots, \frac{k}{2}$. The plaquette terms in the $SU(2)_k$ string-net model can be written as $B_p = \frac{1}{2}(B_p^+ + B_p^-)$ where

$$B_p^+ = \frac{1}{\mathcal{D}_0^2} \sum_{j \text{ integer}} d_j B_p^j\,, \qquad\qquad B_p^- = \frac{1}{\mathcal{D}_0^2} \sum_{j \text{ half-integer}} d_j B_p^j\,. \tag{4.103}$$

The planar p-string condensation on layers of $SU(2)_k$ string-nets is induced by driving a phase transition with large $\widetilde{Z}\widetilde{Z}$ couplings on every $\hat{z}$ edge. This projects into a subspace where the string types on the $\hat{z}$ edges are forced to both be integer, or both be half-integer. The cage operators in the condensed model are given by products $B_c^\pm = B_{pxz}^\pm B_{p'xz}^\pm B_{qyz}^\pm B_{q'yz}^\pm$ using the same notation as above.

The emergent anyon theory in each string-net layer is described by $SU(2)_k \boxtimes \overline{SU(2)}_k$, whose elements we denote by (i, j). The $\mathbb{Z}_2$ 1-form symmetry utilized in the p-string condensation is generated by the $(k/2, k/2)$ boson in this anyon theory. The anyons that braid nontrivially with this boson, and hence are promoted to lineons in the planar p-string condensed model, are of the form $(\frac{i}{2}, j)$ or $(j, \frac{i}{2})$, for i, j, integers, whereas pairs of integers, or half-integers braid trivially with $(k/2, k/2)$ and hence remain planons. The $(k/2, k/2)$ boson itself is a planon that is equivalent to a composite of fractons.

4.5.11 Construction from gauging planar subsystem symmetries

In this section we describe how planar p-string condensation can be induced by gauging planar subsystem symmetries.

The planar p-string condensation introduced above can be realized by gauging a planar subsystem symmetry [42, 207, 208, 136] along a stack of planes, as introduced in Ref. [183], see Ref. [209] for a related discussion. The particular planar subsystem symmetries are generated by a stack of Abelian string operators, see Fig. 4.15a. The domain wall of such a planar symmetry corresponds to a p-string, and gauging the symmetry condenses these domain walls, see Fig. 4.15b. This provides insight into the possible anomalies of the subsystem symmetry which prevent it from being gauged, and render the corresponding p-string condensation inconsistent. In particular, anomalies of the 1-form symmetries, generated by the string operators involved in the planar symmetries, that arise due to braiding are no obstacle to gauging these symmetries as the string operators involved do not intersect, hence fermionic $\mathbb{Z}_2$ and arbitrary $\mathbb{Z}_N$ anyons (for $N > 2$) can be planar p-string condensed. Only anomalies arising from the non on-site nature of the string operators present obstacles to gauging planar symmetries, such as for those generated by a stack of semionic string operators.

We consider a local Hamiltonian on the cubic lattice $H = \sum_v h_v$ with planar subsystem symmetries in the xy planes of the cubic lattice generated by

$$\prod_{x,y} U_{x,y,z}(g)\,, \tag{4.104}$$

where each on-site action is given by a product of string operators segments on the

intersecting layers $U(g) = V^{xz}(g)W^{yz}(g)$. That is, $\prod_x V^{xz}_{x,y,z}(g)$ is an on-site string operator for an Abelian G anyon on an xz layer, and similarly $\prod_y W^{yz}_{x,y,z}(g)$ is a string operator on a yz layer. The domain wall obtained by truncating this symmetry corresponds to a p-string excitation formed by a loop of Abelian g anyon. We can gauge each planar symmetry following the standard procedure for gauging a global 2D symmetry [210, 211, 212, 121], this is known to condense the domain walls, and hence induce planar p-string condensation. Although the symmetries described here are Abelian, the planar gauging can be applied also to non-Abelian symmetries. We describe the general gauging procedure below as it may be useful in future work.

To gauge the symmetry we first introduce $\mathbb{C}[G]$ gauge spins onto the $\hat{x}$ and $\hat{y}$ edges of the cubic lattice, which are given an orientation. Next we introduce projectors on each vertex that implement a generalized Gauss's law within each plane

$$P^{xy}_v = \frac{1}{|G_{xy}|} \sum_{g \in G_{xy}} P^{xy}_v(g)\,, \tag{4.105}$$

$$P^{xy}_v(g) = U_v(g) \prod_{e \to v, e \perp \hat{z}} L_e(g) \prod_{e \leftarrow v, e \perp \hat{z}} R_e(g)\,, \tag{4.106}$$

where $e \to v$ ($e \leftarrow v$) denotes adjacent edges that are oriented towards (away from) the vertex v, and $L(g), R(g)$, denote the left and right regular representations respectively. We also introduce projectors onto zero flux through each xy plaquette

$$F^{xy}_p = \sum_{g_1,g_2,g_3,g_4} \delta(g_1^{\sigma^p_{e_1}} g_2^{\sigma^p_{e_2}} g_3^{\sigma^p_{e_3}} g_4^{\sigma^p_{e_4}} = 1)\, \pi_{e_1\hat{z}}(g_1)\pi_{e_2\hat{z}}(g_2)\pi_{e_3\hat{z}}(g_3)\pi_{e_4\hat{z}}(g_4)\,, \tag{4.107}$$

where $\pi_{e\hat{z}}(g) = |g\rangle_{e\hat{z}} \langle g|$ and the edges $e_1, e_2, e_3, e_4 \in \partial p$ are in order starting from

some vertex in ∂p and following the orientation induced by p with $\sigma^p_{e_i} = 1$ if the orientation of e_i matches and -1 otherwise.

To gauge a local term in the Hamiltonian we extend it onto the gauge qubits and then project onto the subspace of gauge invariant operators as follows

$$\mathcal{G}[h_v] = \mathcal{P}[h_v \prod_{e \in T_{\mathcal{O}_m}} \pi_{e\hat{z}}(1)] \,, \tag{4.108}$$

where T_{h_v} is a tree, within an xy plane, that contains the vertices in S_{h_v}, the support of h_v. The projection onto the subspace of gauge invariant operators is

$$\mathcal{P}[\mathcal{O}] = \sum_{\{g_v\}} \prod_{v \in S_{\mathcal{O}}} P^{xy}_v(g_v)|_{S_{\mathcal{O}}} \; \mathcal{O} \prod_{v \in S_{\mathcal{O}}} P^{xy}_v(g_v)|^\dagger_{S_{\mathcal{O}}} \,, \tag{4.109}$$

where $S_{\mathcal{O}}$ is the set of sites in the support of $\mathcal{O}$. The gauged Hamiltonian is then

$$H_{\text{gauged}} = \sum_v \mathcal{G}[h_v] - \varepsilon \sum_p F^{xy}_p - \lambda \sum_v P^{xy}_v \,, \tag{4.110}$$

and the Gauss's law constraints becomes strict in the limit of $\lambda \to \infty$.

By gauging the planar symmetries, all operators that do not commute with them are projected out. In particular the hopping operators for any anyons in the 2D layers that braid nontrivially with the string operators in each planar symmetry are projected out. This causes these anyons to become stuck between a pair of plains, hence becoming lineons. Any anyons that braid trivially with the planar symmetry string operators remain planons. The gauge charges are equivalent to pairs of anyons that are created by a string operator along $\hat{z}$ that violates the planar symmetry, and

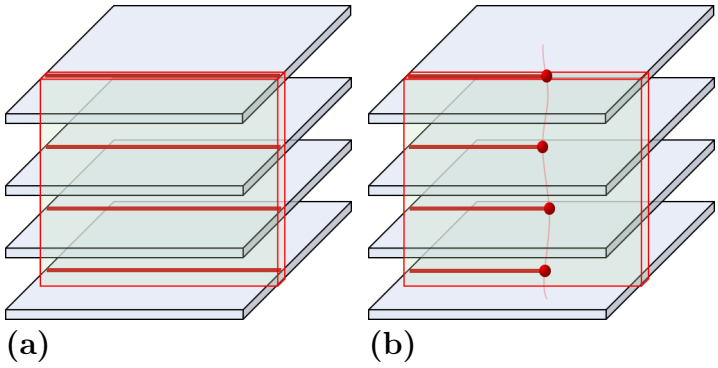

Figure 4.15: (a) A subsystem symmetry on an xy plane (green), consisting of a product of Abelian anyon string operators (red) where the plane intersects topological layers in the xz planes.
(b) The domain wall created by applying a partial subsystem symmetry is a p-string excitation. Gauging the subsystem symmetry condenses these domain walls within the plane, hence inducing planar p-string condensation.
The connection between subsystem symmetries and p-string excitations depicted in (a), (b), holds similarly when topological layers in yz planes are also included, the simpler case has been depicted for clarity of presentation. .

hence are planons given by a composite of lineons. The gauge fluxes are given by gauged twist defects [121, 206, 183], obtained by terminating a domain wall of the symmetry, and hence correspond to fractons. A pair of such fractons separated by a unit along $\hat{x}$ or $\hat{y}$ is equivalent to one of the g anyons that is being p-string condensed, and hence is a planon if the anyon is bosonic or fermionic, and a lineon if the anyon has a nontrivial self braiding phase.

Honeycomb model example

We now present an example lattice construction based on fermionic planar p-string condensation induced by gauging planar subsystem symmetries on layers of Kitaev's honeycomb model [11].

We consider layers supporting chiral Ising anyons, realized by Kitaev's honeycomb

model [11], and apply planar p-string condensation to the $\mathbb{Z}_2$ fermions in each layer. This realizes a model that is closely related to the $SU(2)_2$ example from Sec. 4.5.9, since the anyons only differ by the Frobenius-Schur indicator for the non-Abelian particle [213], which is $+1$ for Ising and -1 for $SU(2)_2$. Hence the resulting fracton models differ only in the Frobenius-Schur indicators of the non-Abelian lineons.

For the lattice model we consider Kitaev's honeycomb model [11] in the chiral Ising anyon phase with a perturbation that respects the fermionic 1-form symmetry and opens an energy gap

$$H(J,\Delta) = -J\sum_{\langle ij\rangle} K_{ij} - \Delta \sum_{\langle ij\rangle\langle ik\rangle} K_{ij}K_{ik} - \Delta \sum_{\langle ij\rangle\langle ik\rangle\langle i\ell\rangle} K_{ij}K_{ik}K_{i\ell}\,,$$

where i,j,k,l, denote distinct points and $\langle ij\rangle$ denote edges in the honeycomb lattice. The chirality of the gapped Ising anyon phase is given by $\nu = \operatorname{sgn}\Delta$. The edge operators K_{ij} depend on the orientation of $\langle ij\rangle$ which we denote by $\alpha = x,y,z$, i.e.

$$K_{ij} = \sigma_i^\alpha \sigma_j^\alpha\,, \tag{4.111}$$

where $\sigma^x = X, \sigma^y = Y, \sigma^z = Z$. Abusing notation to only keep track of the edge orientation and after coarse graining to a square lattice with two qubits per site we have

$$K_x = \begin{array}{c} \\ IX\cdot XI \\ \\ \end{array}\,, \qquad K_y = YY\,, \qquad K_z = \begin{array}{c} IZ \\ | \\ ZI \end{array}\,. \tag{4.112}$$

The fermionic 1-form symmetry restricted to the $\hat{x}$-axis is given by

$$\prod_i (ZZ)_{ij}\,, \tag{4.113}$$

truncating this symmetry operator to a finite line creates emergent fermion excitations at the end points.

We consider a stack of perturbed honeycomb layers (that have been coarse grained to the square lattice) along the xz and yz planes of a cubic lattice such that the $\hat{z}$ axes of the layers align

$$\sum_{\ell_x} H^{yz}_{\ell_x}(J,\Delta) + \sum_{\ell_y} H^{xz}_{\ell_y}(J,\Delta)\,, \tag{4.114}$$

where the $H^{yz}_{\ell_x}$ indicates the honeycomb Hamiltonian in a yz plane at $x = \ell_x$. This model obeys a large symmetry group given by the product of the fermionic 1-form symmetries within each layer, this contains a 3D 1-form symmetry given by taking products of the fermionic string operators over codimension-1 surfaces [183]. Within the 1-form symmetry group is a subgroup of planar subsystem symmetries along the xy planes of the cubic lattice, generated by products of the fermionic string operators over such a plane

$$\prod_{i,j} (ZZ)^{yz}_{ijk} (ZZ)^{xz}_{ijk}\,, \tag{4.115}$$

where yz, xz, denote the plane from which the qubits at coordinate ijk originate. The domain walls of these planar symmetries are p-strings formed by the fermion

excitations in each layer that the p-string intersects.

To induce planar p-string condensation we gauge the subsystem symmetries defined above. This introduces an additional qubit to each $\hat{x}$ and $\hat{y}$ link of the cubic lattice, which we index with half integer coordinates. The gauged Hamiltonian is then given by

$$\sum_{\ell_x} \widetilde{H}^{yz}_{\ell_x}(J,\Delta) + \sum_{\ell_y} \widetilde{H}^{xz}_{\ell_y}(J,\Delta) - \varepsilon \sum_{ijk} F_{ijk} - \lambda \sum_{ijk} G_{ijk}\,, \tag{4.116}$$

where

$$F_{ijk} = X_{(i+\frac{1}{2})jk} X_{(i+\frac{1}{2})(j+1)k} X_{i(j+\frac{1}{2})k} X_{(i+1)(j+\frac{1}{2})k}\,, \tag{4.117}$$

energetically penalizes nonflat $\mathbb{Z}_2$-gauge connections,

$$G_{ijk} = (ZZ)^{yz}_{ijk} (ZZ)^{xz}_{ijk} Z_{(i+\frac{1}{2})jk} Z_{(i-\frac{1}{2})jk} Z_{i(j+\frac{1}{2})k} Z_{i(j-\frac{1}{2})k}\,, \tag{4.118}$$

energetically enforces the planar Gauss's law, which becomes strict in the $\lambda \to \infty$ limit, and the gauged Hamiltonians within each layer are defined by

$$\widetilde{H}(J,\Delta) = -J \sum_{\langle ij \rangle} \widetilde{K}_{ij} - \Delta \sum_{\langle ij \rangle \langle ik \rangle} \widetilde{K}_{ij} \widetilde{K}_{ik} - \Delta \sum_{\langle ij \rangle \langle ik \rangle \langle i\ell \rangle} \widetilde{K}_{ij} \widetilde{K}_{ik} \widetilde{K}_{i\ell}\,,$$

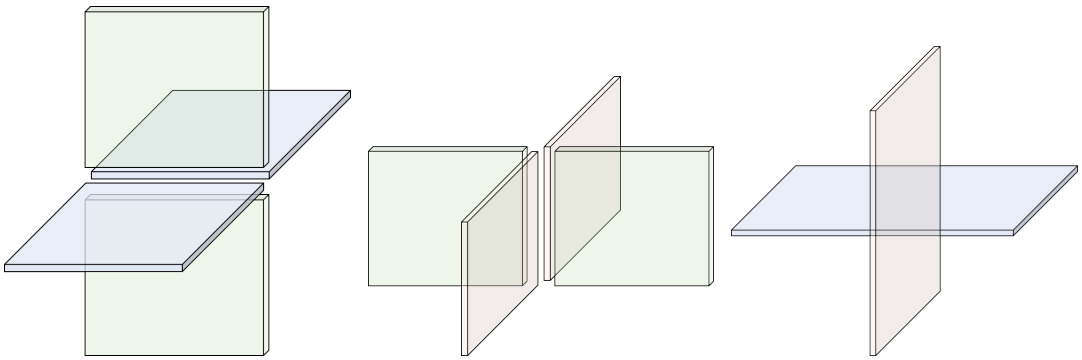

Figure 4.16: (a) A $\hat{y}$-oriented 1-strata where xy-oriented 2-strata supporting $\mathbb{Z}_N$ gauge theory (green) and yz-oriented 2-strata supporting a general topological order that contains $\mathbb{Z}_N$ Abelian anyons, meet.
(b) A $\hat{y}$-oriented 1-strata where xy-oriented 2-strata supporting $\mathbb{Z}_N$ gauge theory (green) and xz-oriented 2-strata supporting a general topological order that contains $\mathbb{Z}_N$ Abelian anyons, meet.
(c) A $\hat{z}$-oriented 1-strata linking xz-oriented 2-strata, and yz-oriented 2-strata, by a tensor product of identity domain walls. .

with minimally coupled local terms

$$\widetilde{K}_x = \begin{array}{c} \\ IX \\ - \\ X \\ - \\ XI \end{array} \ , \qquad \widetilde{K}_y = YY \, , \qquad \widetilde{K}_z = \begin{array}{c} IZ \\ | \\ ZI \end{array} \ . \tag{4.119}$$

This produces a fracton model whose emergent excitation theory is closely related to the $SU(2)_2$ model described in Sec. 4.5.9 up to the Frobenius-Schur indicator of the nonAbelian lineons being -1.

4.5.12 Topological defect network construction

The planar p-string condensed models introduced in this paper can be described by the recently introduced topological defect network construction, providing support for the conjecture made in Ref. [77] that all gapped fracton topological orders fit into this framework. We follow the procedure used in Ref. [183] to turn a gauged

layer construction into a defect network by introducing layers of gauge theory on the subsystem symmetry planes and gapped boundaries where the planes intersect the initial stacks of topological layers

The defect network construction is given by trivial 3-strata, 2D topological orders described by the anyon theory $\mathcal{M}$ on the xz and yz oriented 2-strata, and $\mathcal{A}$ gauge theory (denoted $\mathcal{Z}(\mathrm{Vec}_{\mathcal{A}})$) on the xy oriented 2-strata. The codimension-2 defects on the $\hat{z}$ oriented 1-strata are simply given by the trivial identity domain wall between the pairs of xz 2-strata, and yz 2-strata, meeting there, respectively, see Fig. 4.16c. This is described by the following Lagrangian algebra of bosons that condenses on the defect

$$\mathcal{L} = \sum_{a,b\in\mathcal{M}} (a, \bar{a}, b, \bar{b}) \,, \tag{4.120}$$

where we have used the folding trick to view the defect as a gapped boundary to vacuum of $\mathcal{M}_{xz} \boxtimes \mathcal{M}_{xz}^{\mathrm{rev}} \boxtimes \mathcal{M}_{yz} \boxtimes \mathcal{M}_{yz}^{\mathrm{rev}}$, with the layer subscripts included for guidance. Similarly, the defects on the $\hat{x}$ and $\hat{y}$ oriented 1-strata are equivalent to gapped boundaries to vacuum of $\mathcal{M} \boxtimes \mathcal{M}^{\mathrm{rev}} \boxtimes \mathcal{Z}(\mathrm{Vec}_{\mathcal{A}}) \boxtimes \mathcal{Z}(\mathrm{Vec}_{\mathcal{A}})^{\mathrm{rev}}$ via the folding trick. The following Lagrangian algebra describes the appropriate gapped boundary

$$\mathcal{L} = \sum_{a\in\mathcal{M}} \sum_{b\in\mathcal{Z}(\mathrm{Vec}_{\mathcal{A}})} \sum_{\chi\in\widehat{\mathcal{A}}} \sum_{g\in\mathcal{A}} (a_\chi, \bar{g} \otimes \bar{a}_{\bar{\chi}}, \chi \otimes b_g, \bar{b}_{\bar{g}}) \,, \tag{4.121}$$

where we have utilized the $\mathcal{A}$-grading of $\mathcal{A}$ gauge theory by flux sectors g, see Figs. 4.16a & 4.16b. This construction presents an immediate generalization of the

construction by replacing the gauge theory layers $\mathcal{Z}(\mathrm{Vec}_{\mathcal{A}})$ with more general $\mathcal{A}$-graded anyon theories.

Chapter 5

Weak superfluidity: Weak symmetry breaking and topological order in a 3d compressible quantum liquid

5.1 Introduction

A quantum state is compressible if the charge density is a continuous and strictly increasing function of the chemical potential. Common examples of stable compressible matter include:

1. Symmetry-breaking phase, in particular when the U(1) charge conservation is spontaneously broken by a local order parameter, i.e. a superfluid.

2. For fermionic systems, the Fermi liquid is a compressible phase which does not break any symmetry (U(1) or translation).

Both can be "deformed" to obtain other compressible phases with distinct low-energy dynamics. For example, a Fermi liquid can be coupled to gapless bosonic excitations (e.g. critical fluctuations or gauge fields), leading to various kinds of non-Fermi liquids. For a superfluid, by adding additional interactions one can change the dispersion of the Goldstone boson to alter the low-energy physics. Examples of this include the quantum Lifshitz liquid [214] and Bose-Luttinger liquid [215, 216].

While it is a formidable task to generally classify the low-energy dynamics of gapless phases, one can first characterize them at the kinematic level, in particular their emergent symmetries and the associated quantum anomalies. Recently Ref. [217] has taken this approach to study the low-energy theory of compressible phases. The filling condition can be formulated in a way similar to the 't Hooft anomaly [110, 218], and in particular it is shown that the emergent symmetry group cannot be a compact 0-form and/or finite higher-form symmetry group. The previous two classes of examples illustrate two mechanisms to satisfy the filling condition: the symmetry group of the superfluid phase is $\mathrm{U}(1)^{[0]} \times \mathrm{U}(1)^{[D-1]}$ [219, 220], where D is the spatial dimension. The presence of the $\mathrm{U}(1)^{[D-1]}$ form symmetry is essentially equivalent to the fact that superfluid vortices must form $(D-1)$-dimensional closed surface. The mixed anomaly between the two subgroups is responsible for the filling condition. The same mechanism underlies some more exotic examples of compressible phases of bosons, such as the Bose-Luttinger liquid [216]. For the Fermi liquid, the emergent symmetry is the (0-form) loop group[217] $\mathrm{L}^{D-1}\mathrm{U}(1)$, which describes at the level of kinematics the existence of a Fermi surface. The group is "larger" than any compact Lie group. Deformations of the two types of examples may change the emergent

symmetry group, but do not affect the way that the filling anomaly is realized. In a sense, these two examples represent two "minimal" emergent symmetry groups that allow compressibility in the respective classes. It is clearly an important problem to understand whether there exist other low-energy kinematical structures compatible with a generic filling factor.

Ref. [217] mostly operates within the framework of quantum field theory in continuum with both translation and rotation symmetries. The aforementioned examples can be easily modified to introduce certain anisotropies, for example in boson velocity or the shape of the Fermi surface. However these modifications can all be smoothly turned off without changing the nature of the states i.e. no phase transitions. In particular, they do not affect the kinematical structure. A natural question then is whether there are fundamentally new types of symmetry mechanisms to allow arbitrary filling, once we go beyond the framework of continuum field theory. In fact, there is a trivial toy example that goes beyond what we have discussed so far: consider a stack of decoupled 2D superfluids [1]. Such a phase is obviously compressible but the emergent symmetry group is very different from that of a 3D superfluid. More specifically, each layer has a separate U(1) 0-form symmetry and U(1) 1-form symmetry at low energy. One may object that a stack of 2D superfluids is unstable to infinitesimal boson tunneling, thus does not represent a truly stable phase. Quantum phases with such "subsystem" symmetries have been vigorously studied in recent years, largely inspired by the discovery of fracton topological order [39, 124, 125,

[1] Similarly, one can consider a stack of 2D Fermi liquids. However, such a state has an open Fermi surface consisting of two curves wrapping around the Brillouin zone.

41, 42, 207, 152, 221]. It has been recognized recently that a large class of two- and three-dimensional quantum phases cannot be described as conventional quantum field theories [222, 223, 144, 145, 48, 46, 171, 47, 167, 49]. They are often characterized by exotic global symmetries [207, 136, 224], e.g. those defined on certain submanifolds.

Motivated by this question and building on top of recent works on fracton models [225, 226, 79], in this work we study a new example of a completely stable compressible state in three dimensions, whose low-energy sector is described by an infinite-component Chern-Simons (iCS) theory, consisting of coupled planar U(1) gauge fields (other generalizations of CS-like theory to 3D in the context of fractonic order have been considered in [227] and [168]). Variants of the field theory with fully gapped spectrum have been studied in Ref. [225], which are shown to possess a particular kind of fracton topological order, with all quasiparticles restricted to move in planes. Moreover, it is proposed that the theory provides an example of a "non-foliated" fracton topological phase. Ref. [225] also noticed that the field theory we obtain has a gapless spectrum. One motivation for this work is to elucidate the rich physics of the gapless iCS theory, and provide a lattice realization which can be controllably solved and which manifests the symmetries of the underlying field theory.

Below we briefly summarize the main features of this compressible quantum liquid, focusing on those that distinguish it from the known types of compressible phases previously mentioned. Most importantly, the emergent symmetry group (relevant for the filling anomaly) consists of a 0-form U(1) symmetry group of charge conservation, and a "cylindrical" 1-form symmetry, the meaning of which will be defined later. (Note that an ordinary 3D superfluid has an emergent U(1) 2-form symmetry.) This exotic

emergent 1-form symmetry stems from a rigid string-like superfluid order, where an order parameter for the U(1) 0-form symmetry is supported on a straight line penetrating the entire system. However, there exists no other local order parameter. Thus we dub this phenomenon "weak symmetry breaking" (WSB). The terminology has been previously used in the context of (2+1)d symmetry-enriched topological order [11, 14, 228], when there exists no local order parameter but certain non-local observables break the (0-form) symmetry. In addition, the low-energy theory also exhibits finite 1-form symmetries, corresponding to deconfined, topologically nontrivial quasiparticle excitations. They can be formed from dipoles of vortices of the "weak" superfluid. Thus in a sense the phase of matter intertwines U(1) symmetry breaking and topological order in an interesting way.

Phenomenologically, we find that at low energy there is only a single gapless point. We argue that the gapless state is in fact robust to any local perturbation and therefore represents a stable gapless phase. In particular, the gapless excitations are charge neutral and all local charged excitations are gapped. We also study the transport properties, and find that the phase exhibits a superconducting response in the plane perpendicular to the direction of the non-local order parameter, and insulating in the other.

The chapter is organized as follows: in Sec. 5.2 we first provide a microscopic realization of the compressible liquid with WSB, using a coupled-wire construction, and study its various properties. We derive an infinite-component CS theory description of the low-energy physics, by applying boson-vortex duality transformation in the coupled wire setting. Gapped cases of these field theories have been recently studied

in Ref. [225] as examples of Abelian fractonic phases without any foliation structure. In Sec. 5.3 we then explore the emergent symmetries, anomalies (especially the filling anomaly) and stability of the phase, using the dual gauge theory formulation.

5.2 Coupled wire construction

We start from a microscopic model realizing the phase. The model is built from an array of interacting one-dimensional quantum wires. Such models have proven very fruitful in providing explicit realizations of topological phases in both two and three dimensions [60, 61, 226, 79, 69, 79, 226].

5.2.1 Model Hamiltonian and symmetries

Consider quantum wires arranged in a square lattice. Each wire is described by a $c = 1$ bosonic Luttinger liquid, with a K matrix $K_{\mathrm{w}} = \sigma^x$. We postulate that the Luttinger liquid is realized as the low-energy effective theory of a one-dimensional chain of bosons (or spins). The Hamiltonian is

$$H = \frac{v}{2\pi} \sum_{\mathbf{r}} \int \mathrm{d}x \, [(\partial_x \varphi_{\mathbf{r}})^2 + (\partial_x \theta_{\mathbf{r}})^2]. \tag{5.1}$$

Here $\mathbf{r} = (y, z)$ labels the position of wires in the yz plane. The bosonic fields φ and θ satisfy the canonical commutation relation

$$[\varphi_{\mathbf{r}}(x_1), \partial_{x_2} \theta_{\mathbf{r}'}(x_2)] = 2\pi i \delta(x_1 - x_2) \delta_{\mathbf{r}\mathbf{r}'}. \tag{5.2}$$

We have also assumed that all wires have the same velocity to ensure translation invariance.

We add the following type of interactions to gap out the wires:

$$-g\sum_{\mathbf{r}}\int \mathrm{d}x\ \cos\Theta_{\mathbf{r}}(x), g>0. \tag{5.3}$$

Here $\Theta_{\mathbf{r}}\equiv\Theta_{y,z}$ is defined as

$$\begin{aligned}\Theta_{y,z} = &-\varphi_{yz}+m\theta_{yz}+\varphi_{y+1,z}+m\theta_{y+1,z}\\ &+(n_1\theta_{y,z-1}+n_2\theta_{y,z+1}+n_2\theta_{y+1,z-1}+n_1\theta_{y+1,z+1}).\end{aligned} \tag{5.4}$$

This is a generalization of the coupled wire construction for bilayer quantum Hall states by Teo and Kane [61]. The interaction $\cos\Theta$ is illustrated in Fig. 5.1(b). One can easily show that these fields satisfy the null vector condition[114]:

$$[\Theta_{\mathbf{r}}(x),\Theta_{\mathbf{r}'}(x')]=0, \tag{5.5}$$

so they can be minimized simultaneously. We are interested in the strong-coupling limit $g\to\infty$, at which the cosine terms pin all Θ fields to the minima. This can be achieved either by having a large bare value of g, or turning on inter-wire density-density interactions to make g a relevant coupling.

First we study the global symmetry of the model. Before turning on the coupling Eq. (5.4), each wire has $\mathrm{U}(1)_\varphi\times\mathrm{U}(1)_\theta$ symmetry, the charge densities of which are $\frac{1}{2\pi}\partial_x\theta$ and $\frac{1}{2\pi}\partial_x\varphi$, respectively, and there is a mixed 't Hooft anomaly between the two

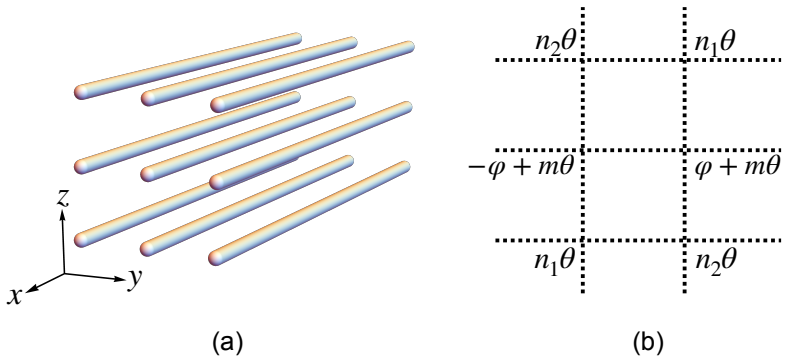

Figure 5.1: The coupled wire construction in this work starts from a 2D array of single-component Luttinger liquids, as illustrated in (a), and then gapping interactions between nearby wires are turned on to create a 3D quantum state. The form of the interaction is illustrated in (b).

U(1) subgroups. One of them, $\mathrm{U}(1)_\varphi$, can be understood as the conservation of boson number, which is assumed to be an exact symmetry of the microscopic Hamiltonian. Here we choose the convention that the boson density is given by $\frac{1}{2\pi}\partial_x\theta$, and the symmetry transformation acts on the fields as

$$\varphi \to \varphi + \alpha, \tag{5.6}$$

where $\alpha \in [0, 2\pi)$ is the U(1) rotation angle. The other subgroup $\mathrm{U}(1)_\theta$ then must be emergent at low energy due to the mixed anomaly. Importantly, the lattice translation symmetry along the wire is realized at low energy as a particular element of $\mathrm{U}(1)_\theta$:

$$T_x : \theta \to \theta + 2\pi\nu, \tag{5.7}$$

where ν is the filling factor of the wire, which is equal to the filling factor of the entire 3D system. When ν is not an integer, the celebrated Lieb-Schultz-Mattis

theorem [229] shows that the 1D wire cannot be fully gapped without breaking the translation symmetry.

The coupling Eq. (5.4) apparently reduces the symmetry group. For each xy plane, there is a $\mathrm{U}(1)_\varphi$ subsystem symmetry:

$$\varphi_{yz} \to \varphi_{yz} + \alpha_z, \tag{5.8}$$

However, the $\mathrm{U}(1)_\theta$ symmetry is broken in general.

We are mainly interested in the special case when $m = -(n_1+n_2)$. For this choice of parameters, we find a $\mathrm{U}(1)_\theta$ subsystem symmetry in each xz plane:

$$\theta_{yz} \to \theta_{yz} + \beta_y. \tag{5.9}$$

This obviously includes a global transformation $\theta_{\mathbf{r}} \to \theta_{\mathbf{r}} + \beta$.

If we set $n_1 = n_2$, then there is a further U(1) dipole symmetry on each xz plane:

$$\theta_{yz} \to \theta_{yz} + z\gamma_y. \tag{5.10}$$

We now consider spatial translations. The full Hamiltonian is obviously invariant under the discrete translations along y and z directions. For the lattice translation T_x, the interaction is invariant if and only if $(m + n_1 + n_2)\nu$ is an integer. If $m = -(n_1 + n_2)$, then ν can be any real number. Otherwise the model is only translation-invariant for certain special rational fillings. We thus conclude that the model with $m = -(n_1 + n_2)$ can be defined *at any filling*. As will be shown below, there is no

spontaneous symmetry breaking for either the global $\mathrm{U}(1)_\varphi$ or $\mathrm{U}(1)_\theta$, in the sense that no local order parameter exists. Therefore the coupled wire model constitutes a new example of compressible quantum phase.

To summarize, we find that at $m = -(n_1 + n_2)$, the system preserves the following global continuous symmetry:

$$\begin{aligned} \mathrm{U}(1)_\varphi &: \varphi_{\mathbf{r}} \to \varphi_{\mathbf{r}} + \alpha, \\ \mathrm{U}(1)_\theta &: \theta_{\mathbf{r}} \to \theta_{\mathbf{r}} + \beta. \end{aligned} \tag{5.11}$$

These two U(1) symmetries have a mixed 't Hooft anomaly, so cannot be realized as on-site symmetries microscopically at the same time. In this work we choose the convention that $\mathrm{U}(1)_\varphi$ is the boson number conservation, and $\mathrm{U}(1)_\theta$ is an emergent symmetry. The lattice translation along wires is embedded into $\mathrm{U}(1)_\theta$.

So far we have only considered the so-called 0-form symmetries. At low energy, the system can develop emergent "higher-form" symmetries [230], whose charges are extended objects. An example relevant to our discussion is the U(1) 1-form symmetry in a 2D superfluid, which is physically equivalent to all superfluid vortices being non-dynamical (i.e. infinitely heavy). In our model, if $m = n_1 = n_2 = 0$, the system is a stack of layers of 2D superfluids, and at low energy each layer has its own U(1) 1-form symmetry. Schematically, the 1-form charge in the layer z for a closed path C is given by

$$Q_z(C) = \oint_C \nabla \varphi_z, \tag{5.12}$$

which counts the total vorticity enclosed by C. When the coupling to θ is turned

on, since $e^{i\theta}$ creates a vortex-anti vortex pair and hops vortices in the layer, the U(1) 1-form symmetry for the layer is explicitly broken. However, when $m = -n_1 - n_2$, the term $\cos(\Theta_{y,z})$ preserves the 1-form charge

$$Q_{z-1}(C) + Q_z(C) + Q_{z+1}(C). \tag{5.13}$$

Note that C must be the same for the three layers. Now considering all layers together, the total 1-form charge

$$\sum_z Q_z(C) \tag{5.14}$$

is conserved by the Hamiltonian at low energy when the cosine term dominates, assuming periodic boundary condition. We refer to the conservation of the total vorticity Eq. (5.14) as a cylindrical 1-form symmetry, since the closed loop C must be exactly aligned throughout all the layers, so the symmetry operator is in fact supported on a cylindrical surface. This should be compared with the 2-form symmetry in a 3D superfluid, where the symmetry operator is supported on arbitrary loops. We illustrate the symmetry operator in Fig 5.2b.

5.2.2 Spectrum and excitations

We now move on to analyze the spectrum of the Hamiltonian. The model is generally not solvable, so we limit ourselves to the strong-coupling limit where the cosine potential terms dominate over the kinetic terms. As shown in Ref. [226], low-energy excitations can be divided into two types: first of all, there are excitations that

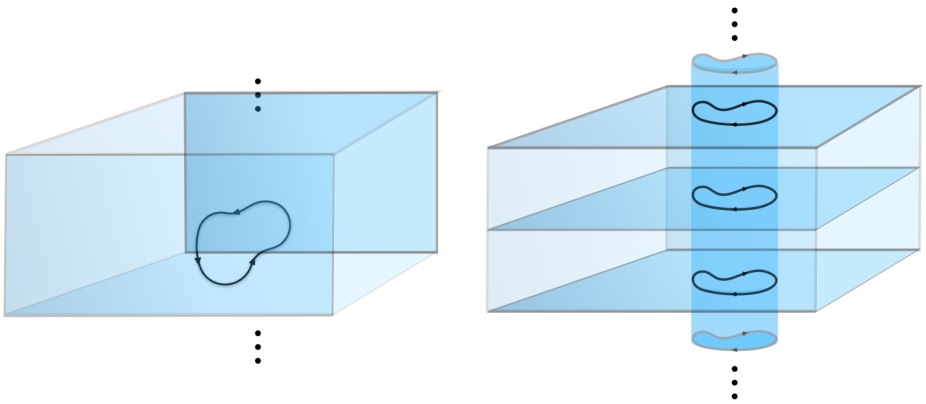

Figure 5.2: (a) The 2-form symmetry operators in a 3D superfluid are supported on closed curves. The corresponding charged objects form closed surfaces (i.e. vortex sheets), hence a 2-form symmetry. (b) The higher-form symmetry operator of the WSB compressible liquid, which is defined in Eq 5.14. The surface is deformable in xy-plane provided it is deformed in the same way in each layer. We refer to this as a cylindrical 1-form symmetry..

describe smooth fluctuations of the bosonic fields, similar to spin waves. They can be analyzed in the "mean-field" approximation, where we expand $\cos\Theta_{\mathbf{r}} \approx 1 - \frac{1}{2}\Theta_{\mathbf{r}}^2$, and then solve the quadratic theory. We find that the spectrum of such Gaussian fluctuations is given by

$$E_{\mathbf{k}} = \sqrt{v^2 k_x^2 + vg(f_\varphi + f_\theta)} \tag{5.15}$$

where

$$\begin{aligned} f_\varphi &= 2 - 2\cos k_y, \\ f_\theta &= 4\left[m\cos\frac{k_y}{2} + n_1\cos(\frac{k_y}{2} - k_z) + n_2\cos(\frac{k_y}{2} + k_z)\right]^2. \end{aligned} \tag{5.16}$$

When $|m| \leq |n_1 + n_2|$, one can make both $f_\varphi = f_\theta = 0$ by setting $k_y = 0, \cos k_z = -\frac{m}{n_1+n_2}$, which is clearly the minimum of $f_\varphi + f_\theta$ since both functions are non-negative. Therefore the spectrum is gapless. For $m = -(n_1 + n_2)$, the minimum is at $\mathbf{k} =$

$(0,0,0)$. Near this point, $E_{\mathbf{k}}$ takes the following approximate form:

$$E_{\mathbf{k}} = \Big[v^2 k_x^2 + vg\Big(k_y^2 + 2(n_2^2 - n_1^2)k_y k_z^3 + (n_1 - n_2)^2 k_y^2 k_z^2 + (n_1 + n_2)^2 k_z^4\Big)\Big]^{1/2}. \tag{5.17}$$

For $n_1 = n_2 = n$, we have

$$f_\varphi + f_\theta = 4\cos^2\frac{k_y}{2}[(m + 2n\cos k_z)^2 - 1] + 4. \tag{5.18}$$

If $|m| > 2|n|$, the minimum of this function is 4 at $k_y = \pm\pi$ and the spectrum is fully gapped. When $|m| \leq 2|n|$, the minimum is 0 with $k_y = 0$ and $\cos k_z = -\frac{m}{2n}$. In this case the spectrum is gapless, with one or two gap-closing points. For $m = -2n$, near the gap-closing point $\mathbf{k} = (0,0,0)$, the spectrum is approximately

$$E_{\mathbf{k}} = \sqrt{v^2 k_x^2 + vgk_y^2 + 4vgn^2 k_z^4}. \tag{5.19}$$

Besides smooth fluctuations, there also exist localized excitations, corresponding to "discontinuities" in the field configurations. At the mean-field level, they can be built out of soliton excitations of the gapping terms that tunnel between different minima. More concretely, for $\cos\Theta_{\mathbf{r}}(x)$, a k-soliton where $k \in \mathbb{Z}$ at x_0 is a configuration where $\Theta_{\mathbf{r}}$ winds by $2\pi k$ over a short distance ξ around x_0. In this limit, these excitations can be thought of as massive quasi-particles. While we do not know the exact profile of such an excitation, we assume that they stay gapped beyond the mean-field analysis, at least for a range of g. We give a more systematic description

of the solitonic excitations in Sec. 5.2.5.

To create such excitations, one can apply vertex operators, such as $e^{i\varphi}$ or $e^{i\theta}$. Note that these two, together with derivatives of φ and θ, generate all local operators in the wire model. It is easy to show that derivatives of φ or θ cannot create localized solitons. Rather they only result in smooth configurations of the fields. Therefore we can focus just on the vertex operators. A crucial fact which we rely on here is that the model satisfies a version of the "topological order" condition as discussed in Ref. [226]. Namely, if a vertex operator has a finite support and commutes with all $\Theta_{\mathbf{r}}$, then it must be a linear combination of $\Theta_{\mathbf{r}}$'s. In other words, any vertex operator with local support has to create gapped excitations, provided it is not some combination of $\Theta_{\mathbf{r}}$'s. Therefore such operators are infinitely irrelevant even when the theory is gapless. This strongly suggests that the gapless theories, when $|m| \leq |n_1 + n_2|$, are stable with respect to weak local perturbations, as long as the topological order condition is obeyed. This is analogous to 3D U(1) gauge theory with gapped charges.

It is important to note that the topological order condition is shown for an infinitely large system. When the system is finite (or finite in one direction), the situation turns out to be quite different. As we discuss next, there can be vertex operators commuting with all gapping terms. Such operators are crucial in understanding the symmetry breaking (or the absence thereof) in the low-energy theory.

5.2.3 String superfluid order

In this section we focus on $m = -(n_1 + n_2)$ and assume that both global $\mathrm{U}(1)_\theta$ and $\mathrm{U}(1)_\varphi$ symmetries are preserved. The topological order condition does not preclude the existence of non-local vertex operators that commute with all plaquette terms. We can consider a closed system with periodic boundary condition along z, in which case we can identify two such non-local operators:

$$\Phi_y = \sum_z \varphi_{yz},\ \Pi_z = \sum_y \theta_{yz}. \tag{5.20}$$

Note that when $n_1 = n_2$ there is an additional operator of interest given by $D_y = \sum_z z\varphi_{yz}$, but it does not exist with PBC. The operator $e^{i\Phi_y}$ has a charge N_z under $\mathrm{U}(1)_\varphi$, where N_z is the size of system in the z direction. Likewise, $e^{i\Pi_z}$ has a charge N_y under $\mathrm{U}(1)_\theta$.

We show in Appendix 5.5.4 that with a finite N_z, when viewed as a quasi-two-dimensional system, the $e^{i\Phi_y}$ operator orders and spontaneously breaks the $\mathrm{U}(1)_\varphi$ symmetry. More precisely, the two-point function decays as

$$\langle e^{i\Phi_y(x)} e^{-i\Phi_{y'}(x')} \rangle \to e^{\frac{L_z}{\rho}(\frac{1}{|\mathbf{r}-\mathbf{r}'|} - \frac{1}{a_0})}, \tag{5.21}$$

where ρ is a constant, and $\mathbf{r} = (x, y)$ is the coordinate in the xy plane. Therefore, fixing N_z, the correlation function approaches a constant when $|\mathbf{r} - \mathbf{r}'|$ is much greater than N_z/ρ. This makes sense since for such large separation the thickness along the z direction becomes negligible. However, going to the 3D limit when N_z is comparable

to the size of the other dimensions, the superfluid order is suppressed and eventually vanishes in the thermodynamic limit $N_z \to \infty$.

Equivalently, one can consider the superfluid stiffness in the quasi-two-dimensional system. The "Josephson" coupling that stabilizes the superfluid order originates from the $\varphi_{y,z} - \varphi_{y+1,z}$ term in $\Theta_{\mathbf{r}}$. However, such a term only accesses a small local portion of the order parameter, which is highly non-local and runs through the entire z direction. As a result, one can show that the superfluid stiffness vanishes as $1/N_z$.

To summarize, we find that the line operator $e^{i\Phi_y}$ develops long-range order breaking the $\mathrm{U}(1)_\varphi$ symmetry, but there exist no local $\mathrm{U}(1)_\varphi$ order parameter. This is what we refer to as the phenomenon of "weak symmetry breaking." We note that similarly $e^{i\Pi_z}$ exhibits long-range order in the $x-z$ plane, although the asymptotic of the correlation function is now more anisotropic. So the $\mathrm{U}(1)_\theta$ symmetry is also weakly broken by the line order parameter.

It is also instructive to consider open boundary conditions along z. Suppose there are two yz surfaces at $z = 0$ and $z = N_z - 1$. We first choose the gapping terms to be

$$- g \sum_y \sum_{z=1}^{N_y - 2} \cos \Theta_{yz}. \tag{5.22}$$

At each y, there are N_z wires but only $N_z - 2$ gapping terms, which leaves certain fields near the boundary unpinned. We focus on the $z = 0$ surface. Unpinned fields on the surface are generated by θ_{y0} and

$$\tilde{\varphi}_{y+\frac{1}{2}} = \varphi_{y+1,0} - \varphi_{y,0} + n_1 \theta_{y,1} + n_2 \theta_{y+1,1}. \tag{5.23}$$

Note that both $\tilde{\varphi}_{y+\frac{1}{2}}$ and θ_{y0} commute with themselves. We see that all unpinned fields are neutral under $\mathrm{U}(1)_\varphi$ symmetry.

Now we further add interactions on the surface, e.g. $\cos(\tilde{\varphi}_{y-\frac{1}{2}} - \tilde{\varphi}_{y+\frac{1}{2}})$ or $\cos(\theta_{y0} - \theta_{y+1,0})$, which spontaneously break the $\mathrm{U}(1)_\theta$ symmetry. In this case, the $e^{i\Phi_y}$ operator no longer commutes with the surface order and thus is not a low-energy observable.

We can also create a completely symmetric and gapped surface, by adding the following perturbations:

$$-\cos\left[\frac{m}{2}(\theta_{y,0} + \theta_{y+1,0}) + \tilde{\varphi}_{y+\frac{1}{2}}\right]. \tag{5.24}$$

One can check that all the cosine arguments commute with each other and there are enough of them to gap out all the degrees of freedom on the surface. In this case, one can slightly modify the definition of Φ_y at the surfaces so that it still commutes with all the gapping interactions. This is done by adding a vertex operator which generates an appropriate phase slip at the end of the string operator: $\Phi_y \to \sum_z \varphi_{yz} - (\frac{n_1-n_2}{2})\theta_{y0}$. Note that when $n_1 = n_2 = -m/2$, Φ_y has the same form as the PBC case.

While we do not have a general proof, we believe one of following scenarios must occur: either the $\mathrm{U}(1)_\theta$ symmetry is spontaneously or explicitly broken at the surface, in which case no (local or non-local) $\mathrm{U}(1)_\varphi$ order parameter exists in the system, or the $\mathrm{U}(1)_\theta$ symmetry is preserved but one can then find a non-local order parameter by modifying Φ_y near the surface.

Since the model has a non-local superfluid order, one may wonder whether there

is any superconducting response once coupled to an external electromagnetic field. Given the model is highly anisotropic, it is not surprising that the answer depends on direction. As shown in Eq. (5.8), the U(1) charge in each layer is conserved by the Hamiltonian as well as the ground state. As a result there cannot be any charge transport in the z direction, i.e. it is insulating. The other directions are quite different. Using the dual gauge theory we compute the effective action for the external field in Appendix 5.5.4, and indeed show that the system is superconducting in the xy plane.

5.2.4 Duality mapping

In this section we describe how the microscopic wire model can be mapped to an infinite-component CS theory coupled to gapped matter fields. The full details of this procedure are presented in Appendix 5.5.2. Schematically, the gauge theory emerges by employing a boson-vortex duality within each horizontal layer of wires. We adopt the method explained in Refs. [231, 232] to the 3D coupled wire model. Note that an alternative method to derive Chern-Simons-type gauge theory from coupled wire models have been proposed in Ref. [67].

Recall that the wire model is described by a rectangular array of Luttinger liquids with conjugate variables (φ, θ) and Lagrangian

$$\begin{aligned}\mathcal{L}[\varphi,\theta] = \sum_{\mathbf{r}} \frac{i}{\pi}\partial_x\theta_{\mathbf{r}}\partial_\tau\varphi_{\mathbf{r}} + \frac{\tilde{v}}{2\pi}\left(\partial_x\varphi_{\mathbf{r}}\right)^2 + \frac{u}{2\pi}\left(\partial_x\theta_{\mathbf{r}}\right)^2 \\ + \frac{v}{8\pi}\left(\partial_x\Delta_y\varphi_{\mathbf{r}}\right)^2 - g\cos(2\bar{\theta}_{\mathbf{r}})\end{aligned} \tag{5.25}$$

where

$$\begin{aligned} 2\bar{\theta}_{\mathbf{r}} &= \Delta_y \varphi_{\mathbf{r}} + \Lambda \theta_{\mathbf{r}} \\ &= (\varphi_{\mathbf{r}+\hat{y}} - \varphi_{\mathbf{r}}) \\ &\quad + (m\theta_{\mathbf{r}} + m\theta_{\mathbf{r}+\hat{y}} + n_1\theta_{\mathbf{r}-\hat{z}} + n_2\theta_{\mathbf{r}+\hat{z}} \\ &\quad + n_2\theta_{\mathbf{r}+\hat{y}-\hat{z}} + n_1\theta_{\mathbf{r}+\hat{y}+\hat{z}}). \end{aligned} \tag{5.26}$$

Here we define $\Delta_y X_{\mathbf{r}} = X_{\mathbf{r}+\hat{y}} - X_r$ and $\mathbf{r} = (y, z)$ is a wire index. Note that the kinetic part of Eq. (5.25) is more general than the free boson Hamiltonian given in Eq. (5.1). In particular, $\frac{v}{8\pi} \left(\partial_x \Delta_y \varphi_{\mathbf{r}}\right)^2$ has been added to the standard Luttinger Liquid kinetic term. This is done because it is convenient for the duality mapping to the vortex theory but its presence does not affect the qualitative physics [231].

Throughout the discussion of the microscopic model we use two equivalent forms of labelling for the wires, $O_{\mathbf{r}+\hat{a}} \equiv O_{y+a_y, z+a_z}$. Anticipating the layered structure of the gauge theory, we treat z as the "layer" index while y is coarse grained to a continuous spatial coordinate. With this motivation in mind, we define the following pair of conjugate variables:

$$\begin{aligned} \tilde{\varphi}_{yz} &= -\textstyle\sum_{y'} \operatorname{sgn}\left(y' - y - \frac{1}{2}\right) \theta_{y'z} \\ \tilde{\theta}_{yz} &= \tfrac{1}{2} \left(\varphi_{y+1,z} - \varphi_{y,z}\right). \end{aligned} \tag{5.27}$$

Here $\tilde{\varphi}_{yz}$ creates a 2π vortex in the φ field in layer z, in between wires y and $y+1$. The operator $\partial_x \tilde{\theta}_{yz}$ is the "charge" operator for this vortex. We can re-express the Lagrangian in Eq. (5.25) in terms of these new fields but the result will be highly

non-local in the y direction. We can restore locality in each layer z via a Hubbard-Stratonovich transformation at the expense of adding new degrees of freedom $a_0^{(z)}(x,y)$ and $a_1^{(z)}(x,y)$. At this stage, the Lagrangian takes the form

$$\begin{aligned}\mathcal{L}[\tilde{\varphi},\tilde{\theta},a_\mu] = \sum_r \frac{i}{\pi}\partial_x\tilde{\theta}_{\mathbf{r}}(\partial_\tau\tilde{\varphi}_{\mathbf{r}} - a^{(z)}_{0,\mathbf{r}}) + \frac{u}{2\pi}\left(\partial_x\tilde{\varphi}_{\mathbf{r}} - a^{(z)}_{1,\mathbf{r}}\right)^2 \\ + \frac{v}{2\pi}\left(\partial_x\tilde{\theta}_{\mathbf{r}}\right)^2 - g\cos(2\tilde{\theta}_{\mathbf{r}} + \frac{1}{2}\Lambda\cdot\Delta_y\tilde{\varphi}_{\mathbf{r}}) \\ + \mathcal{L}^{(z)}_{\text{Maxwell}}.\end{aligned} \tag{5.28}$$

Here, the definition of Λ can be easily inferred from Eq. (5.26), so that the argument of the cosine term matches $2\bar{\theta}_{\mathbf{r}}$. $\mathcal{L}^{(z)}_{\text{Maxwell}} = \frac{u}{2\pi}(\Delta_y a_1^{(z)})^2 + \frac{1}{2\pi\tilde{v}}(\Delta_y a_0^{(z)})^2$. The superscript of this term is no accident; we interpret Eq. (5.28) as a stack of 2D gauge theories in the $a_2^{(z)} = 0$ gauge coupled to matter $(\tilde{\varphi},\tilde{\theta})$. In the context of Eq. 5.28 the gauge fields would appear to be over-labeled since $\mathbf{r} = (y,z)$. We keep the redundant (z) superscript to emphasize this picture of stacks of 2D gauge theories. Such "layered" gauge theories have recently been studied in the context of fracton physics [225] and are reminiscent of the foliated gauge theories developed to describe fracton order [49]. We emphasize that the interpretation of a's as a stack of 2D gauge fields in the xy plane is motivated, and ultimately justified by providing a correct description of the low-energy physics of the model.

The next step is to integrate out the fields $\tilde{\varphi}$ and $\tilde{\theta}$. The details of the derivation can be found in Appendix 5.5.2. In the end we obtain the effective layered Maxwell-CS theory:

$$\mathcal{L}[a] \equiv \frac{iK_{zz'}}{4\pi}a^{(z)}\wedge da^{(z')} + (\text{Maxwell terms}), \tag{5.29}$$

where

$$K_{zz'} = 2m\delta_{zz'} + (n_1 + n_2)\delta_{z,z'\pm 1}. \tag{5.30}$$

The inter-layer Maxwell term contains couplings between components of the electromagnetic field from adjacent layers (z); as an example the B^2 term corresponds to

$$\sum_{z,z'} B^{(z)} \left[\frac{u}{2\pi}\delta_{zz'} + \frac{v}{8\pi}(K^{\mathsf{T}}K)_{zz'} \right] B^{(z')} \quad .$$

So far we have assumed that φ and θ vary smoothly, excluding the "solitonic" excitations of the cosine pinning term. These more singular configurations are the analog of vortices in the usual boson-vortex duality, which should be minimally coupled to the dynamical gauge fields. In Appendix 5.5.2 we show that this is indeed the case; namely the solitons become gauge charges in the dual gauge theory.

OBC in z direction

Now we consider OBC in the z direction and the effect of the various surface gapping terms discussed in Sec 5.2.3 on the resulting dual gauge theory.

First we discuss the symmetrically gapped surface generated by the pinning term in Eq. (5.24). The analysis is similar to the PBC case, except now we must pay attention to the $z = 0$ layer of wires. We decompose $\sum_{\mathbf{r}}$ into $\sum_y \sum_{z>0} + \sum_{y,z=0}$ in Eq (5.25). The terms in the first sum are unchanged while in the second sum, $\sum_{y,z=0}$,

the surface pinning term is $\cos 2\bar{\theta}_{y0}$ where

$$\begin{aligned} 2\bar{\theta}_{y0} = 2\tilde{\theta}_{y0} + \frac{m}{4}\Delta_y(\bar{\varphi}_{y,0} + \bar{\varphi}_{y+1,0}) \\ + \frac{n_1}{2}\Delta_y\bar{\varphi}_{y,1} + \frac{n_2}{2}\Delta_y\bar{\varphi}_{y+1,1} \quad . \end{aligned} \tag{5.31}$$

From here one can integrate out the matter fields and truncate higher order derivative terms where appropriate. The upshot of this is a modification of the K-matrix:

$$\mathbf{K}_{\text{sym,OBC}} = m \begin{pmatrix} -1 & 1 & & & 0 \\ 1 & -2 & 1 & & \\ & \ddots & \ddots & \ddots & \\ & & 1 & -2 & 1 \\ 0 & & & 1 & -1 \end{pmatrix}. \tag{5.32}$$

The B^2 term is also modified near the surface. This can be seen by noting that the term in the Lagrangian corresponds to something proportional to $(1+\alpha K^{\mathsf{T}}K)_{zz'}B^{(z)}B^{(z')}$ for some constant α.

Alternatively, we can explicitly break the $\mathrm{U}(1)_\theta$ symmetry by adding the very natural pinning term corresponding to the middle and top layer of the bulk plaquette term. This partial plaquette is given by

$$\begin{aligned} 2\bar{\theta}_{y0} = 2\tilde{\theta}_{y0} + \frac{m}{2}\Delta_y(\bar{\varphi}_{y,0} + \bar{\varphi}_{y+1,0}) \\ + \frac{n_1}{2}\Delta_y\bar{\varphi}_{y,1} + \frac{n_2}{2}\Delta_y\bar{\varphi}_{y+1,1}. \end{aligned} \tag{5.33}$$

The duality mapping of this surface theory proceeds in the same way as the symmetric

gapped example just discussed. In this case

$$\mathbf{K}_{\text{broken,OBC}} = m \begin{pmatrix} -2 & 1 & & & 0 \\ 1 & -2 & 1 & & \\ & \ddots & \ddots & \ddots & \\ & & 1 & -2 & 1 \\ 0 & & & 1 & -2 \end{pmatrix}. \tag{5.34}$$

5.2.5 Vortices and quasiparticles

Throughout our derivation of the dual gauge theory, we have assumed that the bosonic fields φ and θ vary smoothly in spacetime. As we have already mentioned, the complete spectrum also contains solitonic configurations. We show in Appendix 5.5.2 that the solitons are in fact dynamical charges of the dual gauge fields. Below we describe the universal properties of the soliton excitations. Many details are delegated to Appendix 5.5.1.

Physically, a "fundamental" soliton, i.e. a 2π jump in a single $\Theta_{\mathbf{r}}$ term, is in fact a vortex of the weak superfluid. This can be demonstrated by explicitly constructing a string operator to create a pair of such solitons separated in the y direction. The string operator takes the following form:

$$\prod_{y} e^{i\theta_{yz}(x)}, \tag{5.35}$$

which causes a branch cut of 2π phase jump in the string order parameter, thus the

corresponding excitation is a vortex. It is useful to divide the excitations into vortices and non-vortices. The simplest non-vortex excitation is just a dipole of two vortices, with opposite vorticities k and $-k$, separated along the z direction. Such non-vortex excitations can be considered as being "deconfined" quasiparticles in this phase. We call k the strength of the dipole.

Now we discuss the mobility of excitations. The string operator Eq. (5.35) shows that all excitations can move freely along the y direction. In Appendix 5.5.1 we show that such a fundamental soliton is immobile in the z direction, when $|m| \geq 2|n|$. Notice that these results hold true in both gapped and gapless models. For the gapless theory with $m = -2n$, one can show that a dipole whose strength is a multiple of m can move in the z direction.

The question of mobility along the x direction is more subtle. We present a construction of a x-string operator in Appendix. The string operator is ultra-local in the y direction, but can have some extension in the z direction. For a gapped model, we find that the construction does yield an exponentially localized string operator, as expected. However, the gapless case is quite different. To be concrete let us consider a finite N_z system. For a vortex, the construction fails if PBC or the symmetric OBC is imposed in the z direction. Only when the symmetry-breaking OBC is present one can find a string operator. For a dipole, a string operator always exists regardless of the boundary condition in the z direction. In both cases, however, the constructed string operator decays only algebraically in the z direction away from the localization of the excitation. This observation suggests that the mobility of these excitations along the x direction is also reduced.

In a gapped system, one can define the superselection sectors of quasiparticle excitations as the equivalence classes under local operations. Namely, two excitations are equivalent if they can be transformed to each other by local operator. We can attempt to generalize the notion to our model. We focus on the non-vortex excitations, because there are infinitely many types labeled by the vorticity. Since every non-vortex excitation is mobile along y, we can just consider them at a fixed y. Equivalence between excitations located at different x is less clear since the string operator is only algebraically localized. If however we consider them to be equivalent, we find that there are $m^{N_z-1} \cdot N_z$ classes of non-vortex excitations when PBC is imposed, which agrees with the topological ground state degeneracy of the coupled wire model. More details of the counting can be found in Appendix 5.5.1.

Since the vortices are coupled to the gapless gauge fields, gauge fluctuations induce long-range interactions between the vortices. We compute the interactions when the simplest, most isotropic Maxwell term is added to the dual CS theory (see Eq. (5.57) below). For two unit vortices separated by $\mathbf{r} = (x, y, z)$, let $\rho = \sqrt{x^2 + y^2}$. The interaction potential takes the following asymptotic form:

$$V(\mathbf{r}) \sim \begin{cases} \frac{1}{|z|} & \tilde{g}z^2 \gg \rho \\ \\ \frac{1}{\sqrt{\rho}} & \tilde{g}z^2 \ll \rho \end{cases}. \tag{5.36}$$

From this one can further obtain the interactions between dipoles, which decay with a higher power. Details of the calculations can be found in Appendix 5.5.4.

5.3 Infinite-component CS theory

Our duality mapping suggests that the low-energy physics can be described by an infinite-component Chern-Simons gauge theory, as given in Eq. (5.29). The gapped case $|m| > |n_1 + n_2|$ was studied in greater detail in Ref. [225]. Briefly, such a theory exhibits a kind of fracton topological order, with all quasiparticles being planons. Interestingly, in many cases the Wilson loop operators for these quasiparticles must have exponentially decaying tails in the z direction, and as a result, the braiding statistics between quasiparticles are not strictly local. When this phenomenon happens, the fractonic order appears to be beyond the topological defect network framework [77, 138, 137].

In the following we focus more on the gapless case, and our main task is to analyze the symmetry, anomaly and the issue of stability. We show that the iCS theory indeed captures the universal aspects of the coupled wire model. First of all, we note that the photon spectrum of the iCS theory with only "intra-layer" Maxwell terms was calculated in Ref. [225] and the result agrees [2] with the Gaussian spectrum Eq. (5.17) of the coupled wire model. Below we discuss how other universal aspects of the coupled wire model are encoded in the iCS field theory.

While we are interested in the iCS theory as a (3+1)d system, we start by reviewing the global symmetry and anomaly of a general $\mathrm{U}(1)^{N_z}$ CS theory, which can be thought of as compactifying the 3D system in the z direction (so there are N_z "layers").

[2] At first glance the spectrum of the layered gauge theory arising from Eq. (5.87) would seem to depend only on $n_1 + n_2$ and m, which does not agree with the spectrum derived for the wire model. This discrepancy stems from the fact the y direction has been coarse grained in the layered picture. Restoring higher order derivative terms in y in the gauge theory gives a spectrum matching Eq. (5.17)

i.e. it reduces to a quasi-2D theory for small compactification radius or by allowing non-locality along the compactified direction.

Notice that below we use differential form notations extensively.

5.3.1 Global symmetry and anomaly

We consider the action of a $\mathrm{U}(1)^N$ CS theory:

$$\mathcal{S} = \int_{M_3} \frac{K_{IJ}}{4\pi} a_I \wedge da_J, \tag{5.37}$$

where M_3 is a closed three manifold. $\mathbf{K}$ is a symmetric integer matrix. First we consider the theory with the Chern-Simons term only and assume that there are no matter fields. This is a valid assumption since all vortices are gapped, so well below the gap we can just study the pure gauge theory.

Global symmetry

We now enumerate all the unitary symmetries, including 0-form and 1-form, of the topological action.

First consider the pure topological action Eq. (5.37). The theory has the following discrete symmetries:

$$a_I \to W_{IJ} a_J, \tag{5.38}$$

where $\mathbf{W}$ belongs to $\mathrm{GL}(N, \mathbb{Z})$, i.e. an invertible $N \times N$ integral matrix, such that $\mathbf{W}^\mathsf{T}\mathbf{K}\mathbf{W} = \mathbf{K}$. Physically, when $\mathbf{K}$ is non-degenerate, $\mathbf{W}$ corresponds to a permutation of anyon types in the (2+1)d Abelian topological phase.

In addition, a $\mathrm{U}(1)^N$ gauge theory also has $\mathrm{U}(1)^N$ 0-form symmetries, the conservation of magnetic fluxes. The currents of the symmetries are $\star da_I$, where $\star$ is the Hodge star operator. When $\mathbf{K}$ is non-degenerate, these symmetries are embedded into the 1-form symmetry group.

We now discuss the 1-form symmetry of the model, first assuming that $\mathbf{K}$ is invertible. A general 1-form transformation takes the following form:

$$a_I \to a_I + q_I \lambda, \tag{5.39}$$

where λ is a properly normalized flat connection, i.e. $d\lambda = 0$, and the holonomy of λ along any 1-cycle is an integer multiple of 2π. q_I is an arbitrary real number at this point. When $q_I \in \mathbb{Z}$, the transformation can be viewed as a (possibly singular) gauge transformation. Additionally, one can prove that in order for the partition function of the theory to be invariant, the q_I's have to satisfy the following quantization condition:

$$K_{IJ} q_I \in \mathbb{Z}. \tag{5.40}$$

The derivation can be found in Appendix 5.5.3. If K is invertible, it implies that q_I's must take the values

$$q_I = (K^{-1})_{IJ} k_J, k_J \in \mathbb{Z}, \tag{5.41}$$

and the 1-form symmetry forms a finite Abelian group, the determinant group of $\mathbf{K}$. Each 1-form transformation corresponds to an integer vector $\mathbf{m}$, modulo those that can be written as $\mathbf{Kl}$ for $\mathbf{l} \in \mathbb{Z}^N$, and is in fact one-to-one correspondent to anyon

types. This is well-known, as the 1-form symmetries are generated by Wilson loops. The 1-form symmetry is generally anomalous if the corresponding anyon is not a boson [233].

When $\mathbf{K}$ is degenerate, the null space of $\mathbf{K}$ needs to be considered separately. Suppose that $\mathbf{v} \in \mathbb{Z}^N$ is a null vector, i.e. $\mathbf{K}\mathbf{v} = 0$. Without loss of generality we can assume $\mathbf{v}$ is primitive (i.e. $\gcd(v_1, v_2, \dots) = 1$). In that case, the following 1-form transformation

$$\mathbf{a} \to \mathbf{a} + \alpha \mathbf{v} \lambda \tag{5.42}$$

is always an exact symmetry of the 4d action (without any $2\pi\mathbb{Z}$ shift), where α is an arbitrary real number in $[0, 1)$. Therefore each null vector of K gives rise to a U(1) 1-form symmetry group. Physically, a null vector corresponds to a mode of the gauge fields without CS term, which can be dualized to a superfluid, which has a U(1) 1-form symmetry in the absence of vortices [219]. More generally, if the dimension of the null space is r, then we have $\mathrm{U}(1)^r$ 1-form symmetry.

Now we consider what happens when Maxwell terms are included. The $\mathrm{U}(1)^N$ and 1-form symmetries are not affected at all by the Maxwell terms. The Maxwell terms may break the 0-form symmetry, however. We then have only the subgroup that preserves the Maxwell terms as well.

We make connections between the symmetries identified in the CS gauge theory, especially with the K matrix given by Eq. (5.30), and those found in the coupled wire lattice model which are discussed in Sec 5.2.1. The magnetic U(1) 0-form symmetry of the I-th layer is nothing but the planar $\mathrm{U}(1)_\varphi$ symmetry. The U(1) "1-form" symmetry

defined in Eq. (5.42) can be identified with the conservation of total vorticity Eq. (5.14). Finally, as we will see shortly, we can identify the string order parameter with a "string" monopole operator.

't Hooft anomaly

The emergent symmetry group defined in the previous section generally has 't Hooft anomalies. The discrete part of the 0-form symmetry group has to be analyzed on a case-by-case basis. The anomaly of the finite 1-form symmetry group was studied in Ref. [233], and since it is not particularly relevant to us we do not go into details. So in the following we study the mixed anomaly between the 0-form $\mathrm{U}(1)^N$ and the 1-form symmetry group $\mathcal{A} \times \mathrm{U}(1)^r$.

We consider, without any loss of generality, a U(1) 0-form symmetry with charge vector $\mathbf{t}$. In other words, the U(1) current is given by

$$j = \sum_I t_I \star da_I. \tag{5.43}$$

We turn on a general background gauge field A for the U(1) symmetry:

$$\frac{t_I}{2\pi} \int a_I \wedge dA. \tag{5.44}$$

To check whether this coupling can be compatible with the 1-form symmetries, perform a general 1-form gauge transformation $a_I \to a_I + q_I \lambda_I$ where now λ_I is allowed to be non-flat. The action changes by $-\frac{q_I t_I}{2\pi} \int A \wedge d\lambda$. To restore gauge

invariance, the additional term can be cancelled by inflow from a 4d action

$$S_{\text{bulk}} = \frac{q_I t_I}{2\pi} \int_{M_4} B \wedge dA, \tag{5.45}$$

where B is the background 2-form gauge field.

A similar argument works for the $\mathrm{U}(1)^r$ part of the 1-form symmetry group: under the 1-form gauge transformation $a_I \to a_I + \alpha v_I \lambda$, to maintain gauge invariance we need to have a bulk theory given by

$$S_{\text{bulk}} = \frac{\mathbf{v} \cdot \mathbf{t}}{2\pi} \int_{M_4} B \wedge dA, \tag{5.46}$$

where now B is a 2-form U(1) gauge field, transforming under the 1-form gauge transformation as $B \to B + \alpha d\lambda$.

5.3.2 The filling anomaly

We now analyze the filling anomaly in the layered CS gauge theory. We are mainly interested in K matrices given in Eq. (5.30), although we present the analysis in a form that applies to more general cases. Such theories have a discrete translation symmetry, generated by

$$T_z : a_I \to a_{I+1}, \tag{5.47}$$

provided that the K matrix satisfies $K_{IJ} = K_{I+1,J+1}$. This is the formal way of identifying the index I as labeling layers in the z direction. We assume that $\mathbf{K}$ is "short-ranged" in the z direction, which means that there exists an integer $d \geq 0$

such that $K_{IJ} = 0$ if $|I - J| > d$. For now we assume that either $N_z \to \infty$, or periodic boundary condition is imposed so $a_{I+N_z} = a_I$. This way, the layered CS theory describes a highly anisotropic 3D system.

We are going to show that the (3+1)d theory can exist at any filling. Instead of directly computing the 3D filling anomaly, we take a detour and study the compactified system, with periodic boundary condition imposed along the z direction. Suppose that the 3D system has a filling factor ν (i.e. the average U(1) charge is ν per unit cell). When viewed as a quasi-2D system, the filling factor becomes $N_z\nu$. Here the dependence on N_z reflects the 3D nature.

Before going to the details, we briefly review the theory of the filling anomaly. It has been understood now that even though the filling condition does not correspond to a true, quantized 't Hooft anomaly (essentially because the filling factor is a continuous quantity), its impact on the low-energy physics can be described in the same theoretical framework. We first present a formal argument, following the approach in [234]. The standard method to detect the 't Hooft anomaly of a global symmetry is to couple the system to the background gauge field of the symmetry, and compute the topological response. While translation is a spatial symmetry, at low energy it can be described effectively as an internal symmetry. To this end, we formally introduce $\mathbb{Z}$ gauge fields x^1 and x^2 for the 2D translation symmetry. We also turn on a U(1) background gauge field A. The filling condition can be captured by the following response

$$S_{\text{bulk}} = \nu \int dA \cup x^1 \cup x^2. \tag{5.48}$$

Before getting to the CS gauge theory, we show how the filling anomaly can be embedded into the $\mathrm{U}(1)^{[0]} \times \mathrm{U}(1)^{[1]}$ 't Hooft anomaly discussed in Sec. 5.3.1. Formally, we start from the bulk action

$$\frac{k}{2\pi} \int B \cup dA. \tag{5.49}$$

To realize the filling anomaly, we demand that the translation background gauge field is activated through the 2-form background:

$$B = 2\pi\nu x^1 \cup x^2. \tag{5.50}$$

Then we see that the action gives a filling factor $k\nu$.

We give a physical interpretation as follows. Eq. (5.50) implies that when a loop charged under the $\mathrm{U}(1)^{[1]}$ symmetry moves, it picks up a phase factor given by the flux of the background 2-form gauge field B through the transverse area swept by the loop. Now recall that $x^{1,2}$ are translational gauge fields, $x^1 \cup x^2$ can be heuristically interpreted as the area in the 2D plane. So Eq. (5.50) basically says that a phase $2\pi\nu\mathcal{A}$, where $\mathcal{A}$ is the enclosed area, is attached to the loop. The anomaly action then implies that the loop is identified with magnetic field lines of the $\mathrm{U}(1)^{[0]}$ gauge field. Therefore, the anomaly action and the particular background Eq. (5.50) together can be summarized by the following intuitive picture: a 2π $\mathrm{U}(1)^{[0]}$ flux picks up $e^{2\pi i\nu}$ phase factor when it moves around a unit area. This is exactly the Aharonov-Bohm phase expected from the filling factor.

Such a mechanism is realized by a (2+1)d superfluid. A 2π $\mathrm{U}(1)^{[0]}$ magnetic flux

is trapped in a superfluid vortex. It is well-known that under boson-vortex duality, vortices see a background magnetic field, the strength of which is fixed by the filling factor.

We can apply these considerations to the CS theory. The anomaly is given by Eq. (5.46). The charge vector is simply $t_I = 1$, as we have shown in the duality mapping. We posit that the translation symmetry is realized via the U(1) 1-form symmetry corresponding to the "zero mode" $\mathbf{v} = (1, 1, \cdots, 1)^{\mathsf{T}}$, by the 2-form background given in Eq. (5.50). Together, we find that the coefficient of the topological action is $\mathbf{v} \cdot \mathbf{t}\nu = N_z\nu$. which is the expected filling factor. In fact, it is clear that as long as the charge vector $\mathbf{t}$ and $\mathbf{v}$ are translation-invariant (i.e. invariant under, or a certain multiple), the theory can be defined at arbitrary filling. Physically, whenever a zero mode exists, after compactification the system becomes a quasi-2D superfluid where the $\mathrm{U}(1)^{[0]}$ symmetry is spontaneously broken.

Notice that so far we have assumed periodic boundary condition in the z direction. Now we turn to open boundary condition. In this case, the z translation symmetry is broken. The filling of the quasi-2D system is still $N_z\nu$. The boundary condition at the top and bottom layers now becomes crucial. We have considered two kinds of boundary conditions in the coupled wire model in Sec. 5.2.4, which lead to different K matrices after duality transformation. If the boundary condition preserves all the

symmetries, we found the following K matrix:

$$\mathbf{K}_{\text{sym,OBC}} \propto \begin{pmatrix} -1 & 1 & & & 0 \\ 1 & -2 & 1 & & \\ & \ddots & \ddots & \ddots & \\ & & 1 & -2 & 1 \\ 0 & & & 1 & -1 \end{pmatrix}. \tag{5.51}$$

With this K matrix, $(1, 1, \ldots, 1)^{\mathsf{T}}$ is still a zero mode, and the same argument, as used for the periodic boundary condition, applies.

We also studied a symmetry-breaking surface in Sec. 5.2.4, which yields the following K matrix:

$$\mathbf{K}_{\text{broken,OBC}} \propto \begin{pmatrix} -2 & 1 & & & 0 \\ 1 & -2 & 1 & & \\ & \ddots & \ddots & \ddots & \\ & & 1 & -2 & 1 \\ 0 & & & 1 & -2 \end{pmatrix}. \tag{5.52}$$

This K matrix is non-degenerate, thus representing a fully gapped 2D phase. As discussed in [230] and [233], such a CS theory has a finite emergent symmetry group, incompatible with a generic filling. Thus the only way that the theory can emerge is to to break the symmetries explicitly. This is indeed the case in the coupled wire model.

5.3.3 Monopole operators

U(1) gauge theories generally admit monopole (or "disorder") operators, which are charged under the magnetic U(1) symmetries. For $\mathrm{U}(1)^N$ gauge group, a monopole operator is labeled by the magnetic charge vector $\mathbf{m} \in \mathbb{Z}^N$, i.e. $2\pi m_I$ flux for the a_I gauge field. Physically, it is actually an instanton that inserts $2\pi\mathbf{m}$ flux at a point. Due to the Chern-Simons coupling, the flux insertion necessarily nucleates charges, so we expect that the monopole operator is not gauge-invariant. In order to build a gauge-invariant monopole operator, one has to dress the "bare" operator by matter fields of charge $\mathbf{Km}$. As matter fields are absent (or very massive) in the low-energy theory, a gauge-invariant monopole operator can be introduced at low energy (i.e. well below the mass gap) only when $\mathbf{m}$ is a null vector of $\mathbf{K}$. For a translation-invariant K matrix, null vectors are also translation-invariant. They are precisely the string order parameters in the coupled wire model. Via the well-known Polyakov mechanism, adding monopole operators to the theory causes confinement of the gauge theory. However, if the monopole operator has a translation-invariant magnetic charge vector, it is in fact a highly non-local, string-like object in 3D and cannot appear as a local term in the Hamiltonian. We thus conclude that such theories are stable with respect to confinement caused by monopole proliferation.

We now look closer at the monopole operators, which requires adding Maxwell terms in the action:

$$S_{\text{Maxwell}} = \int \tilde{g}_{IJ} f_I \wedge \star f_J. \tag{5.53}$$

For this purpose, we diagonalize the K matrix:

$$\sum_J K_{IJ} e_J^\alpha = \lambda^q e_I^q, \tag{5.54}$$

where q labels different eigenvectors. Here we normalize e^q such that $\sum_I e_I^q e_I^{q'} = \delta^{qq'}$. Then the K matrix can be written as $K_{IJ} = \sum_q \lambda^q e_I^q e_J^q$. Define new gauge fields $b^q = e_I^q a_I$ and the inverse transformation reads $a_I = e_I^q b^q$. In terms of the new fields, the CS term becomes

$$\sum_q \frac{\lambda^q}{4\pi} b^q \wedge db^q. \tag{5.55}$$

and the Maxwell term becomes

$$\tilde{g}_{IJ} e_I^q e_J^{q'} f^q \wedge \star f^{q'}, \tag{5.56}$$

here $f = db$.

For the simplest choice, we can set $\tilde{g}_{IJ} = \tilde{g}\delta_{IJ}$, then $\tilde{g}_{IJ} e_I^q e_J^{q'} = \tilde{g}\delta^{qq'}$. So the theory becomes

$$\mathcal{L} = \frac{\lambda^q}{4\pi} b^q \wedge db^q - \tilde{g} f^q \wedge \star f^q. \tag{5.57}$$

In our layered CS theory, the translation invariance along z guarantees that different modes do not couple. In general, $\tilde{g}^a$ stays finite even when $N \to \infty$, unless $\tilde{g}_{IJ}$ is exactly proportional to K_{IJ}.

As we have already mentioned, the gauge-invariant monopole operators correspond to null space of the **K** matrix. Such operators only exist when the K matrix is

degenerate, so it has zero eigenvalues, the number of which is the same as the dimension of the null space. We focus on one such mode, and denote by b^0. Since the CS term vanishes, the b^0 mode is just a pure Maxwell theory dual to a superfluid. The charged operator of the superfluid is the monopole operator.

A $2\pi m_I$ instanton for a_I corresponds to a $2\pi e_I^q m_I$ instanton for the b^q gauge fields. At this point, we pause to discuss the Dirac quantization condition. For a^I gauge fields, we have the standard quantization condition:

$$\int_{M_2} \frac{da_I}{2\pi} \in \mathbb{Z}, \tag{5.58}$$

where M_2 is a closed surface. In terms of the new field strength:

$$\sum_\alpha e_I^q \int_{M_2} \frac{f^q}{2\pi} \in \mathbb{Z}. \tag{5.59}$$

Since we are only interested in gauge-invariant operators, we can assume that $\int_{M_2} f^q = 0$ for $\lambda^q \neq 0$. For simplicity, we assume that $\mathbf{K}$ has a unique zero mode $\mathbf{v}$. The normalized eigenvector is $\mathbf{e}^0 = \frac{\mathbf{v}}{\mathbf{v}}$. Then the quantization condition is

$$\frac{v_I}{\mathbf{v}} \int_{M_2} \frac{f^0}{2\pi} \in \mathbb{Z}. \tag{5.60}$$

Since $\gcd(v_1, v_2, \dots) = 1$, we find

$$\int_{M_2} \frac{f^0}{2\pi\mathbf{v}} \in \mathbb{Z}. \tag{5.61}$$

This is the formal way of saying that the fundamental monopole is labeled by $\mathbf{v}$ (when expressed using the original gauge fields a_I).

To restore the standard normalization, we need to rescale $f^0 \to \mathbf{v} f^0$, so the Lagrangian density of the Maxwell term of b^0 now reads

$$\mathcal{L}_0 = -\mathbf{v}^2 \tilde{g} f^0 \wedge \star f^0. \tag{5.62}$$

This theory can be dualized to a superfluid, but now the superfluid density is proportional to $\frac{1}{\mathbf{v}^2 \tilde{g}}$. So the mass generated by instanton proliferation is $\propto \frac{1}{|\mathbf{v}|^2}$ (there is a further fugacity factor, which should actually decay exponentially with $\mathbf{v}^2$).

Now we specialize to the K matrix of the compactified system. In that case, we have $|\mathbf{v}| = \sqrt{N_z}$, thus the superfluid density goes down as N_z^{-1}. The monopole operator, which is charged under the magnetic symmetry of all the layers, is indeed the string superfluid order parameter of the coupled wire model identified in Sec. 5.2.3. The N_z^{-1} decay of the superfluid density also agrees with the result of the two-point correlation function of the order parameter.

One notices an apparent discrepancy between the superfluid density which decays as N_z^{-1} and a finite superconducting response. The resolution is that the charge of the order parameter grows with N_z to compensate the decay of the superfluid density.

5.3.4 Classification of charge excitations

We now discuss the topological classification of charges in the Chern-Simons theory. Again we consider the case of a finite number N_z of layers. Suppose the null space

of the K matrix is spanned by null vectors $\mathbf{v}_j, j = 1, 2, \ldots, r$ where $\mathbf{K}\mathbf{v}_j = 0$. As shown earlier, each null vector corresponds to a 1-form $\mathrm{U}(1)^{(j)}$ symmetry, and the corresponding magnetic U(1) 0-form symmetry is spontaneously broken. One can then show that the total vorticity (with respect to the weak superfluid of the $\mathrm{U}(1)^{(j)}$ symmetry) is given by $\mathbf{v}_j^\mathsf{T}\mathbf{l}$, by e.g. checking the $\mathrm{U}(1)^{(j)}$ 1-form charge of the corresponding Wilson loop.

One can also consider the equivalence classes of non-vortex gauge charges. The definition of equivalence is essentially the same as that of a topological Abelian CS theory with a non-degenerate K matrix, which we briefly review now: a gauge charge $\mathbf{l}$ is a local excitation if and only if it can be written as $\mathbf{l} = \mathbf{K}\mathbf{l}'$ for some integer vector $\mathbf{l}'$. This is true even when $\mathbf{K}$ is degenerate, as already mentioned in Sec. 5.3.3, and easily follows from the equation of motion. Two charges are equivalent if their difference is local. From this definition, it is easy to see that all local excitations must have zero vorticity, as expected in any superfluid. We thus focus on the non-vortex charges, the equivalence classes of which form a finite Abelian group, which is the generalization of the anyon group. To determine the structure of this group, we can simply perform a $\mathrm{GL}(N_z, \mathbb{Z})$ transformation to decouple the null space. In other words, we can find an invertible integer matrix $\mathbf{W}$, such that

$$\mathbf{W}^\mathsf{T}\mathbf{K}\mathbf{W} = \begin{pmatrix} \mathbf{0}_{r\times r} & \\ & \tilde{\mathbf{K}} \end{pmatrix}, \tag{5.63}$$

where $\tilde{\mathbf{K}}$ is a non-degenerate matrix. The structure of the anyon group is determined

by the Smith normal form of $\tilde{K}$. The number of distinct equivalence classes is given by $|\det \tilde{\mathbf{K}}|$. For the K matrix arising from the coupled wire construction, we find that $\tilde{\mathbf{K}}$ is basically the same as the K matrix with symmetry-breaking OBC, but with $N_z - 1$ layers, and $|\det \tilde{\mathbf{K}}| = m^{N_z-1} \cdot N_z$. These results all agree very well that those of the coupled wire model.

5.4 Summary

In this chapter we have introduced a new type of compressible matter: a "weak superfluid," which is a 3D anisotropic phase distinct from the conventional superfluid or Fermi liquid. The weak symmetry breaking is characterized by a "rod" order parameter, which is supported on a straight line along a fixed direction, and at the same time there exist no local order parameters. We argue that the low-energy physics can be captured by a gapless infinite-component Chern-Simons theory introduced in Ref. [225].

We determined the emergent symmetry of the highly anisotropic "weak superfluid", both from the coupled wire model and from the iCS field theory. Most importantly, the weak symmetry breaking leads to a "cylindrical" U(1) 1-form symmetry, where the symmetry transformations are defined on cylinders along the z direction (with arbitrary shape in the xy plane), as depicted in Fig 5.2. The mixed anomaly between the cylindrical U(1) 1-form symmetry and the U(1) 0-form symmetry is responsible for the arbitrary filling condition, i.e. being a compressible phase.

Recently, Ref. [220] identified an interesting conceptual relation between zero-

temperature DC conductivity and "fluxibility", which is a mixed anomaly between charge U(1) symmetry and an emergent symmetry. The latter is also responsible for the arbitrary filling condition. This led to the conjecture [220] that a translation-invariant quantum system is compressible if and only if it is fluxible. In our work, the filling condition is indeed realized in the low-energy theory as a mixed anomaly between the U(1) charge conservation symmetry and the cylindrical 1-form symmetry, which suggests that the system is indeed "fluxible," in an appropriate sense. However, the highly anisotropic emergent symmetry group results in more complicated zero-temperature DC transport, quite different from the isotropic theories considered in Ref. [220].

Our microscopic model was given by a coupled wire construction which stitches together arrays of 1D Luttinger Liquids. We can also understand the phase by imagining gluing together layers of 2D superfluids. In Chapters 3 and 4, other classes of 3D coupled wire models were shown to exhibit fractonic behavior. Interestingly, for appropriate choice of parameters, these models can also be made compressible (i.e. invariant under the anomalous $U(1) \times U(1)$ symmetry defined in Eq. 5.11. Similar to the models studied in this work, they become gapless and exhibit weak symmetry breaking, i.e. there are no local order parameter of any kind. But the non-local order parameter is now supported on a membrane that spans the whole 2D section perpendicular to the wires. It is not yet clear whether the physics can be understood in terms of some variation of the iCS theory. We leave a detailed investigation of these other models for future work.

Another natural question is whether similar WSB phenomena occur in two-dimensional

compressible systems. While we are not aware of any fundamental reasons prohibiting such phenomena in 2D, it is unlikely that a 2D coupled wire model can realize it. The duality transformation employed in this work can be applied to a general coupled wire model, under reasonable conditions. The result is then a 2+1D Abelian CS theory, which is either fully gapped when the K matrix is non-degenerate, or dual to a superfluid when the K matrix is degenerate, which now has a local order parameter (e.g. the quasi-2D limit of the model studied in this work after compactification). It will be interesting to understand whether this is just the limitation of the coupled wire construction, or there is a more fundamental obstruction in 2D.

The iCS models have been shown to realize new and novel phases of matter. The gapped case discussed in [225] provides new examples of type-I fractonic order without any foliation structure. Thus far the iCS theories that have been analyzed have only involved nearest neighbor couplings. It would be interesting to study models with a wider range of couplings between the layers of gauge theories, and explore possible connections with other fracton phases. We have shown here that the coupled wire construction provides a useful tool for building microscopic models which realize these phases at low energy.

5.5 Appendix

5.5.1 String operators for solitonic excitations

In this section we consider the mobility of the solitons. We focus on the most elementary excitation, namely a unit soliton of a single $\Theta_{\mathbf{r}}$ term. We work in the mean-field approximation, assuming large vg.

One can apply a vertex operator to create solitons, and move them around in the yz plane. In this model, it is easy to see that $e^{i\theta}$ can hop a 1-soliton along y. In other words, $\prod_y e^{i\theta_{yz}(x)}$ is a string operator. Note that strictly speaking, the string creates perfectly sharp solitons, which are only valid at $g \to \infty$. At finite g, the soliton is smeared over a length scale ξ and the string operator must be modified to create the smeared profile. But these modifications do not change universal features, such as mobility or the braiding statistics.

We also consider how a single soliton excitation can be transported along the wire. For simplicity we consider the $n_1 = n_2 = n$ case, but the same method works for the more general cases as well. Following the general discussion in Ref. [226], we define

$$\varphi^L_{yz} = \varphi_{yz} + m\theta_{yz} + n(\theta_{y,z-1} + \theta_{y,z+1}). \tag{5.64}$$

We construct a string operator of the following form:

$$W_y(x_2, x_1) = \exp\left(i \int_{x_1}^{x_2} \sum_z w_z \partial_x \varphi^L_{yz} \right). \tag{5.65}$$

where $w_z \in \mathbb{R}$. At the end point x_2, W creates a soliton of strength $\sum_{z'} K_{zz'} w_{z'}$ for the Θ_{yz} term, where y is fixed, and the opposite one at x_1. We thus denote such an excitation at one end of the string by a N_z-dimensional integer vector $\mathbf{v}$, the z-th entry of which is the strength of the soliton in the Θ_{yz} term. Thus finding a string operator of the form Eq. (5.65) reduces to solving the equation $\mathbf{Kw} = \mathbf{v}$.

Thus to move a single soliton of unit strength at $z = 0$, we set $w_z = (K^{-1})_{0z}$. When the bulk is fully gapped (i.e. $2|m| > |n_1 + n_2|$), w as a function of z decays exponentially away from the location of the excitation (it is strictly localized in y), so our string operator is quasi-localized, and the soliton can move along the wire. This agrees with the prediction of the iCS field theory [225], that is the quasiparticles have exponentially localized profiles leading to quasi-localized braiding statistics. In the coupled wire model, the quasiparticle excitation itself is strictly localized as a violation of a certain plaquette term (at least in the mean-field limit), but the string operator is quasi-localized.

In the gapless case, the construction in Eq. (5.65) does not work in general as K is singular, at least when PBC along the z direction is imposed. However, we can still invert the K matrix in the complement of the null space. For $m = -2n$, this subspace consists of all vectors $\mathbf{v}$ such that $\sum_i v_i \neq 0$. For the vectors with non-zero overlap with the null space, as we discussed in the main text they should be thought of as vortices in the weak superfluid. For example, if $\mathbf{v}_0 = (1, -1, 0, \cdots)$, then we can find the following $\mathbf{w}$ which satisfies $\mathbf{Kw} = \mathbf{v}_0$:

$$\mathbf{w} = \frac{1}{m}\Big(-\frac{1}{L_z}, \frac{L_z - 2}{L_z}, \frac{L_z - 1}{L_z}, \cdots, \frac{1}{L_z}, 0\Big). \tag{5.66}$$

$\mathbf{w}$ is no longer quasi-localized. The weight is only inversely proportional to the distance away from the location of the excitation. A string operator moving this excitation along the wire direction can then be constructed using the $\mathbf{w}$.

It is shown in Ref. [79] that two excitations $\mathbf{v}$ and $\mathbf{v}'$ (with the same x coordinate) belong to the same superselection sector, i.e. they can be transformed into each other by acting with local operators, if and only if $\mathbf{v}' = \mathbf{v} + \mathbf{K}\mathbf{u}$ for some integer vector $\mathbf{u}$. This agrees with the mathematical definition of superselection sectors in Abelian CS theories. Let us now enumerate the number of superselection sectors. We can easily show that, all translations of $m\mathbf{v}_0$ are equivalent, and $mL_z\mathbf{v}_0$ is local. It is then straightforward to show that the total number of inequivalent non-vortex excitations is $m^{L_z-1} \cdot L_z$. More generally, we can find the Smith normal form of $\mathbf{K}$, and the number of superselection sectors is the same as the absolute value of the product of all non-zero entries. Notice that here we only count the "non-vortex" excitations, as there are infinite types of vortices labeled by vorticity.

Finally, we consider the mobility of excitations along z. Since $e^{i\theta}$ only moves solitons along y, motion along z necessarily involves $e^{i\varphi}$. It is useful to represent the charge configuration formally by a Laurent polynomial in two variables y and z. Namely, define

$$\sum_{i,j\in\mathbb{Z}} q_{ij} y^i z^j. \tag{5.67}$$

Here q_{ij} is the charge at coordinate i, j in the $y-z$ plane and it should be clear that we do not need to worry about their x coordinates. Such polynomial representation was discussed in Ref. [226].

The operator $e^{i\varphi}$ creates the pattern $(nz^{-1}+m+nz)(1+y)$. Since $1-y$ can be created by $e^{i\theta}$, for mobility along z we can move all excitations to the same y and thus just consider $2(nz^{-1}+m+nz)$. Suppose by applying $e^{ia_j\varphi_j}$ (together with appropriate $e^{i\theta}$'s to move all charges to the same y), we can create a configuration with two solitons of opposite charges separated by a distance l. In terms of the polynomial representation, this amounts to finding a polynomial $f(z)=\sum_j a_j z^j$ such that

$$f(z)(nz^{-1}+m+nz)\propto 1+z^l. \tag{5.68}$$

Suppose that l is large so we essentially look for a string operator along z. For $1\ll j\ll l$ we have

$$na_{j+1}+ma_j+na_{j-1}=0. \tag{5.69}$$

Since $m^2>4n^2$, the corresponding characteristic polynomial has two real roots. As a result, a_j grows exponentially with j (in either directions), which means the charge created at one end costs an exponentially large amount of energy. For $m=-2n$, let $f(z)=a_0+a_1z+\cdots+a_lz^l$, then $f(z)(nz^{-1}-2n+nz)=n[a_0+(a_1-2a_0)z+(a_2-2a_1+a_0)z^2+\cdots+a_lz^{l+1}]$. If we require $a_{j+1}-2a_j+a_{j-1}=0$ for all $1\le j\le l-1$, then we $a_j=a_0+j(a_1-a_0)$. So the only way to have bounded $|a_j|$ is to set $a_1=a_0$, and the excitation created at one end is precisely a vortex-anti-vortex dipole of strength n.

5.5.2 Details of the duality mapping

In this section we provide more detail for the mapping described in section 5.2.4.

Boson-vortex duality

The wire model is described by an array of Luttinger liquids with conjugate variables (φ, θ) and Lagrangian

$$\mathcal{L}[\varphi,\theta] = \sum_{\mathbf{r}} \frac{i}{\pi}\partial_x\theta_{\mathbf{r}}\partial_\tau\varphi_{\mathbf{r}} + \frac{\tilde{v}}{2\pi}\left(\partial_x\varphi_{\mathbf{r}}\right)^2 + \frac{u}{2\pi}\left(\partial_x\theta_{\mathbf{r}}\right)^2 + \frac{v}{8\pi}\left(\partial_x\Delta_y\varphi_{\mathbf{r}}\right)^2 - g\cos(2\bar{\theta}_{\mathbf{r}}) \tag{5.70}$$

where

$$\begin{aligned} 2\bar{\theta}_{\mathbf{r}} &= \Delta_y\varphi_{\mathbf{r}} + \Lambda\theta_{\mathbf{r}} \\ &= (\varphi_{\mathbf{r}+\hat{y}} - \varphi_{\mathbf{r}}) + (m\theta_{\mathbf{r}} + m\theta_{\mathbf{r}+\hat{y}} + n_1\theta_{\mathbf{r}-\hat{z}} + n_2\theta_{\mathbf{r}+\hat{z}} + n_2\theta_{\mathbf{r}+\hat{y}-\hat{z}} + n_1\theta_{\mathbf{r}+\hat{y}+\hat{z}})\,. \end{aligned} \tag{5.71}$$

Here we define $\Delta_y X_{\mathbf{r}} = X_{\mathbf{r}+\hat{y}} - X_{\mathbf{r}}$ and $\mathbf{r} = (y, z)$ is a wire index. The definition of Λ can be easily inferred from Eq. (5.71). Note also that $\frac{v}{8\pi}\left(\partial_x\Delta_y\varphi_{\mathbf{r}}\right)^2$ has been added to the standard Luttinger Liquid kinetic term. This is done because it is convenient for the duality mapping to the vortex theory but its presence does not affect the qualitative physics [231].

In what follows we use the two equivalent forms of labelling for the wires, $O_{\mathbf{r}+\hat{a}} \equiv O_{y+a_y,z+a_z}$. Anticipating the layered structure of the gauge theory, we treat z as the "layer" index and y is to be coarse grained to a continuous spatial coordinate. With

this motivation in mind, we define the following pair of conjugate variables:

$$\begin{aligned}\tilde{\varphi}_{yz} &= -\sum_{y'} \operatorname{sgn}\left(y' - y - \tfrac{1}{2}\right) \theta_{y'z} \\ \tilde{\theta}_{yz} &= \tfrac{1}{2}\left(\varphi_{y+1,z} - \varphi_{y,z}\right).\end{aligned} \tag{5.72}$$

Here $\tilde{\varphi}_{yz}$ creates a 2π vortex in the φ field in layer z, in between wires y and $y+1$. The operator $\partial_x \tilde{\theta}_{yz}$ is the "charge" operator for this vortex. We can re-express the Lagrangian in Eq. (5.70) in terms of these new fields but the result will be highly non-local in the y direction. We can restore locality via a Hubbard-Stratonovich transformation at the expense of introducing new degrees of freedom $a_0^{(z)}(x,y)$ and $a_1^{(z)}(x,y)$ in each layer indexed by (z).

We now rewrite the kinetic part of the Lagrangian using the dual variables $(\tilde{\varphi}, \tilde{\theta})$ and the Hubbard-Stratonovich fields $(a_0^{(z)}, a_1^{(z)})$:

$$\sum_{\mathbf{r}} \tfrac{i}{\pi} \partial_x \theta_{\mathbf{r}} \partial_\tau \varphi_{\mathbf{r}} = \sum_{\mathbf{r}} \tfrac{i}{\pi} \partial_x \tilde{\theta}_{\mathbf{r}} \partial_\tau \tilde{\varphi}_{\mathbf{r}}$$

$$\sum_{\mathbf{r}} \tfrac{v}{8\pi} \left(\partial_x \Delta_y \varphi_{\mathbf{r}}\right)^2 = \sum_{\mathbf{r}} \tfrac{v}{2\pi} \left(\partial_x \tilde{\theta}_{\mathbf{r}}\right)^2$$

$$\sum_{\mathbf{r}} \tfrac{\tilde{v}}{2\pi} \left(\partial_x \varphi_{\mathbf{r}}\right)^2 = \sum_{\mathbf{r}} \tfrac{\tilde{v}}{2\pi} \left(\Delta_y^{-1} \partial_x \tilde{\theta}_{\mathbf{r}}\right)^2 \to \sum_{\mathbf{r}} \left[-\tfrac{i}{\pi} \partial_x \tilde{\theta}_{\mathbf{r}} a_0^{(z)} + \tfrac{(\Delta_y a_0^{(z)})^2}{8\pi\tilde{v}} \right]$$

$$\begin{aligned}\sum_{\mathbf{r}} \tfrac{u}{2\pi} \left(\partial_x \theta_{\mathbf{r}}\right)^2 = \sum_{\mathbf{r}} \tfrac{u}{8\pi} \left(\partial_x \Delta_y \tilde{\varphi}_{\mathbf{r}}\right)^2 \to \sum_{\mathbf{r}} \tfrac{u}{8\pi} \left[\left(\partial_x \tilde{\varphi}_{\mathbf{r}} - a_1^{(z)}\right)^2 + \left(\Delta_y a_1^{(z)}\right)^2 \right] \\ + \sum_{z,y,y'} \tfrac{u}{8\pi} V_{y,y'} \partial_x \left(\Delta_y \tilde{\varphi}_{yz}\right) \partial_x \left(\Delta_y \tilde{\varphi}_{y'z}\right)\end{aligned} \tag{5.73}$$

where $V = \Delta_y^{\mathsf{T}}(1+\Delta_y^{\mathsf{T}}\Delta_y)^{-1}\Delta_y$, which decays exponentially in the difference in wire index y. Up to this point everything is exact. Now we interpret $a_\mu^{(z)}$ as a (2+1)d gauge field, living in layer z, in the $a_2^{(z)}=0$ gauge. The upshot of all this is that we get a theory of layers of vortices minimally coupled to a layered gauge theory. Using Eq. (5.72), we re-express the plaquette term in terms of the vortex variables

$$\begin{aligned} 2\bar{\theta}_{yz} &= 2\tilde{\theta}_{yz} + \frac{1}{2}\Delta_y\left[n_1(\tilde{\varphi}_{y,z+1}+\tilde{\varphi}_{y+1,z-1}) + n_2(\tilde{\varphi}_{y,z-1}+\tilde{\varphi}_{y+1,z+1}) + m(\tilde{\varphi}_{yz}+\tilde{\varphi}_{y+1,z})\right] \\ &= 2\tilde{\theta}_{yz} + \frac{1}{2}\Lambda\cdot\Delta_y\tilde{\varphi}_{yz} \quad . \end{aligned} \tag{5.74}$$

In what follows, when coupled to matter fields $(\bar{\varphi},\bar{\theta})$, we suppress the (z) layer index of the gauge fields and use the $\mathbf{r}$ index in order to make the expressions more succinct. The various indices can be parsed as follows $a_{\mu,\mathbf{r}} = a_{\mu,yz} = a_\mu^{(z)}(x,y)$. At this stage the Lagrangian takes the form

$$\begin{aligned} \mathcal{L}[\tilde{\varphi},\tilde{\theta},a_\mu] = \sum_{\mathbf{r}} \frac{i}{\pi}\partial_x\tilde{\theta}_{\mathbf{r}}\left(\partial_\tau\tilde{\varphi}_{\mathbf{r}} - a_{0,\mathbf{r}}^{(z)}\right) + \frac{u}{2\pi}\left(\partial_x\tilde{\varphi}_{\mathbf{r}} - a_{1,\mathbf{r}}^{(z)}\right)^2 + \frac{v}{2\pi}\left(\partial_x\tilde{\theta}_{\mathbf{r}}\right)^2 \\ - \; g\cos(2\tilde{\theta}_{\mathbf{r}} + \frac{1}{2}\Lambda\cdot\Delta_y\tilde{\varphi}_{\mathbf{r}}) + \mathcal{L}_{\text{Maxwell}}^{(z)}. \end{aligned} \tag{5.75}$$

Here, in the $a_2^{(z)}=0$ gauge, $\mathcal{L}_{\text{Maxwell}}^{(z)} = \frac{u}{2\pi}(\Delta_y a_1^{(z)})^2 + \frac{1}{2\pi\tilde{v}}(\Delta_y a_0^{(z)})^2$. In order to simplify the sine-Gordon term we can introduce another set of conjugate variables:

$$\bar{\varphi}_{\mathbf{r}} = \tilde{\varphi}_{\mathbf{r}} \quad \text{and} \quad \bar{\theta}_{\mathbf{r}} = \tilde{\theta}_{\mathbf{r}} + \frac{1}{4}\Lambda\cdot\Delta_y\bar{\varphi}_{\mathbf{r}}. \tag{5.76}$$

Expressing the Lagrangian in this final basis and also expanding the cosine term

yields

$$\begin{aligned}\mathcal{L}[\bar{\varphi},\bar{\theta},a_\mu] = &\sum_{\mathbf{r}} \frac{i}{\pi}\partial_x\bar{\theta}_{\mathbf{r}}(\partial_\tau\bar{\varphi}_{\mathbf{r}} - a_{0,\mathbf{r}}) + \frac{i}{4\pi}\left(\Lambda\cdot\Delta_y\partial_x\bar{\varphi}\right)_{\mathbf{r}} a_{0,\mathbf{r}} + \frac{u}{2\pi}\left(\partial_x\bar{\varphi}_{\mathbf{r}} - a_{1,\mathbf{r}}\right)^2 \\ &+ \frac{v}{2\pi}\left(\partial_x\bar{\theta}_{\mathbf{r}}\right)^2 - \frac{v}{4\pi}\left(\Lambda\cdot\Delta_y\partial_x\bar{\varphi}\right)_{\mathbf{r}}\partial_x\bar{\theta}_{\mathbf{r}} + \frac{v}{32\pi}\left(\Lambda\cdot\Delta_y\partial_x\bar{\varphi}\right)^2_{\mathbf{r}} \\ &+ g\bar{\theta}^2_{\mathbf{r}} + \mathcal{L}_{\text{Maxwell}}.\end{aligned} \tag{5.77}$$

Integrating out matter fields

In order to get a pure gauge theory the plaquette degrees of freedom $\bar{\varphi},\bar{\theta}$ must be integrated out. The first step in the derivation is to collect all the terms involving $\bar{\varphi}$, up to $\mathcal{O}(\bar{\varphi}^2)$:

$$\begin{aligned}&\mathcal{O}(\bar{\varphi}^2):\ \partial_x\bar{\varphi}_{\mathbf{r}'}\left[\frac{u}{2\pi} + \frac{v}{32\pi}(\Lambda\cdot\Delta_y)^{\mathsf{T}}(\Lambda\cdot\Delta_y)\right]_{\mathbf{r}'\mathbf{r}}\partial_x\bar{\varphi}_{\mathbf{r}} = \partial_x\bar{\varphi}M\partial_x\bar{\varphi} \\ &\mathcal{O}(\bar{\varphi}):\ \underbrace{\left[\frac{-i}{4\pi}\Lambda\cdot\Delta_y a_0 - \frac{u}{\pi}a_1 + \frac{i}{\pi}\partial_\tau\bar{\theta} + \frac{v}{4\pi}\Lambda\cdot\Delta_y\partial_x\bar{\theta}\right]_{\mathbf{r}}}_{\Gamma_{\mathbf{r}}}\partial_x\bar{\varphi}_{\mathbf{r}}\end{aligned} \tag{5.78}$$

We denote the cross term by $\Gamma_{\mathbf{r}}[\bar{\theta},a]\partial_x\bar{\varphi}_{\mathbf{r}}$. Note here we have used a discrete "integration by parts" in parts involving $\Lambda\cdot\Delta_y$ and dropped z boundary terms. This step requires care when considering open boundary conditions in z. Integrating out $\bar{\varphi}$ results in an expression of the form:

$$-\frac{1}{4}\Gamma_{\mathbf{r}'}\left(M^{-1}\right)_{\mathbf{r}'\mathbf{r}}\Gamma_{\mathbf{r}}. \tag{5.79}$$

We are interested in the low energy theory so we can express M^{-1} as a derivative expansion in powers of $\Lambda \cdot \Delta_y$. To accomplish this note that for $M = 1 + D$

$$M^{-1} = (1+D)^{-1} = \sum_{j=0}^{\infty} (-1)^j D^j \ . \tag{5.80}$$

In the present case $M^{-1} \approx \frac{2\pi}{u} - \frac{v\pi}{8u^2}(\Lambda \cdot \Delta_y)^{\mathsf{T}}(\Lambda \cdot \Delta_y)$. We keep the 2nd order term because the a_1^2 term in Γ^2 cancels and the next lowest order term is $(\Lambda \cdot \Delta_y a_1)^2$. Including the left over terms which do not involve $\bar{\varphi}$ and only keeping the lowest order derivative terms in the expansion of Γ^2 gives

$$\begin{aligned} \mathcal{L}[\bar{\theta}, a] = \sum_{\mathbf{r}} \frac{-i}{4\pi} (\Lambda \cdot \Delta_y a_0)_{\mathbf{r}} a_{1,\mathbf{r}} + \frac{v}{8\pi} (\Lambda \cdot \Delta_y a_1)^2_{\mathbf{r}} + \frac{1}{32\pi u} (\Lambda \cdot \Delta_y a_0)^2_{\mathbf{r}} \\ + \frac{i}{\pi} \bar{\theta}_{\mathbf{r}} \left(\partial_x a_0 - \partial_\tau a_1\right)_{\mathbf{r}} + g\bar{\theta}^2_{\mathbf{r}} + \mathcal{L}_{\text{Maxwell}} + \text{Higher order terms} \end{aligned} \tag{5.81}$$

Integrating out $\bar{\theta}$ is now relatively simple and the result is

$$\begin{aligned} \mathcal{L}[a] = \sum_{\mathbf{r}} -\frac{i}{4\pi} \underbrace{(\Lambda \cdot \Delta_y a_1)_{\mathbf{r}} a_{0,\mathbf{r}}}_{\text{CS term}} + \frac{1}{4\pi^2 g} (\partial_x a_0 - \partial_\tau a_1)^2_{\mathbf{r}} \\ + \frac{1}{2\pi\tilde{v}} (\Delta_y a_0)^2_{\mathbf{r}} + \frac{1}{32\pi u} (\Lambda \cdot \Delta_y a_0)^2_{\mathbf{r}} + \frac{u}{2\pi} (\Delta_y a_1)^2_{\mathbf{r}} + \frac{v}{8\pi} (\Lambda \cdot \Delta_y a_1)^2_{\mathbf{r}}. \end{aligned} \tag{5.82}$$

If the y direction is coarse grained and the layer (z) index restored then

$$(\Lambda \cdot \Delta_y a)_z \approx (n_1 + n_2)\Delta_y a^{(z+1)} + 2m\Delta_y a^{(z)} + (n_1 + n_2)\Delta_y a^{(z-1)} \tag{5.83}$$

So the first term in Eq. (5.82), corresponding to a CS term, becomes

$$\mathcal{L}_{\rm CS}[a] = \frac{i}{4\pi}\left[(n_1+n_2)a_1^{(z+1)}\partial_y a_0^{(z)} + 2m a_1^{(z)}\partial_y a_0^{(z)} + (n_1+n_2)a_1^{(z-1)}\partial_y a_0^{(z)}\right] \quad . \tag{5.84}$$

When the gauge constraint, $a_2 = 0$, is relaxed $a_1^{(z)}\partial_y a_0^{(z')} \to \epsilon^{\mu\nu\lambda} a_\mu^{(z)}\partial_\nu a_\lambda^{(z')}$, so the CS part of the Lagrangian has the more familiar form

$$\mathcal{L}_{\rm CS}[a] \equiv \frac{iK_{zz'}}{4\pi} a^{(z)} \wedge da^{(z')} \quad . \tag{5.85}$$

We can similarly investigate parts of Eq. (5.82) associated with the Maxwell terms of the gauge theory. For example, coarse graining y and restoring gauge invariance in the $4^{\rm th}$ term corresponds to

$$(\Lambda\cdot\Delta_y a_0)^2 \to (\Lambda\cdot[\Delta_y a_0 - \partial_\tau a_2])^2 = \left[(n_1+n_2)E_2^{(z+1)} + 2mE_2^{(z)} + (n_1+n_2)E_2^{(z-1)}\right]^2 \quad . \tag{5.86}$$

We see that the typical E_y^2 term present in conventional Maxwell theory is replaced by something which couples the same component (y in this case) of the electric field in different layers. Indeed, a similar term is generated for B but not for E_x, this is not surprising given the anisotropic nature of the underlying microscopic model. The full result for the Maxwell term is given by

$$\mathcal{L}_{\rm Maxwell} = \sum_{zz'} E_1^{(z)}\frac{\delta_{zz'}}{4\pi^2 g}E_1^{(z')} + E_2^{(z)}\left[\frac{\delta_{zz'}}{2\pi\tilde{v}} + \frac{1}{32\pi u}(K^{\mathsf{T}}K)_{zz'}E_2^{(z')} + B^{(z)}\left[\frac{u\delta_{zz'}}{2\pi} + \frac{v}{8\pi}(K^{\mathsf{T}}K)_{zz'}\right]B^{(z')} \quad . \tag{5.87}$$

The upshot of this discussion is that the effective IR Lagrangian is given by:

$$\mathcal{L}[a] \equiv \frac{iK_{zz'}}{4\pi} a^{(z)} \wedge da^{(z')} + \mathcal{L}_{\text{Maxwell}} \quad . \tag{5.88}$$

Note that for the compressible state, $m = -(n_1 + n_2)$, $K^{\mathsf{T}}K \to \partial_z^4$ under coarse-graining in z and so the inter-layer portion of the Maxwell term would appear to be irrelevant in this context.

Coupling to vortices

So far we have assumed that φ and θ vary smoothly, excluding the "solitonic" excitations of the cosine pinning term. These more singular configurations are the analog of vortices in the usual boson-vortex duality, which should be minimally coupled to the dynamical gauge fields. we now extend the duality map to include these excitations.

To this end, we replace the cosine potential $g\cos(2\bar{\theta}_{\mathbf{r}})$ by

$$\frac{-g}{2}(2\bar{\theta}_{\mathbf{r}} - 2\pi n_{\mathbf{r}})^2 \tag{5.89}$$

Here $n_{\mathbf{r}}$ parametrizes the locations of the solitons where $2\bar{\theta}$ jumps by integer multiples of 2π.

From the discussion of the microscopic model we can view n as corresponding to some configuration of vortices created by an operator of the form $e^{i\sum\int n(x,y,z)\partial_x\tilde{\varphi}}$. It is natural to wonder how the introduction of such a field manifests in the dual gauge theory. This can be settled using the mapping of section 5.2.4. Indeed, amending Eq

5.81 gives

$$\begin{aligned}\mathcal{L}[\bar{\theta}, a] = \sum_{\mathbf{r}} \frac{-i}{4\pi}(\Lambda \cdot \Delta_y a_0)_{\mathbf{r}} a_{1,\mathbf{r}} + \frac{v}{8\pi}(\Lambda \cdot \Delta_y a_1)^2_{\mathbf{r}} + \frac{1}{32\pi u}(\Lambda \cdot \Delta_y a_0)^2_{\mathbf{r}} \\ + \frac{i}{\pi}\bar{\theta}(\partial_x a_0 - \partial_\tau a_1 + 2\pi i g n) + g\bar{\theta}^2_{\mathbf{r}} + \frac{g}{4} n^2_{\mathbf{r}} \\ + \mathcal{L}_{\text{Maxwell}} + \text{Higher order terms.}\end{aligned} \tag{5.90}$$

Integrating out $\bar{\theta}$ gives Eq. (5.82) plus a coupling term between the gauge fields and n

$$\mathcal{L}[a, n] = \mathcal{L}[a] + i(\partial_x a_0^{(z)} - \partial_\tau a_1^{(z)})n \to \mathcal{L}[a] - (a_0 i\partial_x n - a_1 i\partial_\tau n). \tag{5.91}$$

This tells us that we can interpret n as a x-dipole of the gauge charge. Namely, $\partial_x n = \rho$ is the charge density. One can expect that if we treat the dynamics of solitons carefully (e.g. solitons moving between wires), one would obtain the full matter-gauge coupling $j \cdot a$. Therefore, as expected, vortices become gauge charges.

5.5.3 Quantization condition for 1-form symmetry transformation

In order to derive the quantization conditions on q_I, it is more convenient to use the 4d definition of the Chern-Simons term. Suppose that M_3 is the boundary of a 4d manifold M_4, i.e. $\partial M_4 = M_3$. The gauge field is also extended to M_4. Then the CS action can be defined as

$$S = \frac{K_{IJ}}{4\pi} \int_{M_4} F_I \wedge F_J. \tag{5.92}$$

Now consider 1-form transformations parametrized by λ_I. We assume that they are extended to the bulk as well, but not necessarily flat. The 4d action changes:

$$\begin{aligned}\delta S &= \frac{K_{IJ}}{4\pi}\int_{M_4}(q_I d\lambda_I \wedge F_J + q_J F_I \wedge d\lambda_J + q_I q_J d\lambda_I \wedge d\lambda_J) \\ &= \frac{K_{IJ}}{4\pi}\int_{M_4}(q_I d\lambda_I \wedge F_J + q_J F_I \wedge d\lambda_J) + \frac{K_{IJ}}{4\pi}q_I q_J \int_{M_3}\lambda_I \wedge d\lambda_J \\ &= \frac{K_{IJ}}{4\pi}\int_{M_4}(q_I d\lambda_I \wedge F_J + q_J F_I \wedge d\lambda_J) \\ &= 2\pi K_{IJ} q_I \int_{M_3}\frac{\lambda_I}{2\pi}\wedge\frac{F_J}{2\pi}\end{aligned} \tag{5.93}$$

Since $\int_{M_3}\frac{\lambda_I}{2\pi}\wedge\frac{F_J}{2\pi}$ is an integer (intersection number), for the partition function to remain the same, we must have $e^{i\delta S}=1$, or $K_{IJ}q_I$ an integer.

5.5.4 Phenomenologies

Order parameter

The stretched superfluid order parameter is given by the string operator $e^{i\Phi_y}$ where $\Phi_y(x)=\sum_z \varphi_{yz}$. We want to compute the two point function: $\langle e^{i\Phi_y(x)}e^{-i\Phi_{y'}(x')}\rangle$. To tackle this we approximate the sine-Gordon term by the quadratic term Θ^2 in the strong coupling limit. The resulting theory is free so we can shift our attention to calculating the $\langle\Phi_y(x)\Phi_{y'}(x')\rangle$, which is equal to

$$\sum_{z,z'}\langle\varphi_{yz}(x)\varphi_{y'z'}(x')\rangle = \sum\!\!\!\!\!\!\int_q \sum\!\!\!\!\!\!\int_{q'}\langle\varphi_q\varphi_{q'}\rangle\sum_{z,z'}e^{iq\cdot r}e^{iq'\cdot r'} = \sum\!\!\!\!\!\!\int_q G_\varphi(q)e^{ik_\perp\cdot(r-r')}\sum_{z,z'=1}^{N_z}e^{ik_z(z-z')}. \tag{5.94}$$

Here $k_\perp = (\omega, k_x, k_y)$ is the momentum perpendicular to z, $q = (k_\perp, k_z)$ and $G(q, q') = \delta_{q,q'} G(q)$, since the theory is free and translation invariant. The sum over z, z' can be easily evaluated

$$\sum_{zz'} e^{ik_z(z-z')} = N_z \sum_z e^{ik_z z} = N_z \delta(k_z). \tag{5.95}$$

Thus

$$\langle \Phi_y(x) \Phi_{y'}(x') \rangle = N_z \int dk_\perp \, e^{ik_\perp \cdot \mathbf{r}} G_\varphi(k_z = 0). \tag{5.96}$$

To work out the two-point function G_φ we re-express the action as

$$S = \sum_q \begin{pmatrix} \varphi(q) & \theta(q) \end{pmatrix} G^{-1}(q) \begin{pmatrix} \varphi(-q) \\ \theta(-q) \end{pmatrix} \quad . \tag{5.97}$$

Recall the mean-field Lagrangian Eq. (5.25) is given by:

$$S = \sum\!\!\!\!\!\!\int_{\mathbf{r},x,\tau} dx d\tau \frac{i}{\pi} \partial_x \theta_{\mathbf{r}} \partial_\tau \varphi_{\mathbf{r}} + \left[\tilde{v} (\partial_x \varphi_{\mathbf{r}})^2 + u (\partial_x \theta_{\mathbf{r}})^2 + g \Theta_{\mathbf{r}}^2 \right] \quad . \tag{5.98}$$

Using this, we get

$$G^{-1}(q) = \begin{pmatrix} \tilde{v} k_x^2 + g f_\varphi(q) & \frac{i k_x \omega}{\pi} + g f(q) \\ \\ \frac{i k_x \omega}{\pi} + g f(-q) & u k_x^2 + g f_\theta(q) \end{pmatrix} \tag{5.99}$$

where

$$f_\varphi = 2 - 2\cos k_y$$

$$f_\theta = 4\left[m\cos\tfrac{k_y}{2} + n_1\cos(\tfrac{k_y}{2} - k_z) + n_2\cos(\tfrac{k_y}{2} + k_z)\right]^2$$

$$f = 2i\big[n_1\sin k_z + n_2\sin(k_y + k_z) + m\sin k_y + n_1\sin\,(k_y - k_z) - n_2\sin k_z\big] \quad . \tag{5.100}$$

We are interested in realizations with the chiral U(1) present which occurs when $n_1 + n_2 = -m$. In this case $f_\varphi f_\theta - |f|^2 = 0$ and so we can express G_φ as follows

$$G_\varphi = \frac{uk_x^2 + gf_\theta}{k_x^2\left[\tilde{v}uk_x^2 + \frac{\omega^2}{\pi^2} + g\left(uf_\varphi + \tilde{v}f_\theta\right)\right]}. \tag{5.101}$$

Setting $k_z = 0$, we have $f_\theta = 0$, and G_φ is simplified to

$$G_\varphi = \frac{u}{\frac{\omega^2}{\pi^2} + u\tilde{v}k_x^2 + 2gu(1 - \cos k_y)}. \tag{5.102}$$

This form makes sense as $k_z = 0$ means θ fields are independent of z, so the wire coupling term decouples into $\cos(\varphi_{yz} - \varphi_{y+1,z})$. For long wavelength limit, we can expand $1 - \cos k_y \approx \frac{k_y^2}{2}$, and rescale $k_x \to \frac{k_x}{\sqrt{\tilde{v}}}, k_y \to \frac{k_y}{g}$,

$$\langle\Phi_y(x)\Phi_0(0)\rangle \sim \frac{N_z}{\sqrt{gx^2 + \tilde{v}y^2}}, \tag{5.103}$$

which can be understood as a superfluid with anisotropic dispersion. Thus the two-

point function for our order parameter has the following scaling:

$$\langle e^{i\Phi_y(x)} e^{-i\Phi_0(0)} \rangle \sim e^{-C\frac{N_z}{\sqrt{gx^2+\tilde{v}y^2}}}. \tag{5.104}$$

Here C is a constant.

Compressibility

The presence of both global U(1) symmetries means the model can be defined at arbitrary filling. This, in turn, suggests compressibility. Here we add more field theoretic justification for this feature. To compute compressibility we add a uniform chemical potential term to the Hamiltonian

$$\begin{aligned} H - \mu N &= H - \mu \sum_{\mathbf{r}} \int \partial_x \theta_{\mathbf{r}} \\ &= \int \frac{1}{2\pi} [\tilde{v}(\partial_x \varphi)^2 + u(\partial_x \theta)^2] - \mu \partial_x \theta - g \cos(2\bar{\theta}) \end{aligned} \tag{5.105}$$

where we have suppressed $\sum_{\mathbf{r}}$ in the last line. The term $\mu\partial_x\theta$ can be absorbed into $(\partial_x\theta)^2$ by completing the square: $\frac{u}{2\pi}(\partial_x\theta)^2 - \mu\partial_x\theta = \frac{u}{2\pi}(\partial_x\theta - \frac{\pi}{u}\mu)^2 - \frac{\pi}{2u}\mu^2$. Next we can shift $\partial_x\theta - \frac{\pi}{u}\mu \to \partial_x\theta$ by redefining $\theta \to \theta + \frac{\pi}{u}\mu x$ but this is also a symmetry of the sine-Gordon term. In particular under this transformation $2\bar{\theta} \to 2\bar{\theta}$. Including the uniform chemical potential the action is given by

$$S[\mu] = S - \frac{\pi V}{2u}\mu^2. \tag{5.106}$$

The compressibility is $\kappa \sim \frac{\partial^2 F}{\partial \mu^2}$ which, for this action, is finite. Note that the above argument rests on the fact that the shift $\theta \to \theta + \frac{\pi}{u}\mu x$ is a symmetry of $2\bar{\theta}$. This is a consequence of the presence of the $U(1)_\theta$ subsystem symmetry. So we are in some way factoring in the stretched order parameter in this calculation.

Electromagnetic response

In order to work out the transport properties of the model we can consider coupling the gauge theory to a 3+1D background field A. The natural current is the monopole current in each layer $j^I_\mu \sim \epsilon^{\mu\nu\lambda}\partial_\nu a^I_\lambda$. Indeed the appropriate minimal coupling can be derived from the microscopic model by replacing $\partial_\mu \varphi \to \partial_\mu \varphi + A_\mu$ and carrying out the mapping of section 5.2.4. For simplicity consider the case with an intra-layer Maxwell term and a common charge t in each layer as in section 5.3.3,

$$\mathcal{L} = \frac{K^{IJ}}{4\pi} a_I \wedge da_J - \tilde{g} f_I \wedge \star f_I + \frac{it}{2\pi} A_I \wedge da_I \tag{5.107}$$

where here $A_I = A(x, y; z = I)$. Note the $A_z(x, y, z)$ does not couple to any current, which reflects the fact that the transport of charge along layers is highly suppressed. This can be seen from the form of the coupling term in the microscopic model. Recall the sine-Gordon term $\Theta_{yz} = \varphi_{yz} - \varphi_{y+1,z} + (\theta \text{ terms })$. Heuristically this condenses a process in which a charged particle created by $e^{i\varphi}$ is hopped along the y direction with some additional complicated back-scattering of vortices between different z layers, but no charges tunnel between layers. As was done in Sec. 5.3.3, we can diagonalize Eq.

(5.107).

$$\mathcal{L} = \sum_q \frac{\lambda^q}{4\pi} b^q \wedge db^q - \tilde{g} f^q \wedge \star f^q + \frac{it}{2\pi} A^q \wedge db^q. \tag{5.108}$$

In what follows we use q subscripts and superscripts interchangeably, (e.g. $O_q \equiv O^q$) since there is no subtlety with raising and lowering operators for the layer index.

It is helpful to integrate out the gauge fields b in order to get a theory purely in terms of the background field A. Note that $\mathcal{L} = \sum_q \mathcal{L}_q$ where, defining $m_q = \frac{\lambda_q}{8\pi q}$ and working in the $\partial_\mu b^q_\mu = 0$ gauge,

$$\mathcal{L}_q = -\tilde{g} f^{\mu\nu,q} f^q_{\mu\nu} + 2m_q \epsilon^{mu\nu\gamma} b^q_\mu \partial_\nu b^q_\gamma + b^q_\mu J^{\mu,q} = 2\tilde{g}\ b^q_\mu \left(\partial^2 \eta^{\mu\nu} - m_q \epsilon^{\gamma\mu\nu}\partial_\gamma\right) b^q_\nu + b^q_\mu J^{\mu,q} \quad . \tag{5.109}$$

One can check that the propagator for this theory is given by

$$D^{\mu\nu}_{qq'}(x,y) = \frac{-\delta_{qq'}}{2\tilde{g}} \int \frac{d^3k}{(2\pi)^3} \frac{1}{k^2 - m_q^2} \left[\eta^{\mu\nu} - m_q^2 \frac{k^\mu k^\nu}{k^4} + i\frac{m_q}{k^2}\epsilon^{\mu\nu\gamma} k_\gamma\right] e^{ik\cdot(x-y)} \quad . \tag{5.110}$$

Integrating out b_q results in the effective action $S[J] = -\frac{1}{2}\iint J(x) D(x,y) J(y)$. Here the current is given by $J^{\mu,q} = \frac{it}{2\pi}\epsilon^{\mu\nu\gamma}\partial_\nu A^q_\gamma$. Working in momentum space the full effective action is given by

$$\begin{aligned} S[A] &= \frac{t^2}{16\pi^2\tilde{g}} \epsilon^{\mu\alpha\gamma}\epsilon^{\nu\beta\xi} \sum_q \int \frac{d^3k}{(2\pi)^3} k_\alpha A^q_\gamma(k) D^{qq}_{\mu\nu}(k) k_\beta A_\xi(-k) \\ &= \frac{t^2}{16\pi^2\tilde{g}} \sum_q \int \frac{d^3k}{(2\pi)^3} \frac{k^2 (A^q)^2 - (k\cdot A^q)^2 - i m_q \epsilon^{\mu\nu\gamma} A^q_\mu(k) k_\nu A^q_\gamma(-k)}{k^2 - m_q^2} \quad . \end{aligned} \tag{5.111}$$

Restricting attention to the $q = 0$ sector, where $m_q = 0$, the Lagrangian has the form

$$\mathcal{L}_{q=0} = \frac{t^2}{16\pi^2\tilde{g}} A_\mu^{q=0}(k) \left(\eta^{\mu\nu} - \frac{k^\mu k^\nu}{k^2} \right) A_\nu^{q=0}(-k) \quad . \tag{5.112}$$

From this we can surmise that the application of a long wavelength ($q \to 0, k \to 0$) vector potential induces a Meissner effect, a hallmark of superconductivity [235].

Interaction between vortices

Making the (z) layer index I of the background field manifest, we have seen that vortices are minimally coupled to the gauge field:

$$\mathcal{L}[a, n] = \mathcal{L}[a] + \sum_I a_\mu^I j^{\mu,I}, \tag{5.113}$$

where $j^{\mu,I}$ is the vortex current in the I-th layer and we have used the layered Maxwell-CS theory of section 5.3.3:

$$\mathcal{L}[a] = \frac{K_{IJ}}{4\pi} a_I \wedge da_J + \tilde{g} \sum_z f_I \wedge \star f_I. \tag{5.114}$$

As before we can diagonalize the K-matrix. For the compressible model i.e. for $m = -(n_1 + n_2)$, the normalized eigenvectors $e_I^q = \frac{1}{\sqrt{N}} e^{iqI}$ have eigenvalues $\lambda_q = 2 - 2\cos q$. In this basis $\mathcal{L} = \sum_q \mathcal{L}_q$ with

$$\mathcal{L}_q = \frac{\lambda_q}{4\pi} b^q \wedge db^q + \tilde{g} f^q \wedge \star f^q + b^q \wedge \star j^q. \tag{5.115}$$

Integrating out the gauge fields, we find the effective action of the currents j_μ is [236]

$$E = \frac{1}{2T}\sum_{qq'}\iint d^3x d^3y\, j^\mu_q(x) D^{qq'}_{\mu\nu}(x,y) j^\nu_{q'}(y). \tag{5.116}$$

where the propagator $D^{\mu\nu}_{qq'}$ is given by Eq. (5.110). Here the measure is given by $d^3x = dx^0dx^1dx^2 = dtdxdy = dtd^2\mathbf{r}$. Notice that here $\mathbf{r}$ denotes the position in the xy plane, different from our convention in the main text.

Consider a vortex-antivortex pair at $(\mathbf{r}_a, z_a)$ and $(\mathbf{r}_b, z_b)$ respectively. This corresponds to $n(x,y;z) = 2\pi\delta_{zz_a}\delta_{yy_a}\Theta(x-x_a) - 2\pi\delta_{zz_b}\delta_{yy_b}\Theta(x-x_b)$ which can be expressed as the following current

$$\begin{aligned} j^\mu_{(z)} &= i\eta^\mu_0[\delta(\mathbf{r}-\mathbf{r}_a)\delta_{zz_a} - \delta(\mathbf{r}-\mathbf{r}_b)\delta_{zz_b}] \\ &= \sum_q i\eta^\mu_0[\delta(\mathbf{r}-\mathbf{r}_a)e^{-iqz_a} - \delta(\mathbf{r}-\mathbf{r}_b)e^{-iqz_b}]\frac{e^{iqz}}{\sqrt{N_z}} \\ &= \sum_q j^\mu_q \frac{e^{iqz}}{\sqrt{N_z}} \end{aligned} \tag{5.117}$$

which minimally couples to the gauge field $j^\mu_{(z)}a^{(z)}_\mu = j^{\mu,I}a^I_\mu$.

Plugging this into Eq 5.116 and ignoring the self energy terms gives the following

$$\begin{aligned}
E &= \frac{1}{2T}\sum_{qq'}\iint d^3x d^3y \frac{e^{iqz_a}}{\sqrt{N_z}}\frac{e^{iq'z_b}}{\sqrt{N_z}} D^{00}_{qq'}\delta^2(x-a)\delta^2(y-b) \\
&= \frac{-1}{4T\tilde{g}}\sum_q \iint dx^0 dy^0 \frac{e^{iq(z_a-z_b)}}{N_z}\int \frac{d^3p}{(2\pi)^3}\, e^{-ix_0p_0}e^{-iy_0p_0}\frac{e^{i\mathbf{p}\cdot(\mathbf{r}_a-\mathbf{r}_b)}}{p^2-\lambda_q^2/\tilde{g}^2}\left(\eta^{00}-\lambda_q^2\frac{p^0p^0}{\tilde{g}^2p^4}\right) \\
&= \frac{1}{4TN_z\tilde{g}}\sum_q \int dx^0 e^{iq(z_a-z_b)}\int \frac{dp^1dp^2}{(2\pi)^2}\,\frac{e^{i\mathbf{p}\cdot(\mathbf{r}_a-\mathbf{r}_b)}}{\mathbf{p}\cdot\mathbf{p}+\lambda_q^2/\tilde{g}^2} \\
&= \frac{1}{2N_z\tilde{g}}\sum_q e^{iq(z_a-z_b)}\int \frac{dp^1dp^2}{(2\pi)^2}\,\frac{e^{i\mathbf{p}\cdot(\mathbf{r}_a-\mathbf{r}_b)}}{\mathbf{p}\cdot\mathbf{p}+\lambda_q^2/\tilde{g}^2}
\end{aligned} \tag{5.118}$$

where in going from line 2 to line 3 we first used $\int dx^0 e^{-ix_0p_0} = \delta(p_0)$ and then carried out the integral $\int dp^0$. In going from line 3 to line 4 we used $\int dy^0 = T$. In the large N_z limit we can replace $\frac{1}{N_z}\sum_q \to \int dq$, so

$$\begin{aligned}
E[r_a, r_b] &\sim \int d^2\mathbf{p}dq \frac{e^{i\mathbf{p}\cdot(\mathbf{r}_a-\mathbf{r}_b)}e^{iq(z_a-z_b)}}{\mathbf{p}^2+\frac{1}{\tilde{g}^2}(2-2\cos q)^2} \\
&\sim \int d^2\mathbf{p}dq \frac{e^{i\mathbf{p}\cdot(\mathbf{r}_a-\mathbf{r}_b)}e^{iq(z_a-z_b)}}{\mathbf{p}^2+\frac{1}{\tilde{g}^2}q^4} \quad .
\end{aligned} \tag{5.119}$$

To evaluate this we identify $q^2/\tilde{g}$ with the mass in a 2D free theory. Placing one of the vortices the origin we have

$$E[\mathbf{r}, z] \sim \int dq e^{iqz} K_0(q^2|\mathbf{r}|/\tilde{g}) = \frac{\pi^2}{\sqrt{8}}\frac{\tilde{g}z}{|\mathbf{r}|}\left[I_{-1/4}\left(\frac{z^2\tilde{g}}{8|\mathbf{r}|}\right)^2 - I_{1/4}\left(\frac{z^2\tilde{g}}{8|\mathbf{r}|}\right)^2\right]. \tag{5.120}$$

Note that in the strong coupling limit $\tilde{g}$ is small.

When $z^2/|\mathbf{r}| \gg \frac{1}{\tilde{g}}$ then we must use the $I_\nu(x\to\infty)$ asymptotic expansion. Note

that $K_\nu = \frac{\pi}{2}\frac{I_{-\nu}-I_\nu}{\sin\pi\nu}$, so $I_{-\nu}^2 - I_\nu^2 = \frac{2\sin\pi\nu}{\pi}K_\nu\,(I_{-\nu}+I_\nu)$. Combining the asymptotic expansion for $K_{1/4}$ and $I_{\pm 1/4}$ gives

$$E \approx \frac{4\pi}{|z|} + \mathcal{O}\left(\frac{|\mathbf{r}|^2}{\tilde{g}^2 z^5}\right). \tag{5.121}$$

In the other limit where $z^2/|\mathbf{r}|$ is comparable or much less than 1 we use the asymptotic form of the limit $I_\nu(x \to 0)$. In this case $I_{-1/4}^2(u) - I_{1/4}^2(u) = \frac{\sqrt{2}}{\Gamma(3/4)^2}\frac{1}{\sqrt{u}} - \frac{\sqrt{u}}{\Gamma(5/4)^2\sqrt{2}} + \ldots$ and so

$$E \approx \sqrt{\frac{\tilde{g}}{|\mathbf{r}|}} + \mathcal{O}\left(z^2\frac{\tilde{g}^{3/2}}{|\mathbf{r}|^{3/2}}\right). \tag{5.122}$$

Having worked out the basic example of the vortex-antivortex pair we can compute the interaction energy of more complicated configurations of vorticees. Consider the case of a pair of vortex dipoles; one at the origin oriented in the $\hat{z}$ direction and one at position $(\mathbf{r}_1, z_1)$ oriented in the negative $\hat{z}$ direction. The current is given by

$$j^\mu_{(z)} = i\eta^\mu_0[\delta(\mathbf{r}-\mathbf{r}_1)(\delta_{z,z_1} - \delta_{z,z_1+1}) - \delta(\mathbf{r})(\delta_{z,0} - \delta_{z,1})]. \tag{5.123}$$

In the limit where $z_1^2/|\mathbf{r}_1| \gg \frac{1}{\tilde{g}}$ the interaction energy is given by

$$E \approx \frac{8\pi a_0^2}{|z_1|^3}, \tag{5.124}$$

where a_0 is the distance between neighboring layers. In the limit where $z_1^2/|\mathbf{r}_1|$ is comparable or much less than 1, which includes the case where the dipoles reside in

the same xy-plane, the interaction energy scales as

$$E \propto -\left(\frac{\tilde{g}}{|\mathbf{r}_1|}\right)^{3/2} \quad . \tag{5.125}$$

Bibliography

[1] K. v. Klitzing, G. Dorda, and M. Pepper. New method for high-accuracy determination of the fine-structure constant based on quantized hall resistance. *Phys. Rev. Lett.*, 45(6):494–497, Aug 1980.

[2] D. Sénéchal. An introduction to bosonization. *CRM Series in Mathematical Physics*, page 139–186.

[3] L. D. Landau and E. M. Lifshitz. *Electrodynamics of Continuous Media, 2nd edition*. Pergamon Press, Oxford, 1984.

[4] V. L. Ginzburg and L. D. Landau. On the Theory of superconductivity. *Zh. Eksp. Teor. Fiz.*, 20:1064–1082, 1950.

[5] D. C. Tsui, H. L. Stormer, and A. C. Gossard. Two-dimensional magnetotransport in the extreme quantum limit. *Phys. Rev. Lett.*, 48:1559–1562, May 1982.

[6] S. M. Girvin and A. H. MacDonald. Off-diagonal long-range order, oblique confinement, and the fractional quantum hall effect. *Phys. Rev. Lett.*, 58:1252–1255, Mar 1987.

[7] N. Read. Order parameter and ginzburg-landau theory for the fractional quantum hall effect. *Phys. Rev. Lett.*, 62:86–89, Jan 1989.

[8] S. C. Zhang, T. H. Hansson, and S. Kivelson. Effective-field-theory model for the fractional quantum hall effect. *Phys. Rev. Lett.*, 62:82, 1989.

[9] X.G. Wen. Topological orders in rigid states. *Int. J. Mod. Phys.*, B:239, 1990.

[10] N. Read and Subir Sachdev. Large- N expansion for frustrated quantum antiferromagnets. *Phys. Rev. Lett.*, 66:1773–1776, Apr 1991.

[11] Alexei Kitaev. Anyons in an exactly solved model and beyond. *Ann. Phys.*, 321(1):2 – 111, 2006.

[12] Michael Levin and Xiao-Gang Wen. Detecting topological order in a ground state wave function. *Phys. Rev. Lett.*, 96(11):110405, Mar 2006.

[13] Alexei Kitaev and John Preskill. Topological entanglement entropy. *Phys. Rev. Lett.*, 96(11):110404, Mar 2006.

[14] Chenjie Wang and Michael Levin. Weak symmetry breaking in two-dimensional topological insulators. *Phys. Rev. B*, 88:245136, Dec 2013.

[15] Gregory Moore and Nicholas Read. Nonabelions in the fractional quantum hall effect. *Nuclear Physics B*, 360(2-3):362 – 396, 1991.

[16] Chetan Nayak, Steven H. Simon, Ady Stern, Michael Freedman, and Sankar Das Sarma. Non-abelian anyons and topological quantum computation. *Rev. Mod. Phys.*, 80:1083, 2008.

[17] Eric Dennis, Alexei Kitaev, Andrew Landahl, and John Preskill. Topological quantum memory. *Journal of Mathematical Physics*, 43(9):4452–4505, Sep 2002.

[18] J. K. Jain. Composite-fermion approach for the fractional quantum hall effect. *Phys. Rev. Lett.*, 63:199–202, Jul 1989.

[19] F. D. M. Haldane. Fractional quantization of the hall effect: A hierarchy of incompressible quantum fluid states. *Phys. Rev. Lett.*, 51(7):605–608, Aug 1983.

[20] B. I. Halperin. Statistics of quasiparticles and the hierarchy of fractional quantized hall states. *Phys. Rev. Lett.*, 52:1583–1586, Apr 1984.

[21] X. G. Wen and A. Zee. Classification of abelian quantum hall states and matrix formulation of topological fluids. *Phys. Rev. B*, 46:2290–2301, Jul 1992.

[22] N. Read. Excitation structure of the hierarchy scheme in the fractional quantum hall effect. *Phys. Rev. Lett.*, 65:1502–1505, Sep 1990.

[23] Ian Affleck, Tom Kennedy, Elliott H. Lieb, and Hal Tasaki. Rigorous results on valence-bond ground states in antiferromagnets. *Phys. Rev. Lett.*, 59:799–802, Aug 1987.

[24] W. P. Su, J. R. Schrieffer, and A. J. Heeger. Solitons in polyacetylene. *Phys. Rev. Lett.*, 42:1698–1701, Jun 1979.

[25] A. Y. Kitaev. *Physics-Uspekhi*, 44:131, 2001.

[26] C. L. Kane and E. J. Mele. Quantum spin Hall effect in graphene. *Phys. Rev. Lett.*, 95:226801, 2005.

[27] A. Kitaev. Periodic table for topological insulators and superconductors. *AIP Conf. Proc.*, 1134:22, 2009.

[28] Shinsei Ryu, Andreas P. Schnyder, Akira Furusaki, and Andreas W. W. Ludwig. Topological insulators and superconductors: tenfold way and dimensional hierarchy. *New J. Phys.*, 12:065010, 2010.

[29] Xie Chen, Zheng-Cheng Gu, and Xiao-Gang Wen. Complete classification of one-dimensional gapped quantum phases in interacting spin systems. *Phys. Rev. B*, 84:235128, Dec 2011.

[30] Xie Chen, Zheng-Cheng Gu, Zheng-Xin Liu, and Xiao-Gang Wen. Symmetry protected topological orders and the group cohomology of their symmetry group. *Phys. Rev. B*, 87:155114, Apr 2013.

[31] Dominic V. Else and Chetan Nayak. Classifying symmetry-protected topological phases through the anomalous action of the symmetry on the edge. *Phys. Rev. B*, 90:235137, Dec 2014.

[32] Zheng-Cheng Gu and Xiao-Gang Wen. Symmetry-protected topological orders for interacting fermions: Fermionic topological nonlinear σ models and a special group supercohomology theory. *Phys. Rev. B*, 90:115141, Sep 2014.

[33] Qing-Rui Wang and Zheng-Cheng Gu. Towards a complete classification of symmetry-protected topological phases for interacting fermions in three dimensions and a general group supercohomology theory. *Phys. Rev. X*, 8:011055, Mar 2018.

[34] Tian Lan, Chenchang Zhu, and Xiao-Gang Wen. Fermion decoration construction of symmetry protected trivial orders for fermion systems with any symmetries G_f and in any dimensions. *arXiv e-prints*, Sep 2018.

[35] Anton Kapustin. Symmetry protected topological phases, anomalies, and cobordisms: Beyond group cohomology. 2014.

[36] Anton Kapustin, Ryan Thorngren, Alex Turzillo, and Zitao Wang. *Journal of High Energy Physics*, 2015(12):52, 2015.

[37] Daniel S. Freed and Michael J. Hopkins. 2016.

[38] Tian Lan and Xiao-Gang Wen. Classification of 3 + 1D bosonic topological orders (ii): The case when some pointlike excitations are fermions. *Phys. Rev. X*, 9:021005, Apr 2019.

[39] Claudio Chamon. Quantum glassiness in strongly correlated clean systems: An example of topological overprotection. *Phys. Rev. Lett.*, 94:040402, Jan 2005.

[40] Jeongwan Haah. Lattice quantum codes and exotic topological phases of matter. may 2013.

[41] Sagar Vijay, Jeongwan Haah, and Liang Fu. A new kind of topological quantum order: A dimensional hierarchy of quasiparticles built from stationary excitations. *Phys. Rev. B*, 92:235136, Dec 2015.

[42] Sagar Vijay, Jeongwan Haah, and Liang Fu. Fracton topological order, generalized lattice gauge theory, and duality. *Phys. Rev. B*, 94:235157, Dec 2016.

[43] Sergey Bravyi and Jeongwan Haah. Quantum self-correction in the 3D cubic code model. *Phys. Rev. Lett.*, 111(20):200501, nov 2013.

[44] Barbara M. Terhal. Quantum error correction for quantum memories. *Rev. Mod. Phys.*, 87:307–346, Apr 2015.

[45] Benjamin J. Brown and Dominic J. Williamson. Parallelized quantum error correction with fracton topological codes. *Physical Review Research*, 2(1), Mar 2020.

[46] Nathan Seiberg and Shu-Heng Shao. Exotic symmetries, duality, and fractons in 2+1-dimensional quantum field theory. *SciPost Phys.*, 10(2), Feb 2021.

[47] Nathan Seiberg and Shu-Heng Shao. Exotic $\mathbb{Z}_n$ symmetries, duality, and fractons in 3+1-dimensional quantum field theory. *SciPost Phys.*, 10(1), Jan 2021.

[48] Michael Pretko. The Fracton Gauge Principle. jul.

[49] Kevin Slagle. Foliated quantum field theory of fracton order. *Phys. Rev. Lett.*, 126:101603, Mar 2021.

[50] Xiuqi Ma, Wilbur Shirley, Meng Cheng, Michael Levin, John McGreevy, and Xie Chen. Fractonic order in infinite-component chern-simons gauge theories, 2020.

[51] Daniel Bulmash and Maissam Barkeshli. Higgs mechanism in higher-rank symmetric U(1) gauge theories. *Phys. Rev. B*, 97(23):235112, jun 2018.

[52] Han Ma, Michael Hermele, and Xie Chen. Fracton topological order from the Higgs and partial-confinement mechanisms of rank-two gauge theory. *Phys. Rev. B*, 98(3), 2018.

[53] B. I. Halperin, Patrick A. Lee, and Nicholas Read. Theory of the half-filled landau level. *Phys. Rev. B*, 47:7312–7343, Mar 1993.

[54] E. Rezayi and N. Read. Fermi-liquid-like state in a half-filled landau level. *Phys. Rev. Lett.*, 72:900–903, Feb 1994.

[55] Chong Wang and T. Senthil. Half-filled landau level, topological insulator surfaces, and three-dimensional quantum spin liquids. *Physical Review B*, 93(8), Feb 2016.

[56] N. P. Armitage, E. J. Mele, and Ashvin Vishwanath. Weyl and dirac semimetals in three-dimensional solids. *Rev. Mod. Phys.*, 90:015001, Jan 2018.

[57] Ryan Thorngren, Ashvin Vishwanath, and Ruben Verresen. Intrinsically gapless topological phases. *Phys. Rev. B*, 104:075132, Aug 2021.

[58] Victor M. Yakovenko. Quantum hall effect in quasi-one-dimensional conductors. *Phys. Rev. B*, 43:11353–11366, May 1991.

[59] S. L. Sondhi and Kun Yang. Sliding phases via magnetic fields. *Phys. Rev. B*, 63:054430, Jan 2001.

[60] C. L. Kane, Ranjan Mukhopadhyay, and T. C. Lubensky. Fractional quantum hall effect in an array of quantum wires. *Phys. Rev. Lett.*, 88:036401, Jan 2002.

[61] Jeffrey C. Y. Teo and C. L. Kane. From luttinger liquid to non-abelian quantum hall states. *Phys. Rev. B*, 89:085101, Feb 2014.

[62] Titus Neupert, Claudio Chamon, Christopher Mudry, and Ronny Thomale. Wire deconstructionism of two-dimensional topological phases. *Phys. Rev. B*, 90:205101, Nov 2014.

[63] Gregory Gorohovsky, Rodrigo G. Pereira, and Eran Sela. Chiral spin liquids in arrays of spin chains. *Phys. Rev. B*, 91:245139, Jun 2015.

[64] Tobias Meng, Titus Neupert, Martin Greiter, and Ronny Thomale. Coupled-wire construction of chiral spin liquids. *Phys. Rev. B*, 91:241106, Jun 2015.

[65] Po-Hao Huang, Jyong-Hao Chen, Pedro R. S. Gomes, Titus Neupert, Claudio Chamon, and Christopher Mudry. Non-abelian topological spin liquids from arrays of quantum wires or spin chains. *Phys. Rev. B*, 93:205123, May 2016.

[66] Thomas Iadecola, Titus Neupert, Claudio Chamon, and Christopher Mudry. Ground-state degeneracy of non-abelian topological phases from coupled wires. *Phys. Rev. B*, 99:245138, Jun 2019.

[67] Yukihisa Imamura, Keisuke Totsuka, and T. H. Hansson. From coupled-wire construction of quantum hall states to wave functions and hydrodynamics. *Phys. Rev. B*, 100:125148, Sep 2019.

[68] Thomas Iadecola, Titus Neupert, Claudio Chamon, and Christopher Mudry. Wire constructions of abelian topological phases in three or more dimensions. *Phys. Rev. B*, 93:195136, May 2016.

[69] Yohei Fuji and Akira Furusaki. From coupled wires to coupled layers: Model with three-dimensional fractional excitations. *Physical Review B*, 99(24):241107, 2019.

[70] Matthew P. A. Fisher and Leonid I. Glazman. Transport in a one-dimensional luttinger liquid. *Mesoscopic Electron Transport*, page 331–373, 1997.

[71] Thierry Giamarchi. *Quantum Physics in One Dimension*. Clarendon press, Oxford, 2003.

[72] F. D. M. Haldane. Stability of chiral luttinger liquids and abelian quantum hall states. *Phys. Rev. Lett.*, 74:2090–2093, Mar 1995.

[73] Thomas Iadecola. Designing topological quantum matter in and out of equilibrium. *Ph. D. Thesis*, 2017.

[74] Pavan Hosur, Shinsei Ryu, and Ashvin Vishwanath. Chiral topological insulators, superconductors, and other competing orders in three dimensions. *Phys. Rev. B*, 81:045120, Jan 2010.

[75] Yohei Fuji. Anisotropic layer construction of anisotropic fracton models. *Phys. Rev. B*, 100(23), aug 2019.

[76] Han Ma, Ethan Lake, Xie Chen, and Michael Hermele. Fracton topological order via coupled layers. *Phys. Rev. B*, 95:245126, Jun 2017.

[77] David Aasen, Daniel Bulmash, Abhinav Prem, Kevin Slagle, and Dominic J. Williamson. Topological defect networks for fractons of all types. *Phys. Rev. Research*, 2:043165, Oct 2020.

[78] Joseph Sullivan and Meng Cheng. Interacting Edge States of Fermionic Symmetry-Protected Topological Phases in Two Dimensions. *SciPost Phys.*, 9:16, 2020.

[79] Joseph Sullivan, Thomas Iadecola, and Dominic J. Williamson. Planar p-string condensation: Chiral fracton phases from fractional quantum hall layers and beyond. *Phys. Rev. B*, 103:205301, May 2021.

[80] Joseph Sullivan, Arpit Dua, and Meng Cheng. Fractonic topological phases from coupled wires.

[81] Joseph Sullivan, Arpit Dua, and Meng Cheng. Weak symmetry breaking and topological order in a 3d compressible quantum liquid, 2021.

[82] Xie Chen, Zheng-Cheng Gu, Zheng-Xin Liu, and Xiao-Gang Wen. Symmetry-protected topological orders in interacting bosonic systems. *Science*, 338(6114):1604–1606, 2012.

[83] T. Senthil. Symmetry-protected topological phases of quantum matter. *Annual Review of Condensed Matter Physics*, 6:299–324, 2015.

[84] Ashvin Vishwanath and T. Senthil. Physics of three-dimensional bosonic topological insulators: Surface-deconfined criticality and quantized magnetoelectric effect. *Phys. Rev. X*, 3:011016, Feb 2013.

[85] Andreas P. Schnyder, Shinsei Ryu, Akira Furusaki, and Andreas W. W. Ludwig. Classification of topological insulators and superconductors in three spatial dimensions. *Phys. Rev. B*, 78:195125, 2008.

[86] M. Z. Hasan and C. L. Kane. Topological insulators. *Rev. Mod. Phys.*, 82:3045, Nov 2010.

[87] Xiao-Liang Qi and Shou-Cheng Zhang. Topological insulators and superconductors. *Rev. Mod. Phys.*, 83:1057, Oct 2011.

[88] Xie Chen, Lukasz Fidkowski, and Ashvin Vishwanath. Symmetry enforced non-abelian topological order at the surface of a topological insulator. *Phys. Rev. B*, 89:165132, Apr 2014.

[89] P. Bonderson, C. Nayak, and X.-L. Qi. A time-reversal invariant topological phase at the surface of a 3D topological insulator. *Journal of Statistical Mechanics: Theory and Experiment*, 9:16, September 2013.

[90] Chong Wang and T. Senthil. Boson topological insulators: A window into highly entangled quantum phases. *Phys. Rev. B*, 87:235122, Jun 2013.

[91] Chong Wang, Andrew C. Potter, and T. Senthil. Gapped symmetry preserving surface state for the electron topological insulator. *Phys. Rev. B*, 88:115137, Sep 2013.

[92] Xie Chen, F. J. Burnell, Ashvin Vishwanath, and Lukasz Fidkowski. Anomalous symmetry fractionalization and surface topological order. *Phys. Rev. X*, 5:041013, Oct 2015.

[93] Chenjie Wang, Chien-Hung Lin, and Zheng-Cheng Gu. Interacting fermionic symmetry-protected topological phases in two dimensions. *Phys. Rev. B*, 95:195147, May 2017.

[94] Meng Cheng, Zhen Bi, Yi-Zhuang You, and Zheng-Cheng Gu. Classification of symmetry-protected phases for interacting fermions in two dimensions. *Phys. Rev. B*, 97:205109, May 2018.

[95] Meng Cheng, Nathanan Tantivasadakarn, and Chenjie Wang. Loop braiding statistics and interacting fermionic symmetry-protected topological phases in three dimensions. *Phys. Rev. X*, 8:011054, Mar 2018.

[96] A. Kapustin and R. Thorngren. Fermionic SPT phases in higher dimensions and bosonization. *Journal of High Energy Physics*, 2017.

[97] Yuan-Ming Lu and Ashvin Vishwanath. Theory and classification of interacting integer topological phases in two dimensions: A chern-simons approach. *Phys. Rev. B*, 86:125119, Sep 2012.

[98] Nathanan Tantivasadakarn and Ashvin Vishwanath. Full commuting projector hamiltonians of interacting symmetry-protected topological phases of fermions. *Phys. Rev. B*, 98:165104, Oct 2018.

[99] Meng Cheng and Chenjie Wang. Rotation Symmetry-Protected Topological Phases of Fermions. *arXiv e-prints*, page arXiv:1810.12308, Oct 2018.

[100] Alex Rasmussen and Yuan-Ming Lu. *ArXiv e-prints*, 2018.

[101] Xie Chen, Yuan-Ming Lu, and Ashvin Vishwanath. Symmetry-protected topological phases from decorated domain walls. *Nature Communications*, 5:3507, Mar 2014.

[102] A. W. W. Ludwig. Topological phases: classification of topological insulators and superconductors of non-interacting fermions, and beyond. *Physica Scripta Volume T*, 168:014001, 2016.

[103] Zitao Wang, Shang-Qiang Ning, and Xie Chen. Exactly solvable model for two-dimensional topological superconductors. *Phys. Rev. B*, 98:094502, Sep 2018.

[104] Lukasz Fidkowski and Alexei Kitaev. Effects of interactions on the topological classification of free fermion systems. *Phys. Rev. B*, 81:134509, Apr 2010.

[105] Lukasz Fidkowski and Alexei Kitaev. Topological phases of fermions in one dimension. *Phys. Rev. B*, 83:075103, Feb 2011.

[106] Ryan Thorngren and Dominic V. Else. Gauging spatial symmetries and the classification of topological crystalline phases. *Phys. Rev. X*, 8:011040, Mar 2018.

[107] Hao Song, Sheng-Jie Huang, Liang Fu, and Michael Hermele. Topological phases protected by point group symmetry. *Phys. Rev. X*, 7:011020, Feb 2017.

[108] Sheng-Jie Huang, Hao Song, Yi-Ping Huang, and Michael Hermele. Building crystalline topological phases from lower-dimensional states. *Phys. Rev. B*, 96:205106, Nov 2017.

[109] Charles Zhaoxi Xiong and A. Alexandradinata. Organizing symmetry-protected topological phases by layering and symmetry reduction: A minimalist perspective. *Phys. Rev. B*, 97:115153, Mar 2018.

[110] Meng Cheng, Michael Zaletel, Maissam Barkeshli, Ashvin Vishwanath, and Parsa Bonderson. Translational symmetry and microscopic constraints on symmetry-enriched topological phases: A view from the surface. *Phys. Rev. X*, 6:041068, Dec 2016.

[111] Lukasz Fidkowski, Ashvin Vishwanath, and Max A. Metlitski. Surface Topological Order and a new 't Hooft Anomaly of Interaction Enabled 3+1D Fermion SPTs. *arXiv e-prints*, page arXiv:1804.08628, Apr 2018.

[112] Meng Cheng. Fermionic lieb-schultz-mattis theorems and weak symmetry-protected phases. *Phys. Rev. B*, 99:075143, Feb 2019.

[113] X.-G. Wen. *Int. J. Mod. Phys.*, B6:1711, 1992.

[114] F. D. M. Haldane. Stability of chiral luttinger liquids and abelian quantum hall states. *Phys. Rev. Lett.*, 74:2090–2093, Mar 1995.

[115] Michael Levin and Ady Stern. Fractional topological insulators. *Phys. Rev. Lett.*, 103(19):196803, Nov 2009.

[116] Michael Levin and Ady Stern. Classification and analysis of two-dimensional abelian fractional topological insulators. *Phys. Rev. B*, 86:115131, Sep 2012.

[117] Jennifer Cano, Meng Cheng, Michael Mulligan, Chetan Nayak, Eugeniu Plamadeala, and Jon Yard. Bulk-edge correspondence in $(2+1)$-dimensional abelian topological phases. *Phys. Rev. B*, 89:115116, Mar 2014.

[118] Lukasz Fidkowski, Jason Alicea, Netanel H. Lindner, Roman M. Lutchyn, and Matthew P. A. Fisher. Universal transport signatures of majorana fermions in superconductor-luttinger liquid junctions. *Phys. Rev. B*, 85:245121, Jun 2012.

[119] P. Lecheminant, Alexander O. Gogolin, and Alexander A. Nersesyan. Criticality in self-dual sine-gordon models. *Nucl. Phys. B*, 639:502–523, 2002.

[120] Chris Heinrich and Michael Levin. Criteria for protected edge modes with Z_2 symmetry. *Physical Review B*, 98:035101, Jul 2018.

[121] Maissam Barkeshli, Parsa Bonderson, Meng Cheng, and Zhenghan Wang. Symmetry, defects, and gauging of topological phases.

[122] Paul Fendley. Free fermions in disguise. *arXiv e-prints*, page arXiv:1901.08078, Jan 2019.

[123] Meng Cheng. Fermionic lieb-schultz-mattis theorems and weak symmetry-protected phases. *Phys. Rev. B*, 99:075143, Feb 2019.

[124] S. Bravyi, B. Leemhuis, and B. M. Terhal. Topological order in an exactly solvable 3D spin model. *Ann. Phys.*, 326:839–866, April 2011.

[125] Jeongwan Haah. Local stabilizer codes in three dimensions without string logical operators. *Phys. Rev. A*, 83:042330, Apr 2011.

[126] Beni Yoshida. Exotic topological order in fractal spin liquids. *Phys. Rev. B*, 88:125122, Sep 2013.

[127] S. Vijay. Isotropic Layer Construction and Phase Diagram for Fracton Topological Phases. January.

[128] Abhinav Prem, Sheng Jie Huang, Hao Song, and Michael Hermele. Cage-Net Fracton Models. *Phys. Rev. X*, 9(2), 2019.

[129] S. Vijay and L. Fu. A Generalization of Non-Abelian Anyons in Three Dimensions. June.

[130] Hao Song, Abhinav Prem, Sheng Jie Huang, and M. A. Martin-Delgado. Twisted fracton models in three dimensions. *Phys. Rev. B*, 99(15), 2019.

[131] Kevin Slagle, David Aasen, and Dominic Williamson. Foliated field theory and string-membrane-net condensation picture of fracton order. *SciPost Phys.*, 6(4):043, dec 2019.

[132] Wilbur Shirley, Kevin Slagle, and Xie Chen. Twisted foliated fracton phases. jul 2019.

[133] Dominic J. Williamson and Trithep Devakul. Type-II fractons from coupled spin chains and layers. jul.

[134] Wilbur Shirley, Kevin Slagle, Zhenghan Wang, and Xie Chen. Fracton Models on General Three-Dimensional Manifolds. *Phys. Rev. X*, 8(3), 2018.

[135] Wilbur Shirley, Kevin Slagle, and Xie Chen. Fractional excitations in foliated fracton phases. 2018.

[136] Wilbur Shirley, Kevin Slagle, and Xie Chen. Foliated fracton order from gauging subsystem symmetries. *SciPost Physics*, 6(4), Apr 2019.

[137] Xiao-Gang Wen. Systematic construction of gapped nonliquid states. *Phys. Rev. Research*, 2:033300, Aug 2020.

[138] Juven Wang. Non-liquid cellular states, 2020.

[139] Tobias Meng. Coupled-wire constructions: a luttinger liquid approach to topology. *The European Physical Journal Special Topics*, 229(4):527–543, Feb 2020.

[140] Titus Neupert, Luiz Santos, Claudio Chamon, and Christopher Mudry. Fractional quantum hall states at zero magnetic field. *Phys. Rev. Lett.*, 106(23):236804, Jun 2011.

[141] Jeongwan Haah. Commuting Pauli Hamiltonians as Maps between Free Modules. *Communications in Mathematical Physics*, 324(2):351–399, 2013.

[142] Arpit Dua, Dominic J. Williamson, Jeongwan Haah, and Meng Cheng. Compactifying fracton stabilizer models. *Phys. Rev. B*, 99:245135, Jun 2019.

[143] Arpit Dua, Isaac H. Kim, Meng Cheng, and Dominic J. Williamson. Sorting topological stabilizer models in three dimensions. *Phys. Rev. B*, 100(15), aug 2019.

[144] Michael Pretko. Subdimensional particle structure of higher rank $u(1)$ spin liquids. *Phys. Rev. B*, 95:115139, Mar 2017.

[145] Michael Pretko. Generalized electromagnetism of subdimensional particles: A spin liquid story. *Phys. Rev. B*, 96:035119, Jul 2017.

[146] Andrey Gromov. Chiral Topological Elasticity and Fracton Order. *Phys. Rev. Lett.*, 122(7):076403, dec 2019.

[147] Shriya Pai and Michael Hermele. Fracton fusion and statistics. *Phys. Rev. B*, 100:195136, Nov 2019.

[148] Y. You, T. Devakul, F. J. Burnell, and S. L. Sondhi. Symmetric Fracton Matter: Twisted and Enriched. *ArXiv e-prints*, May 2018.

[149] Pok Man Tam and Charles L. Kane. Nondiagonal anisotropic quantum hall states. *Phys. Rev. B*, 103:035142, Jan 2021.

[150] Sriram Ganeshan, Alexey Gorshkov, Victor Gurarie, and Victor Galitski. unpublished.

[151] William W. Adams and Philippe Loustaunau. *An introduction to Gröbner bases*, volume 3 of *Graduate Studies in Mathematics*. American Mathematical Society, Providence, RI, 1994.

[152] Rahul M. Nandkishore and Michael Hermele. Fractons. Mar.

[153] Michael Pretko, Xie Chen, and Yizhi You. Fracton Phases of Matter. jan.

[154] Claudio Castelnovo and Claudio Chamon. Topological quantum glassiness. *Philosophical Magazine*, 92(1-3):304–323, 2012.

[155] Isaac H. Kim. 3D local qupit quantum code without string logical operator.

[156] Sergey Bravyi and Jeongwan Haah. Energy landscape of 3D spin hamiltonians with topological order. *Phys. Rev. Lett.*, 107(15):150504, oct 2011.

[157] Benjamin J. Brown and Dominic J. Williamson. Parallelized quantum error correction with fracton topological codes. *Phys. Rev. Res.*, 2(1):1–13, jan 2020.

[158] Trithep Devakul and Dominic J. Williamson. Fractalizing quantum codes. Sep.

[159] Isaac H. Kim and Jeongwan Haah. Localization from superselection rules in translationally invariant systems. *Phys. Rev. Lett.*, 116:027202, Jan 2016.

[160] Abhinav Prem, Jeongwan Haah, and Rahul Nandkishore. Glassy quantum dynamics in translation invariant fracton models. *Phys. Rev. B*, 95:155133, Apr 2017.

[161] Arpit Dua, Pratyush Sarkar, Dominic J. Williamson, and Meng Cheng. Bifurcating entanglement-renormalization group flows of fracton stabilizer models. *Phys. Rev. Res.*, 2(3):33021, sep 2019.

[162] Juven Wang. Non-Liquid Cellular States. February.

[163] Abhinav Prem, Michael Pretko, and Rahul M. Nandkishore. Emergent phases of fractonic matter. *Phys. Rev. B*, 97(8):85116, feb 2018.

[164] Michael Pretko and Leo Radzihovsky. Fracton-elasticity duality. *Phys. Rev. Lett.*, 120:195301, May 2018.

[165] Daniel Bulmash and Maissam Barkeshli. Generalized $U(1)$ Gauge Field Theories and Fractal Dynamics.

[166] Andrey Gromov. Towards Classification of Fracton Phases: The Multipole Algebra. *Phys. Rev. X*, 9(3):031035, dec 2019.

[167] Kevin Slagle and Yong Baek Kim. Quantum field theory of x-cube fracton topological order and robust degeneracy from geometry. *Phys. Rev. B*, 96:195139, Nov 2017.

[168] Dominic J. Williamson, Zhen Bi, and Meng Cheng. Fractonic matter in symmetry-enriched $u(1)$ gauge theory. *Phys. Rev. B*, 100:125150, Sep 2019.

[169] Leo Radzihovsky and Michael Hermele. Fractons from vector gauge theory. *Phys. Rev. Lett.*, 124(5):050402, may 2019.

[170] Nathan Seiberg. Field Theories With a Vector Global Symmetry. *SciPost Phys.*, 8(4):050, sep 2019.

[171] Nathan Seiberg and Shu-Heng Shao. Exotic $U(1)$ Symmetries, Duality, and Fractons in 3+1-Dimensional Quantum Field Theory. mar.

[172] N. Seiberg and S.-H. Shao, arXiv:2004.06115.

[173] Weslei B. Fontana, Pedro R. S. Gomes, and Claudio Chamon. Lattice Clifford fractons and their Chern-Simons-like theory. jun.

[174] Jeongwan Haah. Bifurcation in entanglement renormalization group flow of a gapped spin model. *Phys. Rev. B*, 89(7):75119, feb 2014.

[175] Gábor B. Halász, Timothy H. Hsieh, and Leon Balents. Fracton topological phases from strongly coupled spin chains. *Phys. Rev. Lett.*, 119:257202, Dec 2017.

[176] Timothy H. Hsieh and Gábor B. Halász. Fractons from partons. *Phys. Rev. B*, 96:165105, Oct 2017.

[177] Abhinav Prem and Dominic Williamson. Gauging permutation symmetries as a route to non-Abelian fractons. *SciPost Phys.*, 7(5):068, nov 2019.

[178] D. Bulmash and M. Barkeshli, arXiv:1905.05771.

[179] David T. Stephen, José Garre-Rubio, Arpit Dua, and Dominic J. Williamson. Subsystem symmetry enriched topological order in three dimensions. *Phys. Rev. Res.*, 2(3), apr 2020.

[180] Albert T. Schmitz. Distilling Fractons from Layered Subsystem-Symmetry Protected Phases. oct.

[181] Anton Kapustin and Lukasz Fidkowski. Local commuting projector hamiltonians and the quantum hall effect. *Communications in Mathematical Physics*, 373(2):763–769, May 2019.

[182] R. B. Laughlin. Anomalous quantum hall effect: An incompressible quantum fluid with fractionally charged excitations. *Phys. Rev. Lett.*, 50:1395, 1983.

[183] Dominic J. Williamson and Meng Cheng. Designer non-Abelian fractons from topological layers. apr.

[184] F. A. Bais and J. K. Slingerland. Condensate-induced transitions between topologically ordered phases. *Phys. Rev. B*, 79:045316, Jan 2009.

[185] Chao-Ming Jian and Xiao-Liang Qi. Layer construction of 3d topological states and string braiding statistics. *Phys. Rev. X*, 4:041043, Dec 2014.

[186] Daniel Bulmash and Thomas Iadecola. Braiding and gapped boundaries in fracton topological phases. *Phys. Rev. B*, 99:125132, Mar 2019.

[187] Xiu Qiu, Robert Joynt, and A. H. MacDonald. Phase transitions in a multiple quantum well in strong magnetic fields. *Phys. Rev. B*, 42:1339–1352, Jul 1990.

[188] J. D. Naud, Leonid P. Pryadko, and S. L. Sondhi. Fractional quantum hall effect in infinite-layer systems. *Phys. Rev. Lett.*, 85:5408–5411, Dec 2000.

[189] J.D. Naud, Leonid P. Pryadko, and S.L. Sondhi. Notes on infinite layer quantum hall systems. *Nucl. Phys. B*, 594(3):713–746, February 2001.

[190] X. Ma, W. Shirley, M. Cheng, M. Levin, J. McGreevy, and X. Chen, arXiv:2010.08917.

[191] Charles-Edouard Bardyn, Michele Filippone, and Thierry Giamarchi. Bulk pumping in two-dimensional topological phases. *Phys. Rev. B*, 99:035150, Jan 2019.

[192] R. B. Laughlin. Quantized hall conductivity in two dimensions. *Phys. Rev. B*, 23:5632–5633, May 1981.

[193] B. I. Halperin. Quantized hall conductance, current-carrying edge states, and the existence of extended states in a two-dimensional disordered potential. *Phys. Rev. B*, 25:2185–2190, Feb 1982.

[194] Gregory Moore and Nathan Seiberg. Classical and quantum conformal field theory. *Commun. Math. Phys.*, 123:177, 1989.

[195] Michael Mueger. On the Structure of Modular Categories. *Proc. London Math. Soc.*, 87(2):291–308, jan 2002.

[196] Parsa Hassan Bonderson. Non-Abelian Anyons and Interferometry. Technical report, 2007.

[197] Sriram Ganeshan and Michael Levin. Formalism for the solution of quadratic hamiltonians with large cosine terms. *Phys. Rev. B*, 93:075118, Feb 2016.

[198] A. B. Zamolodchikov and V. A. Fateev. *J. Exp. Theor. Phys.*, 89:380, 1985.

[199] S.B. Bravyi and A. Yu. Kitaev. Quantum codes on a lattice with boundary. 1998.

[200] Alexei Davydov, Michael Müger, Dmitri Nikshych, and Victor Ostrik. The Witt group of non-degenerate braided fusion categories. *J. fur die Reine und Angew. Math.*, 2013(677):135–177, 2013.

[201] Michael A. Levin and Xiao-Gang Wen. String-net condensation: a physical mechanism for topological phases. *Phys. Rev. B*, 71:045110, Jan 2005.

[202] Pavel Etingof, Dmitri Nikshych, and Viktor Ostrik. On fusion categories. *Ann. Math.*, 162(2):581–642, 2005.

[203] Shlomo Gelaki, Deepak Naidu, and Dmitri Nikshych. Centers of graded fusion categories. *Algebr. Number Theory*, 3(8):959–990, 2009.

[204] Chris Heinrich, Fiona Burnell, Lukasz Fidkowski, and Michael Levin. Symmetry-enriched string nets: Exactly solvable models for SET phases. *Phys. Rev. B*, 94(23):235136, dec 2016.

[205] Meng Cheng, Zheng-Cheng Gu, Shenghan Jiang, and Yang Qi. Exactly Solvable Models for Symmetry-Enriched Topological Phases. *Phys. Rev. B*, 96(11):115107, sep 2016.

[206] Dominic J. Williamson, Nick Bultinck, and Frank Verstraete. Symmetry-enriched topological order in tensor networks: Defects, gauging and anyon condensation.

[207] Dominic J. Williamson. Fractal symmetries: Ungauging the cubic code. *Phys. Rev. B*, 94:155128, Oct 2016.

[208] Aleksander Kubica and Beni Yoshida. Ungauging quantum error-correcting codes.

[209] Marvin Qi, Leo Radzihovsky, and Michael Hermele. Fracton phases via exotic higher-form symmetry-breaking. oct.

[210] Michael Levin and Zheng-Cheng Gu. Braiding statistics approach to symmetry-protected topological phases. *Phys. Rev. B*, 86:115109, Sep 2012.

[211] Jutho Haegeman, Karel Van Acoleyen, Norbert Schuch, J. Ignacio Cirac, and Frank Verstraete. Gauging quantum states: From global to local symmetries in many-body systems. *Phys. Rev. X*, 5(1):11024, 2015.

[212] Dominic J. Williamson, Nick Bultinck, Michael Mariën, Mehmet B. Sahinoglu, Jutho Haegeman, and Frank Verstraete. Matrix product operators for symmetry-protected topological phases: Gauging and edge theories. *Phys. Rev. B*, 94(20):205150, nov 2016.

[213] Eric Rowell, Richard Stong, and Zhenghan Wang. *Comm. Math. Phys.*, 292(2):343–389, 2009.

[214] Eddy Ardonne, Paul Fendley, and Eduardo Fradkin. Topological order and conformal quantum critical points. *Ann. Phys.*, 310(2):493–551, Apr 2004.

[215] Shouvik Sur and Kun Yang. Metallic state in bosonic systems with continuously degenerate dispersion minima. *Phys. Rev. B*, 100:024519, Jul 2019.

[216] Ethan Lake, T. Senthil, and Ashvin Vishwanath. Bose-luttinger liquids, 2021.

[217] Dominic V. Else, Ryan Thorngren, and T. Senthil. Non-fermi liquids as ersatz fermi liquids: General constraints on compressible metals. *Phys. Rev. X*, 11:021005, Apr 2021.

[218] Gil Young Cho, Chang-Tse Hsieh, and Shinsei Ryu. Anomaly manifestation of lieb-schultz-mattis theorem and topological phases. *Phys. Rev. B*, 96:195105, Nov 2017.

[219] Luca Delacrétaz, Diego Hofman, and Grégoire Mathys. Superfluids as higher-form anomalies. *SciPost Phys.*, 8(3), Mar 2020.

[220] Dominic Else and T. Senthil. Critical drag as a mechanism for resistivity, 2021.

[221] Michael Pretko, Xie Chen, and Yizhi You. Fracton Phases of Matter. *Int. J. Mod. Phys. A*, 35(06):2030003, 2020.

[222] Cenke Xu. Gapless bosonic excitation without symmetry breaking: An algebraic spin liquid with soft gravitons. *Phys. Rev. B*, 74:224433, Dec 2006.

[223] A. Rasmussen, Y.-Z. You, and C. Xu. Stable Gapless Bose Liquid Phases without any Symmetry. *ArXiv e-prints*, January 2016.

[224] Yizhi You, Trithep Devakul, F. J. Burnell, and S. L. Sondhi. Subsystem symmetry protected topological order. *Phys. Rev. B*, 98(3), 2018.

[225] Xiuqi Ma, Wilbur Shirley, Meng Cheng, Michael Levin, John McGreevy, and Xie Chen. Fractonic order in infinite-component chern-simons gauge theories, 2020.

[226] Joseph Sullivan, Arpit Dua, and Meng Cheng. Fractonic topological phases from coupled wires. *Phys. Rev. Research*, 3:023123, May 2021.

[227] Yizhi You, Trithep Devakul, S. L. Sondhi, and F. J. Burnell. Fractonic chern-simons and bf theories. *Phys. Rev. Research*, 2:023249, May 2020.

[228] Peng Rao and Inti Sodemann. Theory of weak symmetry breaking of translations in z2 topologically ordered states and its relation to topological superconductivity from an exact lattice z2 charge-flux attachment. *Phys. Rev. Research*, 3(2), May 2021.

[229] E. Lieb, T. Schultz, and D. Mattis. Two soluble models of an antiferromagnetic chain. *Annals of Physics*, 16:407, 1961.

[230] Davide Gaiotto, Anton Kapustin, Nathan Seiberg, and Brian Willett. Generalized global symmetries. *Journal of High Energy Physics*, 2015(2), Feb 2015.

[231] David F. Mross, Jason Alicea, and Olexei I. Motrunich. Symmetry and duality in bosonization of two-dimensional dirac fermions. *Phys. Rev. X*, 7:041016, Oct 2017.

[232] Eyal Leviatan and David F. Mross. Unification of parton and coupled-wire approaches to quantum magnetism in two dimensions. *Phys. Rev. Research*, 2:043437, Dec 2020.

[233] Po-Shen Hsin, Ho Tat Lam, and Nathan Seiberg. Comments on one-form global symmetries and their gauging in 3d and 4d. *SciPost Physics*, 6(3), Mar 2019.

[234] Xue-Yang Song, Yin-Chen He, Ashvin Vishwanath, and Chong Wang. Electric polarization as a nonquantized topological response and boundary luttinger theorem. *Phys. Rev. Research*, 3:023011, Apr 2021.

[235] Douglas J. Scalapino, Steven R. White, and Shoucheng Zhang. Insulator, metal, or superconductor: The criteria. *Phys. Rev. B*, 47:7995–8007, Apr 1993.

[236] A. Zee. *Quantum field theory in a nutshell.* 2003.

[237] Yu-An Chen. *Exact bosonization in all dimensions: the duality between fermionic and bosonic phases of matter.* PhD thesis, California Institute of Technology, 2020.

Contents

Appendix A

Appendix

A.1 Fermion-Boson dualities in 1D

Jordan-Wigner transformation and Bosonization

On a 1D lattice there is a convenient duality between fermionic and spin 1/2 (bosonic) degrees of freedom. To begin we can consider a single site. Here there is simple analogy to be made between the basis states of the fermionic and spin Hilbert spaces

$$|\uparrow\rangle \equiv c^\dagger |0\rangle\,, \quad |\downarrow\rangle \equiv |0\rangle \quad . \tag{A.1}$$

Furthermore we can make identifications between the important operators in the different settings

$$\sigma^+ = c^\dagger = \begin{pmatrix} 0 & 1 \\ & \\ 0 & 0 \end{pmatrix}, \quad \sigma^- = c = \begin{pmatrix} 0 & 0 \\ & \\ 1 & 0 \end{pmatrix}, \quad \sigma^z = c^\dagger c - \frac{1}{2} = \begin{pmatrix} \frac{1}{2} & 0 \\ & \\ 0 & \frac{-1}{2} \end{pmatrix} \ . \tag{A.2}$$

Now suppose we have a lattice of spins along a line. The mapping in Eq A.2 runs into a problem when we consider the respective commutation relations for these quantum systems

$$\text{Fermions: } \{c_i, c_j^\dagger\} = \delta_{ij}, \ \{c_i, c_j\} = 0 \qquad \text{Spin } 1/2\text{: } [\sigma_i^a, \sigma_j^b] = i\delta_{ij}\epsilon_{abc}\sigma^c, \ \{\sigma_i, \sigma_j\} = \frac{1}{2}\delta_{ij} \ . \tag{A.3}$$

The issue is that fermionic operators on different sites anti-commute while Pauli operators on different sites commute. All is not lost though, we can still salvage the correspondence between these fundamental two-level systems. We work on the fermionic side first and define the string operator $e^{i\phi_j}$ where $\phi_j = \pi \sum_{i=0}^{j-1} c_i^\dagger c_i$ measures the fermionic occupation between the edge (or some reference site on periodic boundary conditions) and site $j-1$. One can verify that the following operators obey the spin $1/2$ commutation relations of Eq A.3

$$\sigma_j^+ = c_j^\dagger e^{i\phi_j}, \quad \sigma_j^- = c_j e^{-i\phi_j}, \quad \sigma_j^z = c_j^\dagger c_j - \frac{1}{2} \ . \tag{A.4}$$

Succinctly, we see that spin = fermion $\times$ string. Note that we can also invert this mapping because $\phi_j = \pi \sum_{i=0}^{j} c_i^\dagger c_i = \pi \sum_{i=0}^{j} \sigma_i^z + \frac{1}{2}$. Inverting the transformation

gives

$$c_j^\dagger = \left(\prod_{i=0}^{j-1}\sigma_i^z\right)\sigma_j^+, \quad c_j = \left(\prod_{i=0}^{j-1}\sigma_i^z\right)\sigma_j^-, \quad c_j^\dagger c_j = \sigma_j^z + \frac{1}{2} \ . \tag{A.5}$$

Somewhat unsurprisingly, fermion = spin × string.

At an operational level we see that the string operators role is to provide the additional minus sign to enforce the desired commutation relation. Given two spins σ_j^b, σ_k^b with $k > j$, in the fermionic description the support of the string part of σ_k will contain the the raising/lowering part f_j^a of σ_j but not vice-versa. This gives us the desired commuting algebra built out of degrees of freedom which anti-commute. We see that this procedure goes awry in higher dimensions because now there is no canonical ordering of the sites and one may "wiggle" the string operators around. Higher dimension Jordan Wigner transformations require greater care [237].

Bosonization

In the previous section we looked at some dualities between discrete fermionic and bosonic systems. In this section we will discuss their continuum analogues. For canonical treatments of this subject see [71, 2]. To begin with let us consider the simple setting of non-interacting spinless fermions on a 1D lattice. In the momentum basis we can write the Hamiltonian as

$$H_F = \sum_k \varepsilon(k) c^\dagger(k) c(k) \tag{A.6}$$

The dispersion relation $\epsilon(k)$ is shown in Fig. A.1. At low energies it is clear that the relevant states are those near the Fermi points and so it is pertinent coarse grain. We linearize ($\epsilon(k) \to vk$) around the Fermi points and work with the new degrees of freedom and effective Hamiltonian

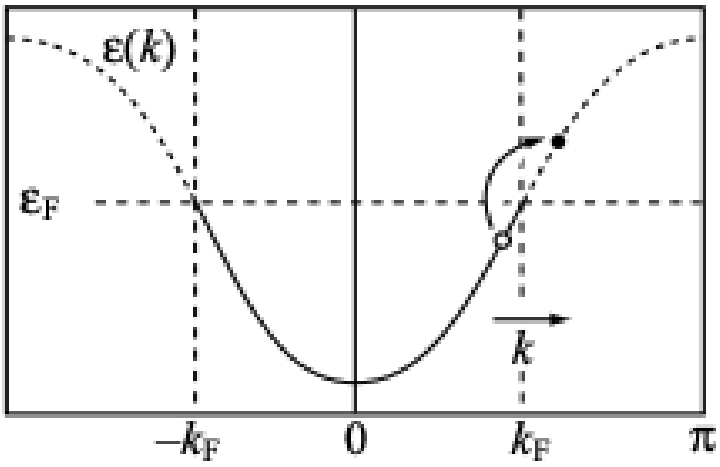

Figure A.1: Plot of the dispersion relation $\varepsilon(k)$ of some translation invariant free fermion system. Figure borrowed from [2].

$$H_F = \sum_{|k|<\Lambda} vk \left(c_L^\dagger(k) c_L(k) + c_R^\dagger(k) c_R(k) \right) \qquad \text{with } c_R(k) = c\left(k_F + k\right), \quad c_L(k) = c\left(-k_F - k\right) \quad . \tag{A.7}$$

With an eye toward coarse graining we can define chiral fermions and use them to construct true Dirac fermion

$$\psi_{R/L}(x) = \left(\frac{2\pi}{L}\right)^{1/2} \sum_{|k|<\Lambda} c_{R/L}(k) e^{\pm ikx} \longrightarrow \Psi(x) = e^{ik_F x}\psi_R(x) + e^{-ik_F x}\psi_L(x) \quad . \tag{A.8}$$

Our effective Hamiltonian can be recast in terms of these continuum fields

$$H_F = -i\frac{v}{2}\int dx \left(\psi_R(x)^\dagger \partial_x \psi_R(x) - \psi_L^\dagger(x)\partial_x \psi_L(x)\right) \ . \tag{A.9}$$

Where we have used Fourier convention where $c_{R/L}(k) = \frac{1}{\sqrt{2\pi L}}\int dx \psi_{R/L}(x) e^{\mp ikx}$.

Let us take a quick aside an consider the following free bosonic Hamiltonian in 1D:

$$H_B = \frac{1}{\pi}\int dx \left(\partial_x \phi_R\right)^2 + \left(\partial_x \phi_L\right)^2 \tag{A.10}$$

where the bosons have commutation relations $[\phi_{L/R}(x), \partial_x \phi_{L/R}(x')] = \pm 2\pi i \delta(x - x')$, $[\phi_L, \phi_R] = i\pi$.

We will be interested in the vertex operators $e^{i\phi_{L/R}}$ of the bosonic degrees and their correlation functions. Throughout this work any exponentiated operator is implicitly normal ordered (e.g. $e^{iA} \equiv :e^{iA}:$). We omit the details here [2] but one can use the mode expansion of the chiral bosons and standard identities about normal ordered operators to arrive at

$$\langle e^{i\phi_L(x)} e^{-i\phi_L(y)}\rangle = \frac{\epsilon}{\epsilon - i(x-y)} \quad \text{and} \quad \langle e^{i\phi_R(x)} e^{-i\phi_R(y)}\rangle = \frac{\epsilon}{\epsilon + i(x-y)} \ . \tag{A.11}$$

The correlation functions for the chiral fermions have the form

$$\langle \psi_L(x)\psi_L^\dagger(y)\rangle = \frac{i}{2\pi}\frac{1}{(x-y)+i\epsilon} \quad \text{and} \quad \langle \psi_R(x)\psi_R^\dagger(y)\rangle = \frac{-i}{2\pi}\frac{1}{(x-y)-i\epsilon}\ . \tag{A.12}$$

Comparing Eqs A.11 and A.12 we see we can make the following identification

$$\psi_L(x) = \frac{1}{\sqrt{2\pi\epsilon}}e^{i\phi_L(x)} \quad \text{and} \quad \psi_R(x) = \frac{1}{\sqrt{2\pi\epsilon}}e^{i\phi_R(x)} \tag{A.13}$$

We can check that the vertex operators reproduce the appropriate fermionic commuation relations $\{\psi_\eta(x), \psi_{\eta'}^\dagger(y)\} = \delta_{\eta\eta'}\delta(x-y),\ \{\psi_\eta(x), \psi_{\eta'}(y)\} = 0$.

Further more we can use Eqs A.13 and A.11 to establish a Fermion-to-Boson dictionary between important operators such as the currents. For example, using

$$\begin{aligned}
\psi_{L/R}^\dagger(x)\psi_{L/R}(x) &= \lim_{\delta\to 0}\frac{1}{2\pi\epsilon}e^{-i\phi_{L/R}(x+\delta)}e^{i\phi_{L/R}(x)} \\
&= \lim_{\delta\to 0}\frac{1}{2\pi\epsilon}e^{-i\phi_{L/R}(x+\delta)-\phi_{L/R}(x)}e^{\langle\phi_{L/R}(x+\delta)\phi_{L/R}(x)\rangle} \\
&= \lim_{\delta\to 0}\frac{1}{2\pi\epsilon}\left(1 - i\delta\partial_x\phi_{L/R} + O(\delta^2)\right)\frac{\epsilon}{\epsilon \mp i\delta} \\
&= \pm\frac{1}{2\pi}\partial_z\phi_{L/R} + \text{divergent piece fixed by normal ordering}
\end{aligned} \tag{A.14}$$

we see that the $U(1)$ charge density $\rho = \psi_L^\dagger\psi_L + \psi_R^\dagger\psi_R = \frac{1}{2\pi}(\partial_x\phi_L - \partial_x\phi_R) = \frac{1}{\pi}\partial\theta$. The free fermion theory also has chiral symmetry $U(1)_{chiral}$ with charge density $\rho_{chiral} = \psi_L^\dagger\psi_L - \psi_R^\dagger\psi_R = \frac{1}{2\pi}(\partial_x\phi_L + \partial_x\phi_R) = \frac{1}{2\pi}\partial_x\varphi$. Here we have introduced an equally valid pair of bosonic variables ($\varphi = \phi_L + \phi_R, \theta = \frac{\phi_L - \phi_R}{2}$), with commuation relations $[\varphi(x), \partial_y\theta(y)] = 2\pi i\delta(x-y)$.

We can consider adding terms to our fermion Hamiltonian. For example we may break the chiral symmetry by adding a mass term

$$\begin{aligned}\Delta H &= m\left(\psi_L^\dagger \psi_R + \psi_R^\dagger \psi_L\right) \\ &= m\left(e^{-i\phi_L} e^{i\phi_R} + e^{i\phi_L} e^{-i\phi_R}\right) \\ &= -\frac{m}{\pi\epsilon}\cos(2\theta)\ .\end{aligned} \tag{A.15}$$

The mass term shows up in the dual bosonic theory as a sine-Gordon term. Alternatively we can add a density-density interaction

$$\begin{aligned}\Delta H &= g\rho^2 = g(\psi_L^\dagger \psi_L + \psi_R^\dagger \psi_R)^2 \\ &= \frac{g}{\pi^2}\left(\partial_x \theta\right)^2 \quad .\end{aligned} \tag{A.16}$$

This time the interaction term renormalizes the kinetic term in the dual bosonic theory.

Generically, adding interactions to the fermionic Hamiltonian will manifest in the dual bosonic theory by either renormalizing the couplings of the kinetic terms or introducing a sine-Gordon term. Throughout this dissertation we will leverage this fact to map fermionic (and bosonic) theories with complicated backscattering interactions to relatively simple bosonic theories.